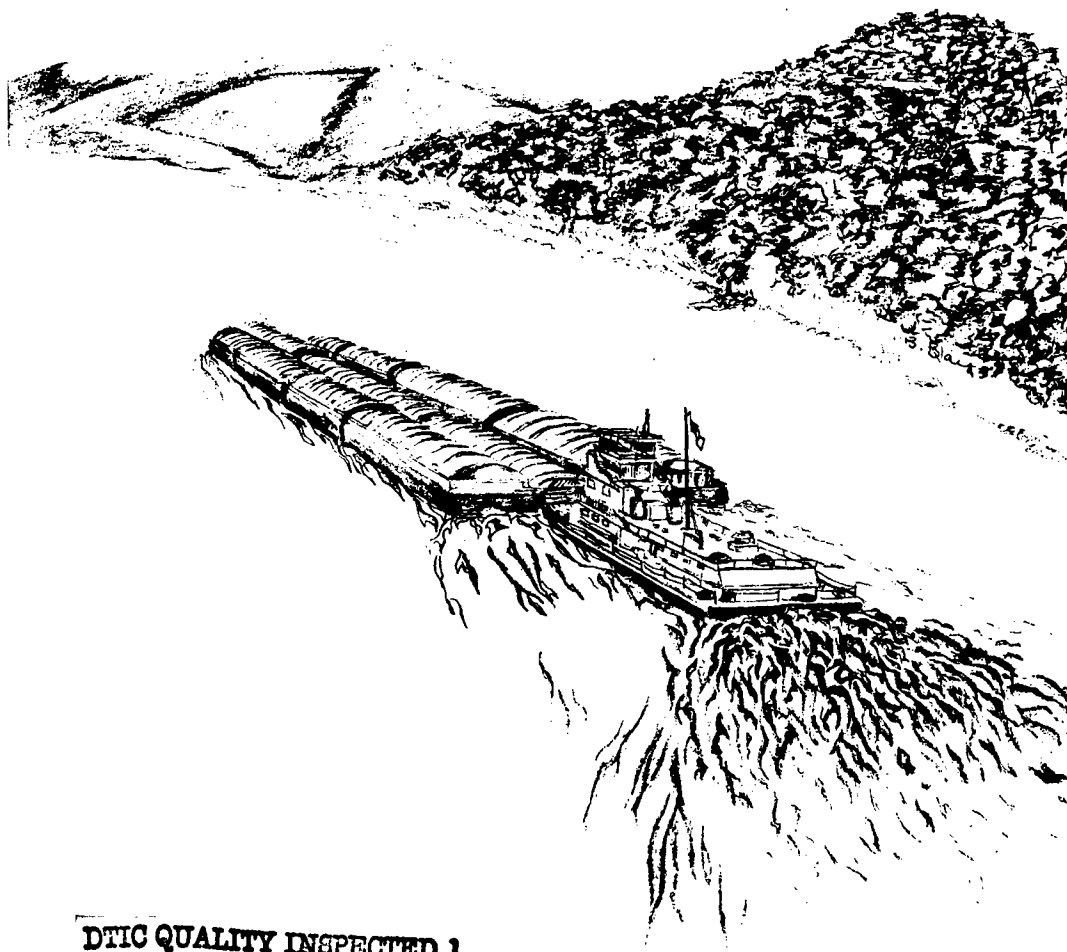


Long Term Resource Monitoring Program

Special Report

98-S001

Physical Changes Associated with Navigation Traffic on the Illinois and Upper Mississippi Rivers



19980904 067

DTIC QUALITY INSPECTED 1

July 1998

DISTRIBUTION STATEMENT A

Approved for public release;
Distribution Unlimited

LTRMP Special Reports provide Long Term Resource Monitoring Program partners with scientific and technical support. The opinions and conclusions in LTRMP Special Reports are those of the author(s) and do not necessarily reflect those of the Environmental Management Technical Center.

All reports in this series receive anonymous peer review.

**Environmental Management
Technical Center**

CENTER DIRECTOR

Robert L. Delaney

APPLIED RIVER SCIENCE

ACTING DIRECTOR

Ken Lubinski

PROGRAM OPERATIONS

ACTING DIRECTOR

Linda Leske

REPORT EDITOR

Jerry Cox

Cover graphic by B. Blair

Mention of trade names or commercial products does not constitute endorsement or recommendation for use by the U.S. Geological Survey, U.S. Department of the Interior.

Printed on recycled paper





United States Department of the Interior
U.S. Geological Survey

Environmental Management Technical Center
575 Lester Avenue, Onalaska, Wisconsin 54650-8552

IN REPLY REFER TO:

September 1, 1998

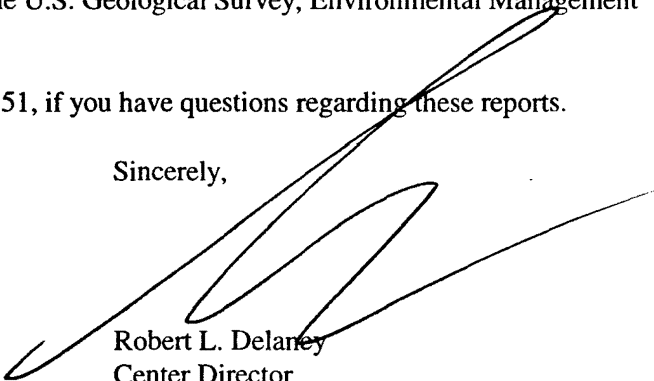
Authors
Libraries

Dear LTRMP Participant:

I am enclosing "Physical changes associated with navigation traffic on the Illinois and Upper Mississippi Rivers" and "Physical changes associated with navigation traffic on the Illinois and Upper Mississippi Rivers (Appendices)" by Nani G. Bhowmik, David Soong, J. Rodger Adams, Renjie Xia, and Bijoy S. Mazumder of Illinois State Water Survey. These reports were produced with partial funding provided by the Long Term Resource Monitoring Program. The opinions and conclusions in the reports are those of the authors and do not necessarily reflect those of the U.S. Geological Survey, Environmental Management Technical Center.

Please contact me at (608) 783-7550, extension 51, if you have questions regarding these reports.

Sincerely,



Robert L. Delaney
Center Director

Enclosure:

LTRMP Special Report 98-S001
LTRMP Special Report 98-S001A

**PHYSICAL CHANGES ASSOCIATED
WITH NAVIGATION TRAFFIC ON THE
ILLINOIS AND UPPER MISSISSIPPI RIVERS**

Project Director

Nani G. Bhowmik

Principal Investigators

Nani G. Bhowmik

David Soong

J. Rodger Adams

Contributors

Renjie Xia

Bijoy S. Mazumder

Illinois State Water Survey

Hydrology Division

2204 Griffith Drive

Champaign, Illinois 61820

Prepared for

U.S. Geological Survey

Environmental Management Technical Center

575 Lester Avenue

Onalaska, Wisconsin 54650

July 1998

River; Apple River Island (RM 546.4, 1 trip), Goose Island (RM 319.3, 2 trips), and Clarks Ferry (RM 468.2, 2 trips) on the Upper Mississippi River.

Analyses of the Data and Results

Each field trip collected data for the ambient and event conditions. These data were analyzed for various parameter determinations. A summary of the results follows.

Site and Ambient Characteristics

The cross-sectional areas of the sites varied from 775 to 2,864 square meters (m²). The average ambient velocity varied from 0.27 to 1.13 meters per second (m/s), and discharge varied from 212 to 2,856 cubic meters per second (cms). The ambient suspended sediment load varied from 917 to 21,169 metric tons per day (mt/d) on the Illinois River and from 10,636 to 37,057 mt/d on the Upper Mississippi River. The highest turbidity measured was 440 nephelometric turbidity units (NTU) on the Illinois River and 585 NTU on the Upper Mississippi River. Ambient suspended sediment concentrations varied from 78 to 934 milligrams per liter (mg/L) on the Illinois River and from 40 to 463 mg/L on the Upper Mississippi River.

The median diameter of bed material within the navigation channel on the Illinois river varied from 0.26 to 0.56 millimeters (mm), whereas within the channel border areas, these values were in the range of 0.25 to 0.74 mm. On the Upper Mississippi River, the median diameter of bed materials within the navigation channel varied from 0.25 to 0.59 mm.

Traffic Characteristics

Most of the events consisted a single tow passage, but the survey also noted two to as many as three tows passing the site in one event. Normally the maximum configuration of a convoy was a planform three barges wide and five barges long pushed by a tow boat in the back. The surveyed results indicated that the average configuration comprised 10 barges on the Illinois and 11 on the Mississippi. The draft varied from 0.61 m (empty barges) to 2.74 m (fully loaded) with an average of 2.2 m on the Illinois and 2.0 m on the Upper Mississippi River. The Illinois River is narrower and shallower and has higher blocking and draft-depth ratios than the deeper and wider Upper Mississippi River. Barge traveling speed, on the other hand, did not differ significantly between the two rivers.

Other Characteristics

Although turbidity and suspended sediment samples were collected at various sites, no system-wide correlation between suspended sediment concentrations and turbidity could be developed.

Data were collected at various sites to compile information on the relative magnitudes of wind-generated waves. During the data collection period, however, prolonged and sustained wind was not present. The maximum wind velocity measured was about 5 miles per hour (mph) and the maximum height of wind-generated waves was 0.11 m.

All event characteristics are summarized in the appendices. Digital data have been organized in ASCII format with a directory for each trip, and these are available from the Environmental Technical Management Center, Onalaska, Wisconsin.

Return Velocity

Some significant observations concerning return velocity follow:

- The highest return flows occurred at the McEver's Island site, which also had the largest blocking factor (0.125).
- In general, upstream-bound barges produced slightly higher return flows in zones closer to the barge and near the shore.
- Mean return flows, as calculated from measured data showed an attenuation from the barge toward shore, except at the McEver's Island site, which showed a reverse trend. Attenuation was not obvious at the Kampsville site for barges bound upstream.
- For sites that were visited twice, data showed that higher return flows were occurring only in zones closer to the barge when discharge was higher. This may be related to the higher horsepower required to push the barge convoy. The trend is most obvious in data from the Kampsville site, where the blocking ratios and draft-depth ratios were comparable between the two trips, but the river flow for Trip 1 was much higher than for Trip 2.
- The measured data showed that the maximum return velocity, $U_{r(max)}$, varied greatly in each zone between the barge and the shore. Not all traffic would produce significant return flows.
- Sites on the Illinois River had higher $U_{r(max)}$ values than those on the Upper Mississippi River. The highest measured $U_{r(max)}$ on the Illinois River was 0.69 m/s, while on the Upper Mississippi River it was 0.32 m/s.
- The impact of navigation traffic on return velocity was greater in the shallower and narrower Illinois River than it was in the deeper and wider Upper Mississippi River.

Maximum Wave Height

The arithmetic means of maximum wave height, $H_{w(max)}$, for upstream-bound and downstream-bound barges were not significantly different. The range of $H_{w(max)}$ varied between 0.01 and 0.30 m. One large wave, 0.66 m high, was produced at Goose Island during Trip 1 by a work barge (a buoy tender). Configurations such as single tows or one barge pushed by a tow produced relatively large waves. In general, higher wave heights were found to be associated with higher discharges.

Maximum Drawdown

The maximum measured drawdown, $H_{d(max)}$, 0.24 m, occurred at McEver's Island, which among all the sites had the narrowest channel width, the shallowest depth, and the highest $U_{r(max)}$ near the shore. This site also had the highest mean and median of $H_{d(max)}$. At the Kampsville site on the Illinois River, slightly higher $H_{d(max)}$ was measured for barges traveling in both directions. Values of $H_{d(max)}$ on the Illinois River were as much as twice those on the Upper Mississippi River.

Velocity Structure

Return flow is conventionally examined only in the longitudinal direction (the flow direction). Field data indicated that upstream-bound barges increased the longitudinal velocity and that downstream-bound barges decreased such velocity in the channel border area. The ratio of increased/decreased velocity to the ambient velocity could reach as high as 300 percent, and larger increases or decreases in net velocity were associated with fully loaded barge convoys. Velocity increased or decreased fairly uniformly in the vertical direction, depending upon the direction of the barge-tows.

Return velocity can also change in the lateral direction. Analysis of velocity vectors indicated that they could rotate by as much as 360 degrees. In some cases, the entire water body was disturbed and the alteration within channel border areas was very small. The altered velocity regime lasted from 2 to 4 minutes.

Suspended Sediment

Suspended sediment samples were collected at multiple stations, similar to the velocity, but emphases were given at channel border areas. The mean increase in suspended sediment was generally higher near the shore and toward the bed than those away from the shore and away from the bed. On the Illinois River, the increase in suspended sediment concentration in channel border areas varied from no change to 426 mg/L. On the Upper Mississippi River, the increase varied from no change to 248 mg/L in channel border areas. In a few sediment samples taken from bottom stations close to the barge traffic (Goose Island, Trip 2), the increase in suspended sediment concentration was fairly small. In general, downstream-bound barges produced a higher (in terms of mean values) and wider range of suspended sediment concentrations than upstream-bound barges. The largest increase in suspended sediment concentrations for the McEver's Island site occurred in a group when the barge-tows were at the farthest distance from shore (more than of 75 percent of the width of the river from the shoreline).

Comparison of Existing Methods and Predictive Relationships

Next an evaluation and comparison were made of the existing methods for computing return velocity, maximum wave height, maximum drawdown, and increased suspended sediment concentrations. The analysis is summarized as follows.

Return Velocity

Ten existing methods were used to compute return velocity for comparison with measured return velocities. Several of the methods performed well depending upon the river and traffic characteristics, and some methods predicted return velocity well on the Illinois River, but overestimated it on the Upper Mississippi River.

Based on dimensional analyses, two regression-type equations were developed for estimating return velocities in the Illinois and Upper Mississippi Rivers, respectively. These equations could be used for the Upper Mississippi River System, particularly at sites that have characteristics similar to those where field data were collected.

Maximum Wave Height

Existing methods were used to compute maximum wave heights for comparison with measured values. These analyses indicated that while some methods could be used to estimate maximum wave heights, none were found to be very good. A regression method has been developed to compute maximum wave height based on several measured parameters.

Maximum Drawdown

Existing methods were also used to compute maximum drawdown for comparison with measured values. In general, most methods performed well for the Illinois River, but did not perform well for the Upper Mississippi River. Consequently, a regression-type equation was developed to estimate maximum drawdown on the UMRS.

Suspended Sediment

The Akers-White, Colby, and Toffaleti methods were used to calculate the ambient suspended sediment load of bed material at each site, and results were compared with the measured suspended sediment loads. The calculated loads included only bed material, while measured loads included bed material and suspended load, and excluded the unmeasured layer immediately above the river bottom. In the deeper parts of several Upper Mississippi River sites, the unsampled zone was much larger because of the maximum depth limit of approximately 18 feet (5.5 m) for the DH-59 sampler.

The Akers-White method gave generally good results for the Upper Mississippi River, while the Colby and Toffaleti methods seriously underestimated ambient suspended sediment loads in both rivers. None of the methods gave accurate results for the Illinois River, probably due to: 1) large wash loads and 2) resuspension and lateral displacement of fines by tow passage. Wash load cannot be computed by bed material sediment formulas. Resuspension and lateral movement coarsen the bed material over the width of the navigation channel and thus reduce the bed material load carried. On the Illinois River, the navigation channel is wider than the channel border area.

The Colby method relies on interpolation between curves for two depths and could not be used reliably to estimate event velocity suspension. The Akers-White method is not designed to estimate event concentrations, but was adaptable. Estimates by the Akers-White method were almost all significantly lower than the measured concentrations. Event concentration estimates were also made with the Toffaleti method. Although the form of the equation and the use of bed material size fractions suggested that the Toffaleti method would be the best method for event calculations, it actually gave low estimates, similar to its underestimation of ambient concentrations and loads.

Remarks

This report presented an extensive set of data that was collected to determine the physical changes within the Upper Mississippi and Illinois Rivers that take place due to the movement of commercial river traffic. Results from the sites where data were collected showed that some of these physical changes could be significant based on the river geometry, ambient conditions, and traffic characteristics. A thorough understanding, evaluation, and prediction of the physical changes associated with navigation traffic is essential for developing comprehensive management alternatives for these large rivers

which are extremely important for commerce and the maintenance of a viable river/aquatic environment.

Table of Contents

	Page
INTRODUCTION.....	1
Project Background.....	1
Scope of Work.....	2
Relationship with the POS.....	3
Original Project Objectives.....	3
Present Project Objectives.....	4
BACKGROUND.....	5
Traffic Characteristics.....	5
Target Physical variables and Biological Effects.....	6
Environmental Variables.....	7
Conceptual Models and Quantitative Relationships.....	7
Typical Values of Selected Dimensionless Parameters on the UMRS.....	8
Barges on the UMRS.....	9
EXISTING METHODS.....	12
Return Velocity.....	12
Drawdown.....	15
Wave Height.....	17
Sediment Resuspension.....	20
Colby Method.....	20
Akers-White Method.....	20
Toffaletti Method.....	21
Dimensional Analysis.....	21
METHOD AND EQUIPMENT DESIGN.....	23
Pilot Data Collection and Instrumentation Setup.....	23
Velocity.....	23
Waves and Drawdown.....	24
Suspended Sediment.....	24
Turbidity.....	25
Site Selection.....	25
DATA COLLECTION.....	26
Reconnaissance Trip.....	26
Site Characterization.....	26
Bathymetry.....	26
Depth, Velocity, and Suspended Sediment.....	27
Instrumentation.....	28
Velocity.....	28
Waves and Drawdown.....	29

	Page
Suspended Sediment and Turbidity	30
Wind Speed and Direction	31
River Stage.....	31
Air and Water Temperature	31
Bed Materials.....	31
Traffic Characteristics.....	31
Coding System.....	32
Event Data Collection Procedure	32
Sampling Frequency	33
Data Reduction	34
Return Velocity.....	34
Maximum Drawdown and Wave Height.....	35
Suspended Sediment Concentration	35
 DATA PRESENTATION	 37
Site Descriptions and Ambient Conditions	38
Date, Time, and Geographic Location.....	38
Cross-Sectional Configuration.....	38
Location and Total Number of Sensors	38
Bed Material Composition in Channel and Channel Border Areas.....	39
Water Level, Velocity, and Temperature.....	39
Suspended Sediment Concentration	39
Traffic Characteristics	39
Wind-Wave Data	40
Event Characteristics.....	40
Database Organization	41
 GENERAL ANALYSES	 42
Traffic Characteristics	42
Maximum Return Velocity.....	43
Maximum Wave Height.....	45
Maximum Drawdown	46
Velocity Structure.....	46
Additional Findings	49
Suspended Sediment Concentrations	49
Goose Island	51
Kampsville.....	52
All Sites	52
Turbidity.....	53
Comparison with Suspended Sediment Concentrations	53

	Page
Particle Size Distribution	55
Kampsville, Trip 1	55
Goose Island, Trip 1.....	55
Goose Island, Trip 2.....	56
Clarks Ferry, Trip 1.....	56
COMPARISON OF EXISTING METHODS AND PREDICTIVE RELATIONSHIPS	57
Return Velocity	57
Regression Equations for Predicting Return Velocity	58
Maximum Wave Height	59
Proposed Regression Method for Estimating Maximum Wave Height ...	60
Maximum Drawdown	60
Proposed Regression Relationship for Maximum Drawdown	61
Suspended Sediment	61
Transport Equations	61
Ambient Sediment Loads.....	62
Event Sediment Loads	64
Comparison of Computed and Measured Concentrations	66
SUMMARY	67
Background	67
Existing Methods	67
Method and Equipment Design.....	67
Data Collection.....	68
Data Presentation.....	68
General Analyses.....	69
Return Velocity	69
Maximum Wave Height	69
Maximum Drawdown.....	70
Velocity Structure	70
Suspended Sediment.....	70
Comparison of Existing Methods and Predictive Relationships.....	70
Return Velocity.....	70
Maximum Wave Height	71
Maximum Drawdown.....	71
Suspended Sediment.....	71
Acknowledgments	72
FIGURES	73

	Page
TABLES.....	147
REFERENCES.....	199
APPENDICES (these are listed in a separate volume)	

FIGURES

	Page
Figure 1. Position of inland waterways and navigation locks and dams on the UMRS	75
Figure 2. General sketch of barge-tow effects	76
Figure 3. Definition sketch for vessel and environmental variables	77
Figure 4. Wave patterns generated by a vessel.....	78
Figure 5. Longitudinal wave profile and wave variables	78
Figure 6. Draft/depth ratios for barge tows on the Upper Mississippi River System, after Adams (1991)	79
Figure 7. Blocking factors for tows one to three barges wide on the Upper Mississippi River System, after Adams (1992)	79
Figure 8. Length Froude Numbers, $F_1 = V_b/(gl)^{0.5}$, for a) barge-tows and b) recreational boats and towboats, after Adams (1992).....	80
Figure 9. Typical Barges on the Upper Mississippi River System.....	81
Figure 10. Schematic diagram showing water motion generated by a moving ship, after Blaauw et al. (1994).....	83
Figure 11. Wave patterns created by a point disturbance for (a) still water, $V = 0$; (b) subcritical flow, $V < c$; (c) critical flow, $V = c$; and (d) supercritical flow, $V > c$, after Henderson (1966).....	84
Figure 12. Schematic diagram of changes in water levels within a navigation channel due to vessel movement, after Blaauw and van der Knapp (1983).....	84
Figure 13. Variation of constraint factor, K , as function of blocking ratio, N , and vessel aspect ration, L/b , after Hochstein and Adams (1989)	85
Figure 14. Graph for determining values of K_w , after Gates and Herbich (1977)	85
Figure 15. McEver's Island Site on the Illinois River, RM 50.1	86

	Page
Figure 16. Post system for velocity data collection.....	87
Figure 17. Vertical array for velocity data collection.....	88
Figure 18. Base-mounted current meters S4 and MMB527.....	89
Figure 19. Wave gage installation.....	90
Figure 20. Sediment towers.....	91
Figure 21. Typical setup for background data collection at McEver’s Island on the Illinois River, RM 50.1.....	92
Figure 22. McEver’s Island data collection setup, Illinois River, RM 50.1	93
Figure 23. Typical instrumentation setup on the Illinois River near Kampsville, RM 35.2.....	95
Figure 24. Wave and drawdown measuring gage	96
Figure 25. Field setup for suspended sediment sampling	97
Figure 26. Recording wind set	99
Figure 27. Staff gage	99
Figure 28. MicroFix system and tow tracking	100
Figure 29. Time series of the x-component of velocity during a barge passage (11-point moving average).....	101
Figure 30. Typical drawdown and wave characteristics due to a barge-tow movement	102
Figure 31. Suspended sediment concentration.....	103
Figure 32. Number of barge-tow events observed per day at each site during the survey.....	104
Figure 33. Number of barges per convoy at each site during the survey	105
Figure 34. Width of barge convoys at each site during the survey	106

	Page
Figure 35. Length of barge convoys at each site during the survey	107
Figure 36. Draft of barge convoys at each site during the survey	108
Figure 37. Distance of barge convoys at each site during the survey.....	109
Figure 38. Speed of barge convoys at each site during the survey.....	110
Figure 39. Horsepower of barge convoys at each site during the survey.....	111
Figure 40. Draft to depth ratio for barge-tow events at each site during the survey.....	112
Figure 41. Blocking factor for barge-tow events at each site during the survey.....	113
Figure 42. Towboat horsepower for barge convoys at each site during the survey.....	114
Figure 43. Comparison of the Illinois State Water Survey and U.S. Army Corps of Engineers (1978) traffic datasets	115
Figure 44. Coordinate system for comparing return velocity.....	116
Figure 45. Typical changes in the longitudinal velocity components at three elevations	117
Figure 46. Distribution of net velocity changes in the lateral direction, Kampsville, Illinois River, RM 35.2	118
Figure 47. Distribution of net velocity changes in the lateral direction, Apple River Island, Mississippi River, RM 546.5.....	119
Figure 48. Distribution of net velocity changes in the vertical direction, Kampsville, Illinois River, RM 35.2	120
Figure 49. Resultant velocity vectors for an upstream-bound barge, McEver's Island.....	121
Figure 50. Resultant velocity vectors for a downstream-bound barge, McEver's Island.....	122

	Page
Figure 51. Velocity vectors of U_r for an upstream-bound barge, Clarks Ferry, trip 2.....	123
Figure 52. Velocity vectors of U_r for a downstream-bound barge, Clarks Ferry, trip 2.....	124
Figure 53. Velocity vectors of U_r for a downstream-bound barge, <i>Mr. Aldo</i> , at Kampsville, trip 1	125
Figure 54. Velocity vectors of U_r for an upstream-bound barge, <i>Floyd H. Blaske</i> , at Kampsville, trip 1.....	126
Figure 55. Changes in the longitudinal component of the velocity at various metering locations due to the movement of an upstream-bound barge convoy.....	127
Figure 56. Changes in the longitudinal velocity component at various metering locations due to the movement of a downstream-bound barge convoy.....	128
Figure 57. Changes in the lateral velocity component at a single meter due to barge-tow movement	129
Figure 58. Variability in suspended sediment concentration due to barge-tow movement	130
Figure 59. Peak and average increase in suspended sediment concentration, (mg/L), Goose Island, RM 319.3, Mississippi River, August 1990.....	131
Figure 60. Sediment concentration variations for a typical day, Goose Island, RM 319.3, Mississippi River.....	132
Figure 61. Sediment concentration variations for a typical day, Kampsville, RM 35.3, Illinois River	133
Figure 62. Suspended sediment concentrations and turbidity values versus time, McEver's Island, RM 50.1, Illinois River	134
Figure 63. Scatter plot of suspended sediment concentration versus turbidity values, McEver's Island, RM 50.1, Illinois River.....	134

	Page
Figure 64. Measured turbidity values and computed suspended sediment concentrations versus time, McEver's Island, RM 50.1, Illinois River.....	135
Figure 65. Comparison of computed and measured $U_{r(max)}$ using the method by Hochstein and Adams (1989).....	136
Figure 66. Comparison of computed and measured $U_{r(max)}$ using the method by Maynard and Siemsen (1991).....	137
Figure 67. Comparison of computed and measured $U_{r(max)}/V_a$, Illinois River.....	138
Figure 68. Comparison of computed and measured $U_{r(max)}/V_a$, Mississippi River.....	139
Figure 69. Comparison of computed and measured $H_{w(max)}$ using the method by USACOE (1980).....	140
Figure 70. Comparison of computed and measured $H_{w(max)}$, using the method by Blaauw et al. (1984).....	141
Figure 71. Comparison of (a) computed and measured $H_{w(max)}/d_f$, and (b) computed and measured $H_{w(max)}$, for the Upper Mississippi River System.....	142
Figure 72. Comparison of computed and measured $H_{d(max)}$ using the method by Hochstein (1967).....	143
Figure 73. Comparison of computed and measured $H_{d(max)}$ using the method by Dand and White (1978).....	144
Figure 74. Comparison of (a) computed and measured $H_{d(max)}/(h-d_f)$, and (b) computed and measured $H_{d(max)}$, for the Upper Mississippi River System.....	145

TABLES

	Page
Table 1. Barge-Tow Variables and Ranges, after Adams (1991).....	149
Table 2. Target Physical Variables, after Adams (1991).....	150
Table 3. Environmental Variables Related to Physical Effects of Commercial Navigation, after Adams (1991).....	150
Table 4. Basic Variables and Dimensions, after Adams (1991).....	151
Table 5. Vessel Passage Parameters, after Adams (1991).....	152
Table 6. River Conditions Used To Generate Power Ratios, after Adams (1991).....	153
Table 7. Unit Towboat Power, after Adams (1991)	153
Table 8. Barge Characteristics (USACOE, 1989).....	154
Table 9. Number of Sites Necessary To Depict Physical Impacts of Navigation on the Upper Mississippi River System	154
Table 10. Number of Trips Necessary To Depict Physical Impacts of Navigation on the Upper Mississippi River System	154
Table 11. Specifications of Instruments Used in the Field.....	155
Table 12. Sampling Rates Used in the Field	156
Table 13. Data Collection Dates and Locations	156
Table 14. Geomorphologic Characteristics of Data Collection Sites.....	156
Table 15. Configuration of River Cross Section, Discharge, and Slope at Data Collection Sites	157
Table 16. Number of Current Meters, Suspended Sediment Sampling Intake Stations, and Wave Gages Used during Field Trips.....	157
Table 17. Lateral Location of Velocity Meters at Field Sites.....	158
Table 18. Vertical Location of Velocity Meters at Field Sites.....	159

	Page
Table 19. Lateral Location of Suspended Sediment sampling Intake Nozzles at Field Sites	159
Table 20. Vertical Location of Suspended Sediment Sampling Intake Nozzles at Field Sites	160
Table 21. Bed Material Size (d_{50}) at Field Sites	161
Table 22. Blocking Factors at Field Sites.....	161
Table 23. Draft to Depth Ratios at Field Sites	162
Table 24. Mean Values of River and Traffic Characteristics at Field Sites	162
Table 25. Mean Maximum Return Velocity within Different Zones from Barge at Field Sites.....	163
Table 26. Minimum and Maximum Return Velocity within Different Zones from Barge at Field Sites.....	164
Table 27. Most Frequently Occurring Intervals of Maximum Return Velocity within Different Zones from Barge at Field Sites.....	165
Table 28. Mean Values of Maximum Return Velocity within Different Zones from Barge, Each River, All Trips.....	166
Table 29. Most Frequently Occurring Intervals of Maximum Return Velocity within Different Zones from Barge, Each River, All Trips.....	166
Table 30. Statistical Properties of Maximum Return Velocity at Field Sites and on Each River	167
Table 31. Range and Mean of Maximum Wave Height at Field Sites.....	167
Table 32. Range and Mean of Maximum Wave Height for the Illinois and Mississippi Rivers.....	167
Table 33. Range and Mean of Maximum Drawdown at Field Sites	168
Table 34. Range and Mean of Maximum Drawdown for the Illinois and Mississippi Rivers.....	168

	Page
Table 35. Mean Increased Suspended Sediment Concentration within Different Zones from Barge at Field Sites	169
Table 36. Range of Increased Suspended Sediment Concentration within Different Zones from Barge at Field Sites	170
Table 37. Mean Increased Suspended Sediment Concentration within Different Zones from Barge for the Illinois and Mississippi Rivers.....	171
Table 38. Range of Increased suspended Sediment Concentration within Different Zones from Barge, for the Illinois and Mississippi Rivers	171
Table 39. Statistical Properties of Increased Suspended Concentration at Field Sites and on Each River	171
Table 40. Suspended Sediment Concentration (mg/L) at Goose Island, RM 319.3, Mississippi River, August 1990.....	172
Table 41. Suspended Sediment Concentration (mg/L) at Kampsville, RM 35.2, Illinois River, October 1990	172
Table 42. Average, Maximum, and Minimum Suspended Sediment Concentration (SSC) at Field Sites.....	173
Table 43. Ratio of Event-Based Suspended Sediment Concentrations to Ambient Suspended Sediment Concentrations (SSC) at Field Sites	175
Table 44. Distribution of Suspended Sediment Particles, Kampsville, Trip 1.....	177
Table 45. Distribution of Suspended Sediment Particles for Specific Events, Kampsville, Trip 1.....	177
Table 46. Distribution of Suspended Sediment Particles, Goose Island, Trip 1	178
Table 47. Distribution of Suspended Sediment Particles for Specific Events, Goose Island, Trip 1	178

	Page
Table 48. Distribution of Suspended Sediment Particles, Goose Island, Trip 2	179
Table 49. Distribution of Suspended Sediment Particles for Specific Events, Goose Island, Trip 2	179
Table 50. Distribution of Suspended Sediment Particles, Clarks Ferry, Trip 1	180
Table 51. Existing Methods for Computing Return Velocity	180
Table 52. Correlation Coefficient and Standard Error of Estimate for Methods of Computing Return Velocity	181
Table 53. Correlation and Standard Error of Estimate for Computed and Measured Return Velocity for Both Rivers and for Directional Movement of the Barges	182
Table 54. Correlation Coefficient and Standard Error of Estimate for Both Rivers for Computed Return Velocity by Two Method on Both Rivers	183
Table 55. Existing Methods for Estimating Maximum Wave Height.....	183
Table 56. Correlation Coefficient and Standard Error of Estimate for Computed and Measured Maximum Wave Height, Illinois and Mississippi Rivers	183
Table 57. Existing Methods for Computing Maximum Drawdown	184
Table 58. Correlation Coefficient and Standard Error of Estimate for Computed and Measured Maximum Drawdown, Illinois and Mississippi Rivers	184
Table 59. Ambient Sediment Load Computations	185
Table 60. Event Peak Suspended Sediment Concentration at Apple River Island, Measured and Computed (Akers-White Method).....	186
Table 61. Event Peak Suspended Sediment Concentration at Clarks Ferry (Trip 1), Measured and Computed (Akers-White Method) Goose Island (Trip 1), Measured and Computed (Toffaleti Method).....	187

	Page
Appendix XVI.	Suspended Sediment Concentrations Data for Kampsville Site, Trip 1 XVI-1
Appendix XVII.	Suspended Sediment Concentrations Data for Clarks Ferry Site, Trip 1 XVII-1
Appendix XVIII.	Suspended Sediment Concentrations Data for Goose <u>Island</u> Site, Trip 2 XVIII-1
Appendix XIX.	Database Organization for All Study Sites XIX-1
Appendix XX.	Sample Plots of Altered Velocity Regimes Due to Movement of Navigation Traffic XX-1
Appendix XXI.	Histograms of Maximum Return Velocities within Various Zones for All Study Sites XXI-1
Appendix XXII.	Sample Plots of Waves and Drawdowns Generated by the Navigation Traffic XXII-1
Appendix XXIII.	Histograms of Maximum Wave Heights XXIII-1
Appendix XXIV.	Histograms of Maximum Drawdown XXIV-1
Appendix XXV.	Typical Plots of Suspended Sediment Concentrations versus Time XXV-1
Appendix XXVI.	Histograms of Suspended Sediment Concentration XXVI-1
Appendix XXVII.	Ratio of Peak to Average Suspended Sediment Concentration Due to Movement of Navigation Traffic ... XXVII-1
Appendix XXVIII.	Comparison of Turbidity and Suspended Sediment Concentration at McEver's Island XXVIII-1
Appendix XXIX.	Suspended Sediment Particle Size Distribution XXIX-1
Appendix XXX.	A Predictive Method for Maximum Return Velocity XXX-1
Appendix XXXI.	Technical Papers Published by Water Survey Researchers in Refereed Journals XXXI-1
Appendix XXXII.	List of Relevant Technical Reports and Presentations Prepared by Water Survey Researchers XXXII-1

INTRODUCTION

Physical changes associated with navigation traffic in a large river environment such as the Illinois or Mississippi River are many and varied. Some of these changes are related to basic hydraulic and physical factors, and can be measured using available instrumentation. Other changes are not quantifiable by direct measurement in the field, and their effects can only be observed over a long period of time.

Relationships between barge-tow movements and the hydraulic and physical characteristics of specified reaches of a river are not fully understood at the present time. This scientific area of large river fluvial hydrodynamics has not been addressed fully with a detailed and comprehensive plan of action. Moreover, because changes in the hydraulic parameters of a river are normally associated with changes in the river's biological activities and/or habitats, a clear understanding of the ambient or original hydraulic characteristics of the river is needed before management decisions can be made.

The present investigation is one of the first attempts to quantify the hydraulic changes associated with the movement of navigation traffic within the Upper Mississippi River System (UMRS). Work is also being done by researchers from the Waterways Experiment Station (U.S. Army Corps of Engineers) on laboratory simulation of flows in the near field of a barge-tow.

This report outlines the research that has been completed by engineers and scientists from the Illinois State Water Survey (ISWS) on physical changes associated with navigation traffic. In addition to research results, materials showing the basic hydraulic structure of large river systems such as the UMRS are included in the appendices.

Project Background

One of the recommendations of the Master Plan (Upper Mississippi River Basin Commission or UMRBC, 1982) for the UMRS was that an Environmental Management Plan (EMP) be initiated in conjunction with the construction of a second (auxiliary) lock at Lock and Dam 26 Replacement near Alton, Illinois. An EMP initiated in 1986 gave the U.S. Army Corps of Engineers (USACOE) responsibility for Habitat Rehabilitation and Enhancement Projects (HREP), and the U.S. Fish and Wildlife Service (USFWS) responsibility for 1) long-term environmental trend assessments (Resources Trend Analysis or RTA), 2) resource problem identification and analysis (PIA), and 3) establishment of an integrated database management system (IDMS) using a geographic information system (GIS). These four components form the complete Long-Term Resource Monitoring Program (LTRMP).

By early 1988, USFWS had established an Environmental Management Technical Center (EMTC) in La Crosse, Wisconsin, and had formulated an operating plan for the LTRMP (Rasmussen and Wlosinski, 1988; USFWS, 1992). The operating plan identified various tasks to be done within each component and established tentative schedules for conducting each task. Within the PIA component, work tasks were assigned under five broad topics:

- Sedimentation - 19 tasks
- Navigation effects - 15 tasks
- Water-level fluctuation - 6 tasks
- Lack of aquatic vegetation - 9 tasks
- Reduced fisheries populations - 8 tasks

Field stations and trend assessment pools or reaches were also identified, and a cooperative agreement was executed between the USFWS (these responsibilities have since been transferred to the National Biological Service, NBS, now part of the U.S. Geological Survey and the Illinois Department of Conservation, IDOC, now the Illinois Department of Natural Resources, IDNR), to provide funding for RTA and PIA projects conducted by Illinois agencies. In 1988, ISWS staff and EMTC staff negotiated a contract to conduct research on two of the PIA tasks: PA(NE)1 - Determine turbulence and shear patterns in the main channel and turbulence in the main channel border associated with commercial vessel passage using vessel speed, size, direction, and river flow and channel characteristics; and PA(NE)4 - Measure the spatial and temporal distribution of changed velocity and suspended sediment conditions in different channel border habitats in relation to passage of commercial vessels.

Scope of Work

The original scope agreed to by both agencies was to acquire an adequate number of two-component electromagnetic current meters, develop and assemble equipment for a new method of suspended sediment sampling, develop and refine field installation of the various equipment, and experiment with data recording frequencies and electronic data recording systems. These tasks were accomplished in four field data collection trips in the fall of 1988 and the spring of 1989.

The first addition to the scope of work was a study of recreational boat waves. This was agreed upon, and the cooperative agreement was extended to March 31, 1990. Additional tasks included: 1) conducting two sets of controlled experiments with a variety of boats, 2) measurement of random boat waves generated by holiday weekend traffic, 3) analysis of the wave data from both controlled and random data sets, and 4) preparation of a report. Bhowmik et al. (1991) is a published report based on this work.

A review of the literature and a need to develop a rationale for the LTRMP problem analysis component resulted in a mutual decision to produce a report on identification of the proper study approach for determining the physical effects of commercial navigation on the UMRS. A report has been prepared and published by EMTC on this topic (Adams, 1991).

Upon review of the pilot-study field trips in 1988 and the prototype trip in May 1989, the project was further extended to allow additional field data collection trips.

After several meetings between the project sponsors and the ISWS, it became clear that characterization of the UMRS reaches needed to be undertaken. Based on this, planform classification of three trend analysis pools was completed and a report

submitted to EMTC for review. After extensive review, comments were forwarded to ISWS, and the final report is expected to be printed by EMTC very soon.

Relationship with the Plan of Study

The investigation being conducted by the ISWS for the EMTC/NBS has some similarity with work outlined under the Plan of Study (POS) for the second lock at Lock and Dam 26 near Alton, Illinois, on the Mississippi River. This plan has been prepared by an interagency team of engineers, scientists, and managers from five UMRS states and three federal agencies with leadership and guidance provided by the USACOE-St. Louis District (USACOE, 1991). The director of the present project and another ISWS investigator represented the State of Illinois on the POS team and were instrumental in the preparation of work units 1, 2, and 5 (descriptions follow).

Even though the Master Plan had not required an Environmental Impact Statement (EIS) for the 600-foot-by-110-foot second (auxiliary) lock at Lock and Dam 26 Replacement, the USACOE-St. Louis District decided that it would be valuable to prepare one. Once the final EIS (USACOE, 1988) had been completed, the need to answer questions about the impacts of navigation on the UMRS ecosystem was clearly understood and acknowledged in the Record of Decision. An Interagency Study Team was convened in 1987 to develop a POS to address the lack of information on the impacts of navigation on the riverine ecosystem. The Study Team agreed upon this statement of its objective:

"The Plan of Study will develop studies which identify and quantify impacts to significant resources within the UMRS resulting from the increased traffic generated by the second lock. Where feasible with the constraints of time and money, studies will attempt to quantify secondary impacts in addition to primary impacts and will examine the effects of recreation craft in addition to those of commercial tows."

The POS (USACOE, 1991) proposed 16 work units, including many biological studies that depended on the results of physical forces and sedimentation studies. Work unit 1 on basic physical forces in main channel and main channel border habitats is similar to the portion of this study based on PA(NE)1. Work unit 2 on sedimentation effects in side channels and backwaters and work unit 5 on physical and biological effects in representative backwaters are similar to other PIA tasks.

The top priorities for both the EMP and the POS are to cooperate and combine efforts to expedite data collection and analysis, to provide good science for decision-making concerning multiple uses of the UMRS, and to do all this at the least possible cost to the people of the United States.

Original Project Objectives

The objectives of the original project were essentially based on PA(NE)1 and PA(NE)4 (Rasmussen and Wlosinski, 1988):

- Collect data on turbulent velocity fluctuations in selected main channel border areas of the UMRS.
- Collect data on the spatial and temporal variations of mean velocity in selected main channel border areas resulting from barge-tow passage.
- Collect data on the spatial and temporal changes in suspended sediment concentrations resulting from barge-tows.
- Collect data on waves and drawdown due to the movement of commercial traffic.
- Collect data on all of the above components in relation to recreational traffic moving at the data collection site during field work.

Present Project Objectives

Based on the above objectives and the funding received from EMTC/NBS through IDNR, field data were collected in 1989, 1990, and 1991 from two sites on the Illinois River and three sites on the Upper Mississippi River (UMR). However, before initiation of the actual analyses, funding for the project was essentially reduced to almost negligible levels, halting data preparation and some data analyses. Then in 1994, the ISWS received additional funding from the USACOE to conduct preliminary analyses of the data collected by ISWS and submit those data in a predetermined form to the EMTC/NBS and USACOE. Following are the objectives of this portion of the project, which is the main focus of this report:

- Provide data collected on the physical changes associated with navigation traffic on the UMR in a computer-useable form to EMTC/NBS and USACOE.
- Provide a description and preliminary analyses of the data.

BACKGROUND

The UMRS consists of about 868 miles of navigable stream of the Mississippi River above the mouth of the Ohio River and approximately 330 miles of the Illinois River. This river system is one of the most important inland transportation arteries in the United States with tremendous economic benefits. The river is also a very important environmental repository for the country, and its wise management and use is essential in order to maintain the river for future generations.

The UMRS (figure 1) is maintained for commercial navigation purposes by 26 locks and dams on the main stem of the Upper Mississippi River and eight locks and dams on the Illinois River. All the locks and dams on the UMR are located above St. Louis, while the river below St. Louis is operated as an open river system.

Physically the Illinois River is narrower and shallower than the Mississippi River. In order to facilitate the movement of barge traffic, the navigation channel is maintained by the USACOE at a minimum width of 91.5 meters (m), or 300 feet (ft), and a minimum depth of at least 2.74 m (9 ft) so that a barge convoy with a maximum draft of 2.74 m can move easily on this system. The minimum depth of water is essentially a little bit greater than 2.74 m.

Traffic Characteristics

Traffic moving on the UMR can vary in size from a single barge pushed by a towboat to a fleet of 15 barges (three wide by five long). In cases of multiple tows, the maximum configuration on the UMR above Lock and Dam (L & D) 27 near St. Louis is three wide and five long. This configuration can occupy a planform area of 32 m (105 ft) by 297 m (975 ft) with a draft of 0.61 m (2 ft) for empty barges and a maximum draft of 2.74 m (9 ft).

Figures 2 and 3 show various parameters that describe the characteristics of typical barge-tow convoys on the UMR. All the major physical variables are shown schematically in these two figures.

Some generalized analyses of the physical variables that govern the movement of the barge-tows on the UMR have already been completed by Adams (1991). The following information is largely from that report.

Table 1 provides the major variables that describe barge-tows on the UMR along with typical values for each. A single barge is defined by its length, width, draft, and bow shape. The draft is directly related to the load and load distribution in the barge. Empty jumbo barges have a draft of about 0.61 m (2 ft), which corresponds to a tare weight of about 425 short tons (1 short ton is equal to 2,000 pounds or 909 kilograms) or 386 metric tons. When loaded to the 2.74-m (9-ft) design draft of the waterway, a jumbo barge carries about 1,350 short tons of cargo. On the UMRS most dry bulk cargo is carried in standard jumbo barges. Petroleum and liquid or gaseous chemicals are carried in tank barges that may be as large as 16.5 m (54 ft) wide by 91.5 m (300 ft) long. Many work barges are generally smaller than cargo barges, but they make up an insignificant part of the commercial traffic on the waterway.

Towboats have different dimensions and propulsive capacities. Towboat size correlates fairly well with horsepower as shown by Latorre (1985). Another variable is the option of open or ducted (Kort nozzle) propellers. Power setting and propeller rotation speed are extremely variable and cannot be included in this general description of vessel movement through the water. However, the distance of the barge-tow from a particular point or area of interest, the angle of the tow to a channel centerline, or "sailing line," and the speed of the tow relative to the flow velocity of the river are important characteristics of barge-tow travel.

Target Physical Variables and Biological Effects

The passage of a vessel has a complex set of primary and secondary effects on the flow pattern in a waterway. Figures 2 and 3 identify many of the primary effects and table 2 lists all target physical variables. The obvious effects are the surface waves generated at the bow and stern and in the wake zone of the vessel as indicated in figures 4 and 5, and turbulent velocities in the propeller jets. Figure 4 shows the various types of waves generated by a moving vessel. Figure 5 defines the wave characteristic variables. Less obvious are the flow field developed by the boundary layer along the barge hulls and its interaction with ambient flows; the "return flow" as the water passes around the barge tow; and drawdown, a long wave effect caused by the accelerated open-channel conditions and directly related to the magnitude of the return flow.

Secondary effects result when the primary effects encounter the river bed, river banks, or a change in channel morphology. They include resuspension of bed material by the accelerated flow or propeller jets; resuspension of bed or bank material by waves; transport of suspended material by the changed velocity field, including turbulence; and changes in velocity, water depth, or flux of suspended material in side channels, tributary mouths, or backwaters.

Biological effects depend on the location, size, and mobility of the organism. Thus plankton and larval fish are essentially free-floating and will be transported with the changed flow velocity or turbulence. There is concern that larval fish in the navigation channel can be hit by the barges or subjected to contact or rapid pressure changes as they pass through a propeller. Adult fish presumably will move away from an oncoming barge-tow, but may not move far enough to be outside the zone from which flow is drawn through the propellers.

Rooted aquatic plants generally colonize shallow-water areas outside the navigation channel and may not be directly affected by barge-tows. However, return flow, drawdown, and wave action can uproot plants by scouring material from around their roots and can prevent establishment of seeds or roots. Benthic organisms such as clams and mussels or insect larvae and worms can be affected by velocity and pressure changes if they are living in the navigation channel. In most cases where such organisms inhabit channel border areas, drawdown can expose them to the atmosphere, and sediment resuspended by the propeller jets or waves can affect their feeding ability. Increased deposition of fine sediment may be beneficial or detrimental depending on a particular species' response to burial or change in substrate size distribution (ASCE, 1990). Additional effects of navigation on the biota may occur at some distance from the navigation channel in side channels, backwaters, or tributaries.

Environmental Variables

Again with reference to figures 2, 3, and 5, there are a number of variables that define the riverine environment and affect the way vessel movement modifies the ambient river conditions. Table 3 lists 12 environmental variables that may be involved in vessel/waterway interactions. The channel cross-sectional geometry is described by width, maximum depth, and horizontal alignment. Depth varies across the channel, and while the depth under the barge-tow is probably the most important variable, it is not known unless the vessel track is known. The vertical and horizontal velocity distribution, including turbulence, and the cross-sectional geometry determine the discharge or volume flow rate of the river.

In addition to the geometric variables mentioned, energy slope and bed roughness affect the velocity and turbulence of river flow, and the rate of attenuation of waves, drawdown, and return flow from barge to shore. The ambient suspended sediment concentration probably does not enter into any of the relationships, but it may contribute to sediment transport by vessel-induced motion. Temperature is a factor when ice formation is possible, and it affects hydraulic variables through the variation in water density (often negligible) and viscosity. Viscosity is a key factor in sediment transport because of its effect on the fall velocity of particles. The bed material particle size distribution and bed forms such as ripples and dunes will affect the suspension of material by the propeller jets and the flow beneath the barges. Wind and wind waves affect vessel performance and maneuvering, so they also play a part in the effects of vessel movement.

Conceptual Models and Quantitative Relationships

The environmental variables described in the previous section produce a large and hard-to-manage set of variables. The interactions of some variables are easier to visualize than others, but to develop a complete model of the effects of vessel traffic on a river system as large and varied as the UMRS seems impossible. Dimensional analysis is one of the traditional methods used to approach complex problems in hydraulics and fluid mechanics.

In dimensional analysis, the requirement that any expression must be dimensionally homogeneous is used to form dimensionless groups and to derive a conceptual form for a particular relationship. Data from field or laboratory measurements are used to quantify the relationship. Frequently dimensional analysis will identify scaling factors that are important to the processes being described. Adams (1991) discussed related dimensionless variables for use in dimensional analyses following the procedure given by Bridgeman (1931) and Rouse (1959).

Basic variables used by Adams and the dimensionless parameters he developed are given in tables 4 and 5, respectively. A detailed description of the procedure involved in the development of dimensionless parameters is given in the original publication by Adams (1991).

Typical Values of Selected Dimensionless Parameters on the UMRS

Typical value ranges for several parameters will now be discussed for barge-tows on the UMRS. From table 5, DR, BF, F_1 , and P_r were selected. Vessel drag forces are defined in terms of Froude and Reynolds numbers and relative roughness. An estimation of boundary layer thickness was also made.

Draft/Depth Ratio. The ratio of vessel draft to the maximum channel depth (on the UMR, the depth of the vessel's track is generally close to the maximum channel depth), DR, indicates the clearance below the vessel. The larger this ratio, the larger the amount of water that must be displaced from beneath the vessel and the greater the acceleration of the water between the bottom of the vessel and the river bed. On inland waterways with a 2.74-m (9-ft) design draft, significant effects can be expected for water depth less than 5.5 m, if the critical draft/depth ratio is 0.5.

This ratio is the easiest to calculate since the range of barge drafts is from 0.61 to 2.74 m and channel depths vary from about 3.5 to 15 m. Figure 6 shows DR values for the common ranges of draft and depth. For the UMRS, operation at DR above 0.90 for fully loaded barges with a 2.74-m draft is likely only near docks or in reaches in need of dredging.

Blocking Factor. The blocking factor, BF, is the ratio of the cross-sectional area of the submerged portion of the vessel, A_b , to the cross-sectional area of the river channel, A_c . Similar to the draft-depth ratio, the blocking factor quantifies the proportion of the cross section available for river flow and the water displaced by the vessel to pass the vessel.

The effective river cross-sectional area can range from the minimum navigation channel size to much larger values. The moderate range of barge widths and drafts and convoy widths defines the range of values for A_b , from 6.5 to 88 square meters (m^2). Figure 7 shows a portion of the total range calculated, and only a small part of this has BF values over 0.1. Each line refers to a particular width of tow in terms of standard jumbo barges, which are 10.7 m (35 ft) wide and either loaded or empty.

On the Illinois River, a typical cross section has a width of 200 m and an average depth of 3 m assuming the cross section to be rectangular in shape, thus A_c is $600 m^2$. The BF values vary from less than 0.009 for a single empty barge to 0.118 for three-wide barges with a draft of 2.74 m. In many reaches of the Mississippi River, the width is about 450 m and the average depth is about 5 m. For such a cross section, the area is $2,250 m^2$, and BF values vary from 0.003 to 0.042 for the same range of barge-tows used for the Illinois River.

Because of the variability in channel width and depth, and the change in depth with discharge, it is difficult to define critical reaches without specific geometric information. Channel geometry also depends on curvature and flow bifurcation at islands. When applied to estimate drawdown and flow velocity at a point, the distance of the sailing line from the point of interest is important as are BF and DR.

Length Froude Number. The Froude number, F , is the primary parameter identifying wave conditions and flow in open channels. The movement of vessels in rivers involves both of these phenomena. The flow of rivers is generally called tranquil, i.e., subcritical, or rapid, i.e., supercritical based on the depth Froude number ($F = V_a/[g(A_c/W_T)]^{0.5}$). The change in this Froude number caused by the passage of a vessel is an

indicator of the amount of acceleration caused by the vessel and is directly related to the blocking factor.

Froude numbers can be defined in several ways. The F_1 length Froude number (see definition in table 5) is an important parameter describing vessel resistance and wave-making characteristics. For convoys of standard jumbo barges, figure 8a shows the range of F_1 . The upper values are in a range of increasing wave-making drag, which peaks at $F_1 \sim 0.5$. Note that cabin cruisers and towboats without barge convoys are not represented on this figure. Smaller craft that can plane will have $F_1 > 1.0$. Figure 8b shows length Froude numbers for recreational boats and towboats. Again, F_1 in towboats is generally less than 0.5, and only small, fast boats will travel at $F_1 > 1.0$. On the other hand, if the vessel depth Froude number, based on vessel speed and the maximum water depth, approaches 1, there is a change in wave patterns, but this is highly unlikely for large convoys such as barge-tows. Some recreational vessels may exceed this condition. When the depth Froude number exceeds 1, transverse waves in the wake are not formed.

Power Ratio. The power ratio, P_r , relates the energy transmitted to the river by the towboat to the energy expended by the river in overcoming friction (Stream Power - Bagnold, 1966, p. 15). Both factors vary over wide ranges. For discharges between 150 and 7,500 cubic meters per second (cms), with typical energy slopes and velocities, the energy expended by the rivers of the UMRS increases from about 20 to 1,250 joules per meter (J/m) of channel length. Note that 1 joule is defined as 1 watt-second. Table 6 gives the values of discharge, slope, and velocity used. Each reach of the waterway has its own hydraulic characteristics.

The energy transferred from a towboat per meter traveled depends on many factors such as installed horsepower, propeller characteristics, overall power train efficiency, speed, load, and acceleration. To estimate energy transfer, the horsepower (HP) is assumed to range from 500 to 7,000, and the absolute tow speed from 0.3 to 8 meters per second (m/s), or 1 to 29 kilometers per hour (kph), or 0.7 to 18 miles per hour (mph), or 1 to 26 feet per second (ft/sec).

These conditions yield a range of energy expenditure from 47 to 17,400 kilojoules per meter (kJ/m) as given in table 7. Note that the rated power is used in P_r without any allowance for power setting, efficiency, or load. The energy per meter of travel transmitted to the river by a 500-HP towboat moving 4 m/s is equivalent to the energy expended by the river with a discharge of 7,500 cms in about 74 m of channel length. A 7,000-HP towboat at full power, moving 0.3 m/s, expends energy equivalent to about 870 kilometers (km) of river for the 150 cms low-flow condition. These values are actually the inverse of P_r as defined in table 5. Figure 8 shows the trend of $1/P_r$ as a function of discharge and towboat power per meter. The power transferred to the waterway by a towboat ranges from about 100 to 1,000,000 times the stream power for conditions on the UMRS.

Barges on the UMRS

As discussed previously, barges on the UMRS are typically configured three wide and five long occupying an area of about 32 m (105 ft) by 297 m (975 ft). Figure 9 shows photographs of barges that are typically found on the UMRS. The three most common

barges are open hopper, covered hopper, and chemical and petroleum barges. Table 8 shows some typical characteristics of the barges that move on the UMRS (USACOE, 1989). According to this report open hopper barges, which can be used for all types of bulk solid cargo, dominate the field, accounting for about 45 percent of the tonnage capacity of all barges operating on inland waterways. Covered hopper barges account for approximately 25 percent of the total tonnage capacity. On the UMRS most dry bulk cargo is carried in jumbo barges.

The typical changes in the physical environment when a barge-tow convoy passes a river reach can be illustrated using an example given by Blaauw et al. (1984) and shown in figure 10. Some of the parameters in figure 10 will be analyzed in subsequent sections.

In laboratory experiments, Maynard (1988) has shown that bow waves exist in front of a towed laboratory barge, and that the bow effect can extend ahead of the tow for about 300 and 550 ft for one-wide and three-wide loaded barges, respectively. Maynard also observed velocity changes under the barge. Velocity changes include a zone just in front of the bow that flows in the same direction as the tow, a rapid reversal in flow just downstream of the bow that results in flow opposite the direction of the tow, and a zone underneath the barge in which the flow decreases or remains about the same depending on water depth. Near the stern, apparent suction effects of the propeller become dominant, resulting in a complex flow pattern.

For the whole channel, effects on the velocity field from a moving barge can be divided into approximately three zones: 1) the zone underneath the barge (Zone 1), 2) intermediate zones adjacent to either side of the barge (Zone 2), and 3) the remaining areas of the channel cross section (Zone 3). Underneath the barge, the hull imposes a moving boundary on top of a flow zone confined by the barge and the channel bed; when the draft/depth ratio is large, flow in this zone normally is greatly affected by the speed and bottom surface of the moving hull, and the flow moves in the opposite direction to the barge and toward the sides. The complexity of flow has been described earlier (Maynard, 1988).

At the edges of the hull of the barge, flow released from Zone 1 interacts with the boundary layer established along the side-wall of the barge. The rapidly moving flow in Zone 2 interacts with the slower ambient flows in Zone 3, forming vertical and horizontal vortices at the interface line to dissipate energies. Therefore, Zone 2 is a transition zone where flows are combinations of the laterally released flow from the bottom of the barge, the return flow, the boundary-layer flow developed along the side-walls of the hull, and the ambient flow.

At the outer regions, hull effects diminish and the flow becomes the vector sum of the return flow and the ambient flow. The magnitude and direction of the return flow in this zone are affected by the channel geometry and the characteristics of ambient flows and by the actual flow pattern surrounding the barge and that induced by the propeller jet. With the presence of return flow, the water surface normally depresses to balance the increased velocity in the total hydraulic head. This is called drawdown, essentially a long (negative) wave that propagates in vast areas toward shorelines or other areas of the channel, channel border, side channel, and connected backwaters.

The propagation of drawdown can be analogous to the propagation of shock waves (Henderson, 1966) in four different directions as shown in figure 11. In the large rivers,

the magnitudes of ambient flow and the corresponding depth render depth Froude numbers to vary from about 0.1 to 0.4 and hardly above 0.5, therefore state b (figure 11) normally does not occur. Wave effects can also become significant when wave-induced orbital water motions reach the river bed in shallow waters. A barge convoy does generate waves, but their magnitudes are generally smaller than those induced by recreational vessels.

In summary, movement of navigation traffic (barge-tows) in restricted waterways such as the Illinois, Mississippi, or Ohio Rivers can generate rapid return flow and water-level depression (drawdown) and waves between the barge and the shoreline. Consequently, the velocity between the barge and the shoreline changes spatially and temporarily (Mazumder et al., 1991). Barge passage generates turbulent velocity fluctuations (Mazumder et al., 1993; Bhowmik et al., 1995a, 1995b), creating surge waves in front of the bow. The velocity structure observed at a fixed point during a barge passage consist of two parts: barge-induced return velocity followed by tow-induced propeller jet velocity. This report concentrates only on the return flow velocity induced by the movement of barge traffic.

EXISTING METHODS

Return Velocity

Many investigators have developed methods to estimate return velocity and drawdown, based on the concept of one-dimensional conservation of mass, momentum, or energy. Some investigators have also discussed methods to compute the spatial variations of return velocity across the channel between the barge and the shoreline. All the methods predict an exponential velocity distribution that decreases laterally with distance from the barge.

Schijf and Jansen (1953) and Tothill (1966) developed methods to predict average return flow and drawdown in a narrow channel with a rectangular or trapezoidal cross section on the basis of one-dimensional energy and continuity equations. The relationships for the conservation of energy and mass were applied to the water motion relative to the barge and are given by:

$$2gh_d = (V_b + V_{ar})^2 - V_b^2 \quad (1)$$

and

$$V_b A_c = (V_b + V_{ar})(A_c - A_b - W_T h_d) \quad (2)$$

where h_d is the average drawdown, V_b is the barge speed, V_{ar} is the average return velocity along the river flow direction, g is the acceleration due to gravity, A_c is the wetted cross-sectional channel area, A_b is the average submerged cross-sectional area of the vessel, and W_T is the top width of the channel.

Sharp and Fenton (1968) and Bouwmeester (1977) developed methods to predict drawdown and return flow beside the barge on the basis of one-dimensional momentum and continuity equations. They assumed that return flow remains uniform across the width of the channel from the barge to the shoreline. Sharp and Fenton's equation for a rectangular cross section neglected the water-level rise in front of the bow, whereas Bouwmeester's equation for a trapezoidal cross section considered the water-level rise. Sharp and Fenton's method is a special case of Bouwmeester's method, which will be discussed here briefly.

Figure 3 and figures 10 and 12 (after Blaauw and van der Knaap, 1983; Blaauw et al., 1984) show what happens when a barge moves in a restricted channel. They also show the forces acting on the control volume of water between section 1 and 2. These forces (F_1 , F_2 , and F_3) are determined by integrating the hydrostatic pressure in the verticals 1, 2, and 3 (see figure 12):

$$F_1 = (1/2)\rho g W_T h^2 - (2/3)\rho g s h^3 \quad (3)$$

$$F_2 = (1/2)\rho g b (r + h_d + d_f)^2 \quad (4)$$

and

$$F_3 = (1/2)\rho g W_T (h - h_d)^2 + \rho g s (h^2 - h_d^2) h - (2/3)\rho g s (h^3 - h_d^3) - (1/2)\rho g b d_f^2 \quad (5)$$

where h is the average water depth, s is the slope of embankment expressed as tangent of bank inclination, b is the beam width of the barge; r is the rise of water level for the barge bow, d_f is the barge draft, and ρ is the density of fluid.

The equation for conservation of momentum is:

$$F_1 - F_2 - F_3 = \rho A_c (V_{rs} + V_a)(V_{ar} - V_a) \quad (6)$$

where V_{rs} is the barge speed with respect to the bank, and V_a is the average ambient velocity. Sharp and Fenton (1968) indicated that V_{rs} is the barge speed relative to the bank, which is equal to $V_b - V_a$, considering the direction of barge movement.

The equation for the conservation of mass for steady flow is:

$$A_c(V_{rs} + V_a) = A_1(V_{rs} + V_{ar}) \quad (7)$$

where $A_1 = W_T(h - h_d) - s(h^2 - h_d^2) - A_b$.

By eliminating the average return velocity V_{ar} from Eqs. (6) and (7), one gets an expression containing drawdown h_d within A_1 as:

$$\frac{F_1 - F_2 - F_3}{\rho A_c g h} = \left(\frac{A_c}{A_1} - 1 \right) \left(\frac{V_{rs} + V_a}{g h} \right)^2 \quad (8)$$

The value of drawdown h_d can be determined by trial and error from Equation (8) using the expression for A_1 , which contains h_d . Note that all parameters in Equation (8) are known except the value of h_d . Once h_d is known, the average return velocity V_{ar} can be obtained from Equation (7).

Blaauw and van der Knaap (1983) modified Bouwmeester's method to determine momentum, M_1 and M_3 , in verticals 1 and 3 (figure 12). The conservation of momentum in verticals 1 and 3 yields:

$$M_1 = \rho A_c V_b^2 \quad (9)$$

and

$$M_3 = \rho A_w (V_b + V_{ar})^2 \quad (10)$$

where $A_w = A_c - A_b - W_T h_d$, which is the wetted cross-sectional area of the channel after drawdown minus the area of the mid-vessel section (Schijf and Jansen, 1953). The continuity equation for steady flow is:

$$A_c V_b = A_w (V_b + V_{ar}) \quad (11)$$

In this case, the conservation of momentum must satisfy the following equation:

$$F_1 - F_2 - F_3 = \frac{\rho A_c (A_b + W_T h_d) V_b^2}{A_c - A_b - W_T h_d} \quad (12)$$

The expression for water-level rise r in front of the bow is given by Bouwmeester (1977) as:

$$r = \left(\frac{d_f W_T}{A_c} \right) \left(\frac{V_b^2}{2g} \right) \quad (13)$$

Substituting the expression of F_1 , F_2 , F_3 , and r into Equation (12), a fourth-degree equation for drawdown h_d is obtained. Thus, h_d is computed by iteration and used for solving the average return velocity V_{ar} .

Fuehrer and Romisch (1977) recommended the following equation to determine the average local maximum return flow $V_{r(max)}$ over the depth beside the barge at subcritical speed:

$$V_{r(max)} = V_b \left\{ \left[1 + \alpha (\varepsilon^2 - 1) \left(\frac{0.08gh}{\varepsilon^2 - 1} \right)^{-0.85} V_b^{1.7} \right] - 1 \right\} \quad (14)$$

where $\varepsilon = 1/(0.96 - A_b/A_c)$,

$$\alpha = 1 \quad \text{for } W_T/b \leq 2.5,$$

and

$$\alpha = 0.114W_T/b + 0.715 \quad \text{for } W_T/b > 2.5.$$

The correction factor α indicates the relative importance of barge width b .

Hochstein and Adams (1989) developed a method to directly compute average return flow V_{ar} relative to the shoreline using the concept given by Hochstein (1967). The expression is:

$$V_{ar} = V_b \{ [(a-1)B + 1]^{0.5} - 1 \} \quad (15)$$

where $a = \{ N/[N(N-1)] \}^{2.5}$

$$B = 0.3 \exp(1.8V_b/V_{cr}) \quad \text{for } V_b/V_{cr} \leq 0.65$$

and

$$B = 1 \quad \text{for } 0.65 < V_b/V_{cr} \leq 1$$

in which $N = A_c/A_b$ and V_{cr} is the so-called first critical velocity, with $V_{cr} = K \left(\frac{gA_c}{W_T} \right)^{0.5}$.

K is the constraint factor defined as a function of blocking ratio N . The reader should refer to Hochstein (1967) for the method used to determine the first critical velocity, V_{cr} . Figure 13 shows the relationship of K developed by Hochstein and Adams (1989). In the figure, L and b are vessel length and width, respectively.

Hochstein and Adams (1989) also developed a method to calculate the distribution of return velocity in the lateral direction by assuming an exponential distribution $V_r(y)$:

$$V_r(y) = k_1 \exp(-y/k_2) \quad (16)$$

where $k_1 = V_r(0) = \alpha V_{ar}$; and $k_2 = W_s/\alpha[1 - e^{-\alpha F(\alpha)}]$, in which $F(\alpha) = 0.42 + 0.521\alpha$ and W_s is the total distance from the barge to the shoreline. Equation (16) can therefore calculate the magnitude of return flow at any lateral point y on the cross section from the barge.

Simons et al. (1981) modified the equation proposed by Hochstein (1967) to determine the attention of return velocity from barge to shore. The magnitude of the return flow near the barge was determined by the barge speed, barge dimension, and cross section of the channel. The equation has the form:

$$V_r(y) = aV_b(\sqrt{a-1}) \exp\{-k(y)\} \quad (17)$$

where $k(y) = \{1 + \alpha^2 y \exp[-\alpha F(\alpha)]/W_s\}$. The variation of return velocity from barge to shoreline is an exponential distribution function.

Berger Associates, Ltd. (1981) also used variations of the exponential distribution to describe the return velocity from the barge to the shoreline. The average local maximum return velocity proposed by Fuehrer and Romisch (1977) was used as the return velocity near the barge. The expression is given by:

$$V_r(y) = V_{r(max)} \exp(-y/k_2) \quad (18)$$

where $V_{r(max)}$ can be computed using Equation (14).

More recently, Maynard and Siemsen (1991) developed a method to compute the cross-sectional return velocity distribution from the tow to the bank using Schijf and Jansen's equation (1953). The return velocity distribution is expressed as:

$$V_r(y) = V_{rsm} \exp\{C(y-b)/(W_s-b)\} \quad (19)$$

where $C = 1.2\{0.024(2A_s/A_b) - 0.266\}$, in which A_s is the cross-sectional area of the river from the centerline of the tow to the shoreline. V_{rsm} is the maximum return velocity on each side of the tow, and is computed as $V_{rsm}/V_{rs} = 0.024(2A_s/A_b) + 0.734$, where V_{rs} is the average return velocity for each side of the tow. V_{rs} is computed as $V_{rs}/V_{ar} = 0.36(A_c/2A_s) + 0.64$, where V_{ar} is given by Hochstein and Adams (1989). Equation (19) also indicates an exponential distribution of return velocity from shoreline to a point close to the barge.

The review of the existing methodology for determining return velocities presented thus far shows that several attempts were made to compute the return flow beside a barge due to its movement within a waterway. Evaluation of their applicability on the UMRS is necessary. Alteration of flow structure in a navigation channel, an important physical process, should also be evaluated and estimated to determine its impact on any sensitive biological habitats.

Drawdown

The materials in this section are given in ISWS Contract Report 271 (Bhowmik et al., 1981b).

There have been several attempts to determine the squat of vessels in canals and harbor entrances because of the problem of grounding and loss of control of vessels in

shallow and restricted waterways at high values of squat. The problem of squat has also become more serious in recent years as larger modern vessels transporting larger cargo need to use channels and harbor entrances designed for smaller vessels.

As discussed in the literature review, squat and drawdown are generally treated as equal to simplify the physical phenomena as one-dimensional flow. Further assumptions made in drawdown or squat analysis include constant vessel velocity in a straight channel, uniform vessel cross section and backflow throughout the flow section, uniform squat over the length of the vessel, and no frictional losses.

Under the above assumptions, Schijf and Jansen (1953) developed a method to estimate the drawdown from one-dimensional energy and continuity equations as follows. Drawdown or squat is given by the equation:

$$H_d = \frac{(V_b + V_{ar})^2 - V_b^2}{2g} \quad (20)$$

in which V_b is the barge speed, V_{ar} is the average return velocity, g is the acceleration of gravity, and H_d is the drawdown.

Equation (20) is the Bernoulli equation, which states that the increase in kinetic energy is equal to the decrease in potential energy if frictional losses are neglected. The terms to the right of the equal sign represent the increase in kinetic energy, while the left-hand term represents the decrease in potential energy.

Balanin and Bykov (1965) used a function involving inverse blocking ratio to multiply the velocity head by barge speed:

$$H_d = \frac{V_b^2}{g} \left[\frac{\left(\frac{A_c}{A_b} - 0.5 \right)}{\left(\frac{A_c}{A_b} - 1 \right)^2} \right] \quad (21)$$

where A_c is the cross-sectional area and A_b is the submerged cross-sectional area of the barge.

Hochstein (1967) proposed:

$$H_d = a_1 V_b^2 (a_2 - 1) \left(\frac{a_3}{2g} \right) \quad (22)$$

in which a_1 , a_2 , and a_3 are the empirical constants: $a_1 = 1$ for open water, $a_2 = [N/(N-1)]^{2.5}$, and $a_3 = 0.3e^{1.8 \frac{V_b}{V_{cr}}}$ for $V_b/V_{cr} \leq 0.65$ or 1 for $0.65 < V_b/V_{cr} < 1.0$, where V_b is the vessel speed, $N = A_c/A_b$, and V_{cr} is the so-called first critical velocity explained earlier.

Galencser (1977) developed another equation for drawdown from prototype and model test results. His equation relates drawdown to the vessel length, beam, draft, velocity, and the channel cross-sectional area and distance from the sailing line as follows:

$$H_d = 2.0 \cdot 10^{-6} \left[\left(\frac{V_b A_b L^2}{y A_c^{0.5}} \right)^{1/3} \right]^{2.8} \quad (23)$$

The equation was developed by finding the equation of the best-fit line between the variable in brackets and the observed drawdown data.

Dand and White (1978) and Gates and Herbich (1977) presented two other drawdown equations that are slightly different. Dand and White's equation was based on scale ship model experiments and is given as follows:

$$H_d = 0.39(V_b - V_a)^2 N^{1.4} \quad (24)$$

The drawdown equation presented by Gates and Herbich (1977) was derived at the National Research Council of Canada (Tohill, 1966) and by Garthune et al. (1948):

$$H_d = \frac{V_b^2}{22.6} \left[\left(\frac{A_c}{A_c - A_b} \right)^2 - 1 \right] \quad (25)$$

where V_b is the velocity of the vessel in knots, A_c is the cross-sectional area of the channel after drawdown, and A_b is the cross-sectional area of the vessel in square feet.

Bhowmik et al. (1981b) performed multivariate analyses on data collected by the ISWS in the early 1980s and arrived at the following equation:

$$H_d = 1.03 \left(\frac{V_b^2}{2g} \right) \left(\frac{A_b}{A_c} \right)^{0.81} \left(\frac{L}{y} \right)^{0.31} \quad (26)$$

Bhowmik et al. (1982) proposed the following relationship:

$$\frac{H_d}{h - d_f} = 0.478 \left(\frac{V_b}{\sqrt{g(h - d_f)}} \right)^{0.5} \left(\frac{A_b}{A_c} \right)^{0.81} \left(\frac{L}{y} \right)^{0.26} \quad (27)$$

The above analysis indicates that there are several relationships and equations that can be tested for validity on the UMRS.

Wave Height

Based on laboratory and field observations, some investigators have developed empirical equations to predict wave height using channel and vessel parameters. Balanin

and Bykov (1965) used vessel velocity and a modified blockage factor as the primary variables to develop the following equation for estimating wave height in the vicinity of a ship:

$$H_w = 2.5 \left(\frac{V_b^2}{2g} \right) \left\{ 1 - \left[1 - \left(\frac{1}{4.2 + N} \right)^{0.5} \right] \left(\frac{N-1}{N} \right)^2 \right\} \quad (28)$$

where H_w is the wave height in ft, V_b is the vessel velocity in ft/sec, g is the gravitational acceleration in ft/sec², N is equal to A_c/A_b , A_c is the cross-sectional area of the channel, and A_b is the submerged cross-sectional area of the vessel in ft², where b is the width of the vessel in ft, and d_f is the draft of the vessel in ft.

Gates and Herbich (1977) developed an equation for calculating wave height at the ship bow. Then H_w at distance y , as defined with cusp line number N_c , was given using deep water wave theory for moving surface point disturbance. Therefore their equation was for unrestricted channels and deep water conditions. This equation has the form:

$$H_w = 1.11 \left(\frac{K_w b_m}{L_e} \right) \left(\frac{V_b^2}{2g} \right) (2N_c + 1.5)^{\frac{1}{3}} \quad (29)$$

in which K_w is a coefficient given in terms of vessel length L (this relationship is shown in figure 14); b_m is the ship maximum beam width; L_e is the distance from the bow stem to the point where b first occurs; and N_c , cusp number ($= 1, 2, \dots$), gives the distance y as:

$$y = \left(\frac{2V_b^2}{g} \right) \left(\frac{(2N_c + 1.5)\pi}{\sqrt{3}} \right) (\sin 19^\circ 28') \quad (30)$$

Hochstein (USACOE, 1980) developed an equation to predict diverging wave height (in feet) in navigation canals that uses English units:

$$H_w = 0.0448 (V_b^2) \left(\frac{d_f}{L} \right)^{0.5} \left(\frac{N}{N-1} \right)^{2.5} \quad (31)$$

Bhowmik et al. (1981b) proposed the following equation based on multiple regression analyses of data collected by the ISWS:

$$H_w = 0.867 \left(\frac{V_b^2}{2g} \right) \left(\frac{d_f}{\pi} \right)^{0.26} \left(\frac{N-1}{N} \right)^{-3.0} \quad (32)$$

where H_w is the maximum wave height and d_f is the draft of the vessel in ft.

Later, Bhowmik et al. (1982) developed a simplified equation for calculating H_w , based on data collected from the UMR. This equation is given as:

$$H_w = d_f 0.133 \left(\frac{V_b}{\sqrt{gd_f}} \right) \quad (33)$$

where H_w represents the maximum wave height, as in Equation (32).

Blaauw and van der Knapp (1983) developed an equation based on a Delft Hydraulic Lab model and prototype canal traffic experiments:

$$H_w = \alpha h \left(\frac{y}{h} \right)^{-\frac{1}{3}} \left(\frac{V_b}{\sqrt{gh}} \right)^{2.67} \quad (34)$$

where h is the representative depth of the cross section and α is a coefficient that depends on the vessel type and the amount of loading. For push tows and loaded barges, $\alpha = 0.8$; for push tows and empty barges or tugboats, $\alpha = 0.35$; and for conventional inland motor vessels, $\alpha = 0.25$.

PIANC (1987) suggested the following equation for tugboats and motor tows:

$$H_w = h \left(\frac{W_s}{h} \right)^{-\frac{1}{3}} \left(\frac{V_b}{\sqrt{gh}} \right)^{4.0} \quad (35)$$

Sorensen and Weggel (1984) and Weggel and Sorensen (1986) developed an interim model for predicting ship-generated wave heights, which is more applicable for recreational craft. In this equation, V is the volume of water displaced by the ship, X is the distance from the ship, H_w is the wave height, and h is the representative water depth:

$$F = \frac{V_b}{\sqrt{gh}}, \quad H^* = \frac{H_w}{\sqrt[3]{V}}, \quad X^* = \frac{X}{\sqrt[3]{V}}, \quad \text{and} \quad h^* = \frac{h}{\sqrt[3]{V}} \quad (36)$$

The dimensionless wave height can be calculated by:

$$H^* = \alpha (X^*)^\eta \quad (37)$$

where η is related to h^* as $\alpha = \beta (h^*)^\delta$. The coefficients β and δ are determined from:

$$\begin{array}{ll} \beta = -0.225\mathbf{F}^{-0.699} & 0.55 > \mathbf{F} \geq 0.2 \\ \beta = -0.342 & 0.80 > \mathbf{F} \geq 0.55 \end{array}$$

$$\begin{array}{ll} \delta = -0.118F^{-0.356} & 0.55 > F \geq 0.2 \\ \delta = -0.146 & 0.80 > F \geq 0.55 \end{array}$$

The coefficient α is related to h^* as:

$$\log \alpha = a + b \log h^* + c \log^2 h^*$$

where $a = -0.6/F$, $b = 0.75F^{-1.125}$, and $c = 2.653F - 1.95$.

Sediment Resuspension

The three riverine sediment transport equations considered in this report are by 1) Colby, 2) Akers-White, and 3) Toffaleti. These equations were developed by the respective authors at different times using different concepts of sediment suspension and transport and the available laboratory and field data sets. All these equations are expressed in English units. However, final results in this report will be expressed as metric tons per day (mt/d) for sediment load and milligrams per liter (mg/L) for sediment concentration.

Colby Method

The Colby method (Colby 1964a, 1964b) requires interpolation between transport curves for four depths and corrections for water temperature, concentration of fine sediment, and median diameter of the bed material. The transport curves are based on a combination of laboratory data, field data, and computations. The correction for fine sediment is only applicable to concentrations greater than one percent or 10,000 mg/L. Though Colby used data from the Mississippi River, most of the 100-foot-depth curve and much of the 10-foot-depth curve are based on calculations, not on measured transport rates. Colby was guided by the Einstein Bed Load Function (Einstein, 1950) as well as by the transport data sets. This method yields the sediment transport rate per foot of stream width. The mean depth, or cross-sectional area divided by the top width, is used for interpolation in the charts. Sediment concentrations could be calculated from the sediment load and water discharge, but there is no way to do this for a particular location, or depth, in the stream cross section. The method is useful for sediment load calculations, but not for sediment concentration prediction.

Akers-White Method

This is one of several sediment transport equations based on the concept of a critical shear stress (Akers and White, 1973). The computation results in an average sediment concentration. If the mean depth and velocity are used, this concentration may be used in the common equation for sediment load:

$$Q_s = 0.0864 C_s \cdot Q_w \tag{38}$$

where Q_s is in mt/d.

Though this equation is also intended for stream transport computations and not point concentration calculations, it is possible to make computations for C_s for given depths and velocities. Concentrations computed with the Akers-White formula are presented in the section on event concentrations.

Toffaletti Method

Toffaletti (1969) based his method on Einstein's bed load concepts and the exponential distribution of sediment in the vertical. He also included separate computations for each bed material size fraction. The geometric mean diameter is used in the computation for each of the common log base-2 size fractions from silt to the largest size present (Vanoni, 1975). The water column is divided into four layers, each with its own expression for the vertical distribution of sediment. The combination of four layers and up to eight size fractions requires much more computation than either the Colby or Akers-White methods. However, it also provides the means to use local bed material gradations, depths, and velocities to compute point concentrations. The vertical layers would allow computation of concentrations at various depths.

Dimensional Analysis

Dimensional analysis is a technique used to simplify complex processes for ease of understanding and to predict future changes based on limited data or limited understanding of the processes. A dimensional analysis was performed to determine the variables that could be used to predict and/or determine the changes associated with navigation traffic. The following variables were considered in this analysis.

Properties of water:

- ρ is the density (FT^2/L^4)
- γ is the specific weight (F/L^3)
- μ is the dynamic viscosity (FT/L^2)

Flow variables:

- V_a is the ambient mean velocity (L/T)
- h is the representative depth (L)
- S_w is the water surface slope (L/L)

Channel geometry:

- S_0 is the channel bed slope (L/L)
- s is the channel embankment slope (L/L)
- W_T is the top width of the transect (L)
- A_c is the cross-sectional area (L^2)

Traffic characteristics:

- A_b is the submerged area of the barge in the cross section (L^2)
- d_f is the effective draft of the barge (L)
- L is the length of the barge fleet (L)

b is the breadth of the barge fleet (L)

V_b is the speed of the barge (L/T) (note that $V_b = V_{ab} \pm V_a$, where V_{ab} is the absolute barge speed and + or - depends on the barge's traveling direction)

y is the distance from the center of a barge to the point of interest (L)

H_p is the towboat horsepower (LF/T)

Return Velocity, V_r :

The relationship for return velocity is given as:

$$V_r/V_a = F(V_d h/\nu, y/W_T, V_b/\sqrt{gL}, A_b/A_c, Pr) \quad (39)$$

where F represents a function, $\nu = \mu/\rho$, and Pr is a power ratio = $(H_p/V_{ab})/(\gamma A_c S_0)$ as given by Stefan and Riley (1985).

Wave Height, H_w :

The parametric relationship for wave height is given as:

$$H_w/h = G(R_e, V_b/\sqrt{gL}, s, A_b/A_c, Pr, y/W_T) \quad (40)$$

in which G represents a different function.

Drawdown, H_d :

Drawdown is related to return flows. In a prismatic channel, the drawdown may be expressed as follows (velocity head in Bernoulli equation):

$$H_d = \frac{(V_b + V_r)^2 - V_b^2}{2g} \quad (41)$$

However, if drawdown is considered as a solitary wave, the basic parametric relationship for drawdown becomes:

$$H_d/h = H(R_e, V_b/\sqrt{gh}, s, A_b/A_c, Pr, y/W_T) \quad (42)$$

where H represents a functional relationship between the variables on the right-hand side and those on the left-hand side of the equation.

METHOD AND EQUIPMENT DESIGN

Field data for evaluating the physical impacts of navigation on the UMRS were collected from both the Illinois and the Mississippi Rivers. Ideally data should be collected from the entire UMRS to cover all the major features, alignments, and morphometric characteristics of the rivers. Data collection sites should be representative so that site-specific information can be applied to other sites. Moreover, it must be kept in mind that data from *all* representative sites on the UMRS cannot possibly be collected, and therefore data and information from selected sites must be used to predict conditions at other locations for which basic data and information are not available.

Another extremely important consideration in the selection of sites is the accessibility of the location to the field crew. Field data collection for a wide variety of parameters requires an extensive amount of instrumentation and highly skilled personnel with ready access to shore support, electricity, temporary shelters, food, etc.

Before initiating the actual data collection, it was necessary to test equipment and procedures to make certain that the proposed techniques and instrumentation would work as planned in the field. It should be mentioned here that this was the first time an effort of this magnitude had been undertaken to collect a set of highly sophisticated data from such a large river system.

Pilot Data Collection and Instrumentation Setup

Before the actual data collection was undertaken, test data were collected from a site visited by ISWS scientists in the early 1980s for a similar data collection project (Bhowmik et al., 1981a-c).

The site for this test run was McEver's Island on the Illinois River at River Mile (RM) 50.1 (figure 15). In 1980, data were collected from this site on sediment resuspension, waves, and drawdown. Given the availability of these background data, McEver's Island was chosen as an ideal site to test instrumentation and techniques before launching a full-scale data collection trip in 1989. Fortunately, the techniques and instrumentation that were tested and modified at this site from October 25-28, 1988, turned out to be appropriate for detailed data collection at other selected sites.

The setups described in this section were developed at the McEver's Island site and used in subsequent data collection trips. Once a setup was tested, verified, and found to be working, it was used at all sites with only minor variations.

Velocity

All velocity data were collected from a fixed-mounted system. Two different mounting systems were used in the field. Subsequent sections of this report provide specifications for various types of meters, wave gages, and other equipment.

Figure 16 shows a sketch and photograph of a system in which either a single velocity meter is attached to a post at a fixed elevation or a set of meters is attached to the vertical post to collect velocity data at different elevations. This system works exceptionally well for water depths ranging from 0.3 m (1 ft) to 1.22 m (4 ft) in channel

border areas extending from very near the shoreline to approximately 33 m (limited by the length of the cable) from the shore. Similar systems were also used to collect velocity data very close to the shoreline. Figure 16 shows the setup that was used to install two-dimensional electromagnetic current meters such as the Marsh McBirney (MMB) 511.

The system used to collect velocity data in deeper water at different elevations is called a vertical array. This setup was designed and tested at McEver's Island to make certain that the system could be installed in the field and that data could be collected and processed easily. Figure 17 shows a sketch of the vertical array along with two photographs before and after deployment in the water. This vertical array could be used in waters from 3 to 3.5 m deep, and was used to install two-dimensional electromagnetic current meters such as MMB 511. These meters were connected to shore stations with cables extending up to 33 m to enable the eventual storage of the velocity data.

The third type of system used for velocity data collection was a fixed-base system in which meters are attached to an aluminum base 1 m in diameter and 0.025 m thick with a supporting post attached at the center of the base. All the bases used were stabilized with the addition of lead weights. Figure 18 shows the two types of meters used in this system, InterOcean S4 and MMB 527. The MMB 527 cable was connected to a shore station, whereas the self-contained S4 had a communication cable connected to a float on the surface, which could be accessed by boat for reprogramming and downloading of data. The ISWS' two MMB 527s could be installed at any location within the channel up to about 90 m and 150 m, respectively, from shore. The self-contained S4 could be installed at any location and at any water depth.

It must be pointed out that all the mounting systems described so far were made of stainless steel, plastic, lead, or aluminum, thus eliminating any possible interference with the magnetic fields of the sensors.

Waves and Drawdown

Wave and drawdown data were collected from an electronic wave gage developed at the ISWS in 1981 (Bhowmik et al., 1981b). The gage was installed on a post with about one-half of the measuring unit kept below the water surface. Figure 19 shows photographs and a sketch of the system. All electronic control systems were kept on shore. The meters were installed in the water at a depth of 0.9 to 1.5 m, and the maximum cable length was 30 m.

Suspended Sediment

Suspended sediment sampling was done from several sediment towers of varying heights and designs (figure 20) with pumping tubes connected to a shore station. Some towers were installed in deeper water close to the navigation channel so that suspended sediment samples could be collected by boat. All event-based samples were collected by pump samplers. All sampling was done about 30 m upstream of the transect where current meters and wave gages were located to avoid any disturbance to the suspended sediments in the water column.

Turbidity

Turbidity data were collected following a procedure similar to the one described for suspended sediments except that water samples were running through the turbidity meter. In fact, turbidity intakes were installed at the same locations where suspended sediment samples were collected.

Site Selection

Numerous meetings between project sponsors, ISWS researchers, and USACOE personnel were held to determine the sites where field data should be collected. Initially, it was decided that data should be collected from several representative sites for different flow conditions to depict the actual conditions in the field. Table 9 shows the approximate number of sites required to depict actual field conditions. During this discussion process, it was decided that data ought to be collected from both rivers to cover a whole range of morphological and physical conditions. It was also determined that data should be collected from straight and curved reaches covering gentle and sharp bends. Table 10 shows the approximate number of trips required to depict the physical impacts of navigation on the UMRS. One can easily see that the resources required to accomplish such an activity would be almost impossible to obtain at the present time.

Based on this evaluation and an evaluation of the planform characteristics of the UMRS, it was felt that at a minimum, field data should be collected from three sites on the Illinois River and from four sites on the Mississippi River for three different flow conditions: low flow, medium flow, and high flow. This meant that a total of 21 data collection trips would be required to depict the actual conditions in the field for the determination of physical impacts of navigation. Subsequent sections describe the number of field trips that were possible, given funding limitations.

The following sites were selected for this study: McEver's Island and Kampsville on the Illinois River, and Apple River Island, Goose Island, and Clarks Ferry on the Mississippi River.

DATA COLLECTION

As already described, sites were selected in close consultation with the EMTC project director and USACOE representatives. During the site selection process, it was determined that the initial attempt to collect field data should be made at sites that are fairly straight. It was also decided that potential sites must be visited and some preliminary data collected during a "reconnaissance trip" before actual data collection began. Finally, it was determined that field data would be collected for a period of about two weeks per trip.

Reconnaissance Trip

After a site was selected for data collection, it was visited at least twice, once for the reconnaissance trip and at least once for event data collection. The reconnaissance trip was designed to collect site-specific information, including river cross-sectional profiles, hydraulic characteristics, sediment loads, and bed material characteristics, and to evaluate access to the site, location of gaging stations, and access to power supply and support facilities.

Site Characterization

The general nature of each site selected for field data collection was determined from topographic maps and reconnaissance visits. Because alluvial channels are dynamic and river flows are constantly changing, preliminary local information on river stage, water discharge, channel geometry, bed material, velocity, and suspended sediment distribution was collected one to two weeks before the field trip. Additional bathymetric and hydraulic data were collected once or twice during each trip. Establishing the location of the primary measurement transect and the locations of the Microfix transponders was also done during the preliminary trip.

Bathymetry

Two methods were used to obtain bathymetric data: 1) recording depth soundings using the MicroFix transponders to show the location of the boat, and 2) measuring the depth along the transect while taking velocity measurements and collecting suspended sediment concentration samples.

A Lowrance X-15 recording depth sounder was used to obtain cross-sectional plots of river depth. Location was determined by MicroFix transponder. For each cross section 10 to 15 positional marks were made on the recording chart to identify the coordinates. Three to five cross sections were sounded at longitudinal intervals of approximately 200 m (600 ft, 0.1 mile). Several longitudinal runs could also be recorded to identify bed forms and irregularities in the longitudinal direction of the channel.

When the water discharge and suspended sediment load were measured, water depths were also measured at 15 to 25 locations for each cross section. Position was determined using the MicroFix transponder.

Bathymetric measurements were used to develop cross-sectional plots of the river channel or contour maps of the river bed near the primary measurement transect. Bathymetric information from the preliminary trip was used to determine the location of current meters and suspended sediment sampling intake towers.

Depth, Velocity, and Suspended Sediment

Once during the preliminary trip and at least once at each of three transects during field data collection, the following set of measurements was made. Water depths and velocity were measured at 15 to 25 verticals in each cross section. Depth-integrated suspended sediment samples and bed material samples were also collected at each vertical. Methods generally follow U.S. Geological Survey (USGS) and federal Interagency Sedimentation Project guidelines. Carter and Davidian (1968) and Buchanan and Somers (1969) describe discharge measurements, Guy and Norman (1982) outline sediment sampling procedures, and Guy (1969) gives laboratory methods for analyzing sediment samples. Guy (1970) discusses general concepts of fluvial sediments.

Guidelines for discharge measurements recommend measuring velocity at 20 or more verticals. Given the need to position a boat by anchoring, and the precision limits of dynamic positioning with the MicroFix transponders, this is the maximum number of verticals that can be measured in channels less than 500 m wide. Generally two or three point methods were used with velocities measured at depths of 0.2 and 0.8 or 0.2, 0.6, and 0.8 percent of the total depth. A Price-type, vertical-axis current meter was suspended from a winch (A-reel) with a streamlined weight below the meter to prevent it from being carried downstream by the current. The discharge was computed from the velocity, depth, and lateral position data following the standard methods (Buchanan and Somers, 1969). Figure 21 shows a typical setup used for collecting depth, velocity, suspended sediment, and bed material data on the Illinois River at RM 50.1 near McEver's Island.

At each location where velocity was measured, a depth-integrated suspended sediment sample was collected with a DH-59 sampler. The DH-59 has a streamlined bronze body that holds a pint glass bottle and has an intake nozzle with an inside diameter of 1/8, 1/4, or 3/8 inch (3.2, 6.4, or 9.6 mm). Nozzle size was selected to obtain samples with volumes between 150 and 400 mL. The DH-59, which is lowered into the water and then pulled up at a constant rate of speed, has a maximum sampling depth of 5.5 m, so in deeper water only the top 5.5 m of water could be sampled. Guy and Norman (1982) describe the sampling procedures in detail. Samples were then returned to the ISWS sediment laboratory for concentration determination following standard methods (Guy, 1969). Total suspended sediment load was calculated from the concentration at each vertical and the water discharge associated with that vertical.

At each measuring position, a bed material sample was obtained, most often with a Petite Ponar sampler, which has an open area 0.15 m on one side and samples the top 0.1 m. The sampled depth depends on the texture of the bed material. Samples were transferred to zip-lock plastic bags for transport to the sediment laboratory for particle size determination as described by Guy (1969). Other samplers used include: 1) Eckman dredge, 2) larger Ponar dredge, 3) Shipek sampler, and 4) BMH-60. Each sampler has advantages in certain river flow and bed material situations.

Other information recorded during each reconnaissance trip included a description of the planform characteristics, presence of bank revetments, wing dams, closing dams and/or side channels, and sloughs. An examination of the site was also made to determine where the velocity meters and sediment towers could be located and where wind gages, shore stations, and shore support systems, such as tents for the field crew, could be erected.

As already noted, each data collection trip lasted from one to two weeks. It took about one and a half days to install the instruments at each site. Once the instruments were installed, they were kept at the site for the entire two-week period to maximize the data that could be collected at each site.

Instrumentation

This section describes in more detail the various instruments and meters used in the field to collect data, along with specifications for those instruments (see table 11). Soong et al. (1990) reported on data acquisition procedures for the navigation study.

Velocity

Velocity data were collected using meters such as the InterOcean Systems S4 and Marsh McBirney 527 and 511. All these meters work on the basic Faraday principle, which dictates that the electromagnetic field around a power source changes as the motion of the particle around that field is altered. These changes in the electromagnetic field alter the voltage that can be correlated with the actual magnitude of the velocity. Once this velocity is calibrated with the change in voltage, a power source such as the S4, MMB 527, and MMB 511 can be used to measure the change in velocity. All three types of meters were used to measure velocity in the field.

Meters such as the S4 and MMB 527 have an internal compass that allows researchers to determine the actual orientation of the measured velocities with respect to a fixed (north) direction. All three types of meters (S4, MMB 527, and MMB 511) measure two components of velocity on a horizontal plane. The MMB 511 does not have a built-in compass and must be installed with a known orientation.

The S4 meter have a built-in data logging system that allows their installation at any location. The MMB 527 and MMB 511 meters require that data logging occurs in a separate unit located on shore. The ISWS used two MMB 527 meters with cables 91.5 m and 152.4 m long; six MMB 511 meters, four with cables 30 m long and two with cables 100 m long; and five S4 meters.

The S4 meter has a spherical shape with a grooved surface and a diameter of 250 millimeters or mm (10 inches). The MMB 527 and MMB 511 meters are also spherical in shape, with a diameter of 103 mm (4 inches) and 39 mm (1.5 inches), respectively. The S4 meter contains all power and signal processing units within its sphere as compared to the MMB 527 and MMB 511 meters, whose power and data conversion units are housed in a separate signal processing unit, normally on shore.

At most sites, two MMB 527 meters, three to five MMB 511 meters, and one to three S4 meters were installed on one side of the river outside of the navigation channel. The S4 meters were installed on the opposite channel border areas since they did not

require any shore support. The MMB meters required shore support stations from which the two velocity components were continuously recorded on data loggers and monitored by a personal computer. The main shore station also provided all other support functions, including power supply, shelter inclement weather, and supply storage. Figure 22 presents four photographs of the McEver's Island site on the Illinois River showing various data collection arrangements. Figure 23 shows a typical setup on the Illinois River at the Kampsville site.

Waves and Drawdown

Surface waves and drawdown were measured with resistance-type wave gages. The measuring system consisted of a wave gage, an interface, a cable connecting the wave gage and the interface, and a portable personal computer. Two wave gages and one interface were built at the ISWS in 1982 (Bhowmik et al., 1982) and were modified for this project to connect to the portable personal computer. Figure 24 shows a sketch and photograph of the wave gage.

Wave height was measured by counting the number of contacts on the wave gages' sensor boards. One gage is equipped with a 0.91-m (36-inch) sensor board with 60 equally spaced sensor grids, the other with a 1.52-m (60-inch) sensor board with 100 equally spaced sensor grids. The distance between sensor grids is 0.015 m (0.05 ft). Each sensor grid connects to an electronic package on the top of the wave gage. PVC pipe cases protect both the sensor board and electronic package from external impacts. For a detailed description of the wave gage structure, readers are referred to Bhowmik et al. (1982).

The wave gage receives power and a 1-kilohertz (kHz) clocking signal from the wave gage interface via a 30.5-m (10-ft), 15-twisted-pair cable. Using these inputs, the wave gage sequences the contacts one by one, starting at the bottom of the gage. When the gage encounters a contact that is out of the water, it stops the sequence and loads that number onto eight data lines to the interface every 0.1 seconds. During the loading process, it inhibits the computer from getting information until the data lines are stable.

The wave gage interface generates 1 kHz timing and power to run the wave gages. Contained within the wave gage interface is a miniature data logging computer, which is controlled by a BASIC software program residing in EPROM (Erasable Programmable Read Only Memory). The maximum sampling rate is ten samples per second and the total storage space is 512 kilobytes. This data logging computer sequentially scans the output of the wave gage and loads the contact number information into its memory. Communication with outside media (main storage, e.g., a personal computer) is through a standard 9-pin RS232 serial port, which is mounted on the outside of the interface.

The maximum deployment range for the wave gages was 30.5 m from the shore as limited by the cable length. Figure 24 shows the mounting system for wave gages. All the control and powering units were kept on shore. Sampling frequency for the wave gages was ten samples per second. Wave and drawdown data were collected for barge events and within selected intervals for wind-generated waves.

Suspended Sediment and Turbidity

The scheme adopted for suspended sediment sampling during the data collection trips involved collecting discrete samples at a number of points in the channel border area (Adams et al., 1989). Suspended sediment sampling between and during two barge passage events was done using ISCO pumping samplers operated in the manual mode. Intakes were mounted on support structures placed on the river bed. Figure 20 shows a sketch and photographs of such a tower used in the field.

All suspended sediment samples were collected in pint glass bottles that hold a 400-mL sample. The bottles were capped and marked for later analysis of sediment concentration in the laboratory. On a rotating schedule each intake was pumped continuously to fill a 5-gallon bucket for particle size determination. Figure 25 shows several photographs of sediment samples being collected and temporarily stored in the field.

During the two pilot field trips in the fall of 1988, only one intake structure was used. It was located about 22 m from shore in 2.5-m-deep water. The intakes were connected to nozzles used for DH-48 depth-integrated suspended sediment sampling. These nozzles were connected to vinyl tubing with a 6.4-mm inside diameter and taped to the support structure pointing in the upstream direction. The ISCO pumping samplers were located on shore and the vinyl tubing was run continuously from the intake to the sampler.

During actual data collection, two or three intake supports were placed in the river at different distances from shore perpendicular to the tow sailing lines. The support structures consisted of a vertical post mounted on a heavy (40-kg) steel base plate (figure 18). Each intake connected to a DH-48 nozzle, with an inside diameter of 0.25 inches (6.4 mm), attached to the support plate at a known distance above the bottom of the base. A length of vinyl tubing, as long as 33 m, connected the intake to an ISCO model 1680 pump unit on shore. Use of the intakes required as many as eight pumps, one for each intake. Each morning and before each event, the pumps were run in reverse for five minutes to flush the intake tubing. A field assistant collected, capped, and marked samples from as many as three intakes during events. Measurement of the time taken to fill the 400-mL sample bottles determined that the velocity in the tubing was about 0.49 m/s. During several events, an intake structure was located close to the sailing line, requiring placement of ISCO pumps and a technician on a boat moored near the intake structure.

The three suspended sediment sample intake structures were aligned perpendicular to the shore with nozzles pointing upstream (figure 20). Intakes were positioned 0.15 and 0.60 m above the bed at all three locations. An additional intake was positioned about 0.75 m below the surface on each structure.

It should be noted that a time delay exists between the time when sample enters at the nozzle and the time when it was collected in the container. Since all the sampling was done on a continuous basis from early morning to the end of the day, the time delay should not make any difference in the overall analyses as all collected samples were delayed by the same time interval.

In addition, two intakes, usually placed near discrete sample intakes, were connected to flow-through cells in Orbico-Hellige turbidimeters. Turbidity values were automatically recorded once a minute on a Campbell Scientific S-10 data logger.

Wind Speed and Direction

Wind data were collected using a recording wind set installed in an open field at each site on a tower approximately 3 to 4 m high. The data were stored in a CR10 data logger. Figure 26 shows the setup used in the field.

River Stage

River stage data were collected at least twice a day at one upstream and one downstream gage. Stages on site were measured using the S4 meters, which were equipped with a depth sensor, and from a staff gage installed at the primary transect near the shore station. Generally this staff gage was read at 30- to 60-minute intervals each day during the field trip. Figure 27 shows a photograph of a staff gage installed in the field.

Air and Water Temperature

Both water and air temperature data were read from thermometers installed on a staff gage in the water and on a tower on shore near the primary shore station. Water temperatures in the channel were also recorded using the S4 current meters.

Bed Materials

Bed material data were collected during each event data collection trip. Samples were collected using either a stainless steel Petite Ponar sampler or a regular Ponar sampler.

Traffic Characteristics

No automated system exists to record traffic characteristics such as speed, distance, configuration, or any other special features.

Traffic data recorded include maneuvering characteristics and barge characteristics such as size, draft, and barge configuration. The four types of barges encountered on the UMRS were 1) open hopper, 2) covered hopper, 3) tank (chemical and petroleum barge), and 4) deck (work barge).

Tow maneuvering characteristics include speed, direction, propulsion, sailing angle relative to the shore, and distance from the shoreline. Tow speed was calculated by recording the total time of passage from a reference point (usually the measuring cross section). The distance from shore was measured using a range finder, as were distances from bow to shore and from tow to shore. The name of the tow was recorded in the field notes so that characteristics such as propulsion could be looked up later. Propulsive characteristics include the number of screws, size of propeller, open or kort nozzles, and horsepower of the barge. These were obtained from publications such as those given in the *Inland River Record 1988-1989* (Owen, 1988).

The sailing angle was obtained using the MicroFix positioning system (Racal Survey, Inc.), which tracked the towboat through the site. The system (pictured in figure 28) consisted of three transponders (T/Rs) and a control management unit (CMU), which

communicated with the T/Rs to determine position. Two T/Rs were placed at known points on the bank, and one T/R and the CMUs were mounted on the work boat. During tow passage, the work boat trailed the tow. Position fixes from the CPU were sent through a serial port and stored on a laptop computer. This system provided a measuring range of 80 km with a resolution of 1 m. Tow maneuvering characteristics, except for sailing angle and propulsion, were recorded in a field note.

Coding System

Data collected from such an array of current meters, suspended sediment samplers, turbidity meters, wave gages, and other instruments must be coded in order to avoid any confusion in the field and also to eliminate any mistakes in the analysis and presentation of the data. Each velocity meter, sediment intake port, and wave gage was given a specific number or code which was used throughout the entire data collection period. The fixed mounted current meters such as MMB 511 and MMB 527 were coded with the manufacturer's name and the serial number of the meter. For example, an MMB 511 meter with serial number 998 was coded with an identification of MMB 511/998 meter, and so on. The location of each sensor was designated by a, b, c, etc., depending upon its location with respect to the shoreline (figure 23). For example, the meter or sediment tower located closest to the shore was designated by "a," the next one by "b," and so on. Similarly, the intake or meter installed near the bed was designated by "1," the next higher one by "2," and so on. Thus "a1" represents the current meter or the sediment sampling intake nozzle closest to the shore and nearest the bed.

Event Data Collection Procedure

Once a representative site was selected, investigators followed an exact procedure for undertaking a field trip to collect data for various events. By definition, an "event" took place when a single barge-tow flotilla passed a sampling site. Following is a step-by-step description of the event data collection process.

- Step 1:* Select site based on input from all concerned parties.
- Step 2:* Gather as much information as possible prior to field work from published or printed sources. This may include stage data, location of gaging stations, discharge, sediment or cross-sectional data, and possible access to the site (based on navigation charts, 7.5-minute quadrangle maps, and other available maps).
- Step 3:* Request and receive appropriate permission to enter the site.
- Step 4:* Test and calibrate all instruments to make certain that they are in working condition.
- Step 5:* Make a reconnaissance trip to the site to collect data, check out the local facilities and boat access areas, and review the site for appropriate locations for current meters, wave gages, sediment sampling stations, shore stations, power supply, etc.
- Step 6:* Proceed to the site either on the following Sunday afternoon or Monday morning.

- Step 7:* Install all meters and erect the tents that will house the shore stations, and field supplies, and provide night accommodations.
- Step 8:* Test all the installed instruments, using certified divers who also work as field data collection personnel. Run all the meters for several hours and resolve any instrument irregularities.
- Step 9:* Initiate data collection from early morning to late afternoon every day. Check all meters several times a day to make certain that they are working properly.
- Step 10:* Continue collecting data. Store sediment samples in a large rented van.
- Step 11:* Dismantle all field setups at the end of the data collection period (normally two weeks), load vans, and return to office.
- Step 12:* Check all the data collected, transfer data from the laptop computers, deliver sediment samples to the laboratory for analyses, and start performing some preliminary analyses. Debrief all field personnel to make certain that nothing was missing during the actual data collection trip.

The steps outlined above were essentially developed during the pilot trip and followed thereafter, and were found to be very effective in collecting field data.

While data collection activities for each event and each day varied somewhat from site to site, they essentially contained the following components: ambient data collection and event data collection during and after tow passage. The time interval selected for collecting data for various parameters was determined by the actual need for the data and the capability of the sensors.

The ISWS developed several computer programs to graphically display the wave, velocity, and water surface elevation records retrieved from data loggers. These programs enabled the field crew to check and correct any irregularities in the field. During data logging, simultaneous monitoring was also available and used in the field to check the normal and expected variations of the parametric values in the field.

Sampling Frequency

The ISWS developed the sampling protocol for suspended sediment concentration. Sampling frequency varied, with one schedule for barge-tow events and another for sampling at other times. During periods without barge-tows, ambient samples were collected from each intake at 20-minute intervals. Table 12 provides the final sampling frequencies used in the field.

When a barge-tow was sighted approaching the measurement reach, preparations were made for an intensive period of sample collection. Beginning 5 to 10 minutes before the tow was expected to pass the sampling line, samples were collected from each intake structure at 1-minute intervals. This means that at the nearshore station (two intakes), each intake was sampled every 2 minutes. At the other two intake structures with three intakes apiece, each intake was sampled every 3 minutes. Sampling at this frequency continued for an hour after the tow passed the intakes. The sampling interval at each intake was then increased to 6 minutes for approximately 30 minutes, and then to 9 minutes for another 30 minutes. After approximately two hours, the sampling interval was increased to 20 minutes. If another tow passed the site at any time during the two hours after the first tow, the event sampling cycle was restarted. This schedule was

followed during the May 1989 trip at the McEver's Island site (RM 50.1) on the Illinois River. Trips to the other sites had slightly modified event sampling schedules, but retained the basic array of eight intakes.

Data Reduction

Data collected in the field were processed to obtain numerical values for each of the parameters. For example, wave data provided information on the number of times and relative elevations where the water surface came into contact with the recording strip on the wave gage. These data were converted to obtain a continuous record of the wave profile for further analyses.

Velocity data collected by the MMB 511s did not contain any directional signal. Those meters were oriented in the field so that one component of the measured velocity was parallel to the axis of the channel and the other component was at a perpendicular angle. These two components of velocity data were collected on the same planar surface. The velocity data collected by the MMB 527s and S4s contained a directional signal through a compass reading. The two velocity components measured by these meters were converted to x and y directions, with x parallel to the main axis of the channel in the flow direction and y perpendicular to the main axis, following the right-hand rule, or 90° clockwise in the +x direction.

All the suspended sediment samples were analyzed in the ISWS sediment laboratory and appropriate plots between suspended sediment concentrations and elapsed time were developed. Similarly, bed material samples and some suspended sediment samples were analyzed in the laboratory to determine the particle size distribution of these materials.

Physical parameters such as return velocity, maximum return velocity, maximum wave height, maximum drawdown, maximum increases in suspended sediment concentrations, duration of increased sediment concentrations, median diameter, standard deviation, and uniformity coefficients of the sediment samples were determined from the various plots and illustrations developed from the collected field data. Examples of how these parameters were determined are given below.

Return Velocity

Return velocity is defined as the velocity component generated during the passage of a barge-tow. Return velocity is in the opposite direction of the barge-tow. Depending upon the magnitudes of the return velocity and the direction of the barge, one can observe the water accelerated or de-accelerated or reversed from a shore. Figure 29b shows a temporal history of the x velocity component (parallel to the main axis of the river, figure 29a) collected at a distance of 36.6 m from the left descending bank (LDB) of the Illinois River looking downstream at RM 50.1 (McEver's Island site). The velocity data shown here were averaged using an 11-point moving average method. Ambient velocity (x-component), defined here as U_{ma} , was determined based on the average of the velocity data collected for a period of 15 minutes before the barge event. The ambient velocity in this case is 0.09 m/s.

The starting and ending point of a barge event were determined based on the time it took the barge convoy to completely pass the site. The beginning time is when the bow passed the instrument line, and the ending time is when the end of the tow passed the instrument line. In the field, all meter clocks were synchronized at the beginning of each day so that the records from all meters would have the same time bases. For the barge event depicted in figure 29, the beginning time (hour:minute:second) was 12:16:45, and the ending time 12:19:13.

Maximum return velocity, $U_{r(max)}$, was derived from return flow plots. Here, $U_{r(max)}$ is defined as the numerical difference between the average ambient velocity and maximum change in the x-component of velocity (from the 11-point moving average plot, not the point plots, which would be of greater magnitude) during the barge-tow event. For the specific example shown in figure 29, the values of various parameters are as follows:

Ambient velocity, $U_{ma} = 0.09$ m/s

Maximum return velocity, $U_{r(max)} = 0.22$ m/s (0.31 - 0.09 m/s)

Duration of the event = 2.5 min

It should be pointed out that the return velocity in this case is positive, i.e., the velocity increased in the downstream direction because the barge was moving upstream. (For downstream-bound barges, the return flow is negative, i.e., it moves in the upstream direction.) Thus when the barge-tow *Reliance* was moving in the upstream direction, the return velocity near the shoreline increased in the downstream direction. Values of U_{ma} , $U_{r(max)}$, and event duration were determined for all barge-tow events, and these values are presented in subsequent sections.

Maximum Drawdown and Wave Height

Figure 30 provides a schematic of maximum drawdown and waves. As a barge-tow convoy approaches a measuring site, such as the Kampsville site on the Illinois River, the water surface elevation starts to drop, creating what is called "drawdown," or H_d , as shown in figure 30. The maximum value of this water surface drop is called "maximum drawdown," $H_{d(max)}$. Similarly, after the initial drop in water surface elevation, the largest waves generated by the barge-tow movement are normally felt near the shoreline. This numerical value, i.e., the difference between the peak and trough of the maximum wave, is called "maximum wave height," $H_{w(max)}$. For all the events, the values of $H_{d(max)}$ and $H_{w(max)}$ were determined. These values are presented in subsequent chapters.

Suspended Sediment Concentration

Increases in suspended sediment concentrations at a measuring station were determined based on plots and data generated from the sediment samples collected at each site. Figure 31 shows a typical plot generated from the field data. Here, ambient suspended sediment concentrations were determined based on the average values of the suspended sediment samples collected in the field before an event. The maximum increase in suspended sediment concentration, $ISSC_{(max)}$, is defined as the difference between the ambient suspended sediment concentration and the maximum measured

sediment concentration. The "duration" for which the sediment concentration remained at an elevated level is the time span that it took for concentrations to return to the ambient conditions.

DATA PRESENTATION

Eight trips were made to five different sites on the UMRS to collect field data for this project. Site-specific analyses and data have already been reported in progress reports to the sponsors (Bhowmik et al., 1993a, b; 1994a-c). Data in this report are presented in the same format used in the progress reports, as outlined below.

I. Site Descriptions and Ambient Conditions

1. Date and time
2. Geographic location
3. Configuration of the cross section
 - Discharge
 - Slope
4. Location of sensors
 - Number of sensors
5. Composition of bed materials in the channel and channel border area
6. Water level 10 minutes prior to event
7. Water velocity prior to event
8. Water temperature prior to event
9. Suspended sediments

II. Traffic Characteristics

1. Date and time
2. Vessel characteristics, i.e., towboat HP/propeller type/size, tow length, and draft (as maximum and mean of draft of tow)
3. Tow configuration, i.e., number of barges in various arrays
4. Tow speed or recreational craft speed
5. Distance from centerline of tow to bank
6. Distance from centerline of tow to sensors
7. Wind wave

III. Event Characteristics

1. Date and time
2. Indication of time at which vessel passed the measurement cross section
3. Induced water velocities
4. Induced wave heights and drawdowns
5. Induced suspended sediment concentrations

Note that items denoted with bullets are included in this report, but were not included in the progress reports.

Site Descriptions and Ambient Conditions

Date, Time, and Geographic Location

Table 13 shows dates of the eight data collection trips and locations of the five sites. Most data collection instruments were installed in the channel border areas of the river. Table 14 gives some of the geomorphologic characteristics of the sites.

Cross-Sectional Configuration

Table 15 gives the average depth and top width for all cross sections. Additional information, such as the water discharge and slope of the water surface profile, is also given in this table.

An analysis of the discharge data shown in table 15 indicates that at the McEver's Island site, a discharge of 212 cubic meters per second (cms) was exceeded 86 percent of the time and at the Kampsville site (trip 1), a flow of 667 cms was exceeded 35 percent of the time. Similarly, for trip 2 at the Kampsville site, a flow of 329 cms was exceeded 65 percent of the time. For the five field trips made on the Mississippi River, the flow exceedence was 30 percent at Apple River, 93 percent at Clarks Ferry (trip 1), 99.5 percent at Clarks Ferry (trip 2), 95 percent at Goose Island (trip 1), and 99.5 percent at Goose Island (trip 2).

Water surface profiles were measured on each trip at least once a day. Appendix I shows data from the pilot trips and actual data collection trips. These data indicate that the average water surface slopes varied from about 0.05 m/km to 0.018 m/km on the Illinois River, and from 0.037 m/km to 0.069 m/km on the Mississippi River, except for trip 2 at Clarks Ferry, where the water surface slope was 0.011 m/km. Table 15 shows the average water surface slope for each trip.

Location and Total Number of Sensors

Sensor information is divided into four categories: 1) number of current meters, intake nozzles for suspended sediments, and wave gages used in the field; 2) lateral and vertical location of the current meters for each trip; 3) lateral and vertical location of the intake nozzles; and 4) distances of the wave gage from the shoreline in each trip.

Table 16 shows the total number of current meters, intake nozzles, and wave gages used during each field data collection trip. Tables 17 and 18 show the lateral and vertical locations of all velocity meters for all trips. Similarly, tables 19 and 20 show the lateral and vertical locations of suspended sediment intake nozzles used for all field trips.

Following are the distances (from the nearest shore) of the wave gage used at each site: Apple River Island – 5.2 m, Goose Island (trip 1) – 17 m, Kampsville (trip 1) – 7.6 m, Clarks Ferry (trip 1) – 15.2 m, Goose Island (trip 2) – 14 m, Kampsville (trip 2) – 9.2 m, and Clarks Ferry (trip 2) – 13.1 m. Wave data were not collected at McEver's Island, where, it should be emphasized, the goal was to collect preliminary data to test instrumentation. Since the same wave gage was used previously (Bhowmik et al., 1981c), this gage was not tested at McEver's Island.

Appendix II gives the relative location of sites on the Illinois and Mississippi Rivers and approximate locations of various sensors. For each site, the appendix shows the location of the primary transect on a navigation chart; a planform sketch of the site,

with sensor locations; and cross-sectional plots of the velocity and sediment towers, respectively.

Figures II-1 through II-4 give information on the McEver's Island site, figures II-5 through II-8 give information for the Apple River Island site, and so on. The figure depicting the navigation chart for each site is not repeated for the second field collection trips at Goose Island, Kampsville, and Clarks Ferry.

Bed Material Composition in Channel and Channel Border Areas

Appendix III gives the particle size breakdown of bed materials at all the sites. The sample locations at each cross section are also listed in this appendix. In addition to the various sizes (d_{10} , d_{16} , d_{50} , etc.), the following parameters were also calculated for each sampling site:

$$\text{Standard Deviation, } \sigma = \frac{1}{2} \left[\frac{d_{85}}{d_{50}} + \frac{d_{50}}{d_{16}} \right] \quad (43)$$

$$\text{Uniformity Coefficient, } U = \frac{d_{60}}{d_{10}} \quad (44)$$

The number of bed material samples collected at each site is as follows: McEver's Island – 13, Apple River Island – 22 (from two transects), Goose Island (trip 1) – 9, Kampsville (trip 1) – 10, Clarks Ferry (trip 1) – 34 (from three transects), and Goose Island (trip 2) – 12. Table 21 shows the ranges of averaged values for d_{50} within the main channel and channel border areas and indicates that the median diameter of bed materials varied from medium to coarse sands at all locations.

Water Level, Velocity, and Temperature

Appendix IV gives ambient water level and water temperature data for all the sites. These data are shown for each site and for various times during every data collection trip. Appendix V shows the values of measured water discharge, computed average velocities, and computed water depths at all the study sites.

Suspended Sediment Concentration

Appendix VI gives the suspended sediment data collected to represent ambient conditions at all sites.

Traffic Characteristics

Appendix VII organizes and presents nonrecreational traffic characteristics, including date and time, vessel characteristics, tow configuration, tow or recreational craft speed, distance from centerline of tow to bank, distance from centerline of tow to sensors, and wind wave. Appendix II gives the relative distances of the sensors from the barge-tows.

The total number of barge-tows that passed each test site for the duration of the field data collection period is as follows: McEver's Island – 13, Apple River Island – 41,

Goose Island (trip 1) – 16, Kampsville (trip 1) – 25, Clarks Ferry (trip 1) – 33, Goose Island (trip 2) – 47, Kampsville (trip 2) – 22, and Clarks Ferry (trip 2) – 28. This indicates that data from a total of 225 barge-tow events were collected from the Illinois and Upper Mississippi Rivers during this project.

Appendix VIII gives recreational traffic characteristics, such as type of vessel, date and time of passage, relative speed, estimated distance from the shoreline, estimated length and direction of movement for all trips.

Following is a summary of the wind-wave data collected at each site, except for McEver's Island, where a wind gage was not installed.

Wind-Wave Data

Kampsville. In general, winds with sufficient magnitudes and prolonged duration were not observed, except on one day in these two trips. On October 17, 1990, persistent winds occurred, and a segment of wind-wave data was recorded between 14:03:24 and 14:12:34. This wind-wave plot is included in Appendix IX. The maximum wave height was 0.11 m, and the significant wave height was 0.053 m. The mean wave height was 0.037 m, and the mean wave period lasted 3 seconds.

Appendix IX summarizes wind direction and speed during trip 1. Speeds varied from about 1 to 8 mph. Except for the afternoon of October 17, wind speeds were low, and no significant visible wind-generated waves were observed.

Apple River Island. Wind speed (Appendix IX) varied from about 0.2 to 6.5 mph. No wind-wave data were recorded at this site.

Goose Island. No wind-wave data were collected at this site. Wind speeds during trips 1 and 2 (Appendix IX) varied from about 0.5 to 11 mph and 1 to 10 mph, respectively.

Clarks Ferry. Because of the presence of numerous large trees around the bankline, no measurable wind-generated waves were observed at the site. Wind speeds (Appendix IX) varied from about 1 mph to 4 to 5 mph.

Event Characteristics

Event characteristics include date, time of passage, induced water velocities, induced wave heights and drawdowns, and induced suspended sediment concentrations.

Appendix X shows the date, passing time, and mean ambient velocities before a barge-tow event for all field trips and data from all the meters. In this appendix, all data have been organized according to collection site. The first two pages of the appendix show the data collected at McEver's Island, and so on.

In Appendix X, U_{ma} and V_{ma} indicate the mean ambient velocities in the longitudinal and lateral directions, respectively. Both of these velocities were determined based on velocity data collected for a period of 15 minutes before a barge-tow event. The authors have noted that a few of the U_{ma} values were quite different from those of other meters and were lower than what one would expect at those locations. Meters were checked before each trip; and data were checked during downloading from meters in the field. Reasons for these discrepancies could be that these meters were subject to the influence of local geometry or other factors such as flowing debris. However, since these

meters still functioned properly in the field, they still recorded the changes during traffic events. Removing the ambient values produced net changes comparable to those recorded on other meters. It is for this reason that the authors kept these meters in the report. These meters include S4/071 (McEver Island trip); S4/151, S4/834, and S4/832 (Clarks Ferry trip 1); and S4/040 (Clarks Ferry trip 2).

Appendix XI shows the changes in velocity that were observed during the passage of navigation traffic at all sites for all events. Here, U_{im} and V_{im} indicate the maximum induced velocities in the longitudinal and lateral directions, respectively. It must be pointed out that these impact velocities, U_{im} and V_{im} , are the net induced velocities; i.e., the ambient velocities at all the metering sites were subtracted from the maximum measured velocities. All the were been organized sequentially starting with McEver's Island and ending with Clarks Ferry (trip 2).

Appendix XII shows the maximum wave height ($H_{w(max)}$) and maximum drawdown ($H_{d(max)}$) at all sites for all events.

Appendices XIII - XVIII present suspended sediment data collected at all the test sites according to the format established for the progress reports (Bhowmik et al., 1994a-c, 1993a-b). Data were organized by site for all the field trips. It should be noted here that suspended sediment samples were not collected for trip 2 at the Kampsville and Clarks Ferry sites.

Database Organization

Digital data were prepared in ASCII format and submitted to the sponsors with the progress reports (Bhowmik et al., 1993a-b and 1994a-c). The directory structure was organized as follows. One directory was created for each trip. Within each directory, velocity, wave and drawdown, and sediment sub-directories were created to identify the types of data reported. Since different types of current meters were used for data collection, sub-directories were created under each of the velocity directories and named after the meters. These data were organized using an INFORMIX-SQL database (gwinfo) on a UNIX-based machine, at the ISWS. This database management system is based on the relational model or a relational database management system (RDBMS). Appendix XIX contains a description of the eight databases for each of the field data collection sites.

GENERAL ANALYSES

Traffic Characteristics

Figure 32 shows the number of events that were observed at the test sites each day of the collection period during daylight hours. The maximum number of daily events was nine, and the minimum was one. The number of barges in convoys for all the test sites (figure 33) varied from a single tow to 24 barges (for a single event). Normally the maximum number of barges in a convoy is 15 with a configuration of three barges wide and five barges long. However, irregular configurations are also common. The average number of barges for each trip varied from 6 to 12.

Figure 34 and 35 respectively, show the width and length of the barge convoys for all trips. Figures 36 and 37, respectively, show the draft of all barge-tow convoys and the distance of the centerline of the convoys from the measuring shoreline.

Figures 38 and 39, respectively, show barge speed and horsepower for all the tows. The speed of the barges varied from about 1 to 6 m/s. The maximum horsepower was a little more than 6,000 HP, and the minimum was about 200 HP.

Figures 40 and 41, respectively, plot the draft to depth ratios and blocking factors for all events. From these two plots, it appears that the maximum draft to depth ratio was about 0.9 at the McEver's Island site on the Illinois River, and the minimum was 0.1 at the Goose Island site (trip 1) on the Mississippi River. Higher draft to depth ratios indicate that the bottoms of the barges were relatively closer to the river bed, which accounts for the increased probability of high impacts to the bed and/or surrounding banks.

The blocking ratio indicates the relative area of a channel that is occupied by traffic. The higher the blocking ratio, the higher the water area that will be disturbed by moving traffic. Figure 41 indicates that for the Illinois River at McEver's Island, the blocking factor was as high as 0.12, indicating that about 12 percent of the cross-sectional area of the river was occupied by the moving barges. This is a relatively high percentage of area to be disturbed by traffic. The lowest blocking ratios were observed on the Mississippi River.

Tables 22 and 23, respectively, show blocking and draft to depth ratios for all the trips and for upstream-bound and downstream-bound barges. In general, downstream-bound barges had higher blocking factors than upstream-bound barges. The mean value for blocking factors varied from 0.024 at Clarks Ferry (trip 2) to 0.115 at McEver's Island.

Table 24 shows the average values of flow velocity (V), discharge (Q), blocking factor (BF), draft to depth ratio (DR), length Froude number (F_l), and depth Froude number (F). The Illinois River had higher BF and DR than the wider and deeper Mississippi River. It is suspected that the impact of tow movement on the channel bed may be less severe for DR values less than 0.5. Thus the Illinois River may be subjected to relatively greater impact than the Mississippi River. At reaches similar to the Kampsville site, the differences in BF and DR between two trips were not significant, even though the earlier trip had much higher discharges than the later one.

In terms of relative speed (i.e., measured speed), downstream-bound and upstream-bound barges were about the same. However, in terms of absolute speed (measured speed minus channel flow speed), the upstream-bound barges were much faster than the downstream-bound barges. Therefore, much more energy was input to the river by upstream-bound barges. Additionally, the absolute speeds on the Mississippi River were higher than those observed on the Illinois River.

Other tow characteristics are related to the system of propulsion, i.e., horsepower and whether or not the tows have open wheels or Kort nozzles. Figure 42 provides the distribution of open wheels and Kort nozzles for all the barges in comparison to their respective horsepower. It appears that the majority of towboats were in the 4,500-HP range.

Data collected by the ISWS from 1988-1991 appear to be representative of the towboats that travel on the Illinois and the Upper Mississippi Rivers. Figure 43 compares the ISWS data with data from a 1978 USACOE study. In almost all classes, the ISWS data on towboat horsepower are similar to those reported by the USACOE.

Maximum Return Velocity

Maximum return flows, $U_{r(max)}$, are positive for upstream-bound barges and negative (against the normal river flow) for downstream-bound barges. Absolute values (i.e., the magnitudes) are used here to simplify the evaluation.

Because $U_{r(max)}$ was measured at various stations and at different distances from the barge, data are subdivided into various categories based on the location of the meter relative to the center of the barge. Figure 44 explains this coordinate system, where y indicates the distance of the sensor from the barge and W_T indicates the top width of the river. The ratio of y to W_T indicates the relative distance of the meter that measured from the center of the barge. Thus the area from the barge to the shore has been subdivided into six zones: with y/W_T values from 0 to 0.15, 0.15 to 0.30, 0.30 to 0.45, 0.45 to 0.60, 0.60 to 0.75, and more than 0.75. Table 25 gives the values of $U_{r(max)}$ for each zone for all the field trips.

General observations can be made as follows:

- Higher return flows occurred at the McEver's Island site, which has the largest blocking factor.
- In general, upstream-bound barges produced slightly higher return flows at zones closer to the barge as well as near the shore.
- The mean $U_{r(max)}$ in each zone had a tendency to attenuate toward the shore, except at the McEver's Island site, which showed a reverse trend. The rate of decrease was also not obvious at the Kampsville site for upstream-bound barges.
- A comparison of data from sites that were visited twice shows higher return flows occurring at higher discharges in zones closer to the barge. This may be related to the higher horsepower required to push the barge convoy. The trend is most visible in trips to the Kampsville site, where BF and DR were comparable, but the river flow for trip 1 was much higher than for trip 2.

Table 26 gives the minimum and maximum values of $U_{r(\max)}$, which can be used to determine the range at each site. An examination of the extreme values of $U_{r(\max)}$ indicates that:

- Not all traffic produced significant values of $U_{r(\max)}$ especially at zones closer to the barge. Fairly small $U_{r(\max)}$ did occur near the barge for both the upstream-bound and downstream-bound barges.
- Sites on the Illinois River had higher $U_{r(\max)}$ values than those on the Upper Mississippi River.
- The highest measured $U_{r(\max)}$ on the Illinois River was 0.69 m/s, while on the Upper Mississippi River it was 0.32 m/s.
- Larger $U_{r(\max)}$ were measured at zones away from the barges. The occurrences were measured from both upstream-bound and downstream-bound barges.
- Higher $U_{r(\max)}$ values occurred at zones closer to the barges during higher discharges. This was measured from Kampsville and Goose Island sites for both upstream-bound and downstream-bound barges.

Table 27 shows the most frequently occurring intervals (MFOIs) of $U_{r(\max)}$ for barges at all sites. The MFOI indicates the most likely occurrence of $U_{r(\max)}$ at a given zone. General observations from this table are as follows:

- The MFOIs of higher $U_{r(\max)}$ occurred with higher discharges on the Illinois River. However, higher or equivalent MFOIs of $U_{r(\max)}$ occurred with lower discharges on the Upper Mississippi River. This may indicate that there is a critical BF value at which higher $U_{r(\max)}$ might be expected.
- Even at narrow reaches such as the McEver's Island site, the MFOIs did not differ from other sites. One exception was found in zones near the shore at McEver's Island, where MFOIs of higher $U_{r(\max)}$ were observed.

Table 28 shows the mean values of $U_{r(\max)}$ for each river, and table 29 gives the MFOIs. From these two tables the following observations can be made:

- For both the Upper Mississippi and Illinois Rivers, the mean values of $U_{r(\max)}$ in zones near the shore were somewhat higher than at other locations.
- The mean $U_{r(\max)}$ on the Illinois River was higher than that on the Upper Mississippi River.
- The attenuation of mean $U_{r(\max)}$ from barge to shoreline was steeper on the Upper Mississippi River than on the Illinois River.

Table 30 shows the statistical properties of $U_{r(\max)}$, such as maximum, minimum, arithmetic mean, median, standard deviation, and standard error for all the trips to the sites. This table indicates that the maximum value of $U_{r(\max)}$ on the Illinois River was 0.69 m/s, and the maximum value on the Mississippi River was 0.32 m/s. The minimum value on the Mississippi River was 0.01 m/s, and the minimum value on the Illinois River was 0.02 m/s. As was expected, the impact of navigation traffic on return velocity was greater in the shallower and narrower Illinois River than it was in the deeper and wider

Mississippi River. Appendix XX shows a sample of plots for altered velocity regimes on both rivers.

$U_{r(max)}$ data have been divided into three additional categories: upstream-bound barges, downstream-bound barges, and all barge events. Appendix XXI gives histograms of these data. An examination of the histograms shows that $U_{r(max)}$ values within most zones have skewed distributions, and some of them may have bimodal distributions. Since the number of data points in each zone for each trip is generally less than 30, it is not possible to use the sample mean for the population mean. But it should be noted that the difference between the mean and the median is fairly small within each zone for all the trips and also for the upstream-bound and downstream-bound barges.

Maximum Wave Height

The maximum wave height, $H_{w(max)}$, measured at each of the sites was analyzed to determine the range (interval between the maximum and minimum values) and the mean. Table 31 gives these values for upstream-bound barges, downstream-bound barges, and all barges. Following are some general observations that can be made from this table:

- The mean values for upstream-bound and downstream-bound barges did not show significant differences.
- Although the range of $H_{w(max)}$ varied between trips, values typically ranged from 0.09 to 0.12 m.
- The largest wave, 0.66 m high, was produced at Goose Island during trip 1 by a work barge (a buoy tender). Configurations such as single tows or one barge pushed by a tow produce relatively large waves. In this case, the barge caused large deviations between mean and median, and skewed the values for that trip.
- Comparing the mean values of $H_{w(max)}$ at sites visited twice suggests that higher $H_{w(max)}$ occurred on trips with higher discharges. For instance, the first trip to Goose Island had the highest discharge among all the trips and also showed the highest mean value of $H_{w(max)}$. Conversely, the McEver's Island trip had the lowest discharge and the lowest mean value of $H_{w(max)}$.

A possible explanation to the last observation includes that more power was used at higher discharges to overcome the flow's forces or the differences in channel geometries and other factors. Table 32 gives the mean and the range of $H_{w(max)}$ for both rivers. These data show that the direction of barge traffic had little effect on the magnitude of $H_{w(max)}$. In general, the mean was about the same on both rivers, and the measured maximum wave height occurred on the Mississippi River. However, if the single maximum wave height measured at the Goose Island site is removed, then the range would be similar on both rivers.

Appendix XXII shows selected time histories of waves and drawdown generated by the movement of navigation traffic on the Illinois and Mississippi Rivers. Appendix XXIII gives general analyses of $H_{w(max)}$ as in histograms.

Maximum Drawdown

Maximum drawdown, $H_{d(\max)}$, for all sites was analyzed to determine the range and mean for each trip. Table 33 shows the results of these analyses, and table 34 shows the mean values and ranges of $H_{d(\max)}$ for each river. Appendix XXIV contains histograms of maximum drawdown. Several observations can be made concerning drawdown:

- Higher $H_{d(\max)}$ occurred at narrower reaches.
- The maximum measured $H_{d(\max)}$ (0.24 m) occurred at the McEver's Island site. Of all the sites, this location had the narrowest channel width, the shallowest depth, and the highest $U_{r(\max)}$ near the shore. This site also had the highest mean and median $H_{d(\max)}$.
- Somewhat higher $H_{d(\max)}$ was measured for barges traveling in both directions at the Kampsville site on the Illinois River. These values also occurred at higher discharges. However, such an observation cannot be made for sites on the Upper Mississippi River. Although many predictive relationships for drawdown are correlated with return flow, the mean $U_{r(\max)}$ in table 28 does not indicate such a direct correlation. Obviously, factors associated with channels, geometry, etc., can affect this correlation.
- Mean values of $H_{d(\max)}$ for sites on the Illinois River were as much as twice those on the Upper Mississippi River.

Apparently blockage ratio is an important factor on the magnitudes of drawdown.

Velocity Structure

Barge-tow movements interact with the ambient velocity structure at a river cross section, creating complicated flow regimes and distributions. However, field data showed that increases and/or decreases in net velocity in either the vertical or lateral direction are related to barge loading and maneuvering characteristics, including speed, draft, distance, and direction of movement. Several plots have been developed from field data to illustrate the relationship between velocity changes and these factors.

Figure 45 shows the typical changes in longitudinal velocity components at three elevations at the Kampsville site (trip 1) during the movement of two barge-tow convoys, *Mr. Aldo* and *Floyd Blaske*. Specific information on these two barge convoys is given in the figure. *Mr. Aldo* was moving downstream, so the consequent changes in return velocity were in the upstream direction (i.e., reducing the ambient velocity). The absolute average velocity at an elevation of 0.3 m above the bed decreased from about 0.3 m/s to about 0.03 m/s. Similar decreases in velocity were also measured at elevations of 1.2 m and 2.4 m above the bed. Approximately 15 minutes later, *Floyd Blaske* passed the site in the upstream direction, and the longitudinal velocity increased at all elevations. The increase was about 100 percent at an elevation of 0.3 m above the bed.

The variations shown in figure 45 were observed at most sites even though the magnitudes of increase were different. Appendix XX gives some sample plots of velocity changes.

Figure 46 shows the lateral distribution of $U_{r(\max)}$ due to the movement of barge-tow convoys for four upstream-bound barge convoys at Kampsville. An examination of this figure indicates that the maximum net increase in velocity due to the passage of the barge convoy *Jeff Boat* was about 0.36 m/s at a distance of about 50 percent of one-half the width of the river. *Jeff Boat* was pushing a three-by-five convoy with a draft of 2.74 m, and moving at a speed of 1.88 m/s. Examination of this and other figures indicates that fully loaded convoys with this configuration (three-by-five) were generally associated with large increases or decreases in longitudinal velocity within the channel border areas of the river.

Figure 46 also shows data from barge-tow convoys moving downstream at Kampsville. Similar variability in $U_{r(\max)}$ in the lateral direction was observed at other sites as well, as shown in figure 47 for Apple River Island on the Mississippi River.

The movement of navigation traffic also changes the velocity profile in the vertical direction. Figure 48 shows the $U_{r(\max)}$ in the vertical direction for many of the traffic events depicted in figure 46. This figure not only demonstrates that the movement of barge traffic changes the ambient vertical velocity profile, but also shows that the magnitude of these changes is related to the barge configuration, draft, and direction of movement. For example, for the barge-tow convoy *Jeff Boat*, moving upstream, the maximum increase in net velocity was more than 0.3 m/s. Similarly, for the convoy *Mary Ann*, also moving upstream but pushing empty barges, the maximum increase in velocity was less than 0.1 m/s.

The velocity structure normally changed in both the lateral and vertical directions; in fact, the resultant velocity sometimes rotated 360 degrees before it re-established its normal pattern after the passage of the barge-tows. Figures 49 and 50, respectively, show the changes in the total velocity vectors for a period of 30 minutes at three different locations on the Illinois River (McEver's Island site) for one upstream and one downstream barge convoy. An examination of figure 49 (an upstream-bound barge) shows that the total velocity vector essentially rotated 360 degrees for the meter close to the shore, while at the two locations away from the shore the magnitude of velocity increased by about 300 to 400 percent. This indicates that upstream-bound barges increased the velocity by several hundred percent at this shallower and narrower reach of the Illinois River. However, figure 50 indicates the variability of the velocity vectors was somewhat different for the downstream-bound barge. The barge convoy in this case essentially caused the velocity vector to rotate by 360 degrees at all three locations.

The alteration of velocity vectors due to barge-tow movements was also observed at other sites for a variety of barge-tow configurations and distributions. Figures 51-54 show the vectors of net velocity at each meter during barge passage. As can be seen from these figures, the velocity vector changed over time and with the advent of the tow traffic. The duration of velocity alteration varied from meter to meter, but the alteration of the velocity structure due to traffic movement was detected at all metering sites. In fact, at all meters, the altered velocity regimes were detected almost instantaneously or slightly before the passage of a barge-tow convoy. This suggests that the movement of barge-tows can disturb the entire water body within a river cross section.

Figure 55 depicts a temporal history of velocity data collected during the passage of a barge-convoy (Bhowmik et al., 1991) for the Illinois River at McEver's Island. The

velocity component in this figure is again parallel to the direction of the main flow. Even though not all meters were located at the same elevations at all stations, comparisons can be made about the changes in velocity at various locations for the same event and for the same time interval.

The tow *Reliance* pushed 15 barges upstream with an effective (average) draft of 2.1 m at a speed of 2.63 m/s (figure 55). The net increase in velocity at 10.7 m from the shore was higher than the increase observed at distances of 15.2, 37, and 45.7 m from the shore. Moreover, 0.15 m above the bed, increases at distances 10.7 and 37 m from the shore were higher than those observed 0.92 m above the bed at a distance of 15.3 m. The net increase in flow velocity was as much as 0.4 m/s, and the increase lasted for about 3 minutes. Figure 55 also illustrates the time lag between maximum increases in velocity at various locations. The increased velocity was initially felt close to the shore before it was felt at locations away from the shoreline.

Figure 56 shows the changes in velocity at six different meters when the tow *W.C. Norman*, pushing 12 fully loaded barges, moved downstream at a speed of 1.95 m/s. Again, the changes shown are the net velocity changes obtained by subtracting the ambient velocity (approximately 0.35 m/s as averaged value. Though the ambient velocity at each meter was used to obtain the net velocity at that meter) from the measured velocity during this event. It is clear that the downstream movement of this barge-tow configuration generated return flows in the upstream direction that were strong enough to temporarily alter the direction of flow at all locations. Figure 56 also indicates that changes in velocity were higher near the bed than away from the bed. The return flow was as much as 0.3 m/s and lasted for about 3 minutes.

Velocity components perpendicular to the main flow (figure 57) demonstrate that the pattern of altered velocity regimes was quite complex and that the return flow did not only move parallel to the shoreline. The resultant velocity should be considered in any further analyses even though the velocity component parallel to the shoreline is normally considered in one-dimensional modeling efforts.

Following are some general observations concerning velocity changes:

- Upstream-bound barges increased the longitudinal velocity, while downstream-bound barges decreased the longitudinal velocity within channel border areas.
- The increases and/or decreases in velocity were as much as 300 percent or more of ambient velocity or more.
- Higher increases/decreases in net velocity were normally associated with fully loaded barges.
- Velocity increased/decreased rather uniformly in the water column (depth).
- In some cases, velocity vectors rotated 360 degrees due to the passage of barge-tow convoys, especially those moving in the downstream direction.
- In some cases, the velocity field in the whole cross section was disturbed by the movement of barge-tow convoys.
- Altered velocity regimes lasted from about 2 minutes 30 seconds to as long as 4 to 5 minutes.
- The rotating characteristics of velocity should be considered in any future modeling effort.

Additional Findings

This research afforded an opportunity to gather a substantial amount of field data from the Illinois and Mississippi Rivers. These data were used in additional analyses of the hydrodynamic behavior of large floodplain rivers (Bhowmik et al., 1995b; Mazumder et al., 1991, 1993). These analyses were extremely useful in describing the turbulence characteristics of large rivers and how they vary during commercial navigation traffic.

The analyses indicated that velocity, velocity fluctuation, turbulence intensity, and turbulence shear stress were all relatively high toward the main channel area. Moreover, all of these flow parameters decreased toward the channel border areas. Therefore, the main channel area above the river bed is the most active zone as far as turbulence is concerned. These observations are important in understanding the creation of turbulent eddies, sediment transport processes, and bank erosion mechanisms. It should also be noted that the turbulence intensities (x- and y-components) and turbulence shear stress were found to be high at elevations 10 to 20 percent of the depth from the bed.

Turbulence velocity data collected during barge-tow events suggest that the maximum turbulence shear stress generated by barge movement at a dimensionless distance of about 0.8-0.9 from the centerline of the channel (dimensionless distance is presented in terms of $y/(W_T/2)$, see Mazumder et al., 1993) is as much as ten times higher than that averaged over the duration of background velocity. The movement of barge traffic in a river can generate larger eddies and more transverse shear than natural river flows.

The qualitative behavior of longitudinal turbulence intensity distribution for both upstream- and downstream-bound barge movements was similar, whereas the behavior of the transverse turbulence intensity was somewhat different. The intensity of the longitudinal turbulence velocity component had a higher value than the transverse component. This is quite comparable to the turbulent boundary layer near the wall in a closed channel. In fact, the turbulence intensities following events in both longitudinal and transverse directions were as much as four times the background turbulence intensities.

The turbulent kinetic energy generated by the event increased, reached a maximum value between 0.8 and 0.9 of $y/(W_T/2)$, and then decreased. This shows that the maximum turbulent kinetic energy produced by velocity changes is significantly higher than background values in a natural river.

Suspended Sediment Concentrations

Appendix XXV gives a set of typical plots depicting suspended sediment increases during barge-tow events on both rivers. The corresponding histograms for these increases are also presented (Appendix XXVI). Data similar to those shown in these appendices were analyzed to determine the mean increases in suspended sediment at zones away from the barges. Table 35 shows the mean increase in suspended sediment concentrations at various zones from the sailing line for all field trips, and table 36 shows the range of increase in suspended sediment concentration for all field trips. Following are some general observations from these two tables:

- For data collected in channel border areas, the mean increase in suspended sediment was generally higher near the shore than near the sailing line. Adams (1992) and Adams and Delisio (1991) reported similar observations.
- The increase in suspended sediment concentrations in channel border areas varied from no change to as high as 426 mg/L on the Illinois River. The maximum increase occurred at the McEver's Island site, which also had the highest values of drawdown and return velocity.
- On the Upper Mississippi River, the increase in suspended sediment concentration varied from no change to as high as 248 mg/L in the channel border areas. The maximum increase occurred at Apple River Island. Note that bed material in the channel border area at this site was finer than at the other two Mississippi River sites. Higher drawdown and wave heights were also observed at the Apple River Island site.
- In a few sediment samples taken from stations close to the barge during trip 2 at Goose Island, the increase in suspended sediment concentration was fairly small. This was associated with the relatively small DR values at this site (table 23).
- On the basis of collected data, downstream-bound barges produced higher mean values and a wider range of suspended sediment concentration values than upstream-bound barges.

Table 37 shows the mean increased suspended sediment concentration for each river, and table 38 shows the range of increased suspended sediment concentrations. An examination of these tables shows that the largest increase in suspended sediment concentrations occurred at a distance of approximately 20 percent of the width of the river from the shoreline.

Table 39 shows the maximum, minimum, arithmetic mean, median, standard deviation, and standard error of estimate for suspended sediment concentration increases for all sites. The table shows that the Illinois River had relatively large increases in suspended sediment concentrations compared to increases on the Mississippi River. This was also found to be true in terms of the standard deviation values, 70 mg/L on the Illinois River and 34 mg/L on the Mississippi River.

The variability of suspended sediment concentrations during a barge-tow event can be illustrated with a set of time series plots at various locations in the lateral and vertical directions. Figure 58, for example, shows such variations induced by the towboat *Mobil Leader*, which had twin screws, 5,000 HP (725 kw), and ducted or Kort nozzle propellers. The tow was pushing a six-wide loaded barge with a 2.74-m draft, sailing about 122 m from shore in the upstream direction at a speed of 3.62 m/s. The three parts of figure 58 illustrate the changes in suspended sediment concentration at three stations and two to three different elevations. These data were taken from the near-shore zone, where the bed material of approximately 40 percent sand, 40 percent silt, and 20 percent clay.

For station a, located 14 m from shore, the maximum increased suspended sediment concentration 0.15 m above the bed was about 10 to 12 times the ambient sediment concentration. Similarly, 0.6 m above the bed, the increased concentration was about six to seven times the ambient concentration. These increases were smaller than

those at the other two stations (station b, 18 m from the shore, and station c, 24 m from the shore). However, in all cases, there is a distinct trend: the increase in suspended sediment concentration near the bed at the 0.15 m elevation was always greater than those observed at the 0.6 m, 1.2 m, or 1.8 m elevations. As a matter of fact, there was a vertical gradient at all the stations; that is, the increase in concentration was greatest near the bed with a gradual decrease toward the surface. It should be pointed out here that the top intake at all locations was about 0.75 m below the water surface. Data collected from other barge events showed similar variability.

The variability in increased suspended sediment concentrations at different elevations and at various sites is further examined using the ratio in figure 59, for a single barge-tow event on the Upper Mississippi River at the Goose Island site. Here the ratio of the peak and average increases is shown against the average ambient suspended sediment concentration. Appendix XXVII shows similar variability at several other locations, especially in the vertical direction. Figure 58 shows that the increased suspended sediment concentrations took from half an hour to several hours to settle. Because barge-tow events can occur several times a day, the daily variability of suspended sediment concentrations is illustrated below for several barge-tow events at two sites, Goose Island and Kampsville.

Goose Island

The Goose Island site is located at RM 319.3 in Pool 21 of the Mississippi River, about 9 km downstream of Lock and Dam 21 at Quincy, Illinois. During the survey, the main channel was 400 m wide. The average depth increased from 5 to 6 m between August 20 and August 29, 1990, and the main channel discharge increased from 1,600 to 3,000 cms in this period. Ambient sediment concentrations were similar at all intakes, with daily average ambient concentrations decreasing from about 200 to 170 to 160 mg/L and then increasing to about 190 mg/L on successive days of sample collection. The average tow passing the site had 12 barges traveling at a speed of 2.5 m/s, and passed 310 m from shore. Appendix VII gives traffic characteristics recorded at this site.

Suspended sediment samples were collected during 14 of 17 barge-tow passages at the site. Five sediment intakes were mounted on three support structures: station a, with intakes 0.23 m above the bed in water 0.60 m deep, 8 m from shore; station b, with intakes 0.23 and 0.61 m above the bed in water 1.2 m deep, 16.5 m from shore; and station c, with intakes 0.23 and 1.52 m above the bed in water 2.1 m deep, 26 m from shore. On August 25, 1990, a triple passage event with one downstream-bound tow and two upstream-bound tows occurred within a half-hour period and one double passage event with one downstream-bound tow and one upstream-bound tow occurred within 15 minutes. Figure 60 shows a daily record for the intakes at stations a1 and c1 and times of passage by the tows.

During an individual event the concentration at each intake varied (figure 60). For the nine single tow events the duration of increased concentrations ranged from 19 to 50 minutes and averaged 36 minutes with a standard deviation of 9 minutes. Table 40 summarizes statistics for all events for intakes a1 and c2. The event increase values show the average increase above ambient levels during the event. Event maximum and

minimum values represent the largest and smallest increases above ambient values during any event.

Kampsville

Figure 61 shows similar daily variability for the Kampsville site (RM 35.2) on the Illinois River, approximately 56.6 km upstream from the river's junction with the Mississippi River at Grafton, Illinois. During the survey, the channel was 300 m wide. The average depth increased from 3.4 to 4.0 m between October 10 and October 19, 1990, and the main channel discharge increased from 410 to 775 cms in this period. Ambient suspended concentrations varied spatially and temporally, with higher concentrations at the bottom intakes and at the stations further from shore. Ambient concentrations ranged from about 1,000 mg/L the first day at intake a1 to about 400 mg/L at intake c1 on the second and third days. Twenty-nine barge-tows passed the site during this time. The average tow had 11 barges, traveling at a speed of 2.7 m/s, and passed 140 m from shore. Appendix VII gives traffic characteristics recorded for this site.

Seven sediment intakes were mounted on three support structures: station a, with intakes 0.15 and 0.46 m above the bed in water 0.60 m deep, 7.6 m from shore; station b, with intakes 0.15 and 0.76 m above the bed in water 1.6 m deep, 15.2 m from shore; and station c, with intakes 0.15, 0.91, and 1.37 m above the bed in water 2.4 m deep, 23 m from shore. Sediment samples were collected for one continuous event during which two downstream-bound tows and three upstream-bound tows passed within a three-hour period. Samples were also collected from two double events, one with two upstream-bound tows within 5 minutes, and the other with one upstream-bound tow and one downstream-bound tow within 40 minutes. Figure 61 shows a daily record for intakes a1 and c1 and indicates the times of passage of the tows.

Events lasted an average of 44 minutes with a standard deviation of 12 minutes and ranged from 30 to 62 minutes. The event sampling schedule produced samples for all 16 tows (15 events) at station a, 10 events at station b, and 8 events at station c. Table 41 summarizes statistics for all events at intakes a1 and c3. Event increase values represent the average increase above ambient levels during the event. The event maximum and minimum values represent the largest and smallest increases above ambient values during any event. Increases were largest near the shore.

All Sites

Plots of daily suspended sediment concentration changes due to barge events have been developed for all the sites (see appendix XXV). A parallel analysis of the ratios of increased suspended sediment concentrations during an event to ambient suspended sediment concentrations was performed for each intake. Table 42 shows the minimum, average, and maximum ambient suspended sediment concentrations measured at each site for each trip and for each individual sampling intake. The minimum ambient suspended sediment concentration was 28 mg/L at the McEver's Island site at intakes a1 and a2, and the maximum concentration was 563 mg/L at intake c1 at the Kampsville site during trip 1.

The event/ambient ratios varied widely (table 43). The maximum ratios were observed on the Illinois River at McEver's Island, where at intake a1, the ratio was a little

over 13, indicating a 1,300 percent increase in suspended sediment concentrations. The minimum increase in suspended sediment concentrations during an event was about 10 percent.

Some conclusions on suspended sediments are outlined below:

- Suspended sediment concentrations were found to increase relatively more within the near-shore zone than in the zone close to the main channel.
- The relative increase in suspended sediment concentration at the bottom intake at McEver's Island (Illinois River) was as much as two times the increase observed at the bottom intake at Apple River Island (Mississippi River).
- Higher ambient suspended sediment concentrations were recorded during trip 1 at both the Kampsville and Goose Island sites. Although the relative increases in suspended sediment concentrations at both sites and all elevations were similar, these increases were smaller than those observed when the ambient suspended sediment concentrations were smaller.
- The increase in event suspended sediment concentrations in the water column was similar to that for ambient conditions.

Turbidity

It is well established that an increase in suspended sediment concentrations can indicate an increase in the turbidity level of the water. However, it must be noted that turbidity is the optical property of water, and it may or may not correlate well with suspended sediment concentrations. Turbidity was measured from an Orbico-Hellige nephelometric turbidimeter that was set up with suspended sediment sample collectors. Vinyl tubing from the intake nozzles was connected to a Masterflex peristaltic pump for turbidity measurement and then routed to a flow-through cell in the Orbico-Hellige nephelometric turbidimeter. Data on turbidity were collected from a number of sites during routine suspended sediment sampling and developed into plots, such as those for McEver's Island (appendix XXVIII).

Comparison with Suspended Sediment Concentrations

Adams and Delisio (1991) analyzed turbidity and suspended sediment data, and their observations are reported here. Their data were obtained in June 1989 at McEver's Island, RM 50.1 on the Illinois River (80.6 km upstream of the confluence with the Mississippi River). The river flow rate was 594 cms, approximately the average flow rate, and it was exceeded about 38 percent of the time. The average depth was 3.78 m and the average velocity was 0.57 m/s. The suspended sediment load was 11,700 mt/d (135 kg/sec), with an average concentration of 225 mg/L. Bed material was primarily sand in the center of the river and a mixture of sand, silt, and clay near the shore.

As described by Adams et al. (1989), sediment and turbidity were sampled at fixed points in the river. The intake support structure was located 25 m from shore at a water depth of 2 m. Suspended sediment concentration samples were collected 0.91 m (36 inches) above the river bed, and turbidity was measured at 0.45 m (18 inches) and

0.91 m (36 inches) above the river bed. The bed material composition in the vicinity of the intakes was about 40 percent sand, 40 percent silt, and 20 percent clay.

Figure 62 shows the turbidity in nephelometric turbidity units (NTU) and the suspended sediment concentration in mg/L versus time at the 0.91-m elevation. During the measurement period, the suspended sediment concentration at this elevation decreased from 215 to 180 mg/L. A similar decrease in turbidity was observed at both intake levels. Both regression equations (with an initial time of 0000 hours) have the same decay coefficient. The suspended sediment concentration shows a standard deviation above the regression line of 7.5 mg/L and a maximum difference of 53.7 mg/L, while turbidity has a standard deviation of 1.8 NTU and a maximum difference of 7.9 NTU. Other simultaneous turbidity and suspended sediment concentration data sets (e.g., tow passage data sets) also show less variability for turbidity than for sediment concentrations.

Figure 63 shows a scatter plot and the regression line between the suspended sediment concentration and turbidity at the 0.91-m elevation, which depicting considerable scatter. Note that r^2 is only 0.52 for the linear least-squares regression line. This regression equation, $C_s = 15.6 + 130 \text{ NTU}$, was used to calculate suspended sediment concentrations at the 0.45-m elevation from the measured turbidity values at the same level (figure 64).

The set of turbidity data plotted in figure 64 shows somewhat more variation than the set at the 0.91-m elevation, with a standard deviation of 3.5 NTU and a maximum difference of 20.3 NTU. The difference in decay coefficients results from the computation of the concentrations from the turbidity values. If the decay equation for NTU (figure 64) is substituted into the previous equation, the following equation is obtained:

$$C_s = 15.6 + 500.2 \exp(-0.061 \text{ NTU})$$

which preserves the decay coefficient by the introduction of the constant. The r^2 values for all the time series regressions are about 0.85.

The special data set described here was collected to determine the temporal variability of suspended sediment concentration and turbidity over an extended period of ambient conditions. Good time-series data were obtained for a two-hour period of gradually decreasing suspended sediment concentrations. The standard deviation about the regression line was about 5 percent of the concentration value. This means that under typical slowly varying conditions in larger rivers such as the Illinois and Upper Mississippi Rivers, it is correct to assume slowly varying suspended sediment concentrations with moderate to small temporal variability.

The attempt to obtain a correlation equation relating sediment concentration and turbidity over the two-hour period was not successful, however. The general trend was similar, but the variability of turbidity was considerably less, and the correlation was not very good.

Particle Size Distribution

In addition to suspended sediment concentration and turbidity, data were also collected for particle size determination. On a rotating schedule, each intake was pumped continuously to fill a 5-gallon container. In this way sufficient sediment was gathered for the determination of particle size distribution.

Sixty-two samples were collected. Of these, 53 were taken for background analysis and 9 for event information. All samples were composed of fine sand, silt, and clay particles. Although 1-gallon containers were used for storing samples at Kampsville, the dry sample weights shown in tables 44-50 are similar to those for samples collected in 5-gallon containers on the Mississippi River. The percentages of fine sand, silt, and clay shown are based on the dry weight for each sample. Appendix XXIX contains plots of particle size distribution.

Kampsville, Trip 1

Background Information. The sand portion at Kampsville (RM 35.2 on the Illinois River) ranged from 0.2 to 0.9 percent except for intake c3 on October 13, 1990, when it was about 4.4 percent (table 44). Clay was the primary composition of suspended sediment, ranging from 53 to 79 percent. The minimum percentage of clay also occurred at the same time that maximum sand percentages were detected.

In general, higher suspended sediment concentrations occurred near the bottom and toward the channel. This distribution is clearly represented in the dry weight data of October 13.

Event Information. Event data were collected at the Kampsville site on October 15, 1990, for the barge *Ardyce Randall*. Table 45 indicates that the dry weights for this event were heavier than the background data collected earlier, indicating sediment resuspension. It can also be observed that materials added to the water column during an event had similar percentages of sand, but silt increased and clay decreased. In terms of lateral distribution, the event data contained more clay near the shore and more silt toward the channel, but the sand percentage did not vary much.

Goose Island, Trip 1

Background Information. Compared to Kampsville, suspended sediment at Goose Island (RM 319.3 on the Mississippi River) contained a higher percentage of sand (table 46). Although the dry weights of the samples were not significantly greater than those at Kampsville, the samples were collected in 5-gallon containers rather than the 1-gallon containers used at Kampsville. Sand ranged from 0.3 to 15.7 percent, with an average of 4.0 percent. It seemed that the percentage of sand was consistently higher at the near-channel station (intake c1). Silt ranged from 17.8 to 40.3 percent with an average of 30.6 percent, while clay varied from 50.4 to 80.2 percent, with an average of 65.4 percent.

Event Information. Event data were collected at Goose Island on August 26, 1990, for barges *Kevin Michael* and *Sumac*. The total sediment weight did not increase for these events, and sand percentages decreased (table 47).

Goose Island, Trip 2

Background Information. During the 1991 survey at Goose Island, suspended sediment particle sizes did not change significantly from the previous year. The sand portion ranged from 1.0 to 5.6 percent, with an average of 3.2 percent; silt ranged from 30.3 to 53.7 percent, with an average of 42.6 percent; and clay ranged from 41.3 to 67.3 percent, with an average of 54.3 percent (table 48). Station d was farther into the channel, and station e was a temporary station set up to collect data near the navigation channel. The particle sizes at these intakes, however, were not significantly different from data collected at stations near the shore.

Event Information. All event data were collected for the barge *Evey-T* on July 23, 1991. Comparisons of lateral distribution can be made because the samples were taken from stations b, d, and e. Table 49 indicates that the total sample weights were greater near the shore and decreased toward the channel; the same is true for the percentage of sand. However, while total weights increased from the bottom toward the surface, the percentage of sand decreased somewhat away from the bottom. Overall, the total weights increased more during barge passage than during the background measurements.

Clarks Ferry, Trip 1

Background Information. At Clarks Ferry (RM 468.2 on the Mississippi River), an attempt was made to collect samples near the navigation channel (station e). The sand percentage near the shore was small; at near-shore stations (excluding e1 and e2), the percentage of sand ranged from 0.1 to 1.4 with an average of 0.6. However, the percentage of sand at e1 and e2 was 41.4 and 78.0, respectively (table 50). Similarly, the percentage of silt ranged from 26.6 to 48.2 at near-shore stations, with an average of 38.26, and the percentage of clay varied from 50.4 to 73.3, with an average of 61.1. The percentage of silt was higher than that of clay at intakes near the channel.

COMPARISON OF EXISTING METHODS AND PREDICTIVE RELATIONSHIPS

Existing equations for return velocity, maximum wave height, maximum drawdown, and increased suspended sediment concentrations were evaluated using the field data collected for this project. Presently, there are some ten predictive equations available to compute U_r , $H_{w(max)}$, and $H_{d(max)}$, respectively. However, some of these equations were not derived for vessels such as barges and some were developed for barges but were based on restricted idealized (e.g., prismatic) cross sections. By applying the measured hydraulic and traffic characteristics into these equations, the analysis computed each physical parameter and evaluated the best fit by comparing correlations between measured and predicted values. Results for each physical parameter are as follows.

Return Velocity

The return velocity (U_r) generated by tow traffic must be quantified to determine its impact on the river environment. Nine existing methods are available to compute U_r . Table 51 provides references for these methods. Bhowmik et al. (1995a) developed method 10 on the basis of selected data from the Illinois River at the Kampsville site. Appendix XXX gives a brief description of this method.

Methods 1-5 shown in the table assume that the magnitude of return flow does not change from barge to shore. Despite the fact that they are derived from different methodologies (momentum and energy approaches), these methods calculate the "average return flow." Methods 6-9 shown in table 51 essentially use an initial value for return flow near the barge, and multiply it by an exponential decay function to describe the attenuation of the return velocity. Here, maximum return velocity is assumed to be present at the barge-water interface and a zero value is assumed to exist at the shoreline.

In order to compare the return velocities computed by methods 1-5 (table 51), the measured "average return flow" needs to be calculated from data at all the meters. However, when comparing measured values with those computed by methods 6-10, the maximum return velocity measured at each meter was used.

With this stipulation, return velocities for each of the trips were computed using methods 1-10. Correlation coefficients, r , and the standard error of estimate (SE) were also computed for each equation and for each site. Higher SE values represent larger deviations between the measured and computed values. Table 52 shows the regression coefficient and SE for all ten methods for all barge events and sites. It appears that of methods 1- 5, 4 and 5 perform fairly well, whereas in the second set of methods, 6, 8, 9, and 10 perform fairly well.

Method 6 converts a calculated average U_r into a lateral velocity distribution using a distribution function. The other methods within this second set use either the barge speed (method 7) or calculated U_r near the barge as the initial value in the determination of the lateral distribution function. Method 6 uses the U_r computed by method 5 as the average U_r . Thus, wherever method 5 performs well, method 6 should also perform well.

It should also be noted that methods 6 and 8 use the same distribution function except for the initial values of U_r . Method 8 uses maximum U_r near the barge (calculated by method 4) as its initial conditions.

It should be pointed out that embedded assumptions in these methods cannot be met in a natural environment. In most cases, barge traffic is never at the centerline, the river cross section is not prismatic, the flow is not uniform, underwater structures such as dikes and dunes can alter the flow structure, and upstream bends and transition zones are always present. These natural variabilities cannot be modeled or duplicated, and as such, some empirical relationships based on physical factors and field data may have to be used to compute the return velocities in inland waterways.

Extensive analyses were done to verify which methods perform well when the data are combined for both rivers or separated according to whether the traffic was moving upstream or downstream. Based on these analyses, table 53 gives the correlation coefficients and SE for all methods. Here again, it appears that several methods perform fairly well, although method 6 appears to be better in predicting return velocity.

Further analyses of the computed values of U_r by methods 6 (Hochstein and Adams, 1989) and 9 (Maynard and Siemsen, 1991) were done, and table 54 provides the correlation coefficients and SE between computed and measured U_r . Figures 65 and 66, respectively, show the computed and measured values of U_r based on methods 6 and 9.

These plots indicate that Hochstein and Adams' method normally underestimates U_r in the Illinois River and overestimates U_r in the Upper Mississippi River. On the other hand, Maynard and Siemsen's method predicts fairly well the return flows on the Illinois River and overpredicts them for the Upper Mississippi River. In all cases, the predictions indicate significant scatter compared to measured values.

Regression Equations for Predicting Return Velocity

The analyses presented so far indicate that some existing methods can be used to predict the return flows in navigable waterways with some success. For this project, an attempt was made to determine whether a regression-type equation could be developed to predict the maximum return flows in the lateral direction, particularly within channel border areas.

The regression equations developed may have corrected forms, but the coefficients are valid only for the range of data sets used in the analyses. Therefore caution must be exercised in extrapolating these equations for other sites and for return velocities larger than the study's values. These equations may be valid for similar sites with similar hydraulic and geometric conditions.

The regression method described here depends heavily on nondimensional parameters. Return velocity, $U_{r(\max)}$, is dimensionalized using the average ambient velocity, V_a . The dimensionless ratio, $U_{r(\max)}/V_a$, is related to four independent dimensionless variables as given in the following equation:

$$U_{r(\max)}/V_a = f(V_b/\sqrt{gh}, y/W_T, A_b/A_c, P_r) \quad (45)$$

where V_b/\sqrt{gh} is the Froude number describing the traveling speed of the barge, y is the distance from the centerline of the barge along the lateral transect, W_T is the top width of

the river, A_b is the submerged cross-sectional area of the barges, A_c is the river cross-sectional area, and P_r is the power ratio (table 5). All these parameters can be obtained from the field except for the power term. Due to the difficulties in getting the set power values from the barges during measurement, the registered power for each barge is used here.

A stepwise regression analysis was performed to arrive at the final regression relationship. Two equations were developed, one for the Illinois and one for the Mississippi Rivers. The magnitudes of return velocities, collected under different hydraulic and geometric conditions from these two rivers by the barge traffic, necessitated the development of two separate equations. It is quite possible, however, that the equation developed for the Illinois River could be used for reaches of the upper Mississippi River where hydraulic and geometric conditions are comparable. The equation for the Illinois River is:

$$\frac{U_{r(\max)}}{V_a} = 10^{0.98} \left(\frac{V_b}{\sqrt{gh}} \right)^{0.77} \left(\frac{A_b}{A_c} \right)^{0.171} (P_r)^{0.30} \left[0.96 - 3.69 \left(\frac{y}{W_T} \right) + 6.08 \left(\frac{y}{W_T} \right)^2 \right] \quad (46)$$

where $r^2 = 0.235$, correlation coefficient = 0.48, and SE = 0.16.

The equation for the Upper Mississippi River is:

$$\frac{U_{r(\max)}}{V_a} = 10^{1.26} \left(\frac{V_b}{\sqrt{gh}} \right)^{0.73} \left(\frac{A_b}{A_c} \right)^{0.08} (P_r)^{0.22} \left[0.54 - 1.35 \left(\frac{y}{W_T} \right) + 1.12 \left(\frac{y}{W_T} \right)^2 \right] \quad (47)$$

with $r^2 = 0.45$, correlation coefficient = 0.67, and SE = 0.10.

Using the installed HP instead of actual HP for calculating the P_r is a shortcoming of these equations. Overall, these two regression equations improve the prediction slightly over existing methods. However, as shown in figures 67 and 68, there is considerable scatter. Although χ^2 tests indicate that distributions of measured and computed data are similar (probability ≈ 1.0), the regression model is relevant to measurements at low levels (through paired T tests).

Maximum Wave Height

A review of the literature indicates that there are ten methods that can be used to predict the maximum wave height generated by moving vessels. As mentioned in the section on existing methods, some of these equations were developed for recreational boats or deep draft vessels. Table 55 provides references for all ten methods and indicates the type(s) of vessels for which the methods were developed. In a previous study of some of these methods, method 3 was found to perform well for the Kanawha River in West Virginia (Kuo et al., 1988).

Table 56 presents evaluations of these ten equations based on the measured data, which show the correlation coefficient, standard error of estimate, and if the predicted

values over- or underestimated the measured data, or the predicted maximum wave heights scattered both sides of the perfect-fit-line.

Overall, the methods perform better for the Illinois River than for the Upper Mississippi River. Most methods underestimate $H_{w(\max)}$ for the Illinois River but overestimate $H_{w(\max)}$ for the Mississippi River. For the Illinois River, method 7 provides the best fit, followed by method 6 or method 2. For the Mississippi River, method 2 fits best, followed by method 6. If these methods are applied to the whole data set, methods 2, 6, and 7 appear to predict the measured values better than the others. The computed (methods 2 and 6) and measured values are shown for the entire UMRS and separately for the Illinois and Mississippi Rivers (figures 69 and 70).

Methods 1, 2, and 3 use blocking ratios and methods 4, 6, 7, and 8 use depth Froude numbers with barge speed as a parameter. Methods 6 and 7, which have very similar forms, also use draft to depth ratios. It appears that the methods using depth Froude numbers give more consistent results than the other methods.

Proposed Regression Method for Estimating Maximum Wave Height

In order to evaluate whether or not an effective regression-type equation can be developed for predicting maximum wave heights on the UMRS, a stepwise regression analysis was performed using the nondimensional parameters described in the section on existing methods:

$$\frac{H_{w(\max)}}{d_f} = g \left(R, \frac{V_b}{\sqrt{gL}}, \frac{V_b}{\sqrt{gh}}, s, \frac{A_b}{A_c}, \frac{y}{W_T} \right) \quad (48)$$

The stepwise regression analysis yielded the following relationship:

$$\frac{H_{w(\max)}}{d_f} = 0.0005 \left(\frac{V_b}{\sqrt{gL}} \right)^{-0.90} \left(\frac{V_b}{\sqrt{gh}} \right)^{1.18} \left(\frac{A_b}{A_c} \right)^{-0.86} \left(\frac{y}{W_T} \right)^{0.33} \quad (49)$$

where $r^2 = 0.48$, correlation coefficient = 0.69, and SE = 0.705.

Figure 71 (a) compares the computed (using equation 49) and measured values of $H_{w(\max)}/d_f$ for all the data sets collected for the present project. A χ^2 test indicates that the distributions of measured and computed $H_{w(\max)}/d_f$ are similar (probability ≈ 1.0). The computed data reasonably represent the actual data in a paired T test. Figure 71 (b) shows the actual values of computed and measured $H_{w(\max)}$.

Maximum Drawdown

Ten methods are available to compute maximum drawdown. Table 57 provides references for all ten methods. Most of the methods (except for 2, 8, and 9) take Bernoulli's equation and modify it with factors such as blocking ratios and barge length to distance ratios. Method 1 is a direct application of Bernoulli's equation. It should also be noted that the drawdown computed by methods 1, 8, and 9 can be used to calculate

uniform return velocity. In a previous study of some of these methods, method 5 was found to perform well for the Kanawha River in West Virginia (Kuo et al., 1988).

All ten methods were used to compute drawdown on the UMRS, and correlation coefficients were developed from the measured and calculated values. Table 58 provides these correlation coefficients, SE, and notations with respect to the apparent fit.

A review of the table shows that in general all methods perform well for the Illinois River data sets. However, the predictability declines significantly for Mississippi River data sets. The computed (methods 7 and 4) and measured values are shown for the entire UMRS and separately for the Illinois and Mississippi Rivers (figures 72 and 73).

Proposed Regression Relationship for Maximum Drawdown

An attempt was made to develop a regression relationship for computing and predicting maximum drawdown, $H_{d(\max)}$, on the UMRS. For this analysis, maximum drawdown was made dimensionless by using depth, h , according to the following functional relationship:

$$\frac{H_{d(\max)}}{h} = H \left(R, \frac{V_b}{\sqrt{gh}}, s, \frac{A_b}{A_c}, \frac{y}{W_T} \right) \quad (50)$$

After the stepwise regression analysis, the final form of the relationship for estimating maximum drawdown becomes:

$$\frac{H_{d(\max)}}{(h-d_f)} = 0.499 \left(\frac{V_b}{\sqrt{g(h-d_f)}} \right)^{0.86} \left(\frac{A_b}{A_c} \right)^{0.78} \left(\frac{y}{W_T} \right)^{-0.50} \quad (51)$$

where $r^2 = 0.64$, correlation coefficient = 0.80, and SE = 0.30.

Figure 74 shows the plot of the computed versus measured values of $H_{d(\max)}/(h-d_f)$ for all the data sets collected for the present project. A χ^2 test indicates that the distributions of measured and computed $H_{d(\max)}$ are similar (probability ≈ 1.0). The computed data represent the actual data well in a paired T test. Figure 74 (b) shows the actual values of computed and measured $H_{d(\max)}$.

Suspended Sediment

This section describes the comparative analysis that was performed using existing equations to predict the effects of vessel passage on sedimentation parameters, including suspended sediment concentrations.

Transport Equations

The three riverine sediment transport equations used in the first-level analysis of suspended sediment concentrations — by Colby, Akers-White, and Toffaleti — are discussed in the section on existing methods. These equations were developed at different times using different concepts of sediment suspension and transport and with the

laboratory and field data sets available to the authors. All of the equations are expressed in English units. Calculations will also be made using English units because the equations lack dimensional homogeneity and are extremely complex. (Multiple unit conversions in each equation would introduce several chances for systematic error.) However, note that final results are expressed in mt/d for sediment load and mg/L for sediment concentration.

All three methods were used to compute bed material sediment loads at each site. Field measurements were done with depth-integrating samplers that could not sample the 4 inches (100 mm) just above the river bed. In the deeper parts of the Upper Mississippi River channels, the sampling depth was limited to 18 feet (5.5 m) by the DH-59 sediment sampler. Suspended sediment particle size samples were composed mostly of silt and clay materials with some fine and very fine sand. Most bed material samples contained primarily sand and gravel, with only small amounts of silt and clay.

A common approach in sediment transport analysis has been to consider the fine sediment as “wash load,” or material from the watershed, rather than as material scoured from the bed or banks of the alluvial river. An approach proposed by Laursen (1958) was to combine the sediment in the water column with the bed material to obtain a total size distribution for use in the transport equation. Laursen presented this concept, but did not suggest a way to obtain the total bed material composition.

The methods used here (Colby, Akers-White, and Toffaleti) and Laursen’s method were all developed from a mixture of theoretical equations, concepts about sediment movement, and results of laboratory studies and field measurements. All can be criticized for empirical inconsistency since each of the sediment load curves tends to pass through clusters of data, even those transport curves that were developed using the more complex Toffaleti and Laursen methods. The Akers-White method appears to have gained accuracy through the incorporation of several additional years of field, laboratory, and theoretical work on sediment transport. However, the great variability of sediment concentrations and transport rates at a single location along a stream seems to exclude the possibility of empirical or analytical closure to less than an order of magnitude.

Estimating increases in sediment concentration caused by velocity changes at the perimeter of the river due to vessel passage increases the complexity of the problem. Incremental increases in velocity at the bed and banks of the river can suspend additional bed material. The increased velocity is associated with propeller jets near the sailing line and with wave, drawdown, and return flow action away from the sailing line. Wave and drawdown suspension are commonly observed along the banks in shallow water. Once the bed or bank material is in suspension, it is convected with the ambient sediment in the river. Field measurements of suspended sediment concentration cannot distinguish between stream sediment load (bed material load), wash load, and material suspended by vessel passage. Adams (1992) presents a more detailed discussion of the mechanics of vessel passage in inland waterways.

Ambient Sediment Loads

At some point during each data collection field trip, water discharge and suspended sediment load were measured at the principal cross section. (Suspended sediment concentration data were not collected during two of the trips, Goose Island in 1990 and Clarks Ferry in October 1991, and water and sediment flow rates in the side channel were

measured only during the 1991 trip to Goose Island.) The four Mississippi River data sets are discussed first followed by the three Illinois River data sets. Table 59 presents a summary of the computations using each of the three sediment transport equations and the measured sediment loads.

Mississippi River. All of the Mississippi River sites are located in reaches with one or more islands and a large side channel. Between 8 and 21 verticals were occupied for velocity and suspended sediment concentration measurements. Average suspended sediment concentrations ranged from 80 mg/L at Apple River Island to 150 mg/L at Goose Island (1990). Measured suspended sediment loads ranged from 10,636 to 37,057 mt/d.

As shown in table 59, the Akers-White method gives the best estimates of sediment load, with ratios of computed to measured loads ranging from 0.822 to 1.297. The Colby method generally underestimates sediment loads, with ratios of computed to measured loads between 0.290 and 0.715. The Toffaleti method seriously underestimates the sediment load, with ratios of computed to measured loads around 0.1. This analysis also supports the use of the Akers-White method for estimating local suspended sediment concentrations following the impact of vessel-generated waves and return velocities.

One point of interest is the side channel measurements at Goose Island in 1991. The main channel water discharge was 1,880 cms, the side channel discharge was 729 cms, and the average suspended sediment concentrations were 125 mg/L in the main channel and 77 mg/L in the side channel, making the sediment loads 20,323 and 4,850 mt/d in the main and side channels, respectively. The total water flow rate was 2,609 cms and the total sediment transport rate was 25,173 mt/d. Different concentrations of sediment in the main and side channels forced the main channel to carry about 81 percent of the sediment and about 72 percent of the water.

Illinois River. The Illinois River is narrower and shallower than the Mississippi River, and it has a lower gradient. The higher slope, discharge, and sediment concentration at Kampsville in October 1990 were caused by runoff from a fall storm. As shown clearly in table 59, none of the methods give adequate estimates of the suspended sediment loads in the Illinois River. Two factors may account for this: 1) most of the suspended sediment was wash load, and 2) fines had been removed by towboat propeller jets.

Demissie et al. (1992) give an excellent summary of erosion, transport, and deposition of sediment in the Illinois River valley. They clearly show that most of the sediment in the Illinois River is contributed by major tributaries, and that the deposition rate in the valley is about 8.5 million metric tons per year.

Adams (1992) discusses the range of draft to depth ratios for the UMRS. Since most towboats have drafts near the 9-foot (2.74-m) maximum, this value is appropriate for use in a discussion of propeller jet resuspension. At both sites on the Illinois River, the draft/depth ratio was 0.78 (maximum) and 0.68 (average). These values exceeded the presumed ratio of 0.5 as a threshold for sediment entrainment by propeller jets.

Removal of finer particles from the main channel by tow passage results in coarser bed material than would be present without barge-tows. This, in turn, causes underestimation of the sediment load by any transport equation. Also, without

incorporating the finer suspended sediment in the transportable bed material composition, there is no way to include wash load in the sediment load calculations.

Event Sediment Loads

As described earlier in the report, a number of velocity meters and suspended sediment intakes were used at each site. With more experience and additional instruments, the complexity in the deployment increased with each trip. For an event to be included in this analysis, there had to be data sets for one or more suspended sediment intakes and velocity data sets from current meters located reasonably close to each of the intakes.

Velocity data collection methods changed with the acquisition of additional meters and automatic data logging systems for all current meters. Event peak values were used in the sediment transport equations to estimate the peak suspended sediment concentration resulting from tow passage.

Following is a discussion of how well the Akers-White and Toffaleti methods predicted sediment concentrations during tow passage (the Colby method is not suitable for this computation).

Akers-White Computations. The Akers-White method was used to estimate sediment concentrations during tow passage events because of the single calculation involved and the relative accuracy of the equation in predicting sediment transport rates on the Mississippi River. However, this method does not compute a concentration profile in the vertical or the concentration at a specific point in the water column. Thus only one computed value is given for each location in the cross section of a set of sediment intakes. The four Upper Mississippi River data sets are discussed first followed by the two Illinois River data sets.

Apple River Island. Six sediment intakes were installed at four locations on the transect. Sediment and velocity data sets were obtained for 12 events (table 60). Computed values were less than measured values for all intakes at all stations. The measured peak concentrations generally decreased with distance from the shore. At stations c and d, which had two intakes, the measured concentrations were lower at the higher intake.

Clarks Ferry, Trip 1. Eight sediment intakes were installed at four locations across the transect. Data were collected for eight tow passage events (table 61). Comparisons were limited by the small amount of sediment data collected during this field trip, partially due to structural weakness in an experimental sediment intake support used in deeper water and because of the sandstone river bed in front of the field station. The calculated values were all very small compared to the measured concentrations.

Goose Island, Trip 1. Five sediment intakes were installed at three distances from the shore. Sediment and velocity data were collected for 13 events (table 62). As at Clarks Ferry and Apple River Island, the computed concentrations were much lower than the measured concentrations. The ratio of computed to measured values rarely exceeded 10 percent.

Goose Island, Trip 2. Six sediment intakes were mounted on fixed supports at four locations on the transect, and two intakes were sampled from a boat anchored at the buoy line. Data were collected for 20 tow passage events during this field trip (table 63). The

computed concentrations were essentially zero for station a and very small at stations b and c. At stations d and e the computed concentrations were similar to the measured concentrations. The ratio of computed to measured concentrations ranged from 14 to 170 percent at stations d and e.

McEver's Island. Eight suspended sediment intakes were sampled at three locations on the transect. Sediment and velocity data were recorded for eight events. As might have been expected from the poor estimation of suspended sediment load, the computed concentrations were generally much lower than the measured concentrations. Table 64 gives the measured and computed peak concentrations for each of the eight events.

Kampsville, Trip 1. For most of the events during this trip, five suspended sediment intakes were sampled at three locations on the transect. During passage of the *Ste. Genevieve*, however, three additional intakes were sampled from a boat anchored on the edge of the navigation channel as defined by the buoy line. Sediment and velocity data were collected for 21 tow passage events. The computed concentrations were zero for all events at stations a and b. At stations c and d, the computed concentrations were much lower than the measured values (table 65). Some of the discrepancy between computed and measured concentrations for this field trip may be explained by the high ambient suspended sediment concentrations, around 300 mg/L, due to a fall storm runoff event on cleared fields in the Illinois River watershed. This material can all be labeled wash load.

Toffaletti Computations. This equation was used to estimate sediment concentrations during tow passage events because it treats the bed material as a number of size fractions based on the standard bed material classification and because it incorporates the vertical distribution of sediment concentrations in the computation. The method includes this latter detail to improve the estimate of the average concentration in the vertical rather than to allow computation of concentrations at the elevation of individual sediment intakes above the river bed. Thus, only one computed value is given for each location of sediment intakes in the cross section. The four Mississippi River data sets are discussed first followed by the two Illinois River data sets.

Apple River Island. Six sediment intakes were sampled at four locations on the transect. Sediment and velocity data sets were obtained for 12 events (table 66). Computed values were lower than measured values for all intakes at all stations. Most concentrations were only a fraction of the values computed using the Akers-White method (table 60).

Clarks Ferry, Trip 1. Eight sediment intakes were installed at four locations across the transect. Data were collected for eight tow passage events (table 67). Comparisons were limited by the small amount of sediment data collected during this field trip. The calculated values were all very small compared to the measured concentrations and generally smaller than the results of the Akers-White method.

Goose Island, Trip 1. Five sediment intakes were installed at three distances from the shore. Sediment and velocity data were collected for 13 events (table 68). As at Clarks Ferry and Apple River Island, the computed concentrations were much lower than the measured concentrations.

Goose Island, Trip 2. Six sediment intakes were mounted on fixed supports at four locations on the transect. Two intakes were sampled from a boat anchored at the buoy

line. Data were collected for 20 tow passage events during this field trip (table 69). The computed concentrations were very small for all five stations. For events for which the Akers-White method predicted significant concentrations, the Toffaleti method predicted small values. At stations d and e the difference between the two methods is greater, as may be seen by comparing tables 63 and 69.

McEver's Island. Eight suspended sediment intakes were sampled at three locations on the transect. Sediment and velocity data were recorded for eight events. As might have been expected from the poor estimation of suspended sediment load, the Toffaleti method gave concentrations that were much lower than the measured concentrations. Table 70 gives the measured and computed peak concentrations for each of the eight events.

Kampsville, Trip 1. For most of the events during this trip, five suspended sediment intakes were sampled at three locations on the transect. During passage of the *Ste. Genevieve*, however, three additional intakes were sampled from a boat anchored on the edge of the navigation channel as defined by the buoy line. Sediment and velocity data were collected during 21 tow passage events. The computed concentrations were zero for all events at stations a and b. At stations c and d, the computed concentrations were much lower than the measured values (table 71). Some of the discrepancy between computed and measured concentrations for this field trip may be explained by high ambient suspended sediment concentrations, around 300 mg/L, due to a fall storm runoff event on cleared fields in the Illinois River watershed. For this site, the Toffaleti method yielded concentrations that were about one-half of those calculated by the Akers-White method.

Comparison of Computed and Measured Concentrations

The measured velocities used in these computations were basically return-flow increases caused by displacement of water around the barge-tow. The near-shore erosion of fine material by wake waves and the infill wave of drawdown were not estimated at all. Much of the suspended sediment was finer than the local bed material and was transported farther after resuspension than the sands in the bed material samples.

As discussed earlier, the Colby method is not applicable to this type of computation. The Toffaleti method offers several refinements such as vertical distribution of concentration and the use of a bed material size distribution in size fractions instead of a single representative diameter. Review of the estimated event concentrations in tables 60-71 shows that the Akers-White method gave somewhat better estimates than the Toffaleti method. However, neither was accurate enough to be recommended.

Also evident from the tables is the fact that measured concentrations often decreased from the bank toward the navigation channel, but computed concentrations always increased from shore to channel. See tables 64 and 70 or tables 62 and 68 for examples of these trends.

SUMMARY

The Illinois State Water Survey, with assistance from the Environmental Management Technical Center of the National Biological Service and the U.S. Army Corps of Engineers (USACOE), has conducted a detailed field investigation on the physical changes associated with the movement of navigation traffic on the Illinois and Mississippi Rivers. This report summarizes the results of that investigation. Research results have also been presented at technical society meetings and published in a number of journals. Appendix XXXI includes three articles published in refereed journals, Appendix XXXII lists references for other relevant publications.

Following is a synopsis of the information presented in each major section of this report.

Background

This section outlines the project background and scope of work, and explains how the project objectives correlated with the Plan of Study (POS) developed by the USACOE for the Melvin Price Lock and Dam on the Mississippi River near Alton, Illinois. Included is a description of the Upper Mississippi River System (UMRS) and navigation traffic characteristics such as typical barge configurations and barge-tow variables. The report discusses the physical and biological effects of vessel passage on flow patterns in a waterway and outlines the environmental variables involved in vessel-waterway interactions. Also described are dimensional analysis and selected dimensionless parameters, including draft/depth ratio, blocking factor, length Froude number, and power ratio.

Existing Methods

This section describes the methods available to compute and/or predict return velocity, drawdown, wave height, and sediment resuspension. The section concludes with a nondimensional analysis of traffic and river-related variables subsequently used to develop predictive relationships.

Method and Equipment Design

This section describes the procedures used to design the field data collection system, including a fairly detailed testing of the system at the McEver's Island site on the Illinois River. Since such a large-scale data collection project had not been undertaken before, extensive planning and field testing were required before an acceptable procedure could be adopted for use in the field. Procedures for selecting various sites are also described in this section.

Data Collection

This section describes the techniques used for collecting background and event data from the Illinois and Mississippi Rivers. Ambient velocity and sediment concentrations, bed material characteristics, the planform of the river, and cross-sectional and discharge data from one or two transects were collected at each site.

Data collection from large rivers such as the Illinois and Mississippi requires the development of specialized mooring and mounting systems and the use of nonferrous materials such as aluminum or stainless steel for electromagnetic current meters. Systems that were designed and tested at the Illinois State Water Survey before being used in the field are described here, as are all the data collection equipment used in the field. This section also explains how field data were collected, the frequency of field measurements for various parameters, and the techniques used to handle the large volume of data.

Data Presentation

The ambient conditions at each data collection site are presented in this section. To summarize, the cross-sectional areas of the sites varied from 775 square meters (m^2) to 2,864 m^2 . The average ambient velocity varied from 0.27 meters per second (m/s) to 1.13 m/s, and discharge varied from 212 cubic meters per second (cms) to 2,856 cms. The ambient suspended sediment load varied from 917 metric tons per day (mt/d) to 21,169 mt/d on the Illinois River and from 10,636 to 37,057 mt/d on the Mississippi River. The highest turbidity measured was 440 nephelometric turbidity units (NTU) on the Illinois River and 585 NTU on the Mississippi River. Ambient suspended sediment concentrations varied from 78 milligrams per liter (mg/L) to 934 mg/L on the Illinois River and from 40 to 463 mg/L on the Mississippi River.

The median diameter of bed material within the navigation channel on the Illinois river varied from 0.26 millimeters (mm) to 0.56 mm, whereas within the channel border areas, these values were in the range of 0.25 to 0.74 mm. On the Mississippi River, the median diameter of bed materials within the navigation channel varied from 0.25 to 0.59 mm.

Traffic during an event varied from a single tow to as many as three tows. Normally the maximum configuration of the tow was a planform consisting of tows three wide by five long. The average configuration comprised 10 tows on the Illinois and 11 on the Mississippi. The draft varied from 0.61 meters (m) to 2.74 m with an average of 2.2 m on the Illinois and 2.0 m on the Mississippi River. The narrower and shallower Illinois River had higher blocking and draft-depth ratios than the deeper and wider Mississippi River. Barge traveling speed, on the other hand, did not differ significantly between the two rivers.

Although turbidity and suspended sediment samples were collected at various sites, no system-wide correlation between suspended sediment concentrations and turbidity could be developed.

Data were collected at various sites to compile information on the relative magnitudes of wind-generated waves. During the data collection period, however, prolonged and sustained wind was not present. The maximum wind velocity measured

was about 5 miles per hour (mph) and the maximum height of wind-generated waves was 0.11 m.

All the event characteristics are summarized in various appendices. Digital data have been organized in ASCII format with a directory for each trip.

General Analyses

This part of the report describes findings for the parameters observed during data collection.

Return Velocity

Following are some significant observations concerning return velocity:

- The highest return flows occurred at the McEver's Island site, which also had the largest blocking factor (0.125).
- In general, upstream-bound barges produced slightly higher return flows in zones closer to the barge and near the shore.
- Mean return flows, as calculated for different zones from the barge, showed an attenuation from the barge toward shore, except at the McEver's Island site, which showed a reverse trend. Attenuation was not obvious at the Kampsville site for upstream-bound barges.
- A comparison of data from sites that were visited twice shows higher return flows occurring in zones closer to the barge at higher discharges. This may be related to the higher horsepower required to push the barge convoy. The trend is most visible in trips to the Kampsville site, where the blocking ratio and draft-depth ratio were comparable, but the river flow for trip 1 was much higher than for trip 2.
- Not all traffic produced significant values of maximum return velocity, $U_{r(max)}$, especially at zones closer to the barge. Fairly small values of $U_{r(max)}$ near the barge occurred for both upstream-bound and downstream-bound barges.
- Sites on the Illinois River had higher $U_{r(max)}$ values than those on the Mississippi River. The highest measured $U_{r(max)}$ on the Illinois River was 0.69 m/s, while on the Mississippi River it was 0.32 m/s.
- Large $U_{r(max)}$ did occur at zones away from both upstream-bound and downstream-bound barges.
- The impact of navigation traffic on return velocity was greater in the shallower and narrower Illinois River than it was in the deeper and wider Mississippi River.

Maximum Wave Height

The mean values of maximum wave height, $H_{w(max)}$, for upstream-bound and downstream-bound barges were not significantly different. The range of $H_{w(max)}$ varied between 0.01 and 0.30 m. During trip 1 at Goose Island a work barge (a buoy tender) produced one large wave, 0.66 m high. Configurations such as single tows or one barge pushed by a tow produced relatively large waves. In general, higher wave heights were found to be associated with higher discharges.

Maximum Drawdown

The maximum measured drawdown, $H_{d(max)}$, 0.24 m, occurred at McEver's Island, which of all the sites had the narrowest channel width, the shallowest depth, and the highest $U_{r(max)}$ near the shore. This site also had the highest mean and median $H_{d(max)}$. At the Kampsville site on the Illinois River, slightly higher $H_{d(max)}$ was measured for barges traveling in both directions. Values of $H_{d(max)}$ on the Illinois River were as much as twice those on the Mississippi River.

Velocity Structure

Field data indicated that upstream-bound barges increased the longitudinal velocity near the channel border area and that downstream-bound barges decreased the velocity in the channel border area. The increases/decreases were as high as 300 percent, and larger increases/decreases in net velocity were associated with fully loaded barge convoys. Velocity also increased or decreased in the vertical direction depending upon the direction of the barge-tows.

Although return velocity is conventionally examined only in the longitudinal direction, it can also change in the lateral direction. Analysis of velocity vectors indicated that they could rotate by as much as 360 degrees. In some cases, the entire water body was disturbed and the alteration within channel border areas was very small. The altered velocity regime lasted from 2 to 4 minutes.

Suspended Sediment

The mean increase in suspended sediment was generally higher near the shore than near the sailing line. On the Illinois River, the increase in suspended sediment concentration in channel border areas varied from no change to 426 mg/L. On the Mississippi River, the increase varied from no change to 248 mg/L in channel border areas. In a few sediment samples taken from stations close to the barge (Goose Island, trip 2), the increase in suspended sediment concentration was fairly small. In general, downstream-bound barges produced higher mean values and a wider range of suspended sediment concentrations than upstream-bound barges. The largest increase in suspended sediment concentrations occurred when the barge-tows were at a distance of more than 75 percent of the width of the river away from the shoreline (Table 36).

Comparison of Existing Methods and Predictive Relationships

This section of the report evaluates and compares equations for computing return velocity, maximum wave height, maximum drawdown, and increased suspended sediment concentrations.

Return Velocity

Ten existing methods were used to compute return velocity for comparison with measured return velocities. Several of the methods performed well depending upon the river and traffic characteristics, and some predicted return velocity well on the Illinois River, but overestimated it on the Mississippi River.

Based on dimensional analyses, two regression-type equations were developed for estimating return velocities in the Illinois and Mississippi Rivers, respectively. These equations could be used for the UMRS, particularly at sites that have characteristics similar to those where field data were collected.

Maximum Wave Height

Other existing methods were used to compute maximum wave heights for comparison with measured values. These analyses indicated that while several methods could be used to estimate maximum wave heights generated by barge traffic, none were found to be very good. A regression method has been proposed to compute maximum wave height based on several measured parameters.

Maximum Drawdown

Existing methods were also used to compute maximum drawdown for comparison with measured values. In general, most methods performed well for Illinois River data, but did not perform well for the Upper Mississippi River data sets. Consequently, a regression-type equation was developed to estimate maximum drawdown on the UMRS.

Suspended Sediment

The Akers-White, Colby, and Toffaleti methods were used to calculate the ambient suspended sediment load of bed material at each site, and results were compared with the measured suspended sediment loads. The calculated loads included only bed material, while measured loads included bed material and suspended load, and excluded the unmeasured layer immediately above the river bottom. In the deeper parts of several Mississippi River sites, the unsampled zone was much larger because of the maximum depth limit of approximately 18 feet (5.5 m) for the DH-59 sampler.

The Akers-White method gave generally good results for the Mississippi River, while the Colby and Toffaleti methods seriously underestimated ambient suspended sediment loads in both rivers. None of the methods gave accurate results for the Illinois River, probably due to: 1) large wash loads and 2) resuspension and lateral displacement of fines by tow passage. Wash load cannot be computed by bed material sediment formulas. Resuspension and lateral movement coarsen the bed material over the width of the navigation channel and thus reduce the bed material load carried.

The Colby method relies on interpolation between curves for two depths and could not be used reliably to estimate event velocity suspension. The Akers-White method is not designed to estimate event concentrations, but was adaptable. Estimates by the Akers-White method were almost all significantly lower than the measured concentrations. Event concentration estimates were also made with the Toffaleti method. Although the form of the equation and the use of bed material size fractions suggested that the Toffaleti method would be the best for event calculations, it actually gave low estimates, similar to its underestimation of ambient concentrations and loads.

ACKNOWLEDGMENTS

Staff from the Illinois State Water Survey (ISWS) conducted this project as part of their regular duties. Many other ISWS staff members, present and past, contributed to this project, including William Bogner, Jim Slowikowski, Ed Delisio, Il Won Seo, Vijay Rangarajan, and Walter Reichelt. Maitreyee Bera contributed significantly by constructing the database and performing detailed computations for the report.

Lori Nappe, Lacie Jeffers, and Kathy Brown typed the report; Linda Hascall and David Cox prepared many of the illustrations; and Eva Kingston and Sarah Hibbler edited the manuscript.

This research project was partially funded by the Environmental Management Technical Center of the U.S. Geological Survey, and the U.S. Army Corps of Engineers. Project activities were conducted through the Illinois Department of Natural Resources. Any opinions, findings, and conclusions or recommendations expressed in this report are those of the authors and do not necessarily reflect those of the sponsors.

The authors are grateful to Jerry Rasmussen and Joe Wlosinski, U.S. Fish and Wildlife Service, for their initial and continued support of this project. Others whose assistance has been crucial to this project are Bob Delaney and Ken Lubinski, Environmental Management Technical Center of the National Biological Service, both of whom played an extremely vital role in making certain the project was continued and successfully completed.

The authors are also grateful to the U.S. Army Corps of Engineers for their continued financial support of the project. Numerous staff from the U.S. Army Corps of Engineers field office and many local and private landowners provided the necessary access to the field sites. The Illinois Department of Natural Resources and its professional staff, including Marvin Hubbell and Bill Donels, assisted with and provided all necessary help for processing the contractual agreements.

The project required so many field, office, and other support staff that it is almost impossible to mention the names of everyone involved. The authors express their sincere thanks and gratitude to all of them.

FIGURES

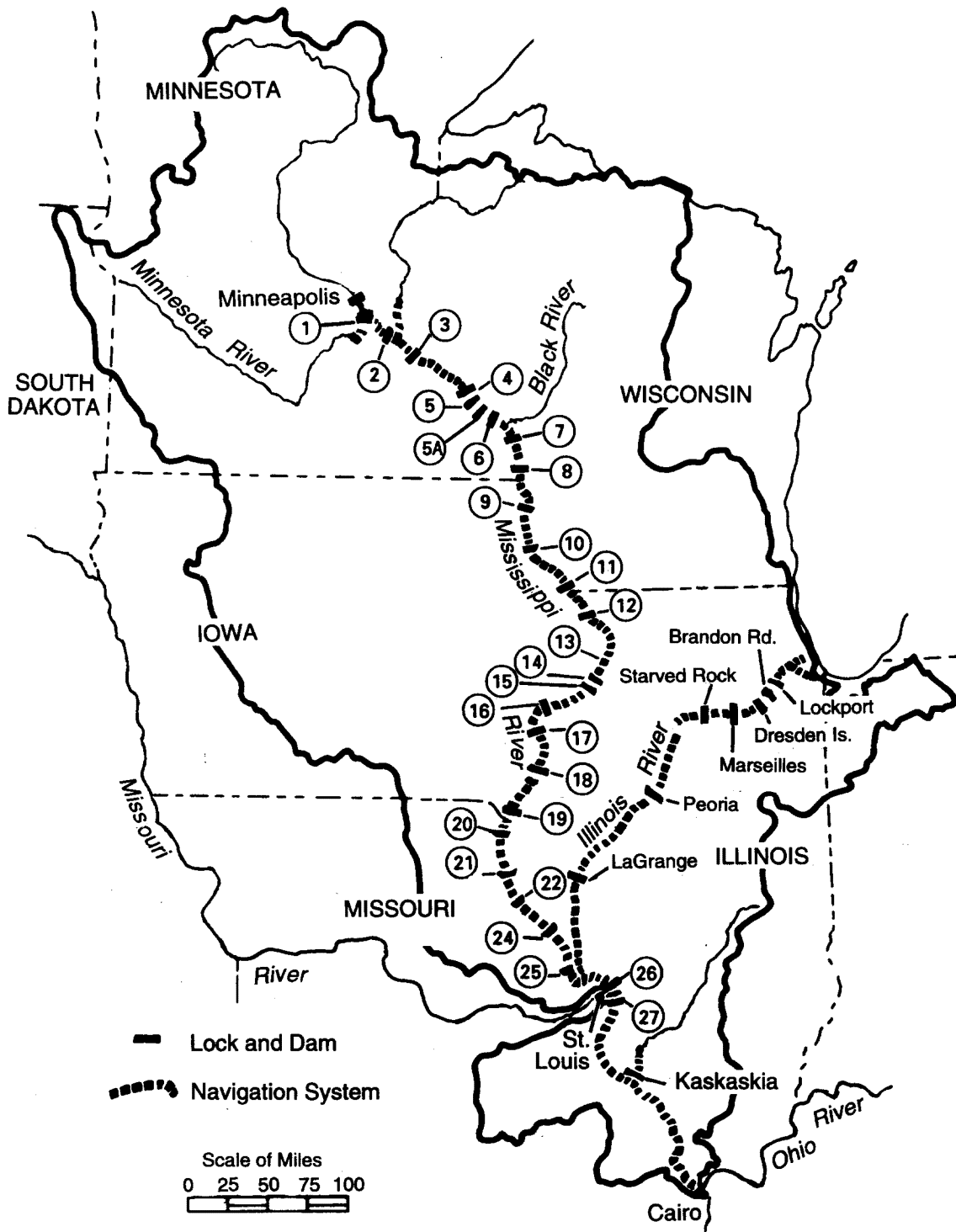
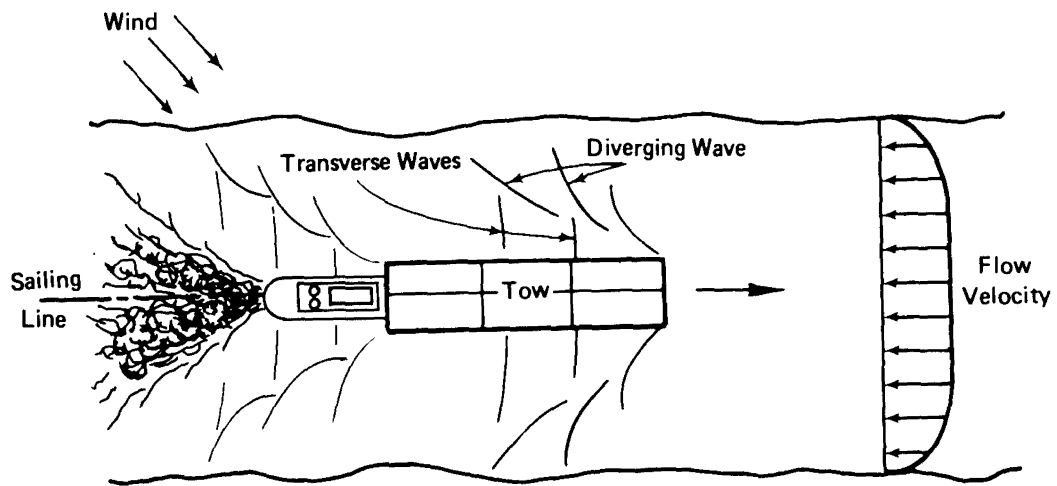
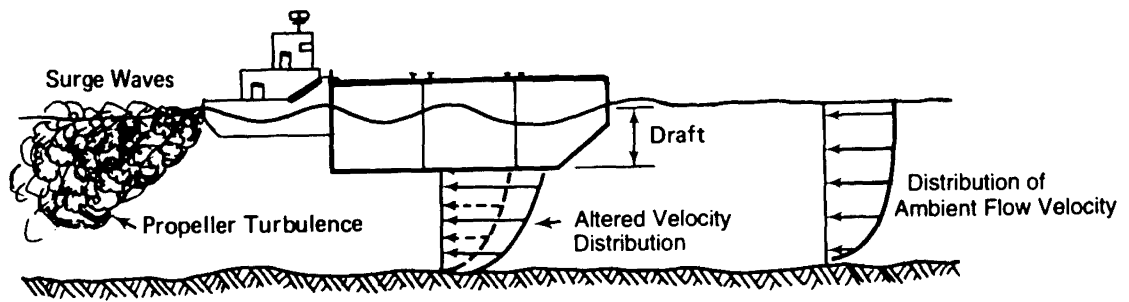


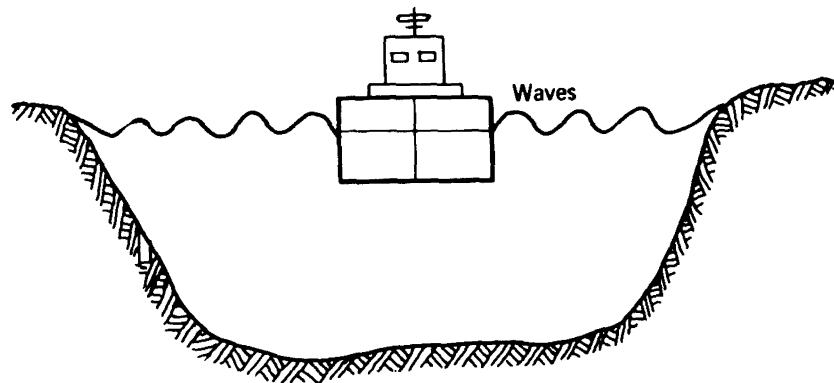
Figure 1. Position of inland waterways and navigation locks and dams on the UMRS



PLAN

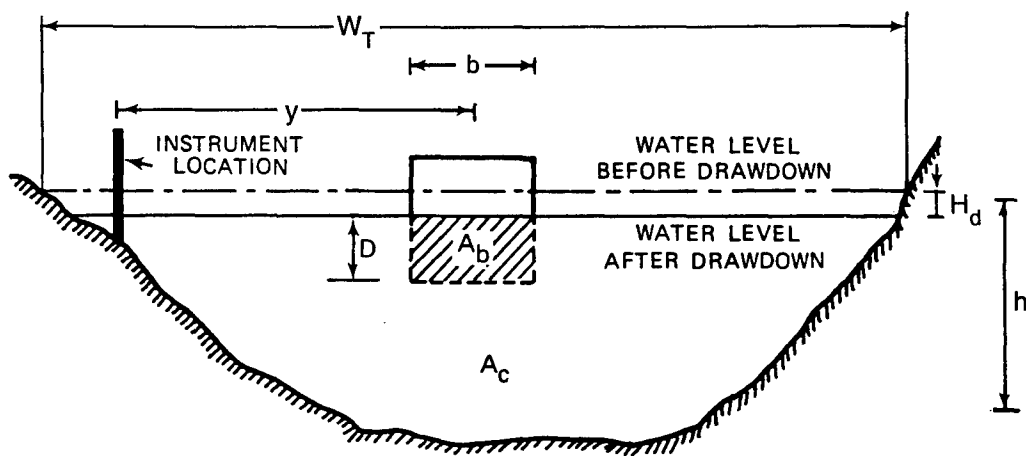
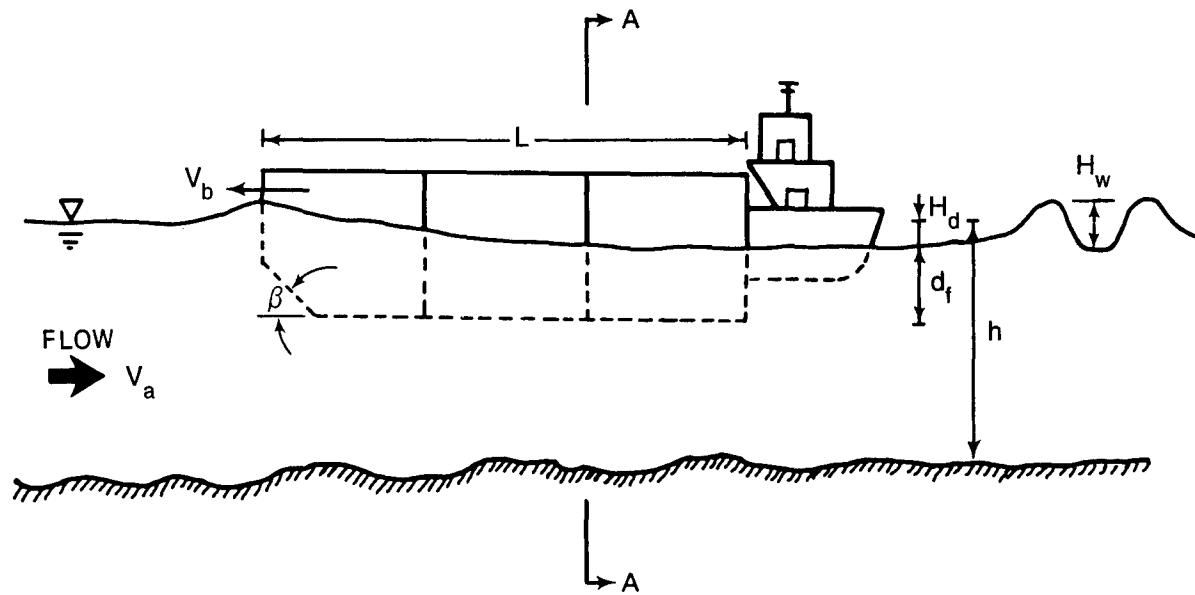


SECTION



CROSS SECTION

Figure 2. General sketch of barge-tow effects



CROSS SECTION A-A

Figure 3. Definition sketch of vessel and environmental variables

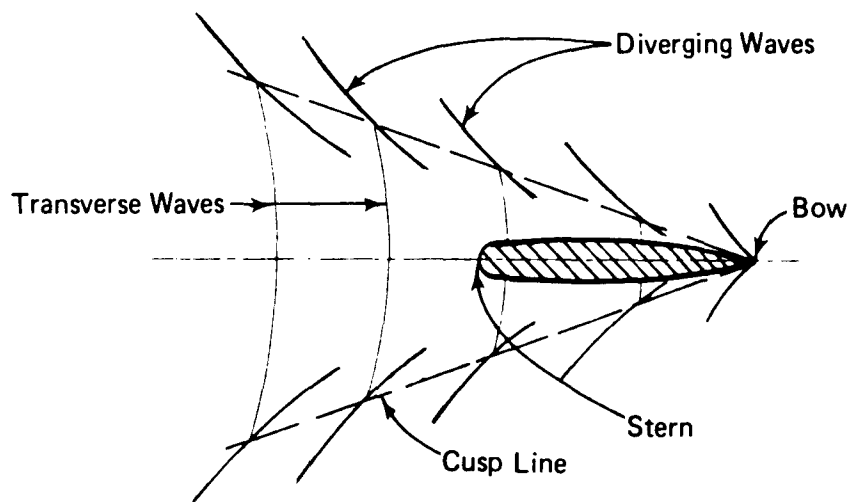


Figure 4. Wave patterns generated by a vessel

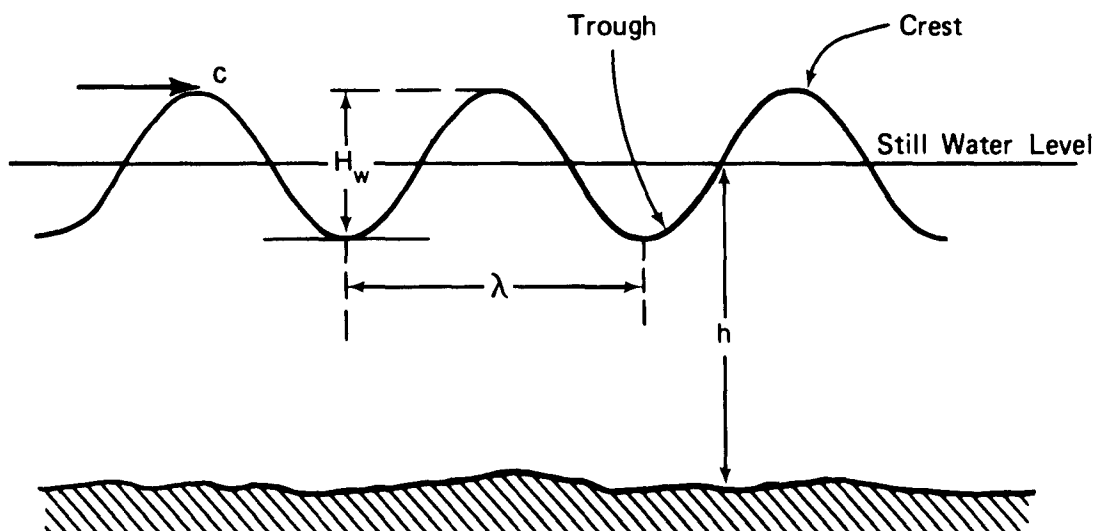


Figure 5. Longitudinal wave profile and wave variables

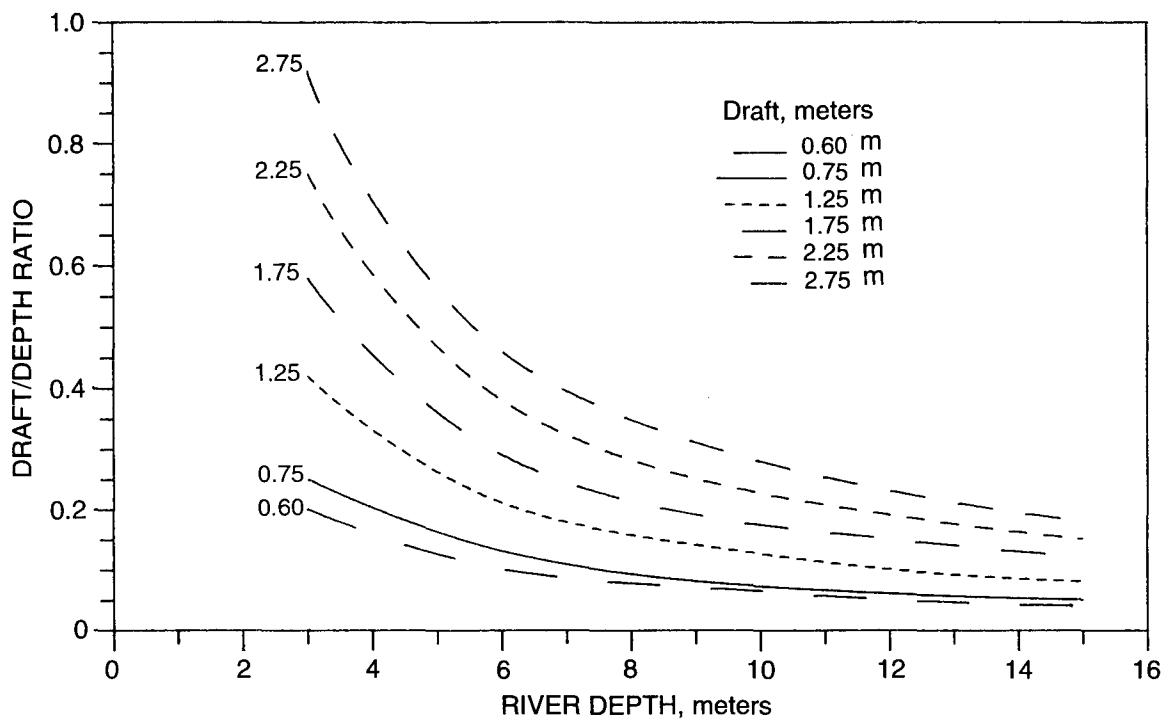


Figure 6. Draft/depth ratios for barge tows on the UMRS, after Adams (1991)

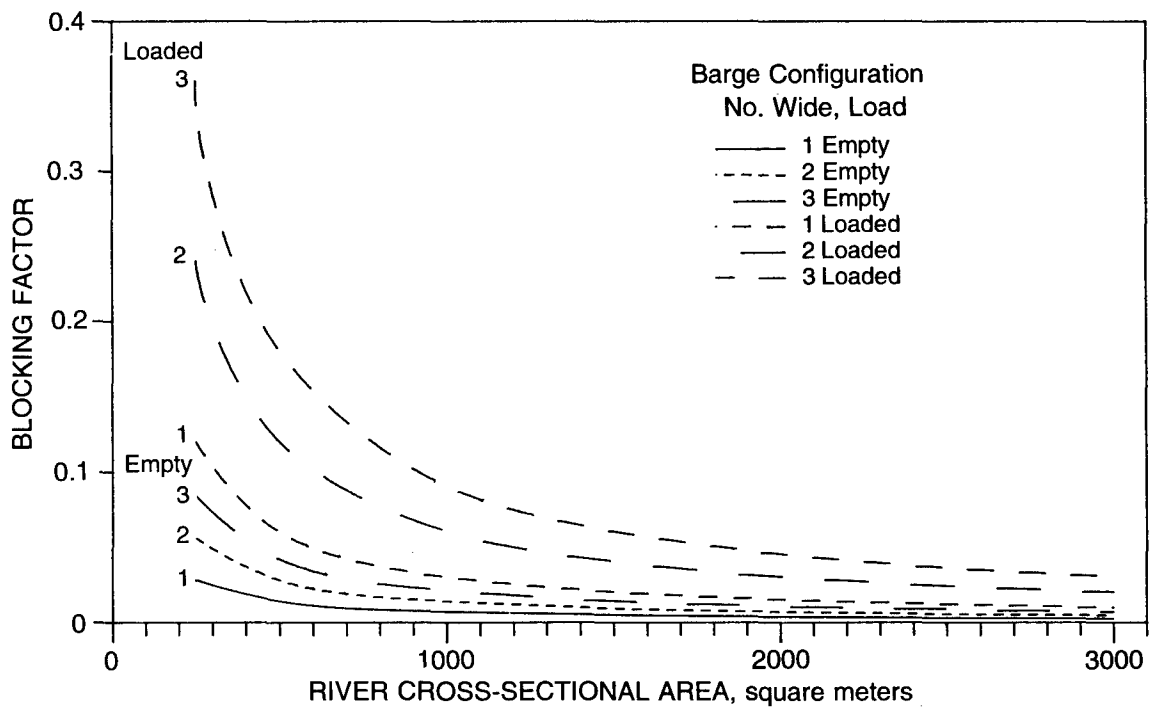


Figure 7. Blocking factors for tows one to three barges wide on the UMRS, after Adams (1992)

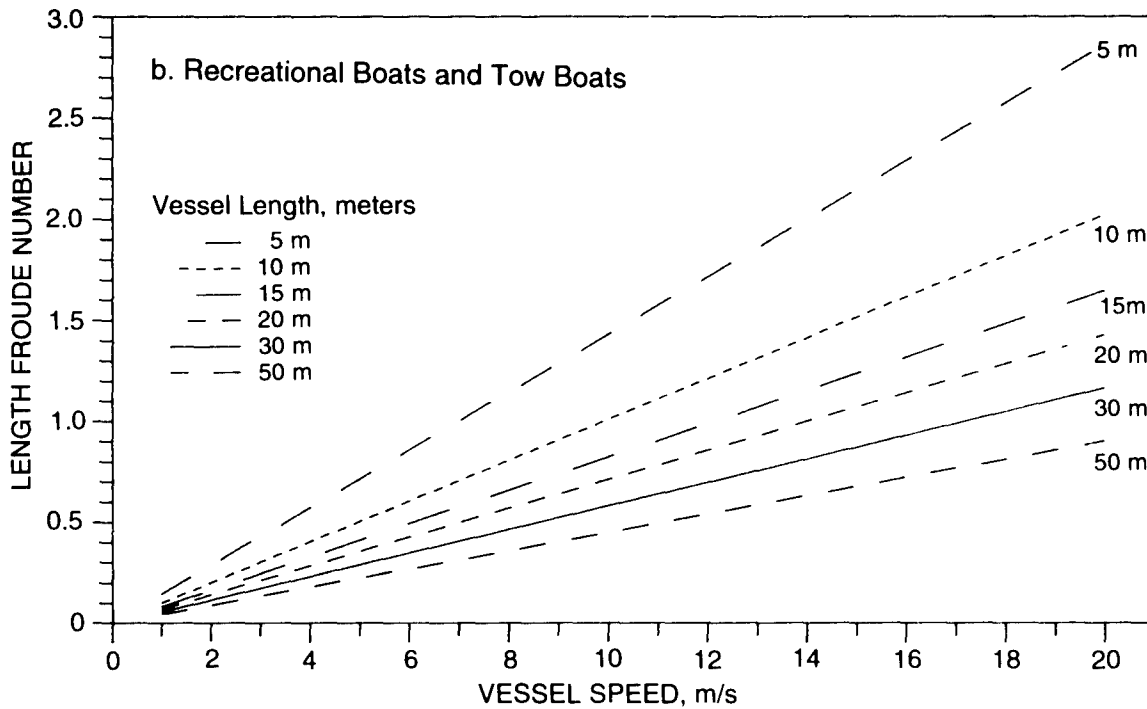
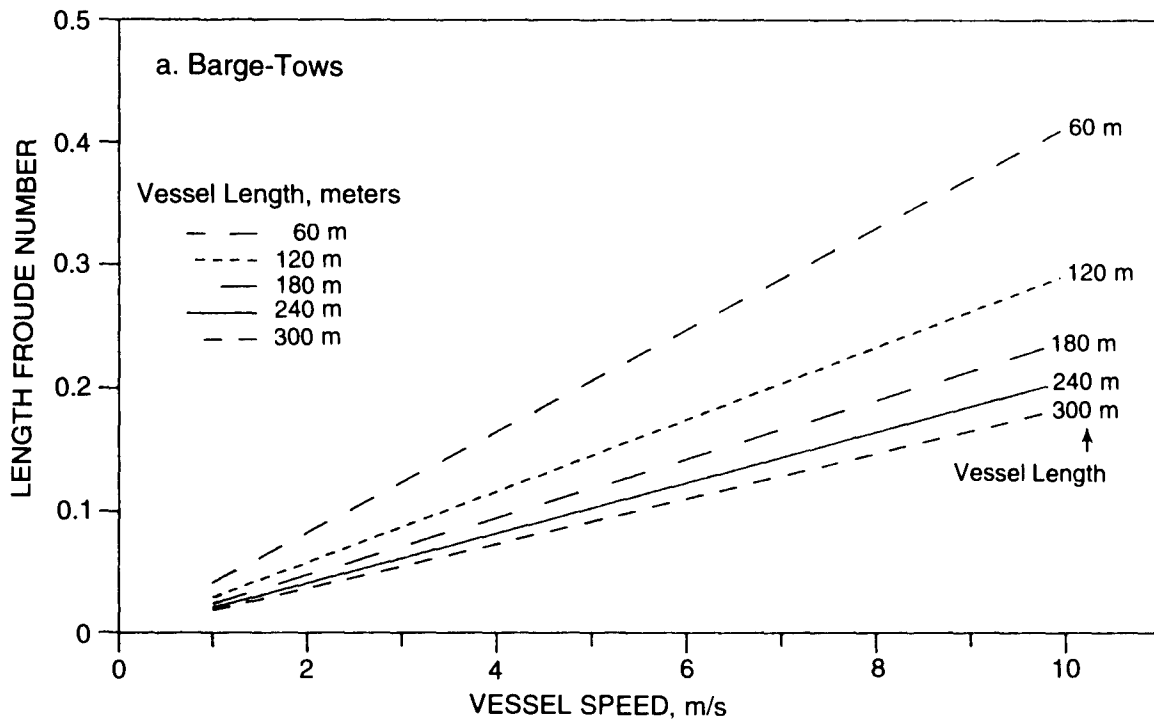
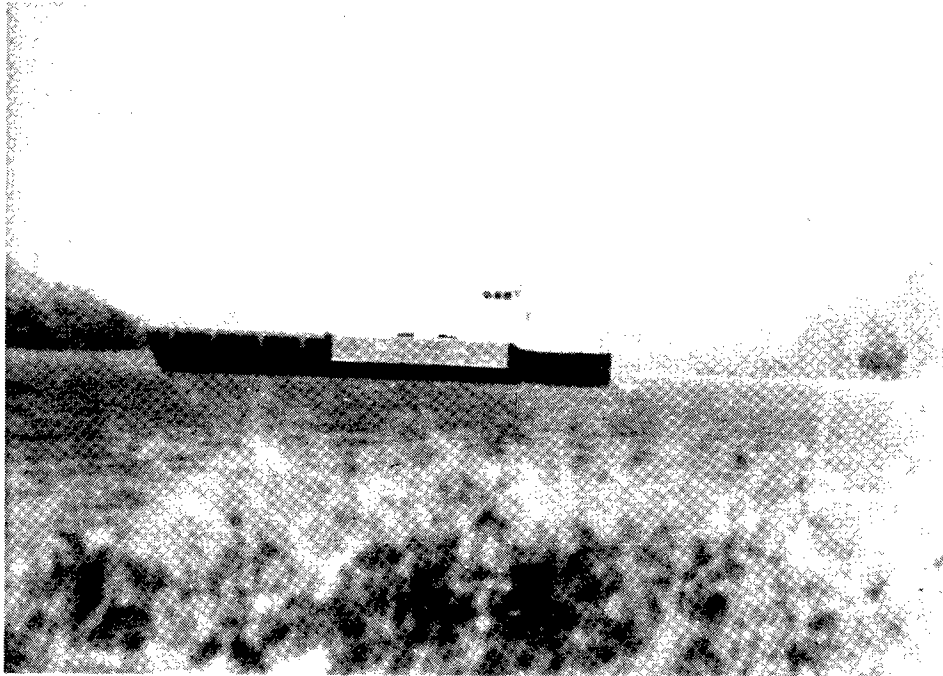
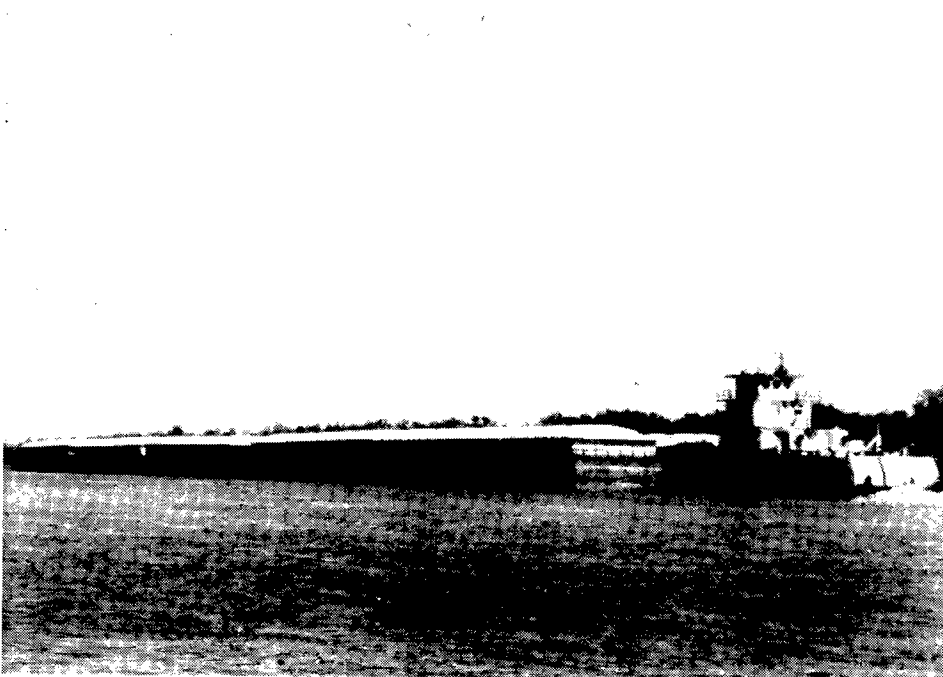


Figure 8. Length Froude Numbers, $F_1 = V_b/(gl)^{0.5}$, for a) barge-tows and b) recreational boats and towboats, after Adams (1992)

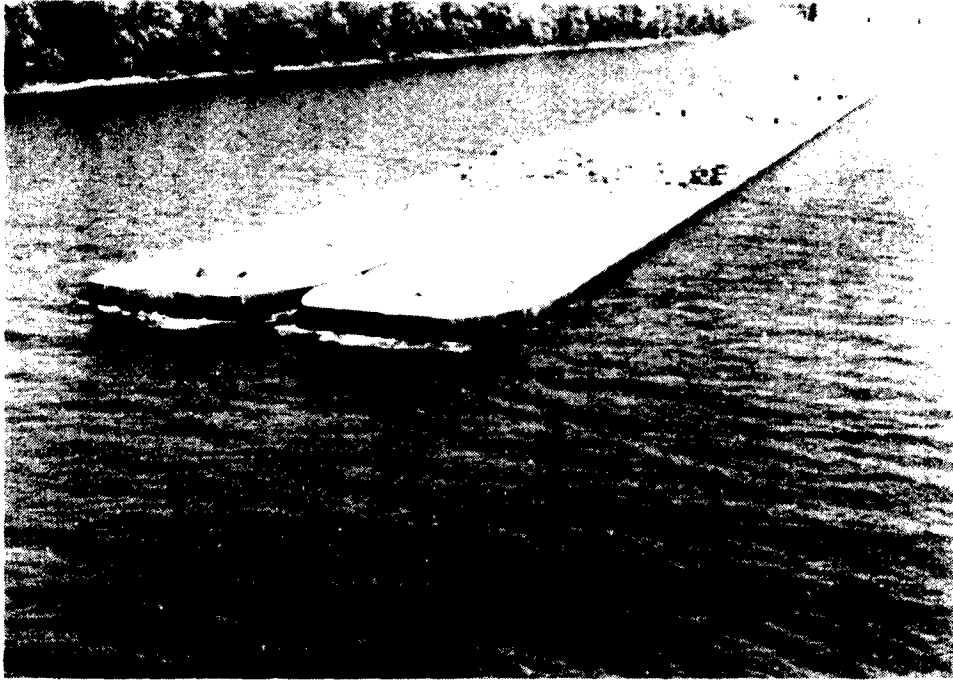


a. Petroleum Barges



b. Cargo Barges

Figure 9. Typical barges on the UMRS



c. Chemical Barges



d. Petroleum Barges

Figure 9. Concluded

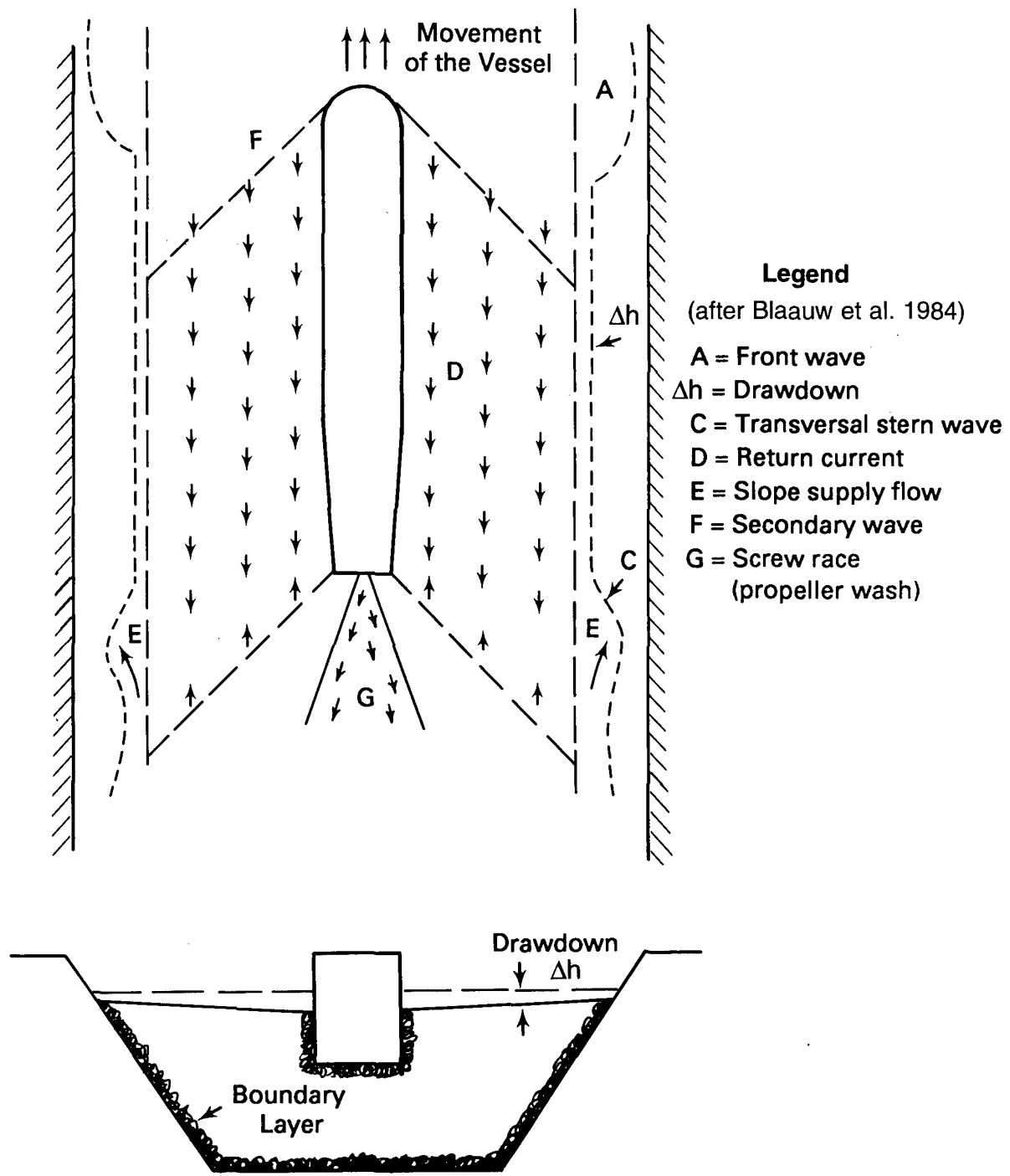


Figure 10. Schematic diagram showing water motion generated by a moving ship, after Blaauw et al. (1994)

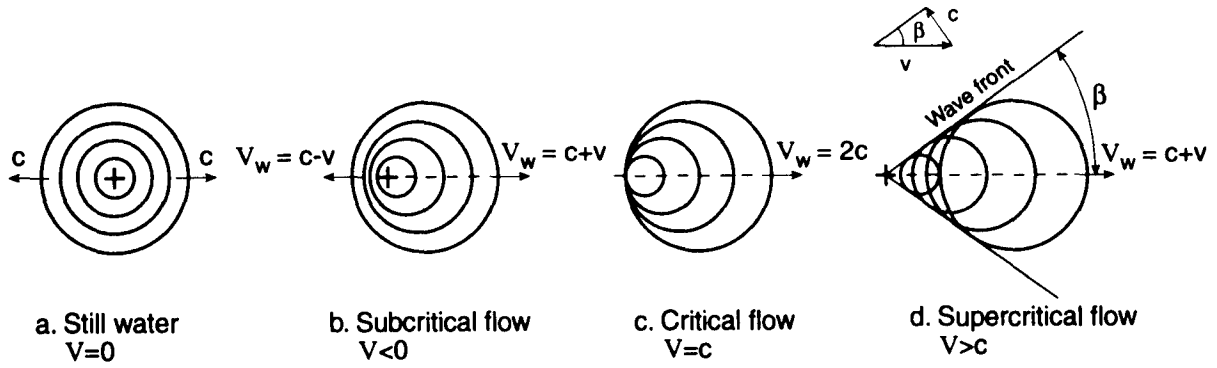


Figure 11. Wave patterns created by a point disturbance for (a) still water, $V = 0$; (b) subcritical flow, $V < c$; (c) critical flow, $V = c$; and (d) supercritical flow, $V > c$, after Henderson (1966)

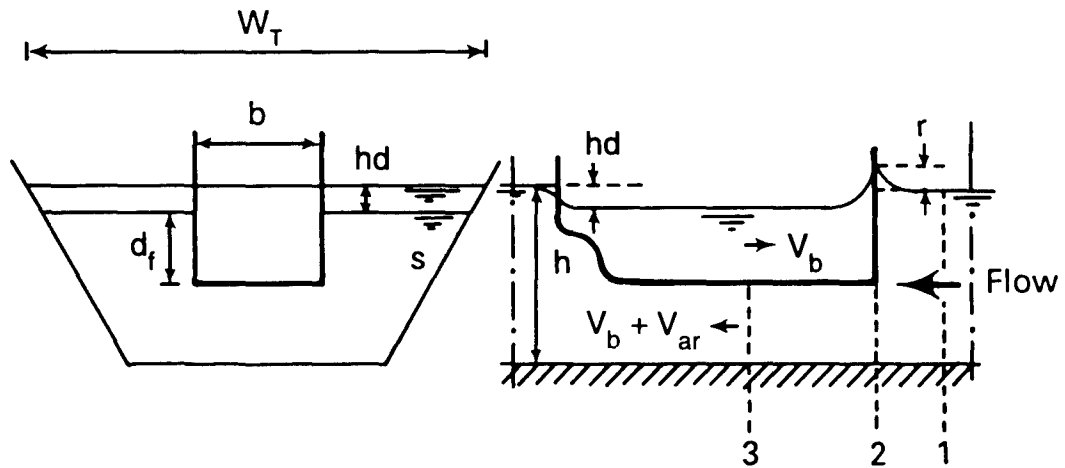


Figure 12. Schematic diagram of changes in water levels within a navigation channel due to vessel movement, after Blaauw and van der Knapp (1983)

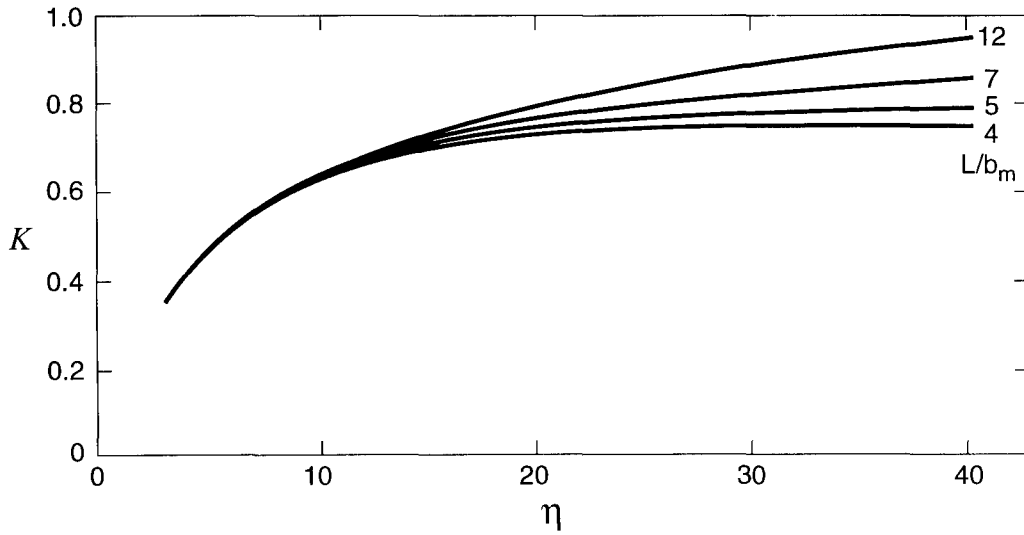


Figure 13. Variation of constraint factor, K , as function of blocking ratio, N , and vessel aspect ratio, L/b , after Hochstein and Adams (1989)

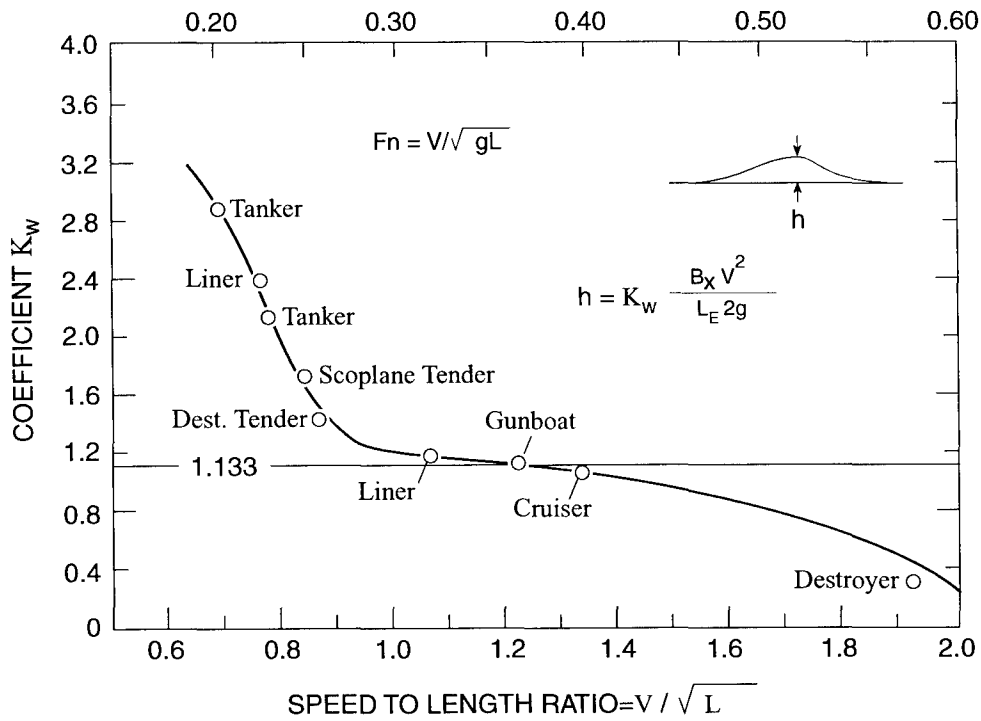


Figure 14. Graph for determining values of K_w , after Gates and Herbich (1977)

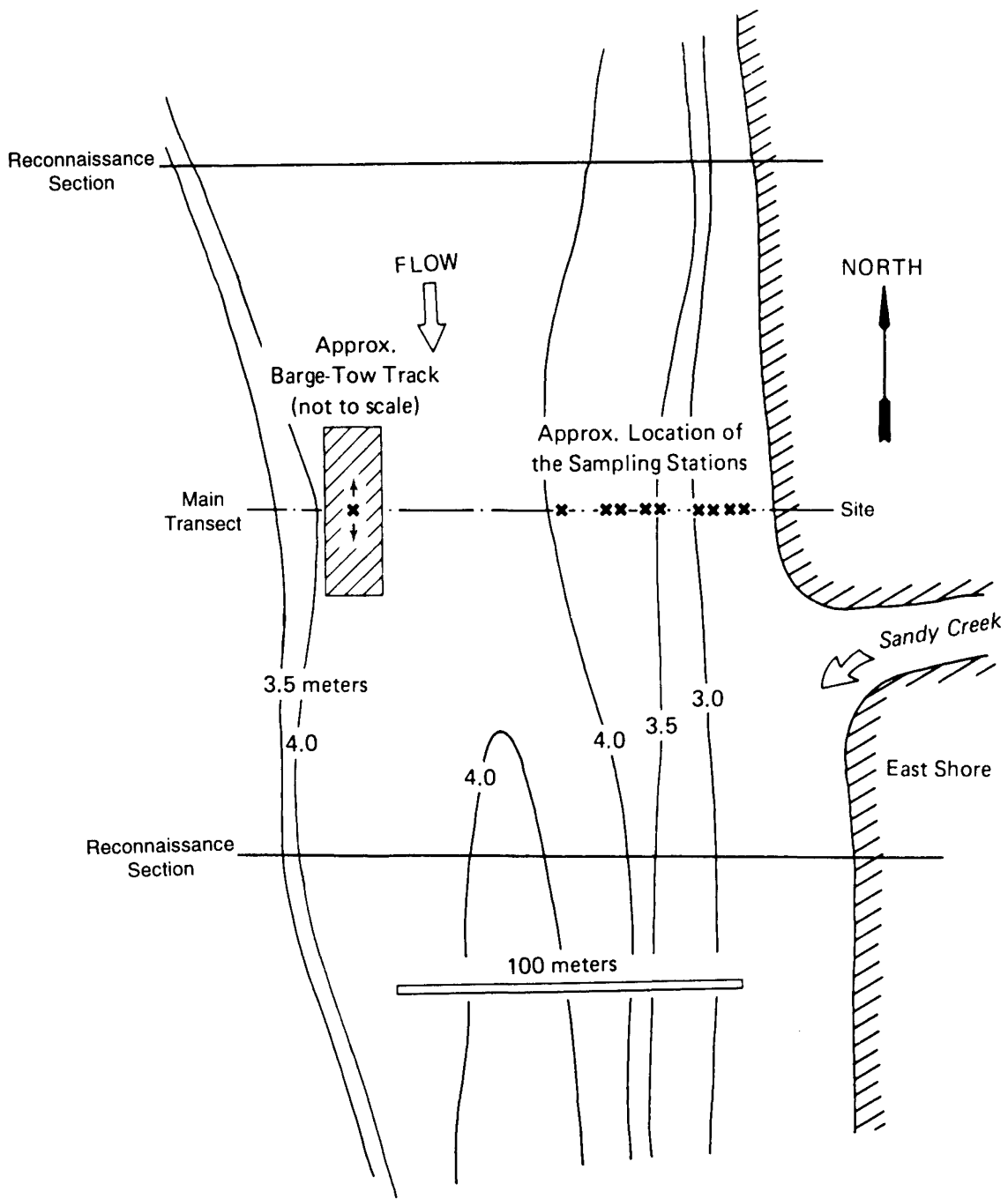
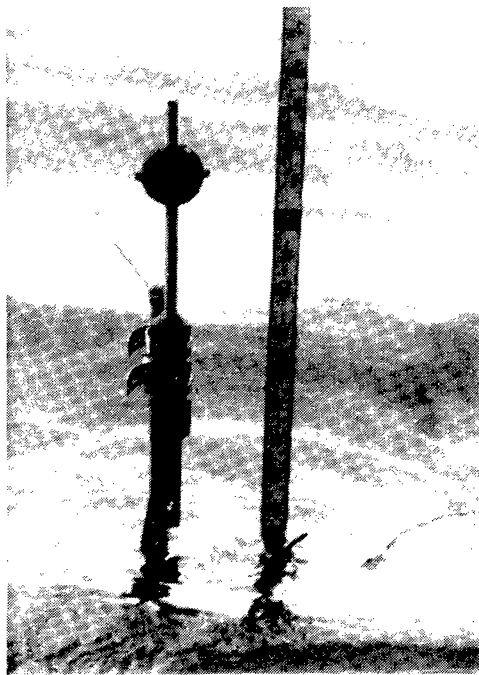
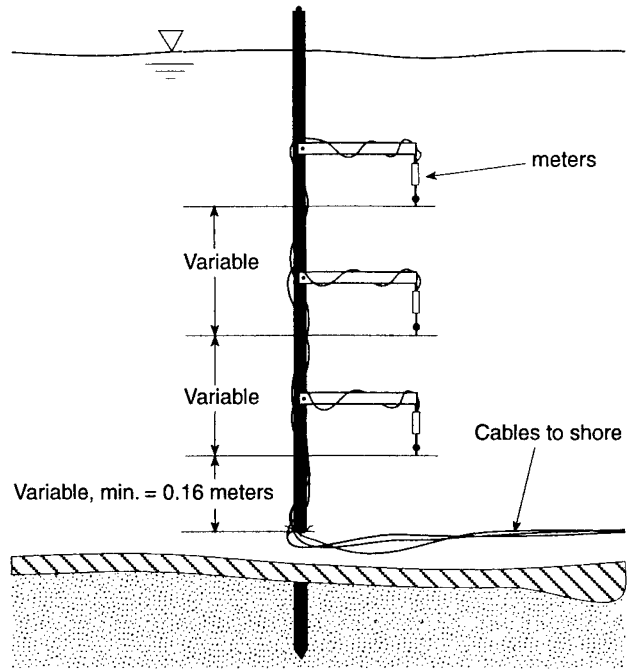
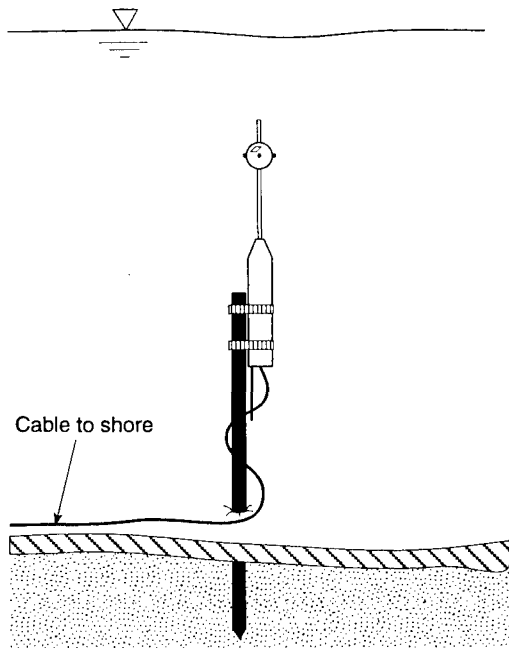
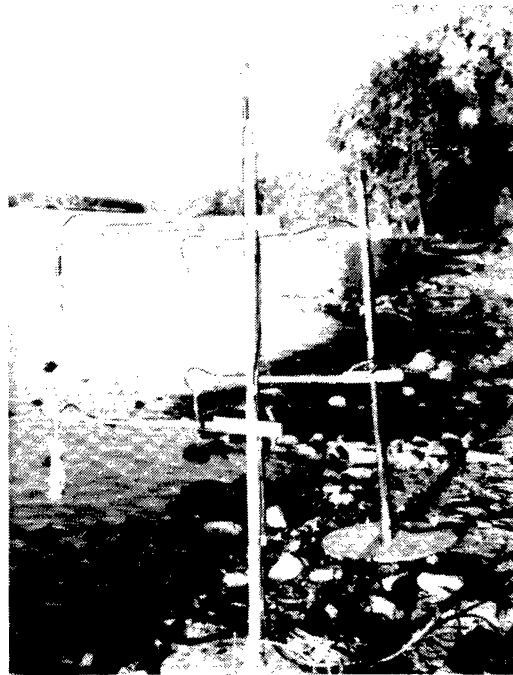


Figure 15. McEver's Island Site on the Illinois River, RM 50.1

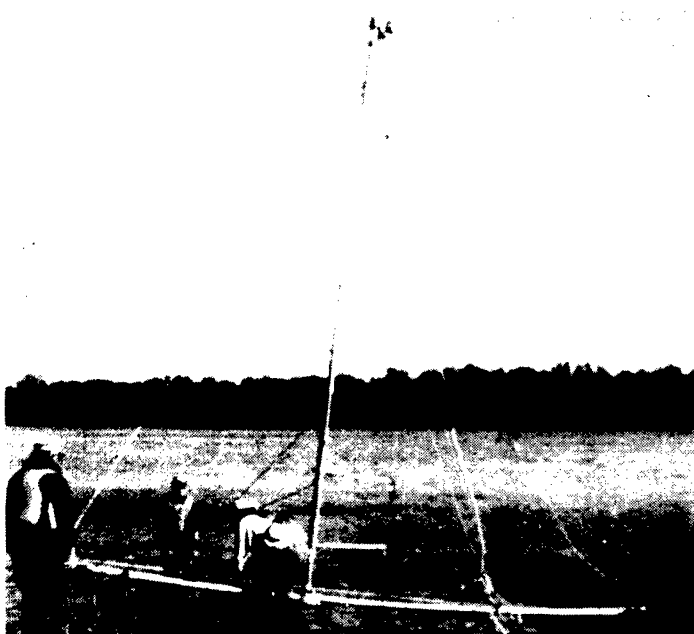
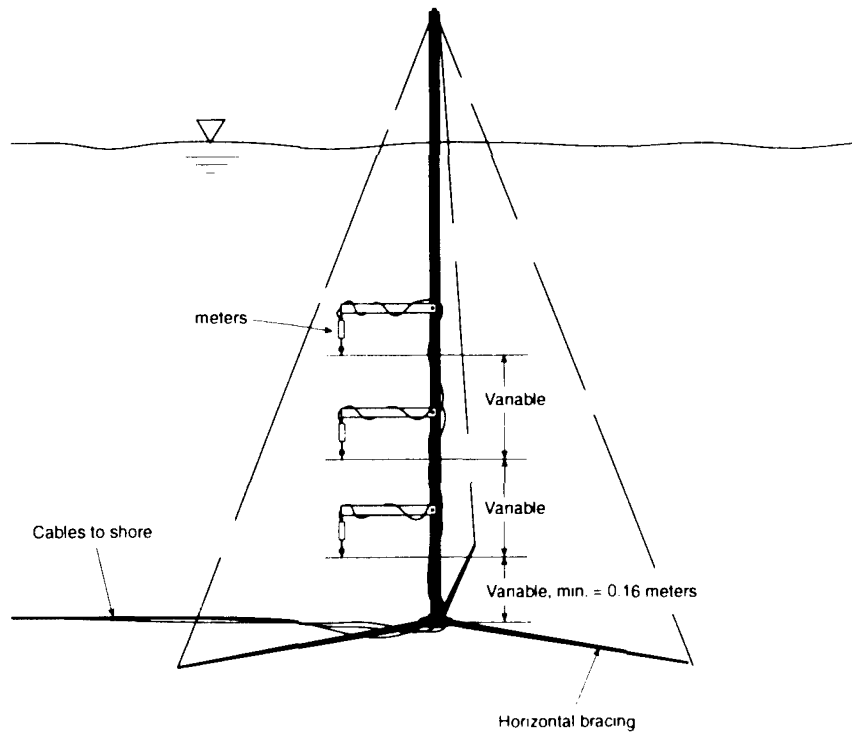


a. MMB511 Single Meter Setup

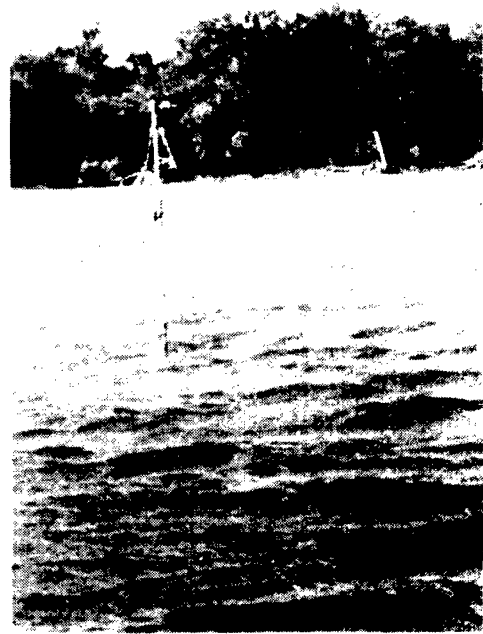


b. MMB511 Array Setup

Figure 16. Post system for velocity data collection

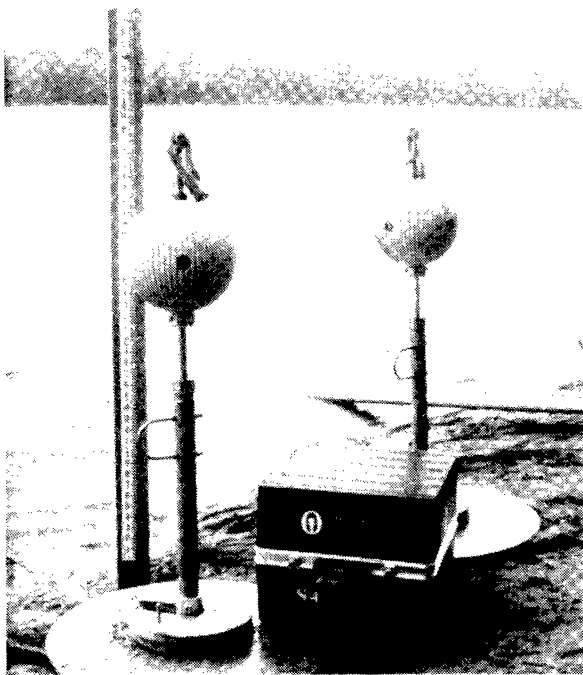
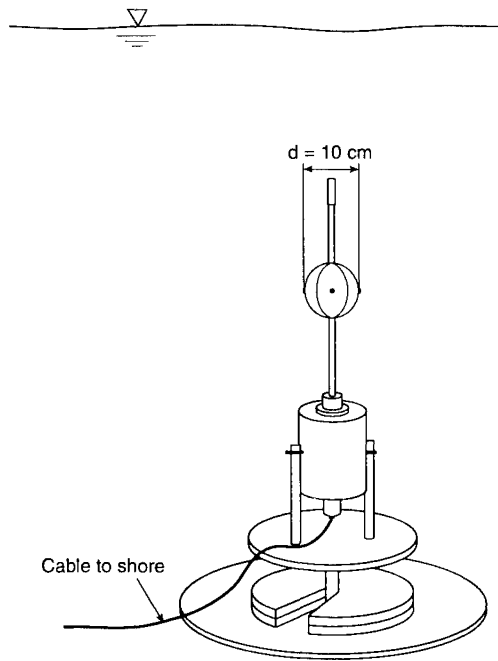
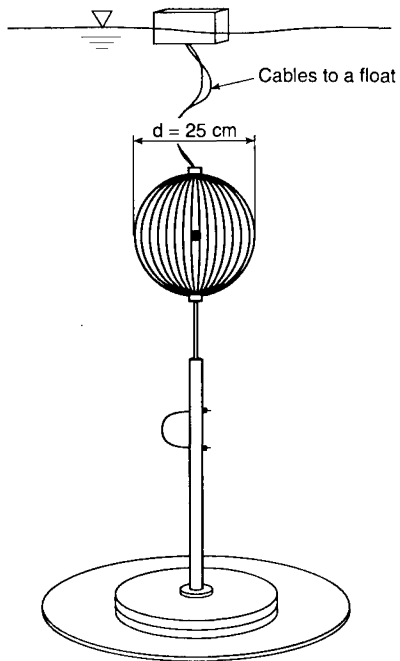


Before Deployment

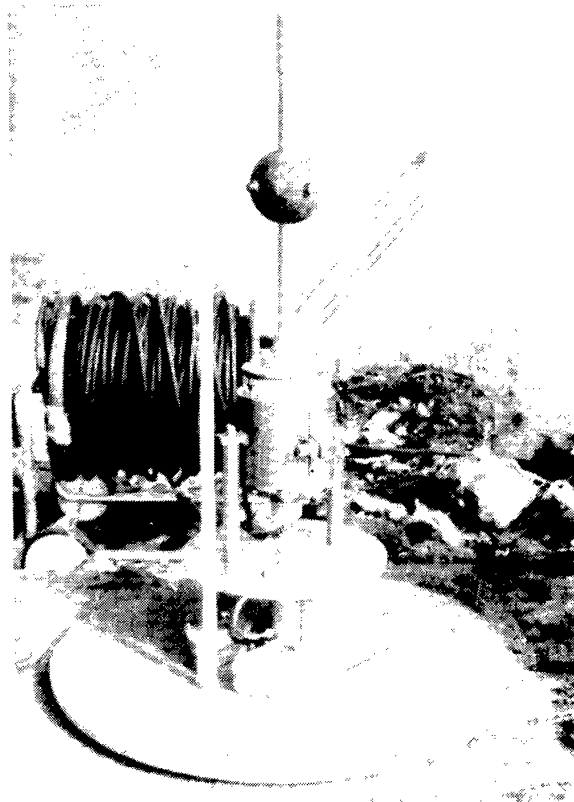


After Deployment

Figure 17. Vertical array for velocity data collection

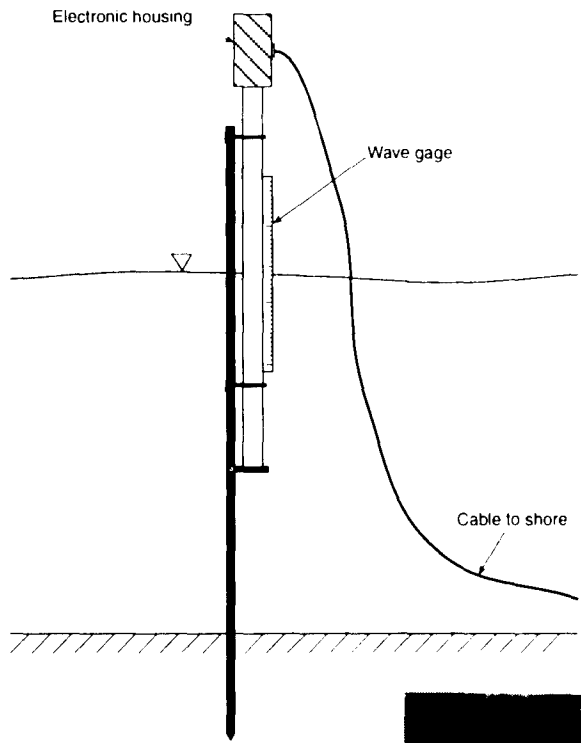


a. S4 Meters on Supporting Bases



b. MMB527 Meter on Supporting Base

Figure 18. Base-mounted current meters S4 and MMB527

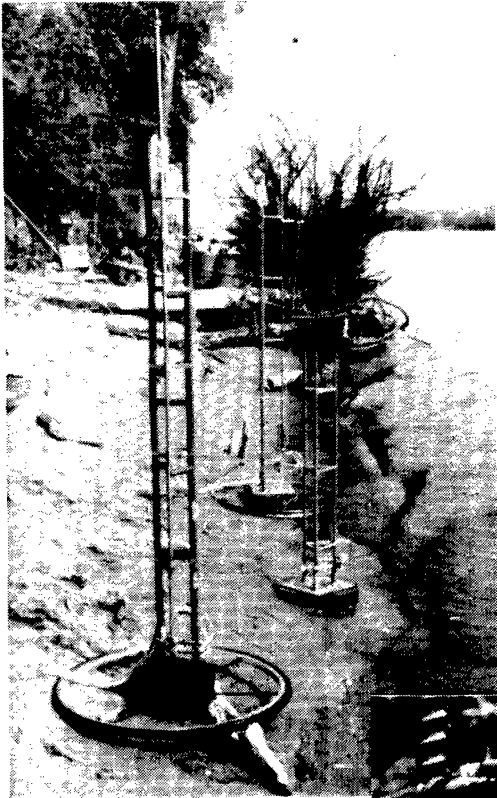
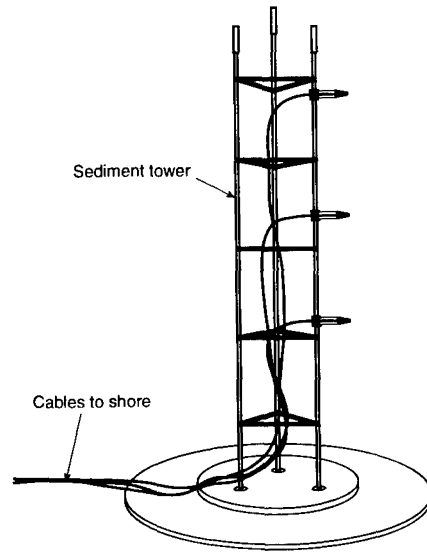


Wave Gage Setup in the Field



Measuring Surface Wave Data during Event

Figure 19. Wave gage installation



Sediment Towers

Sediment Tower and Intake Nozzles

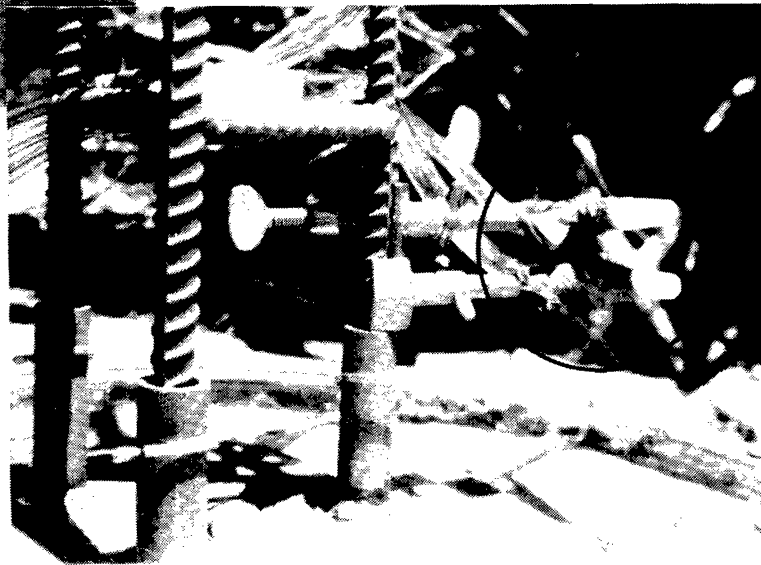


Figure 20. Sediment towers

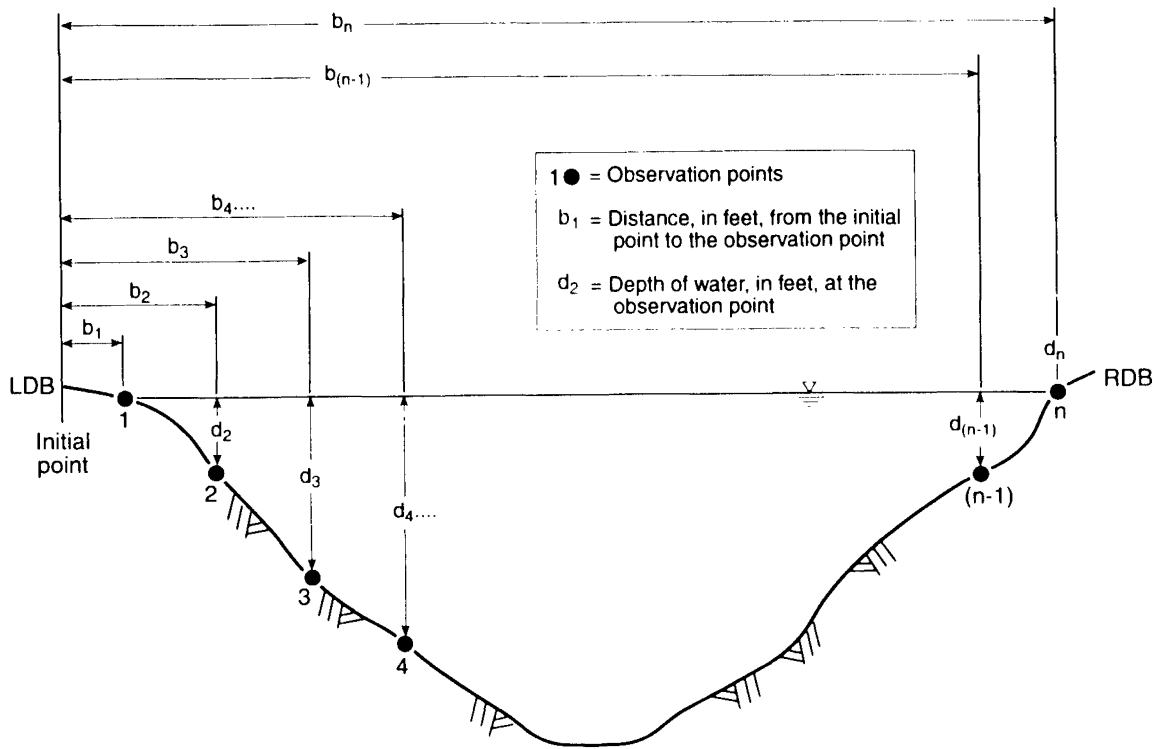
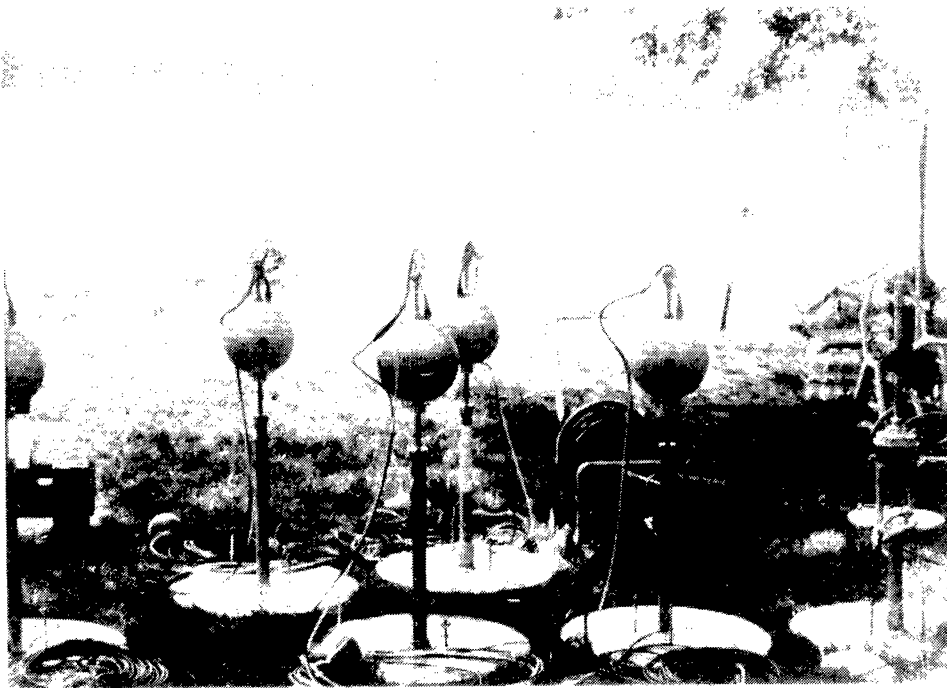


Figure 21. Typical setup for background data collection at McEever's Island on the Illinois River, RM 50.1



a. Equipment Used in the Field



b. Laying Out Equipment in the Main Transect

Figure 22. McEver's Island data collection setup, Illinois River, RM 50.1



c. Collecting Event Data



d. Collecting Event Data

Figure 22. Concluded

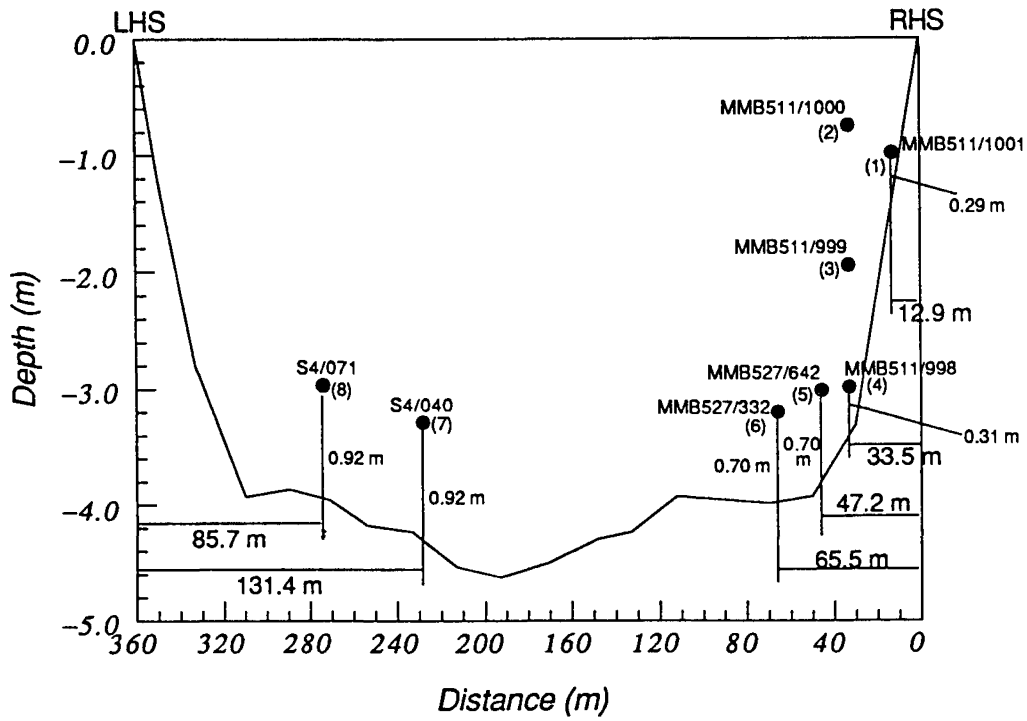


Figure 23. Typical instrumentation setup on the Illinois River near Kampsville, RM 35.2

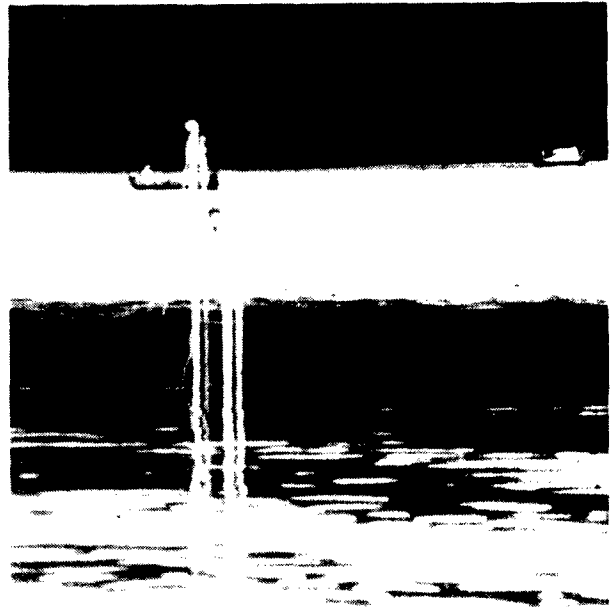
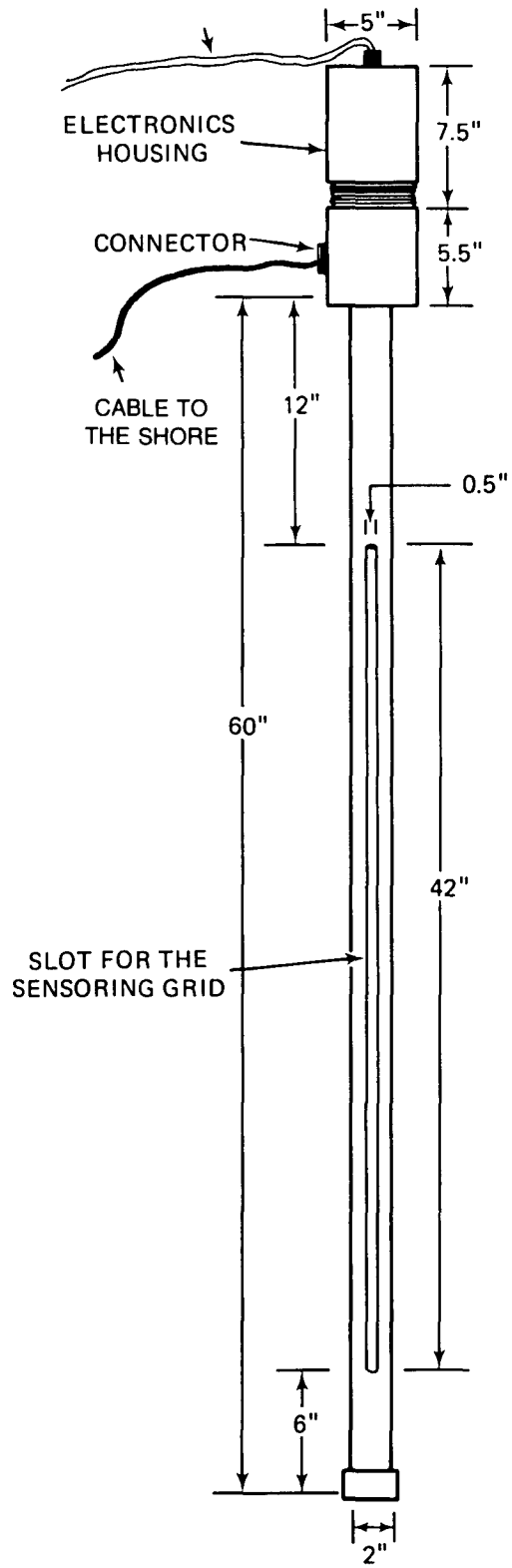
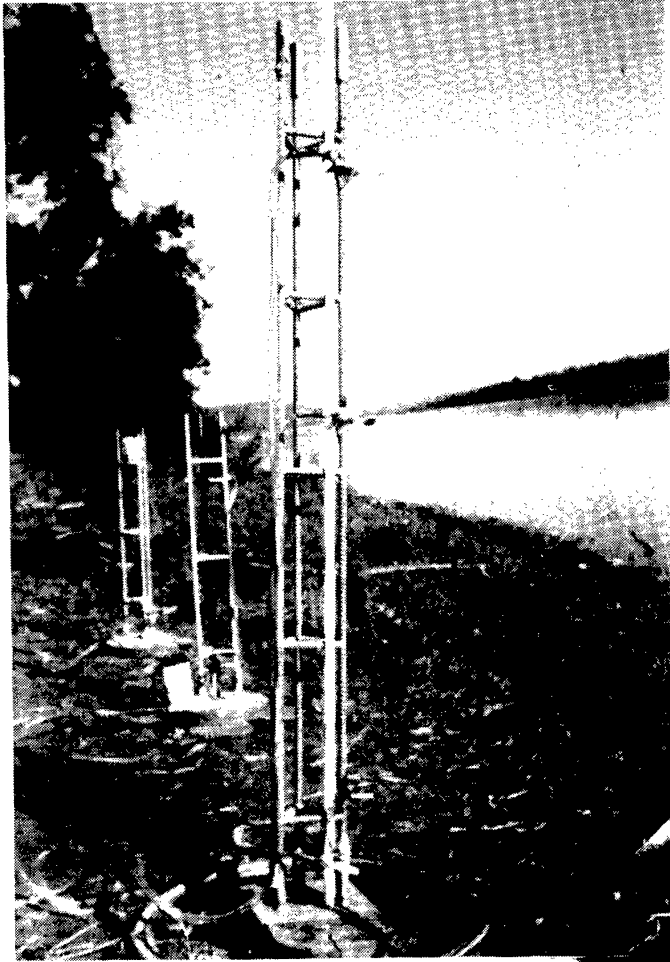


Figure 24. Wave and drawdown measuring gage

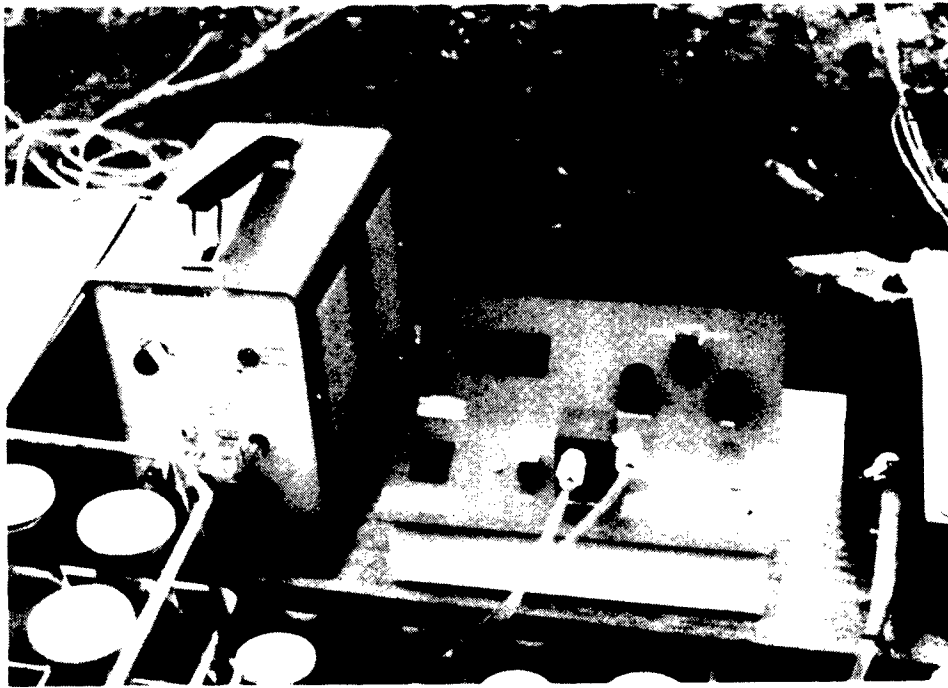


a. Sediment Tower

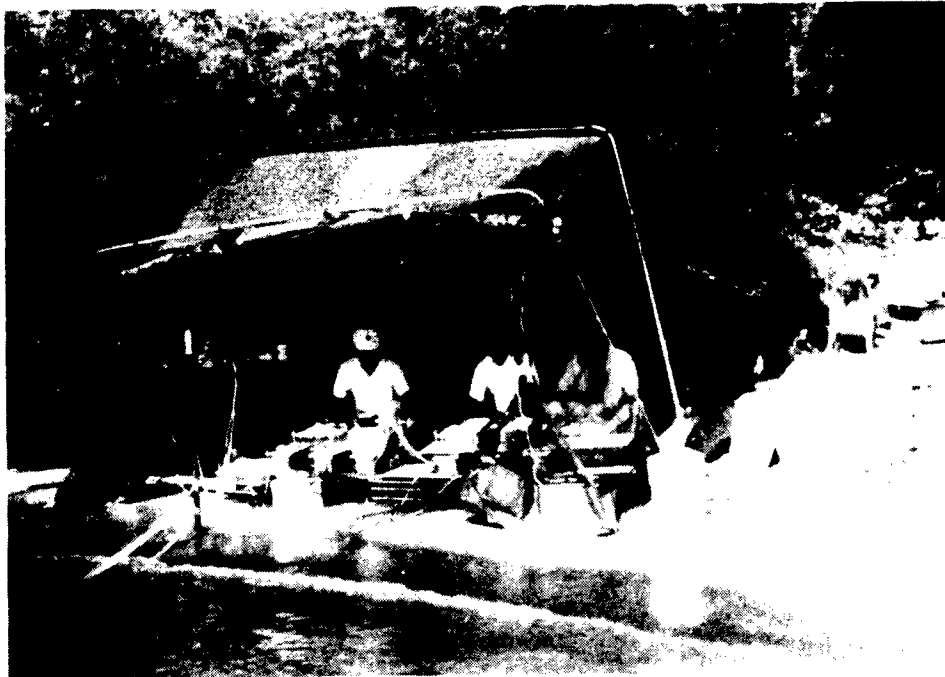


b. Shore Station (note tower in the water)

Figure 25. Field setup for suspended sediment sampling



c. Pump and Turbidity Meter



d. Shore Station

Figure 25. Concluded



Figure 26. Recording wind set

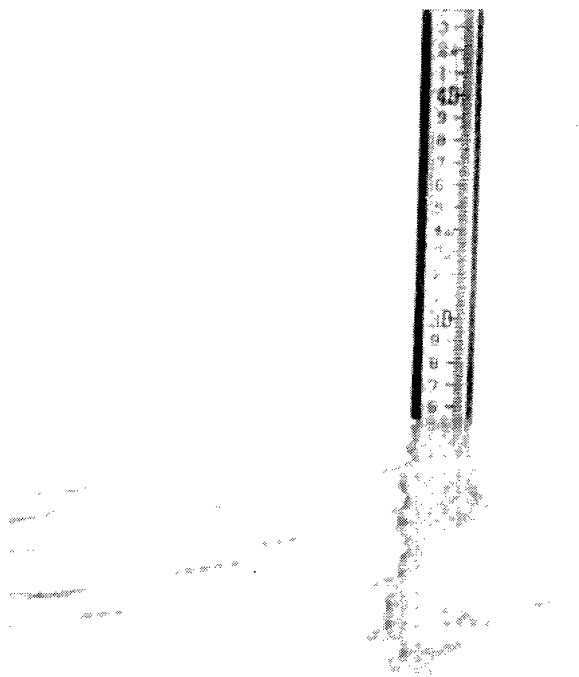


Figure 27. Staff gage

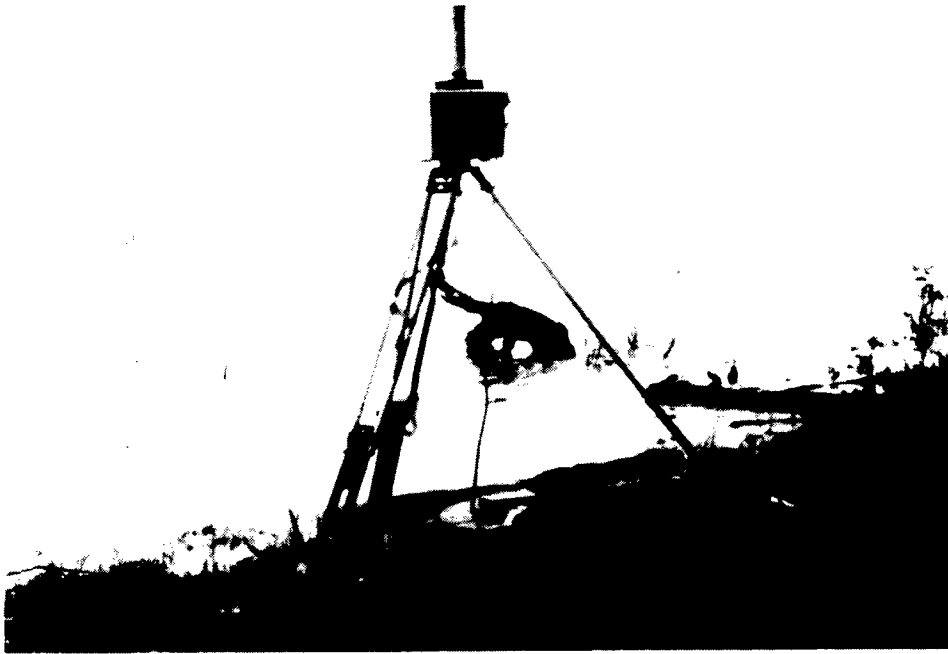
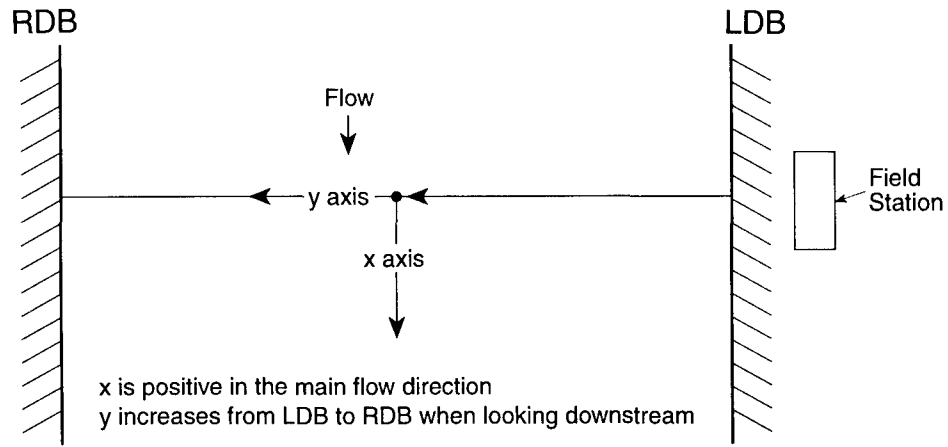
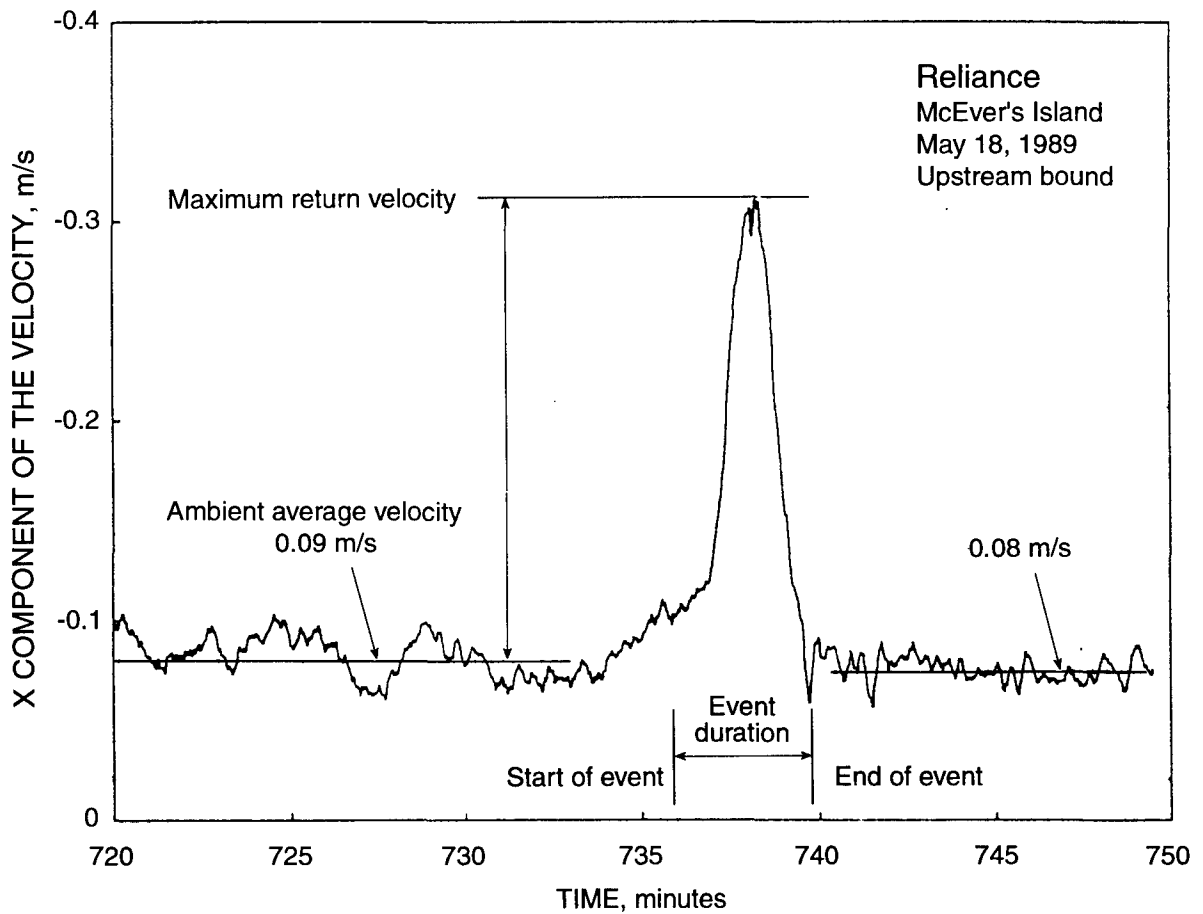


Figure 28. MicroFix system and tow tracking



a. Definition Sketch of the River Plan Form



b. Return Velocity Determination

Figure 29. Time series of the x-component of velocity during a barge passage (11-point moving average)

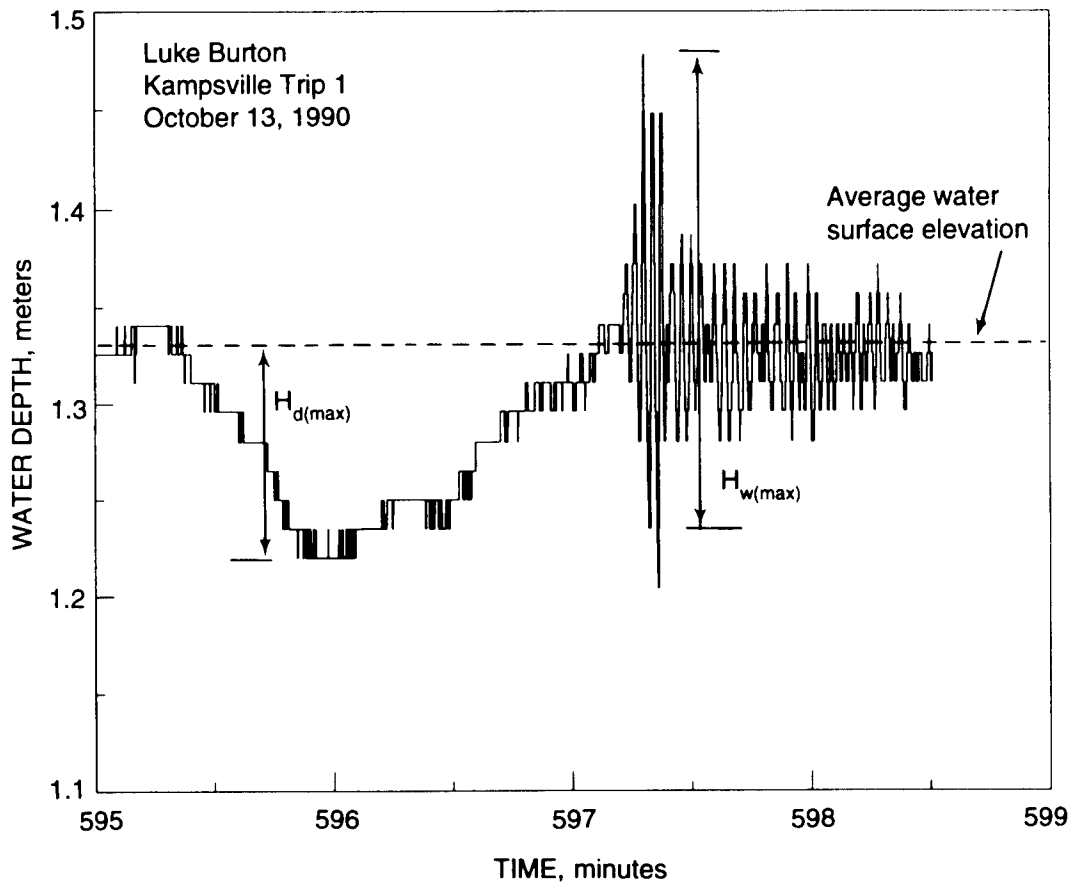


Figure 30. Typical drawdown and wave characteristics due to a barge-tow movement

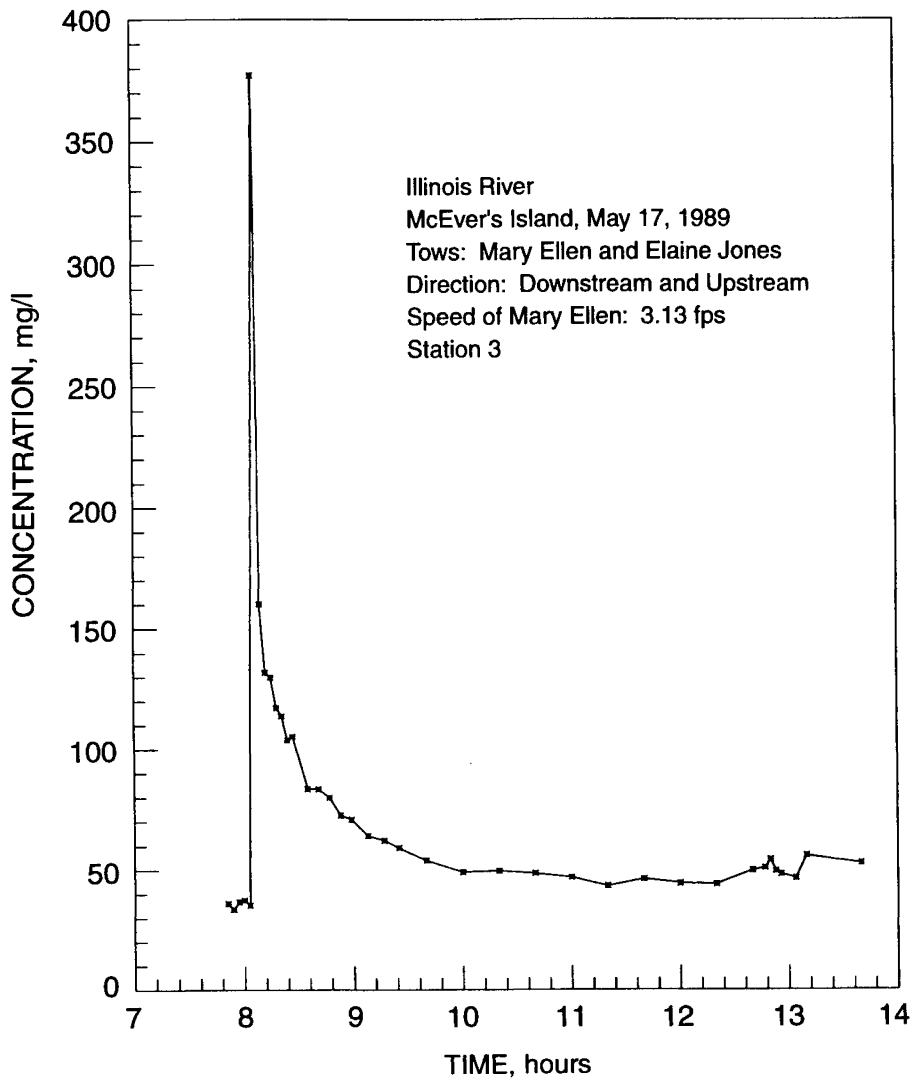


Figure 31. Suspended sediment concentration

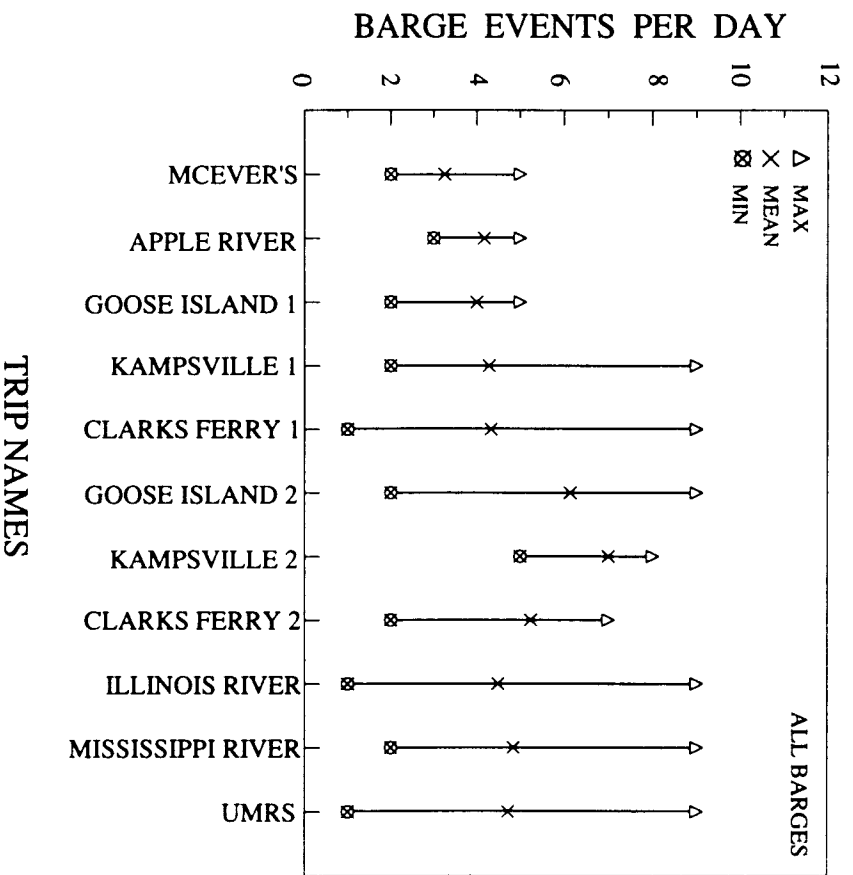


Figure 32. Number of barge-tow events observed per day at each site during the survey

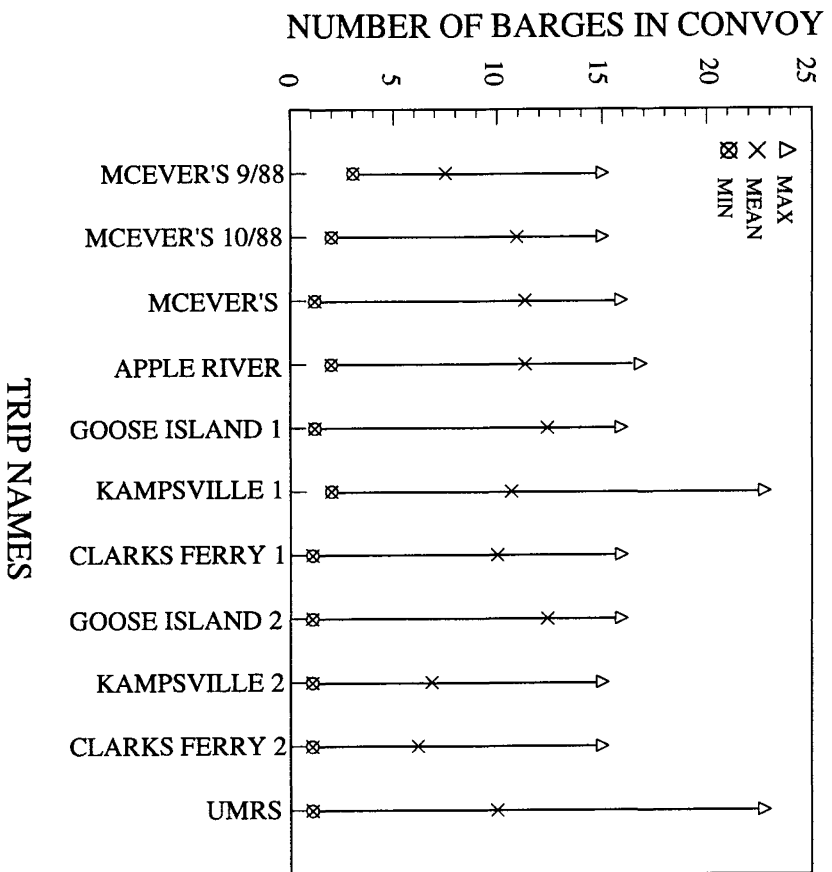


Figure 33. Number of barges per convoy at each site during the survey

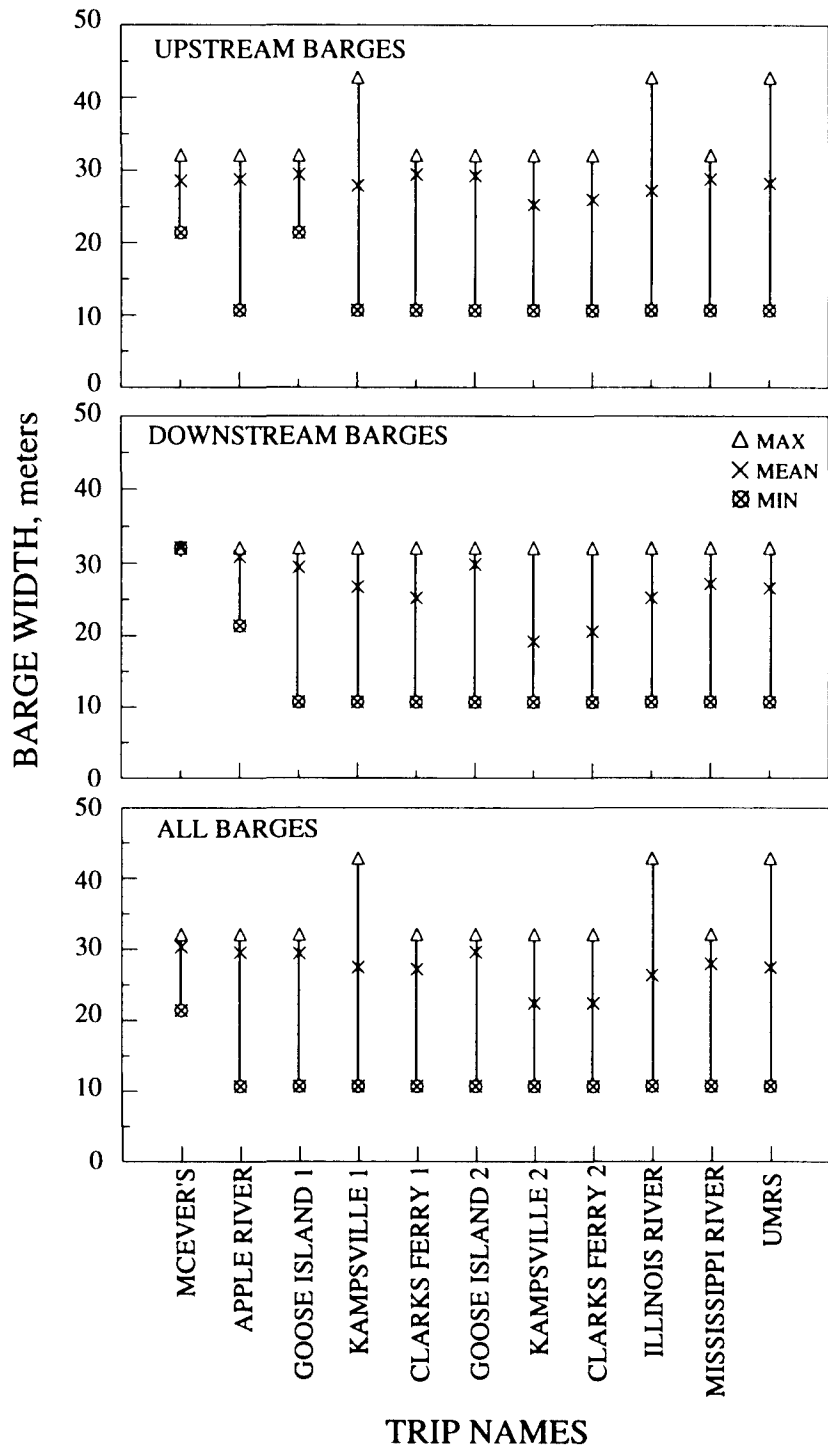


Figure 34. Width of barge convoys at each site during the survey

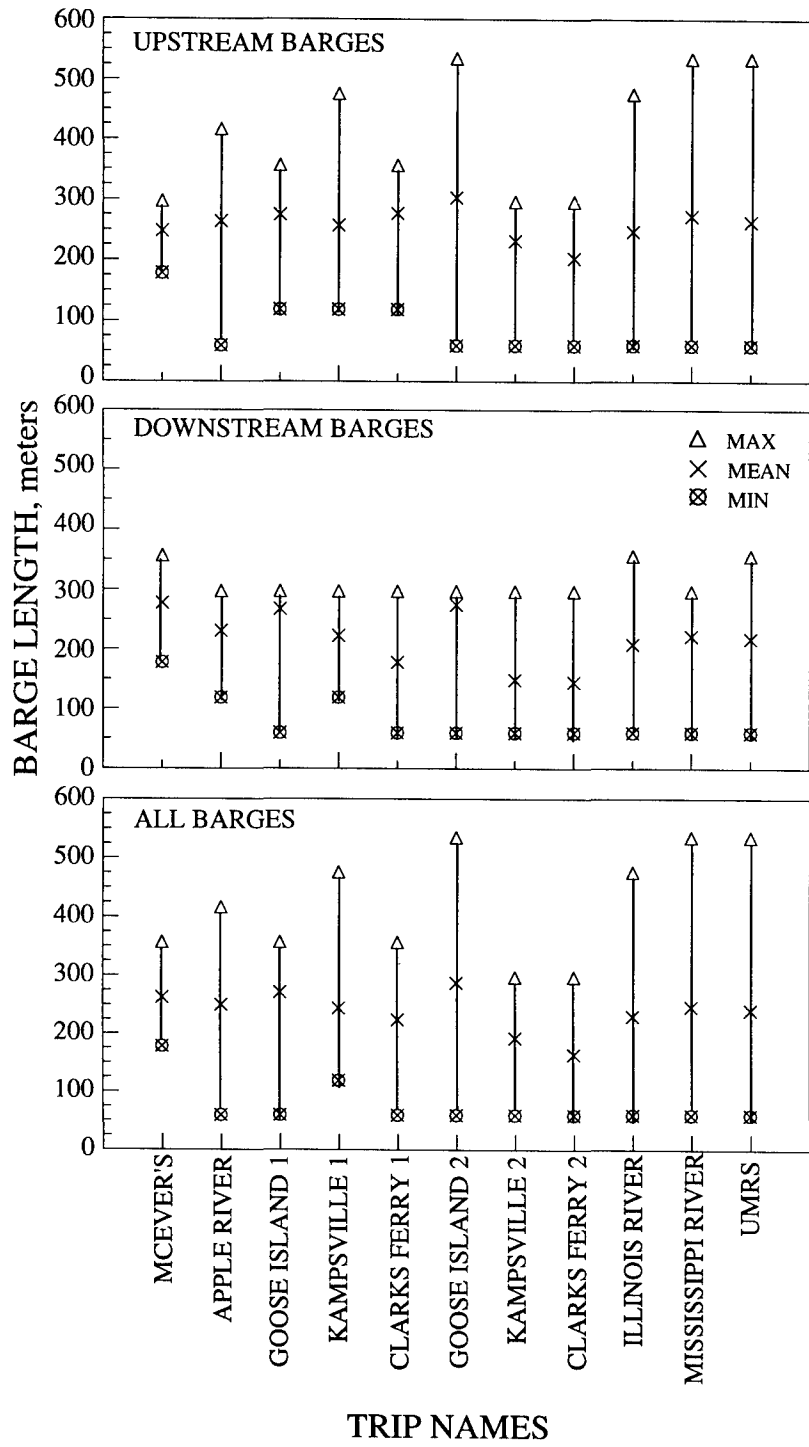


Figure 35. Length of barge convoys at each site during the survey

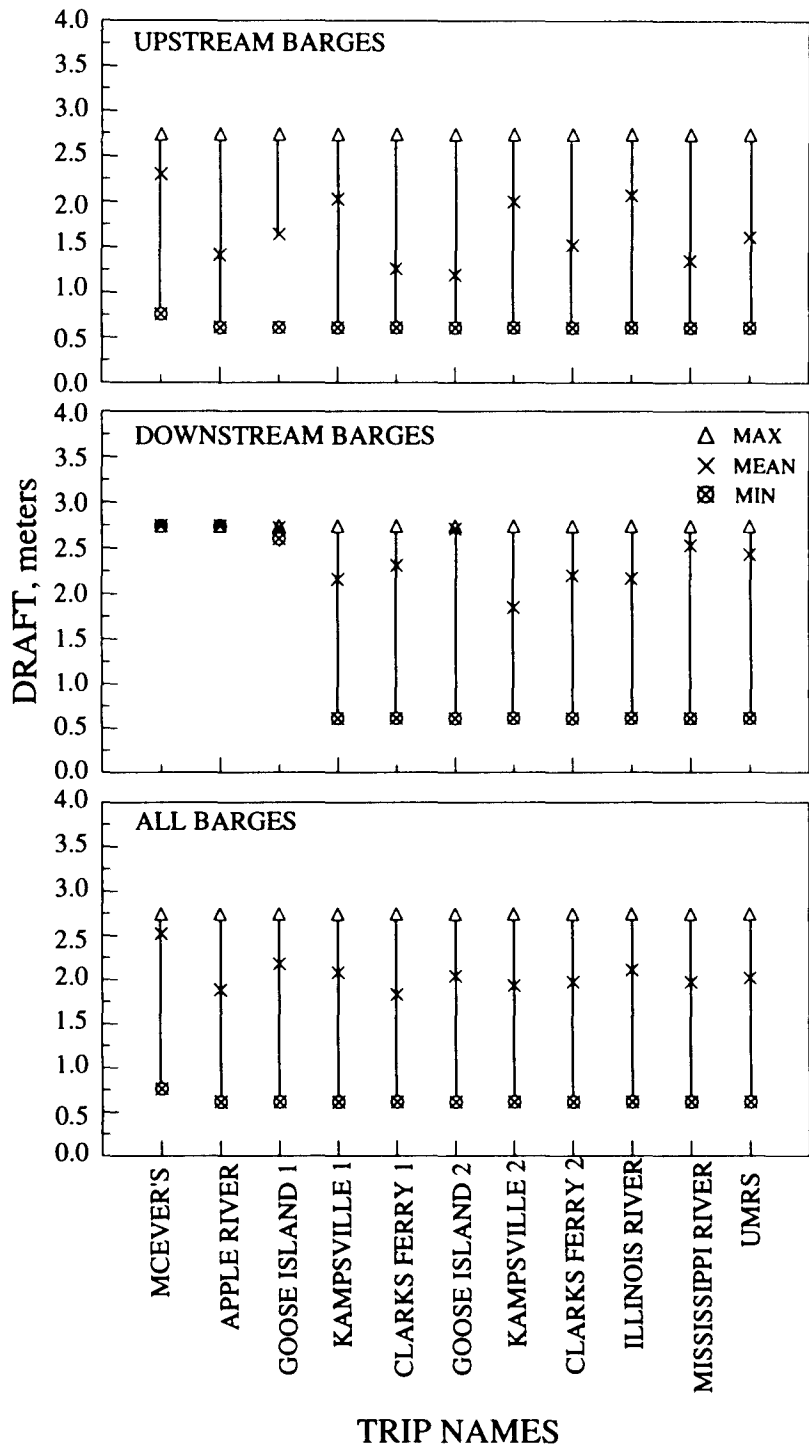


Figure 36. Draft of barge convoys at each site during the survey

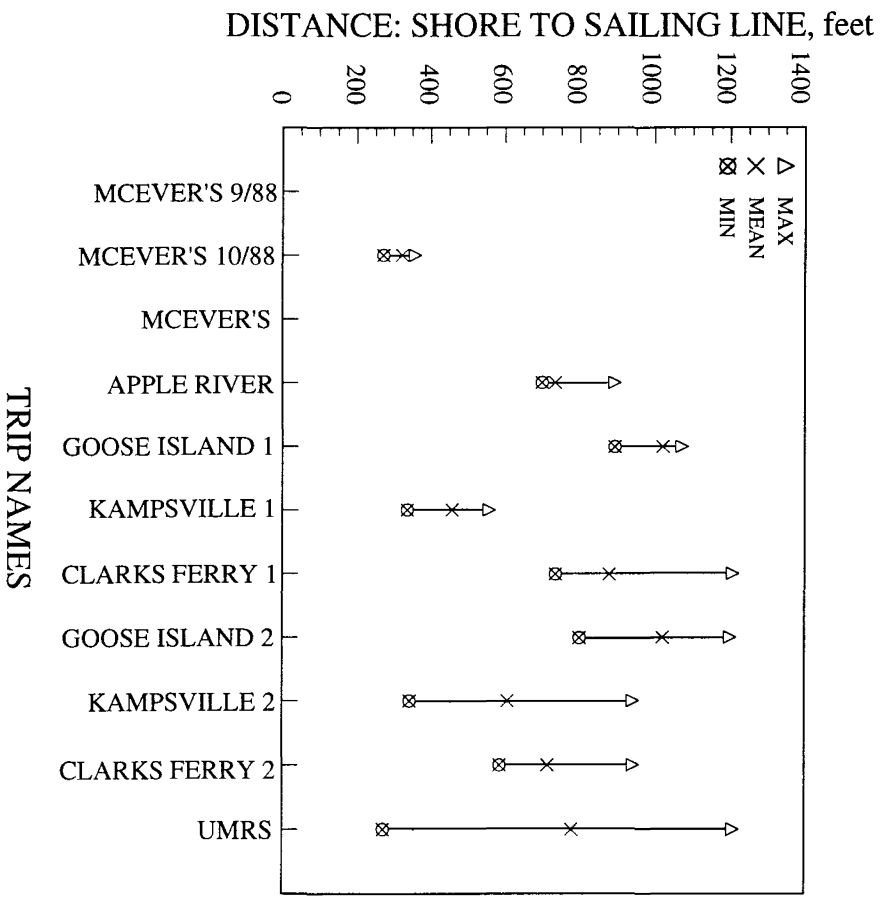


Figure 37. Distance of barge convoys at each site during the survey

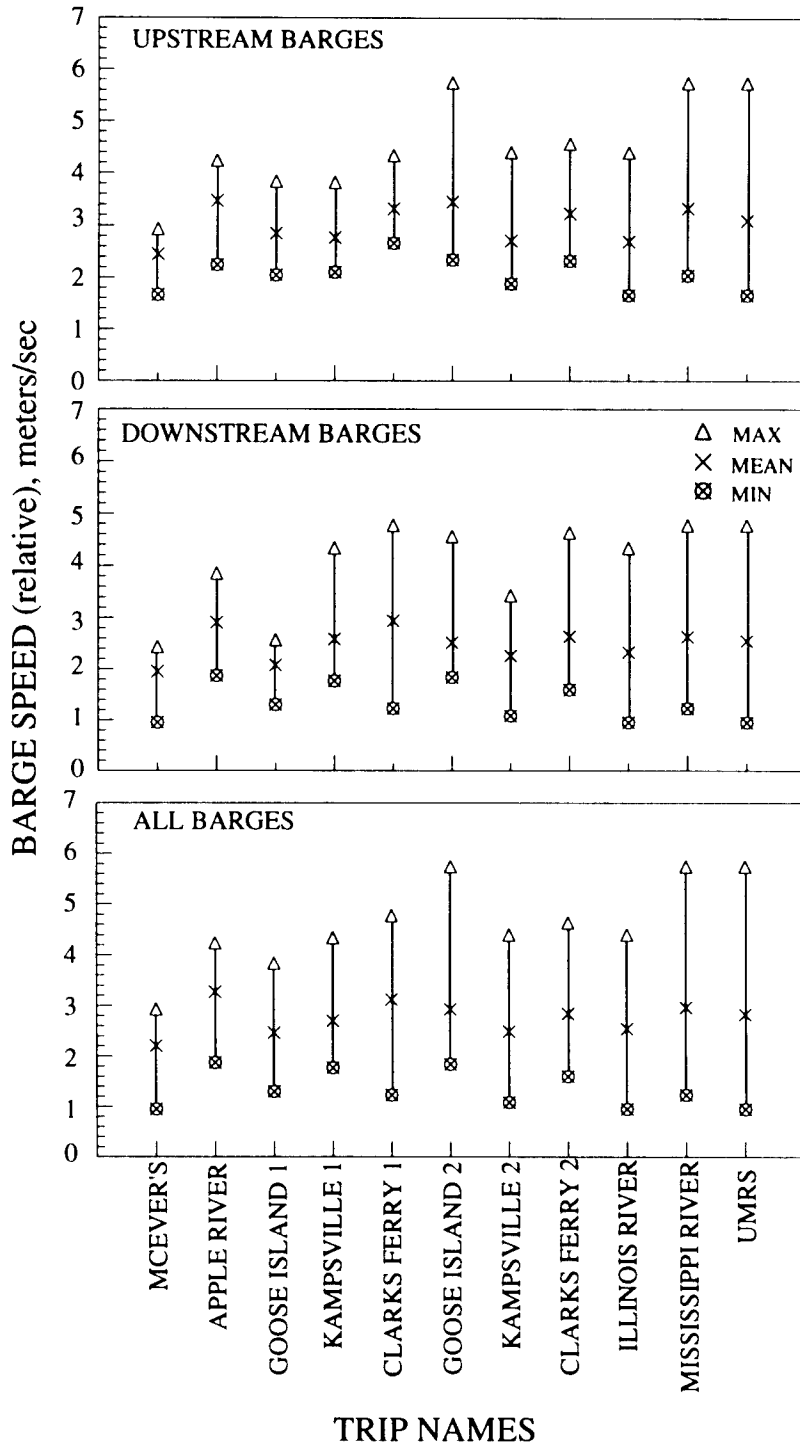


Figure 38. Speed of barge convoys at each site during the survey

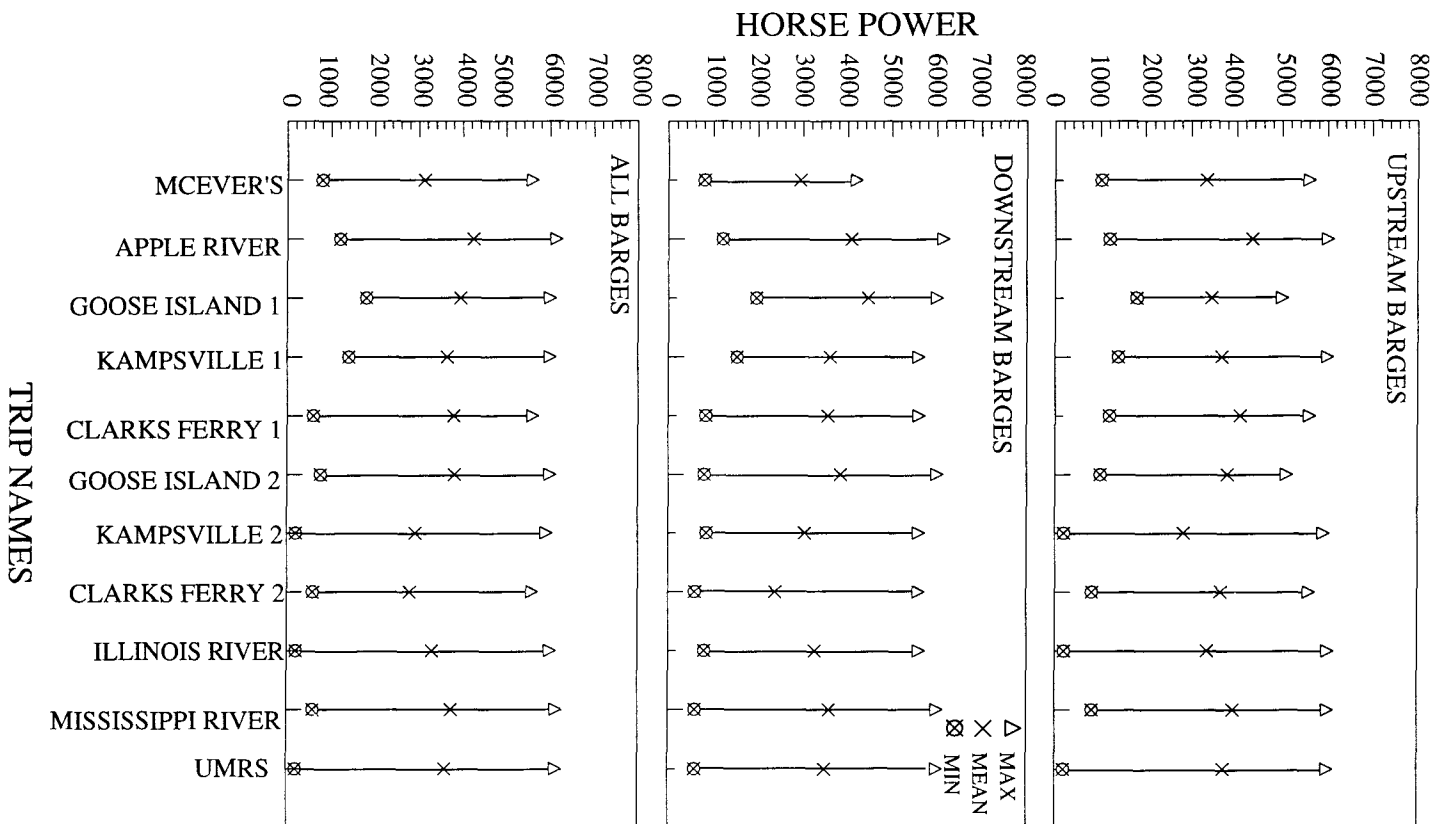


Figure 39. Horsepower of barge convoys at each site during the survey

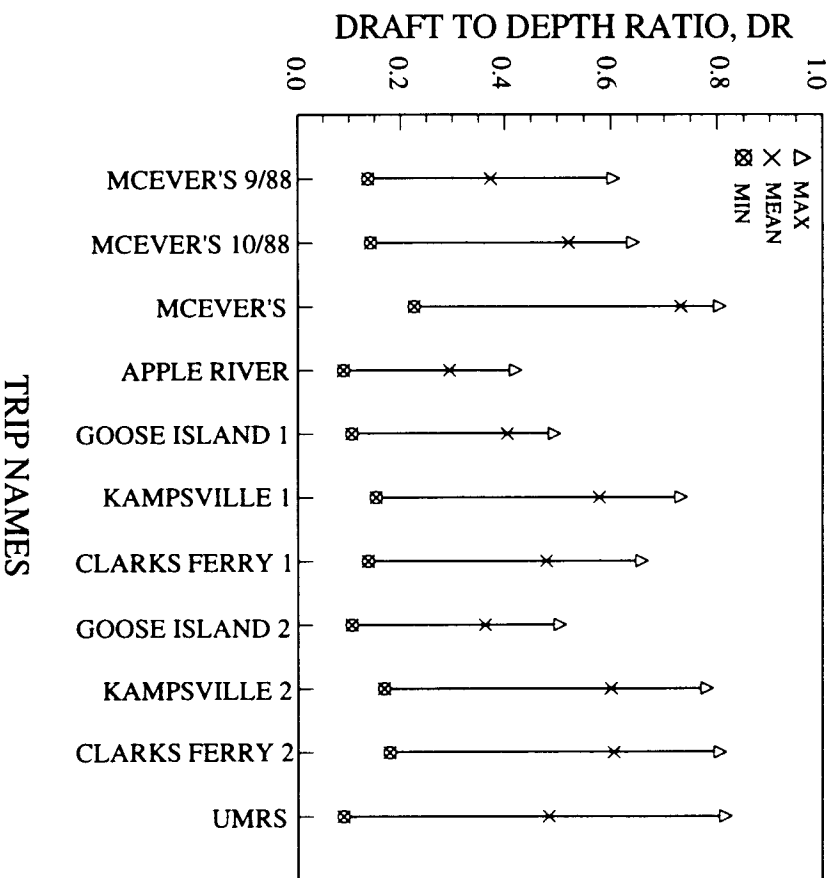


Figure 40. Draft to depth ratio for barge-tow events at each site during the survey

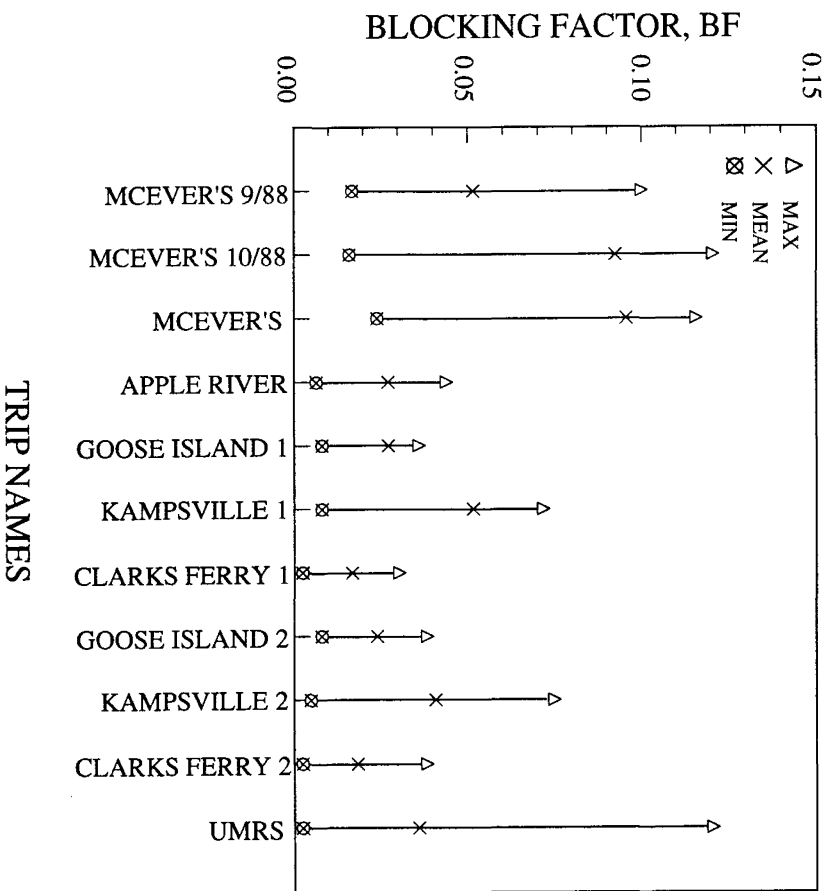


Figure 41. Blocking factor for barge-tow events at each site during the survey

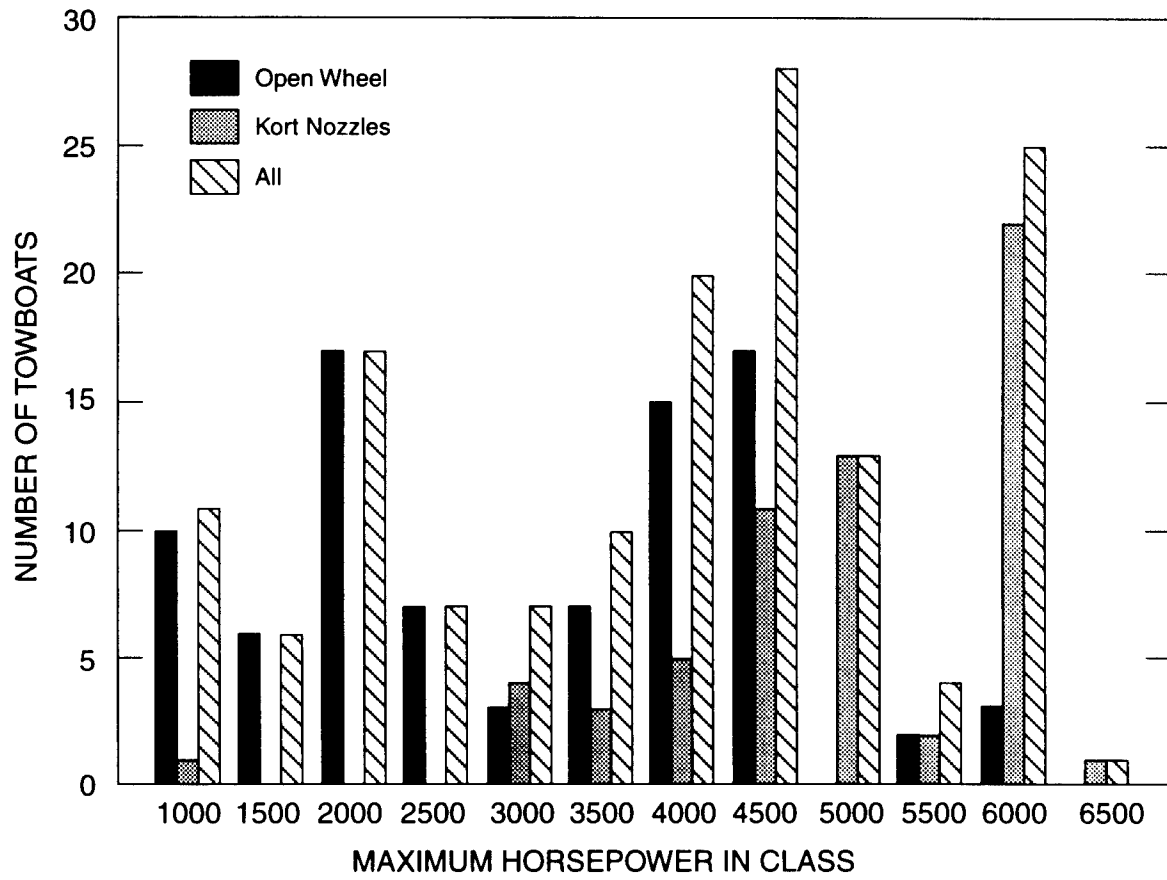


Figure 42. Towboat horsepower for barge convoys at each site during the survey

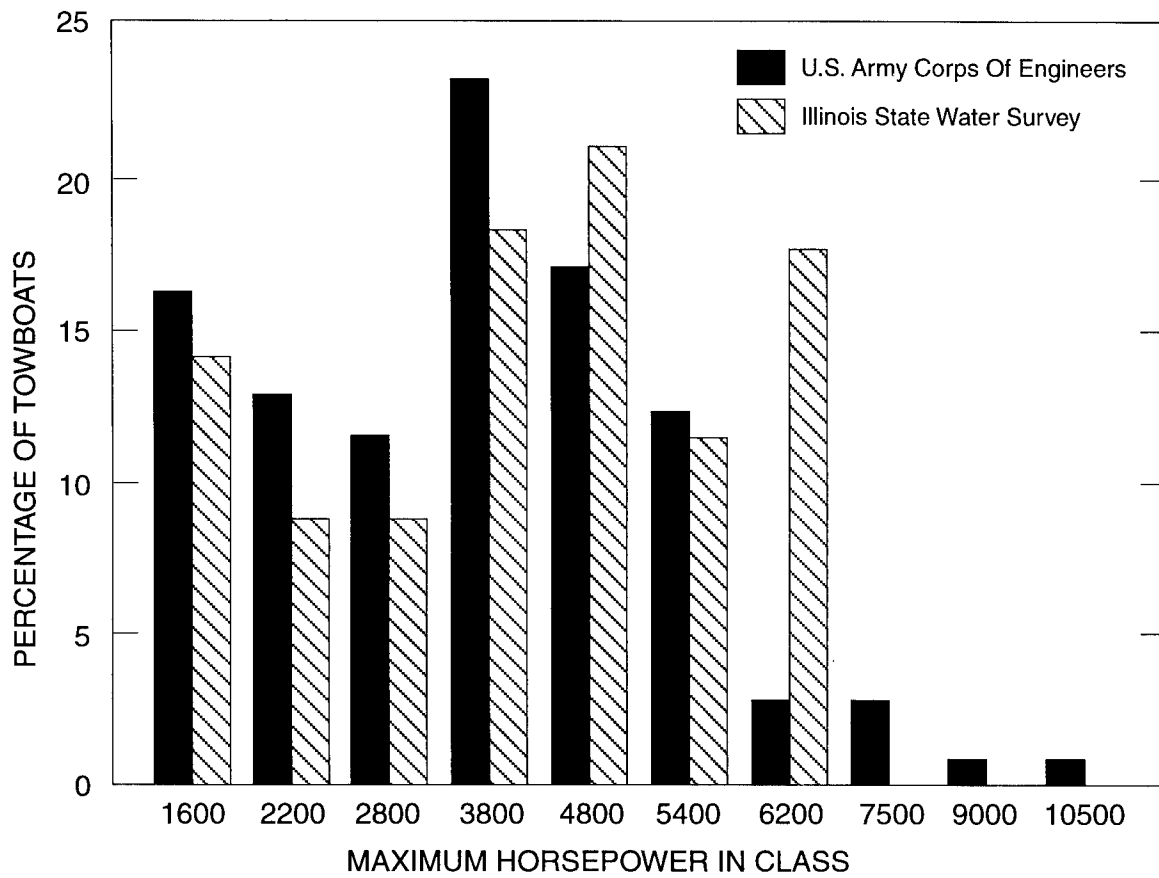


Figure 43. Comparison of the Illinois State Water Survey and U.S. Army Corps of Engineers (1978) traffic datasets

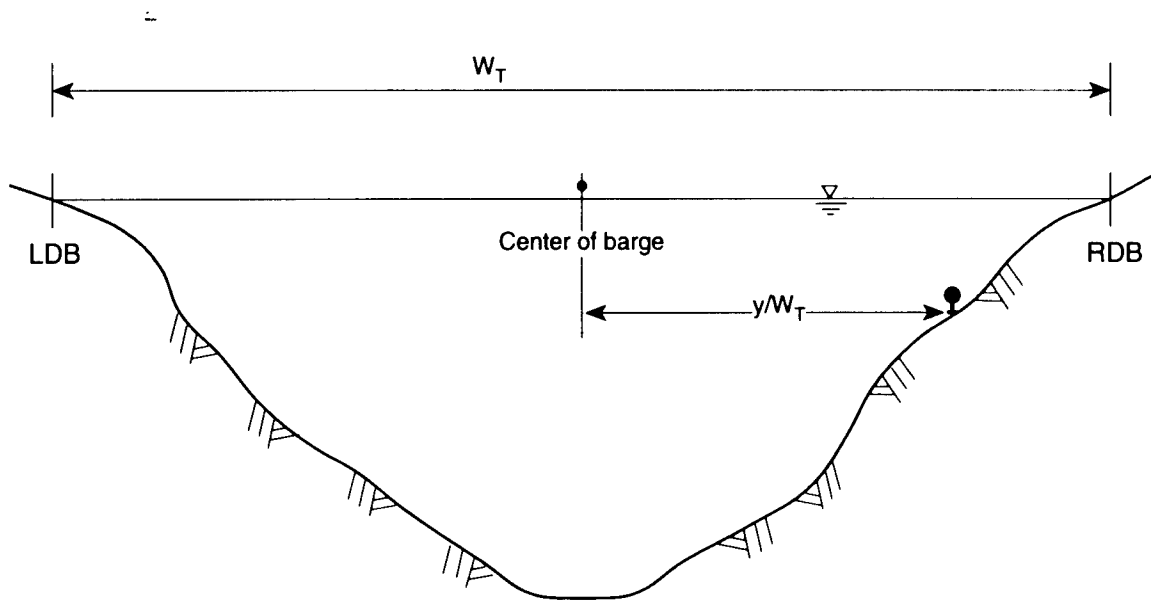


Figure 44. Coordinate system for comparing return velocity

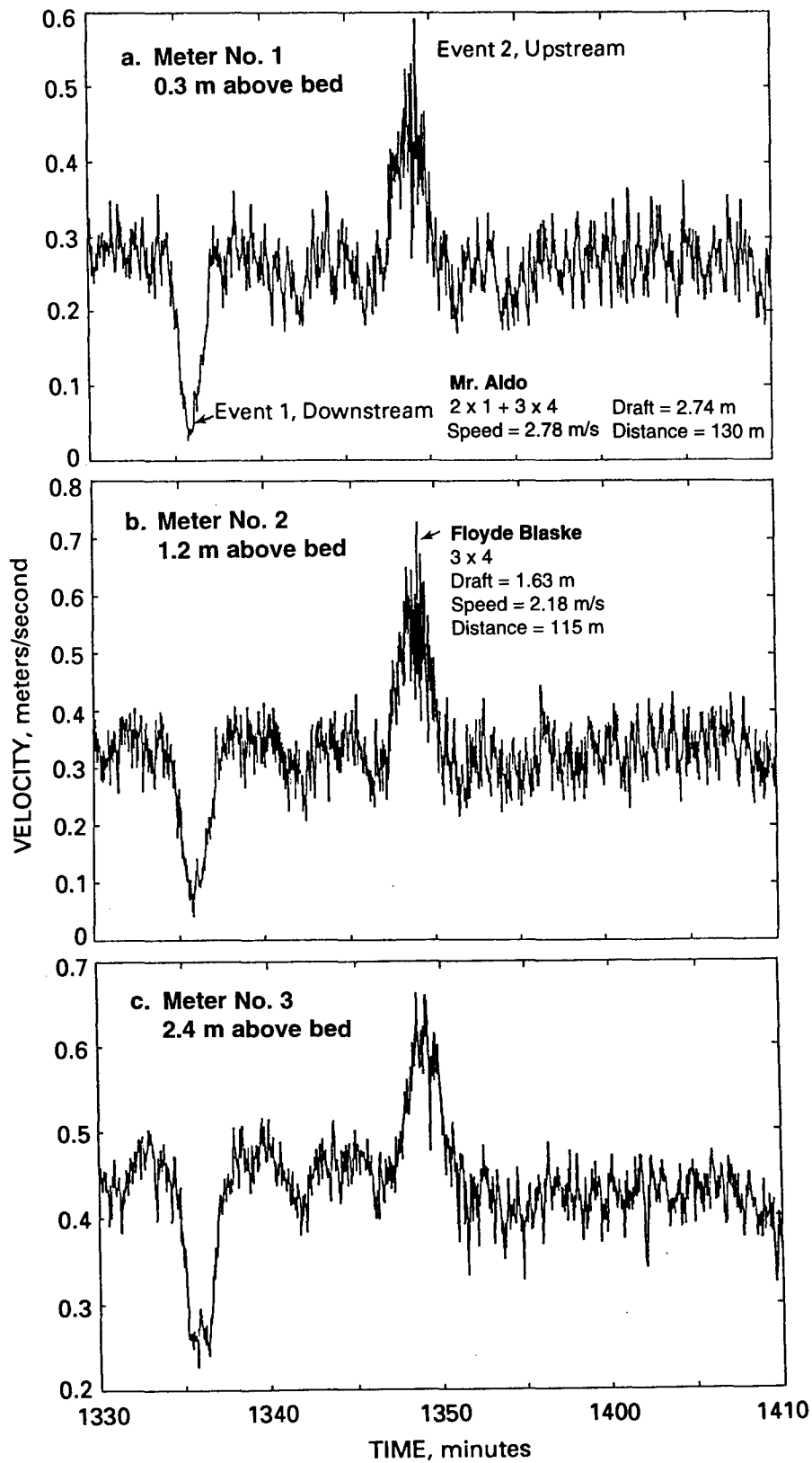


Figure 45. Typical changes in the longitudinal velocity components at three elevations

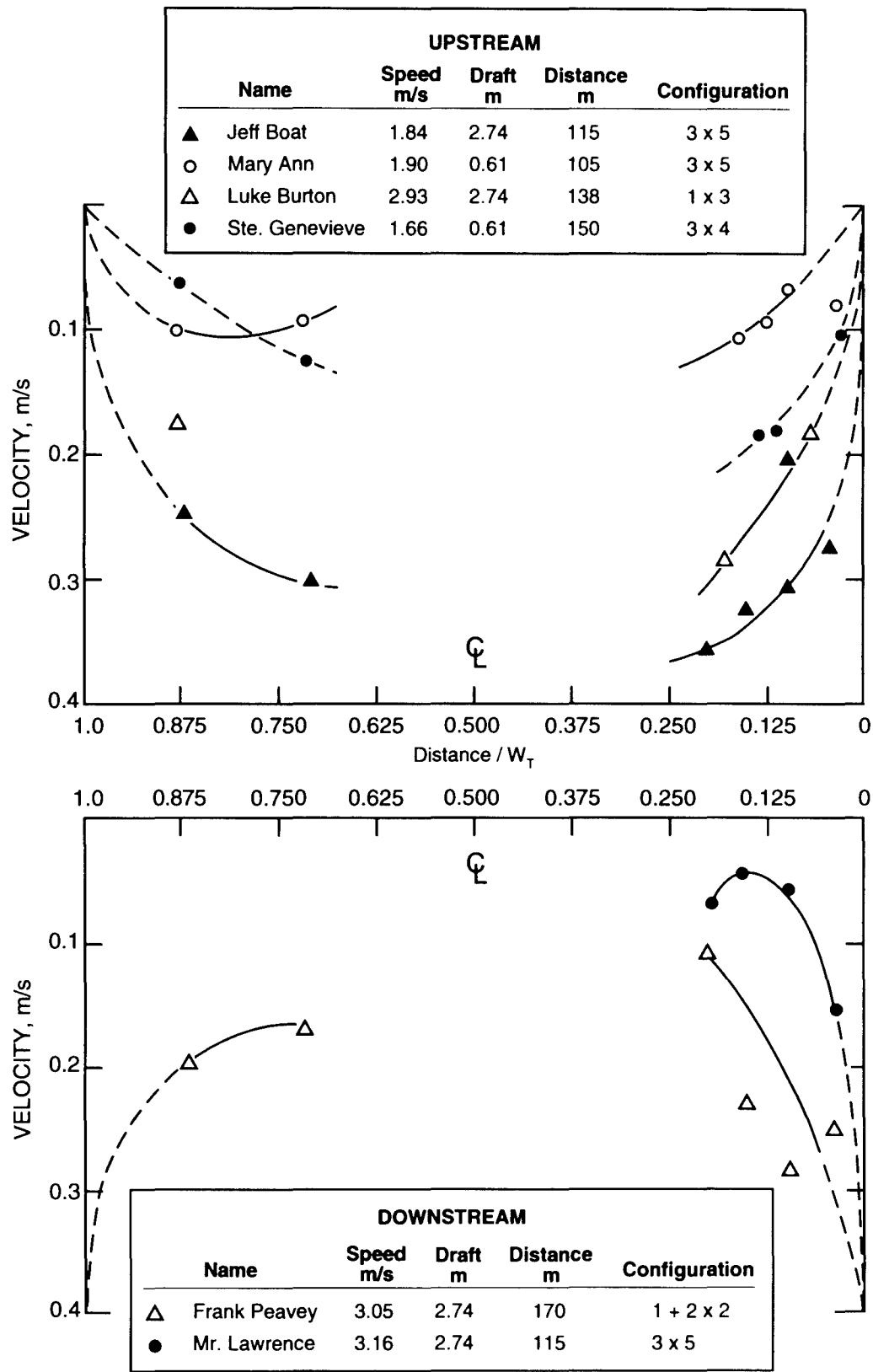


Figure 46. Distribution of net velocity changes in the lateral direction, Kampsville, Illinois River, RM 35.2

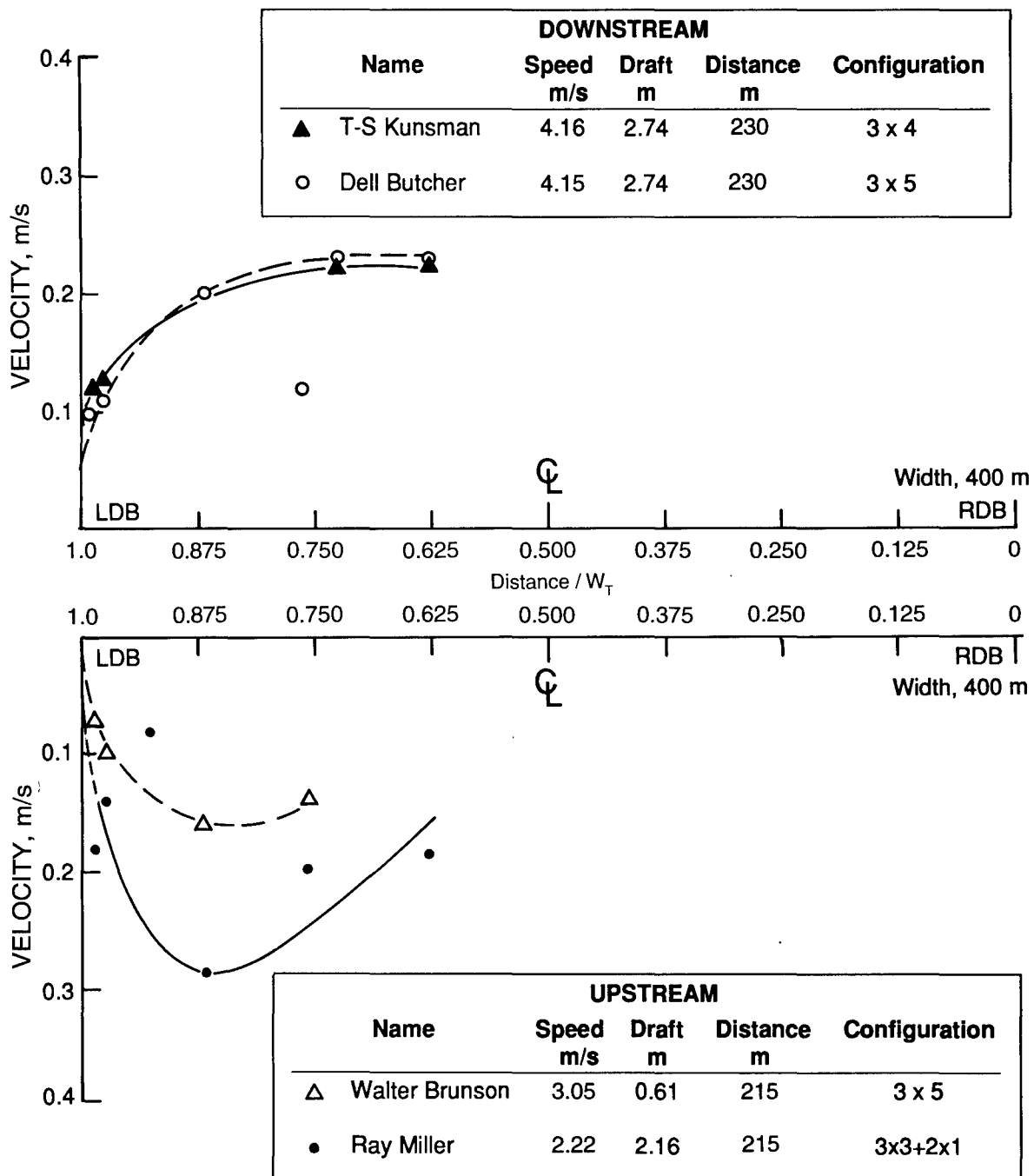


Figure 47. Distribution of net velocity changes in the lateral direction, Apple River Island, Mississippi River, RM 546.5

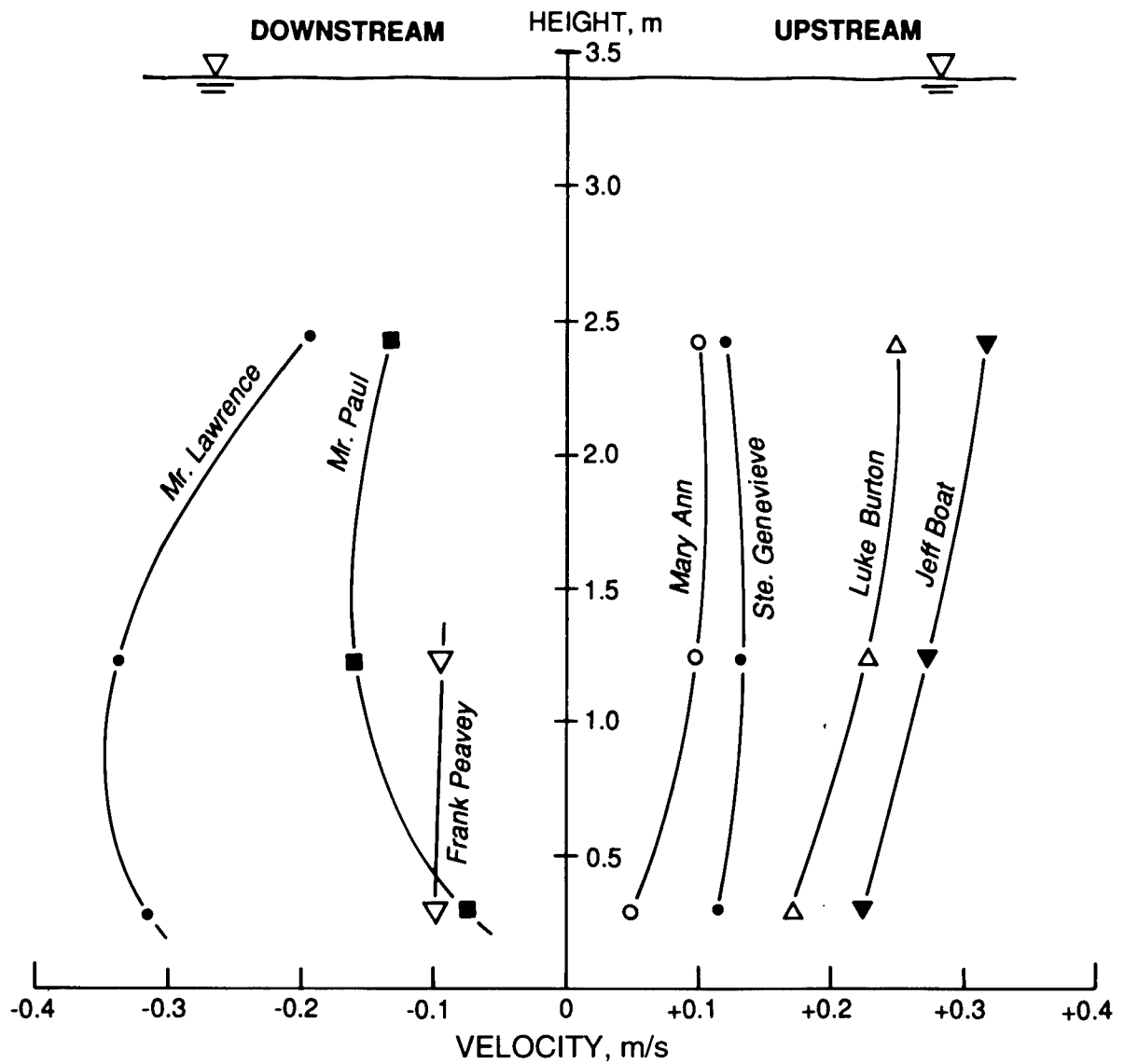


Figure 48. Distribution of net velocity changes in the vertical direction, Kampsville, Illinois River, RM 35.2

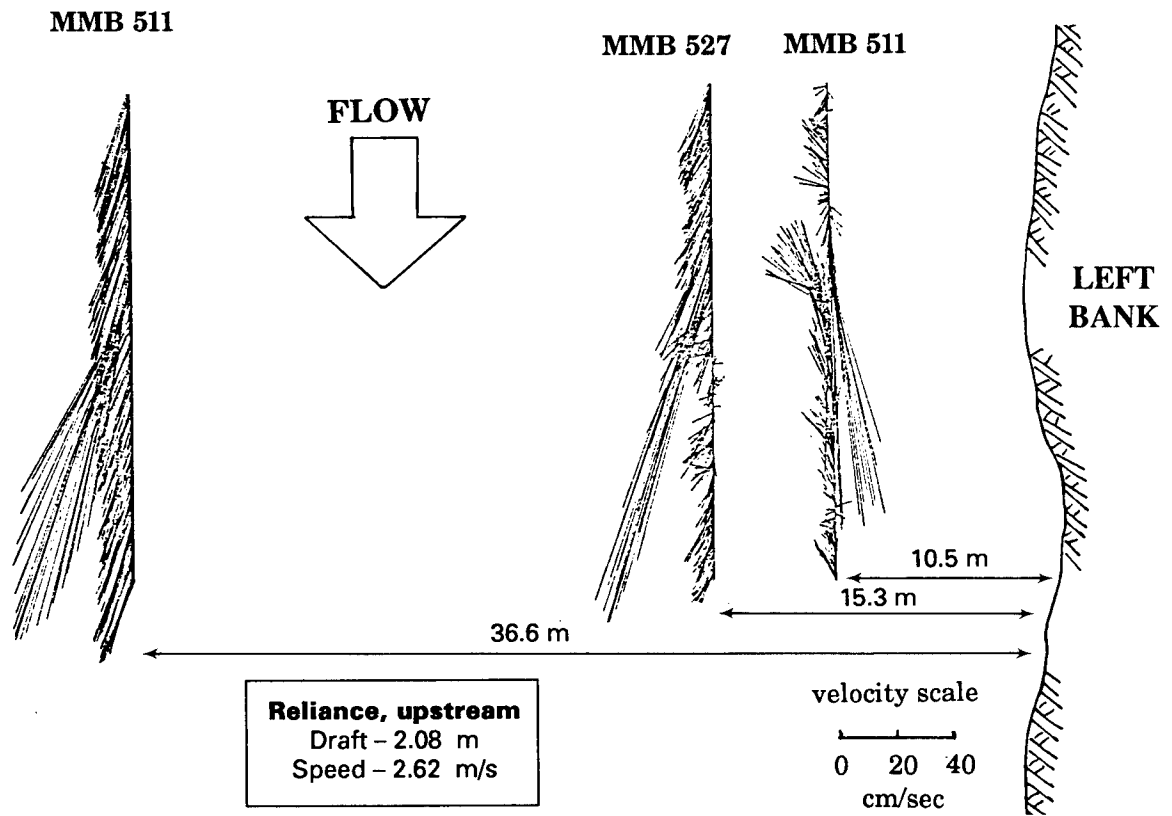


Figure 49. Resultant velocity vectors for an upstream-bound barge, McEver's Island

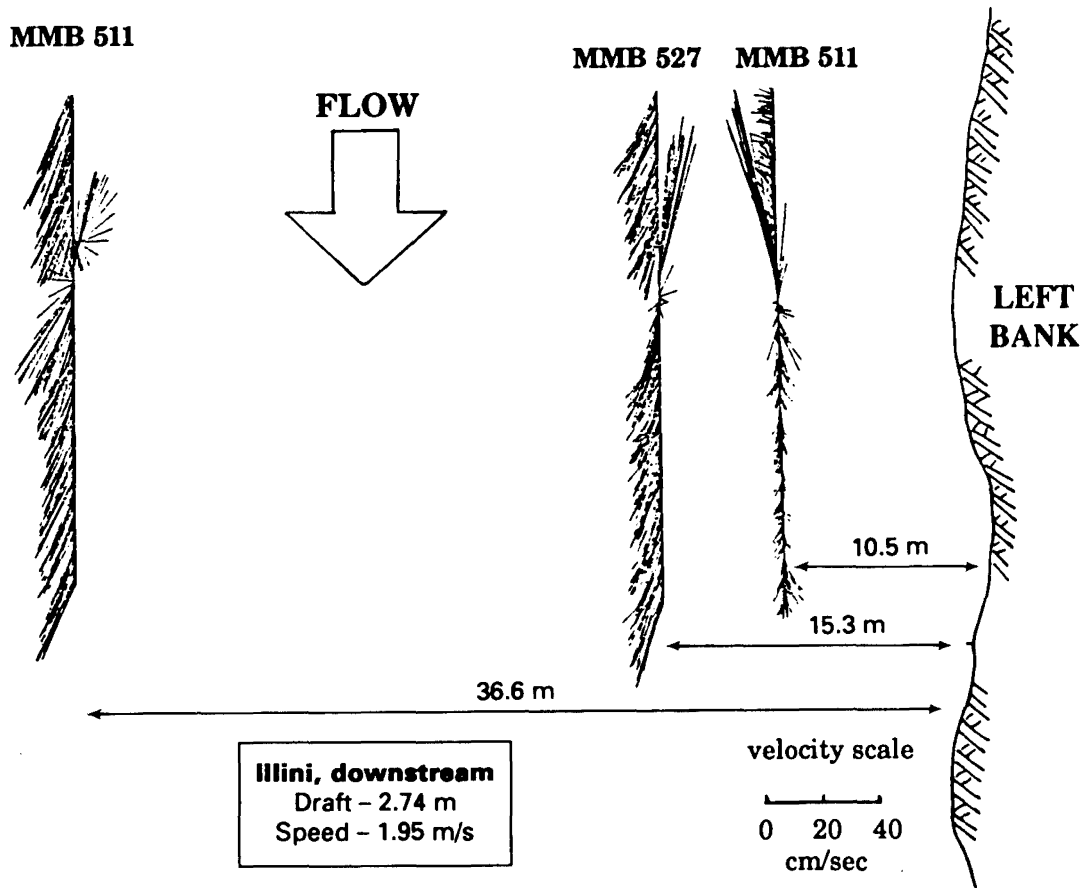


Figure 50. Resultant velocity vectors for a downstream-bound barge, McEver's Island

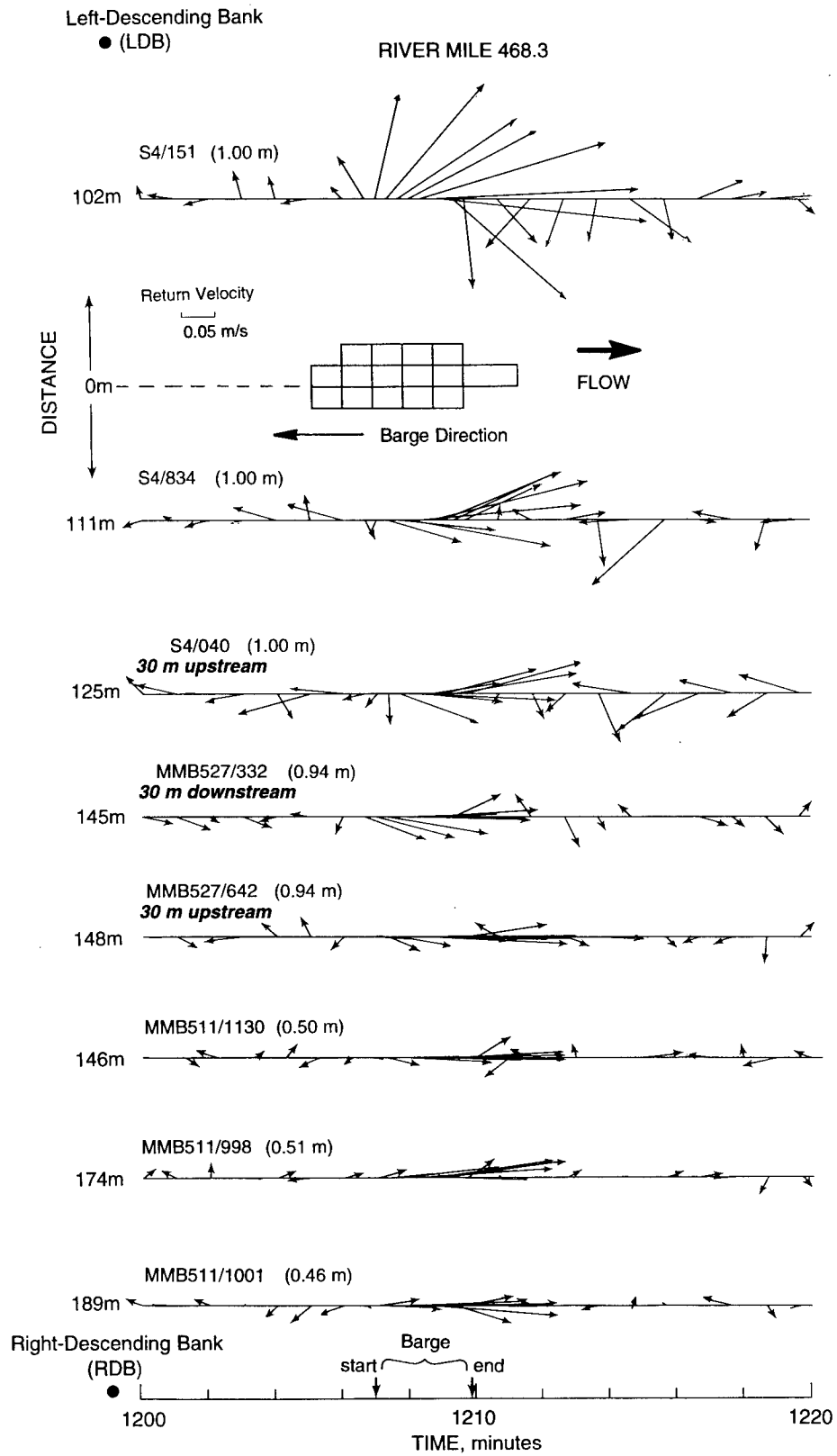


Figure 51. Velocity vectors of U_r for an upstream-bound barge, Clarks Ferry, trip 2

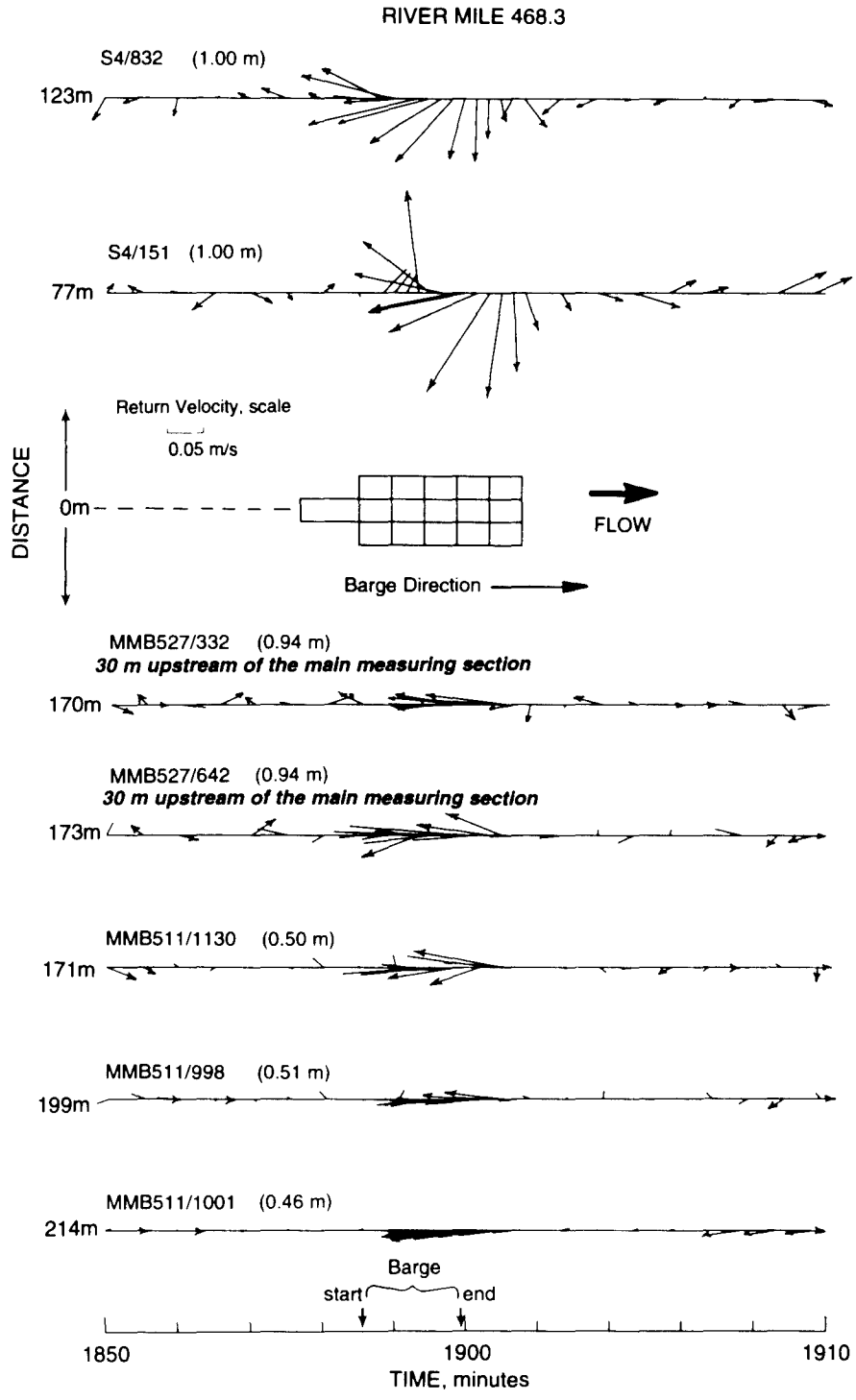


Figure 52. Velocity vectors of U_i for a downstream-bound barge, Clarks Ferry, trip 2

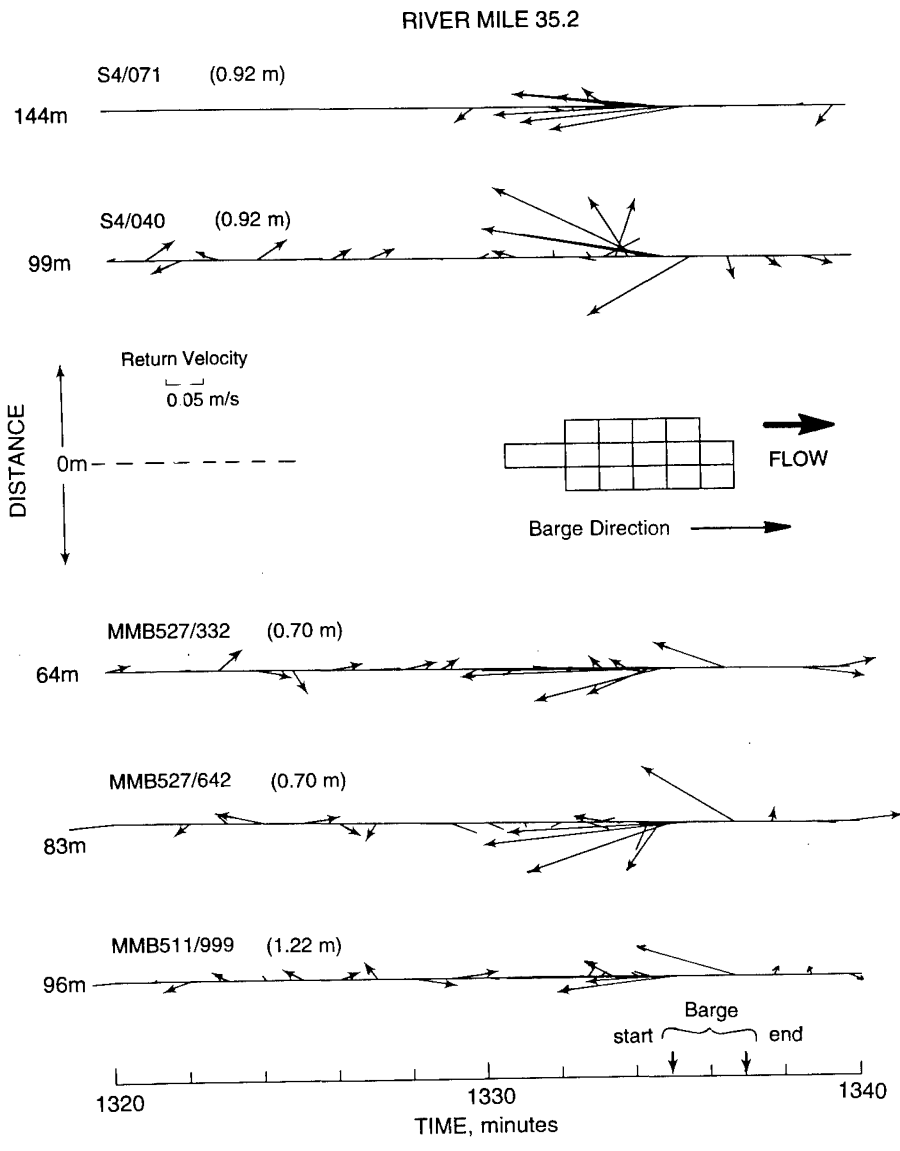


Figure 53. Velocity vectors of U_r for a downstream-bound barge, *Mr. Aldo*, at Kampsville, trip 1

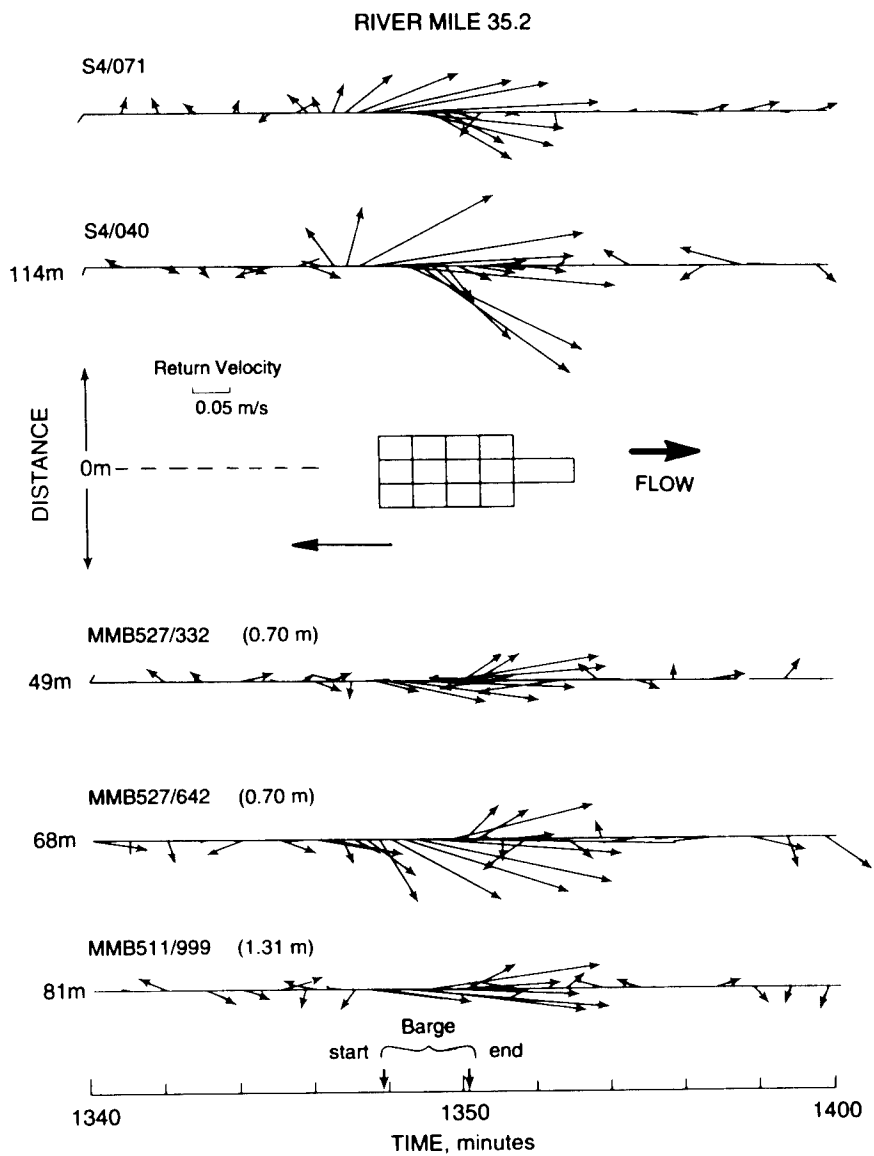


Figure 54. Velocity vectors of U_r for an upstream-bound barge, *Floyd H. Blaske*, at Kampsville, trip 1

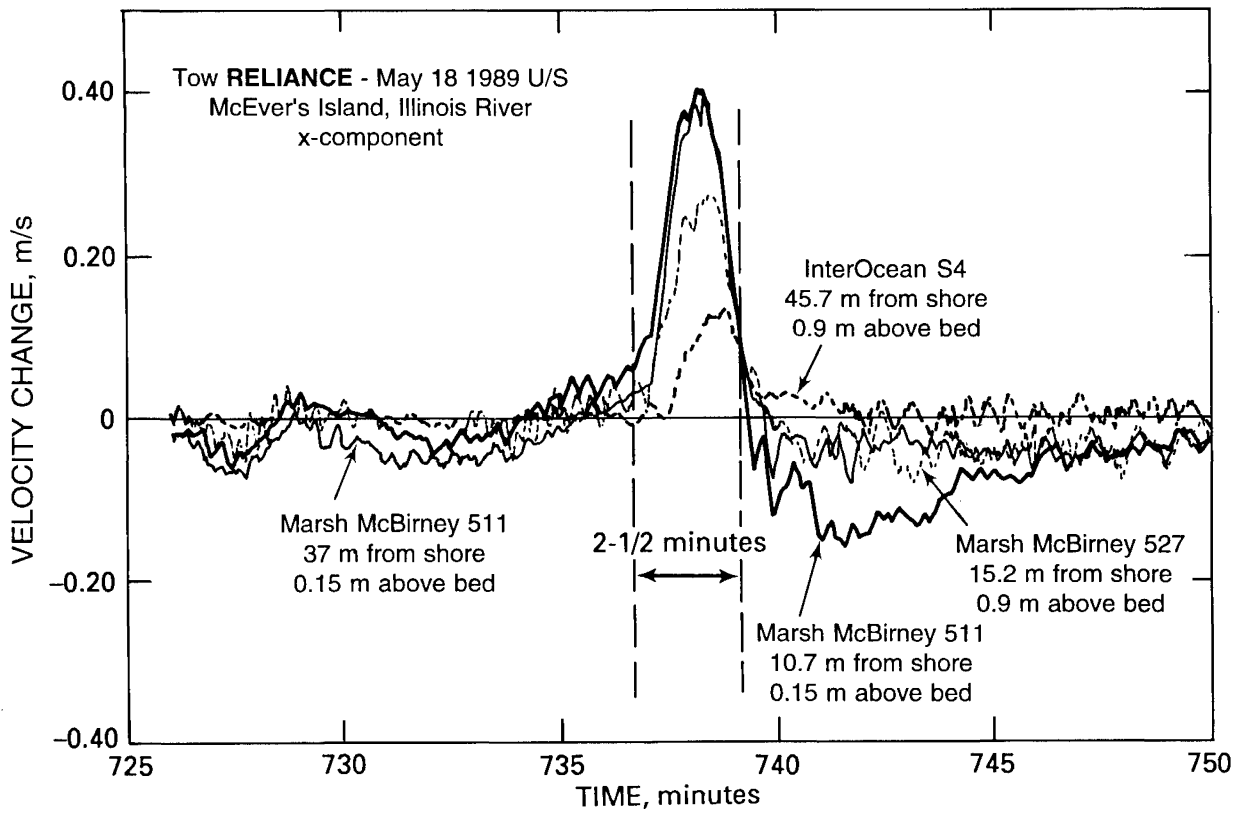


Figure 55. Changes in the longitudinal component of the velocity at various metering locations due to the movement of an upstream bound barge convoy

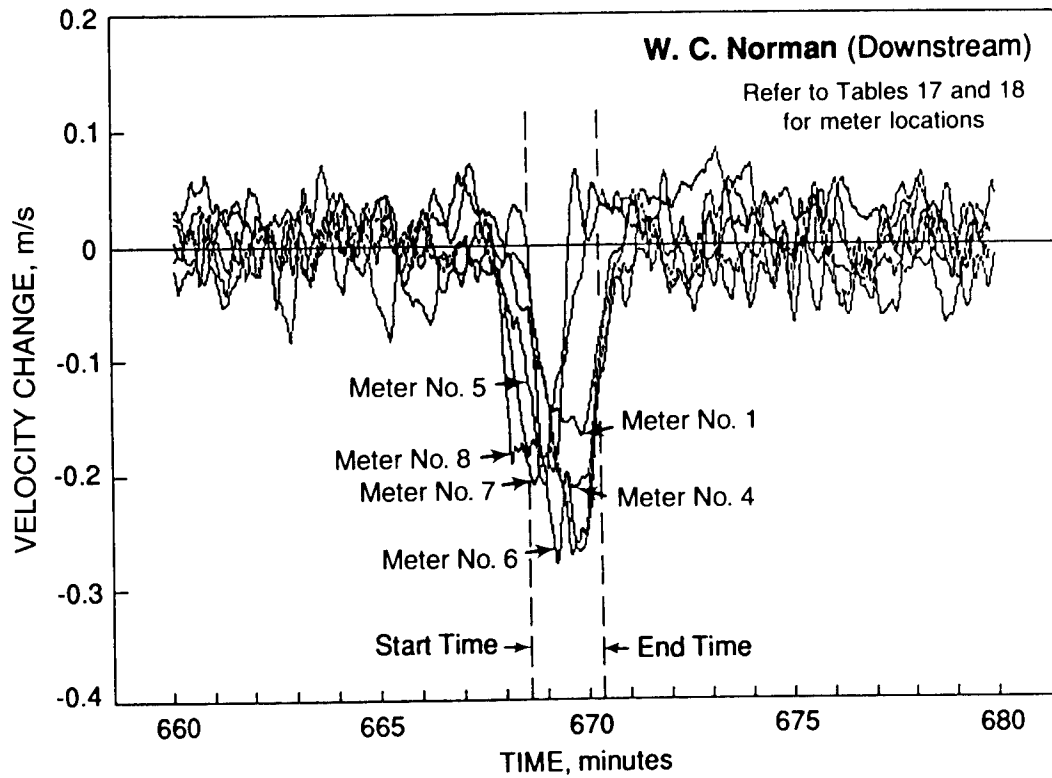


Figure 56. Changes in the longitudinal velocity component at various metering locations due to the movement of a downstream-bound barge convoy

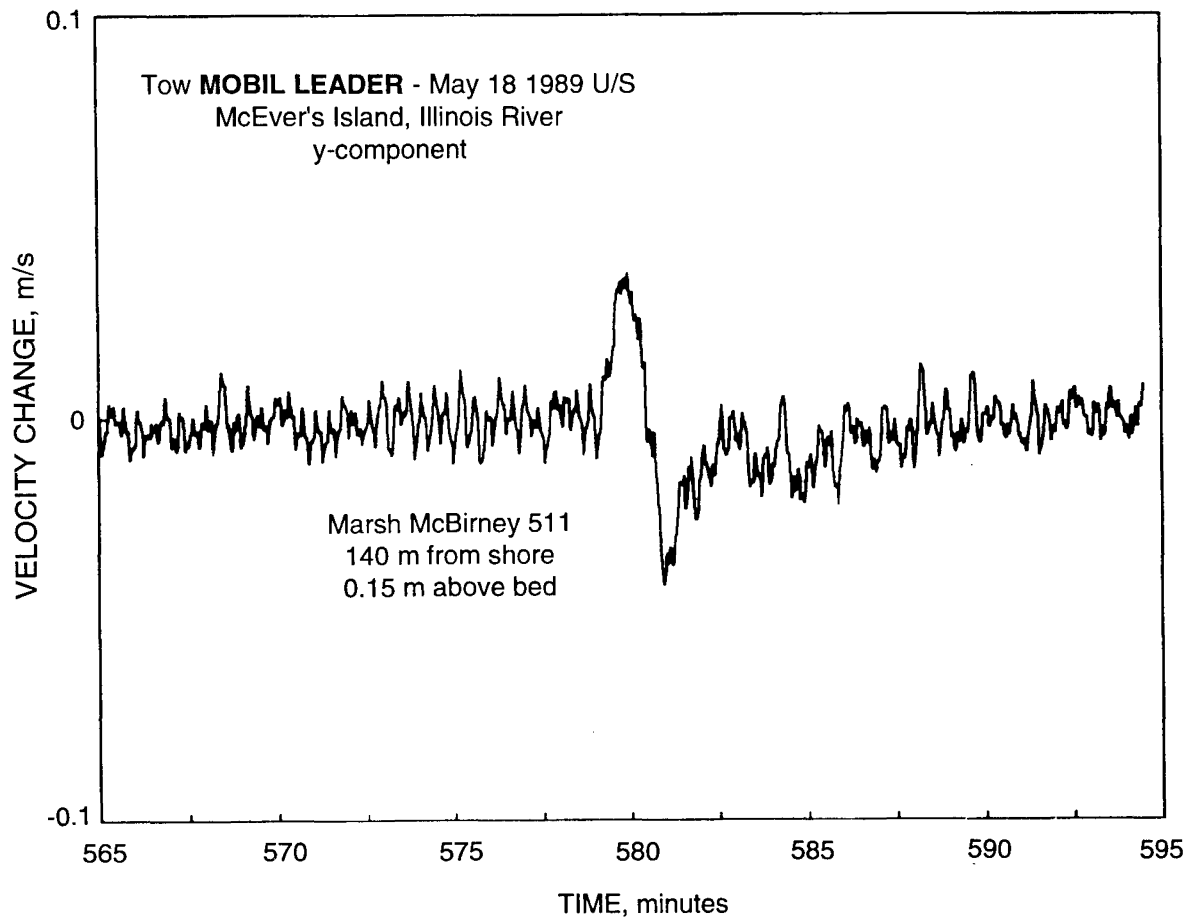


Figure 57. Changes in the lateral velocity component at a single meter due to barge-tow movement

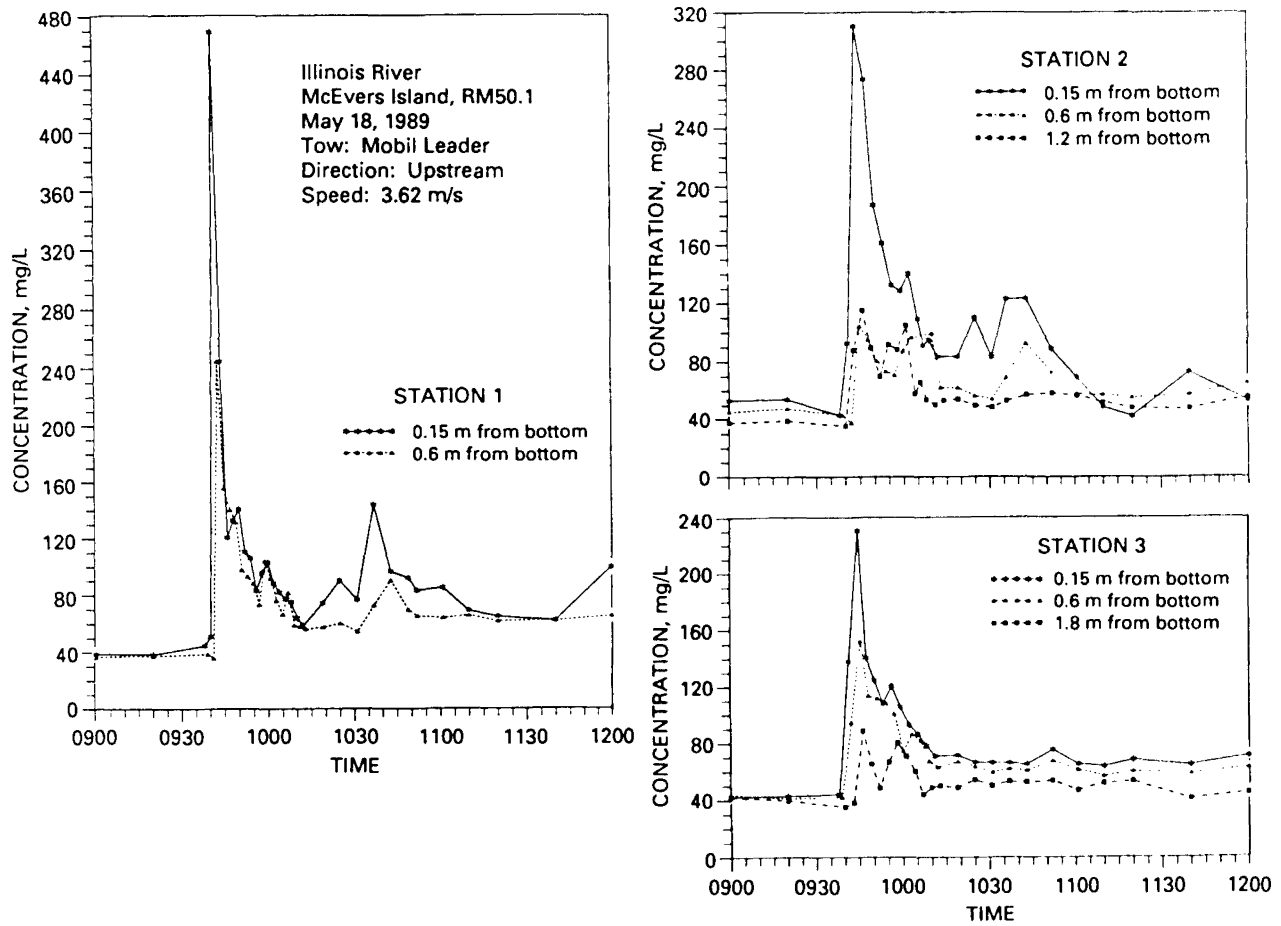


Figure 58. Variability in suspended sediment concentration due to barge-tow movement

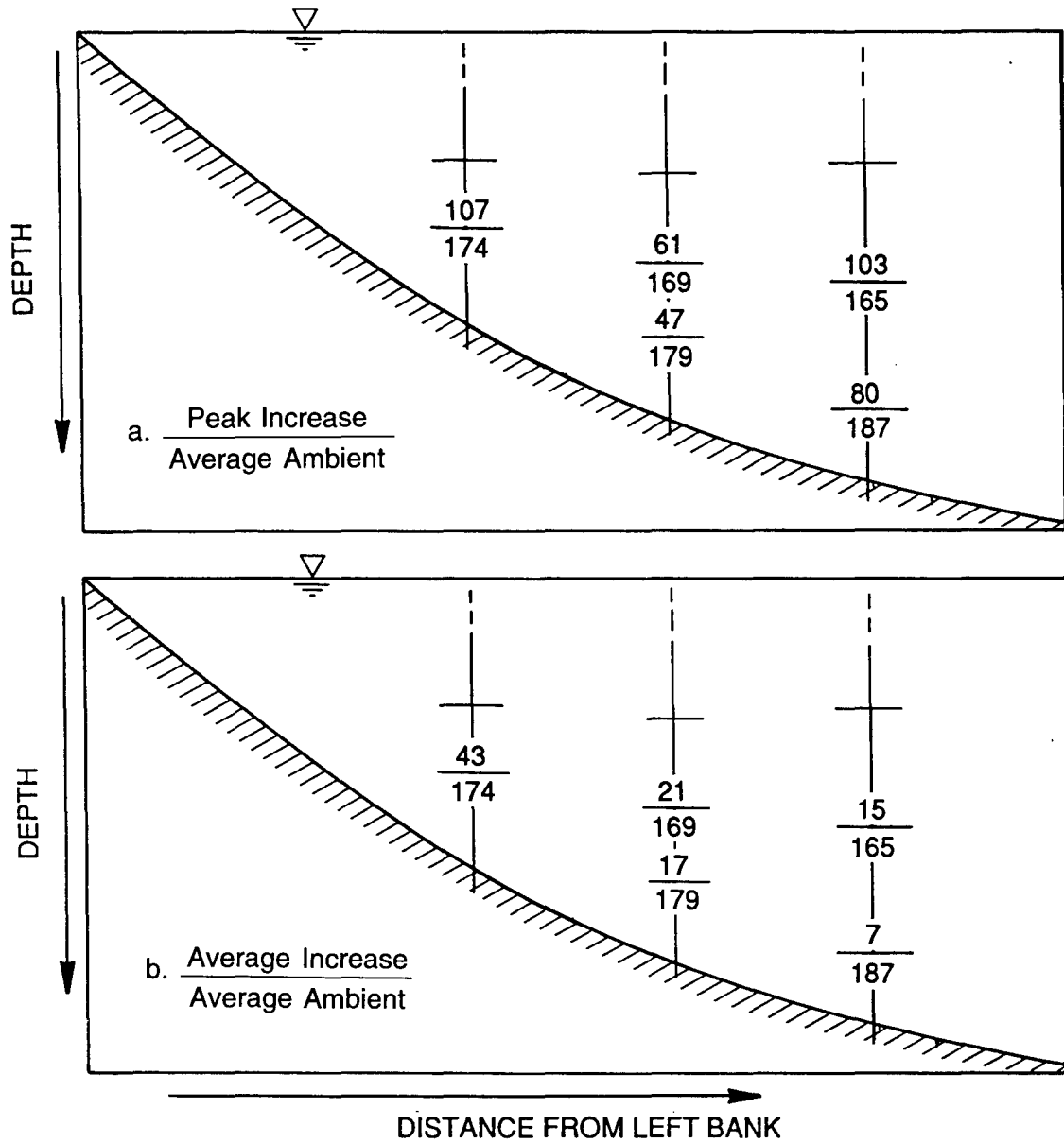


Figure 59. Peak and average increase in suspended sediment concentration, (mg/L),
Goose Island, RM 319.3, Mississippi River, August 1990

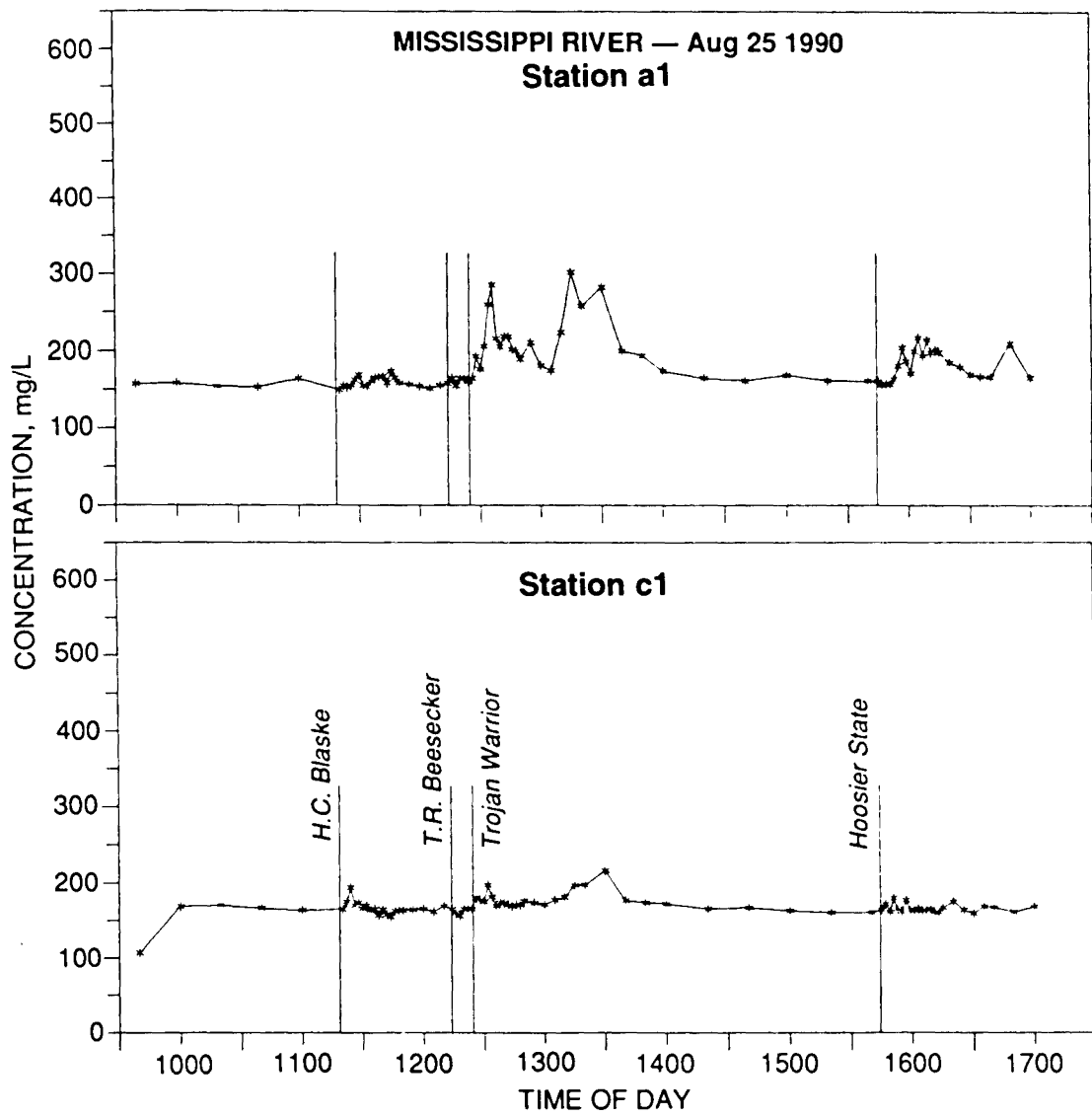


Figure 60. Sediment concentration variations for a typical day, Goose Island, RM 319.3, Mississippi River

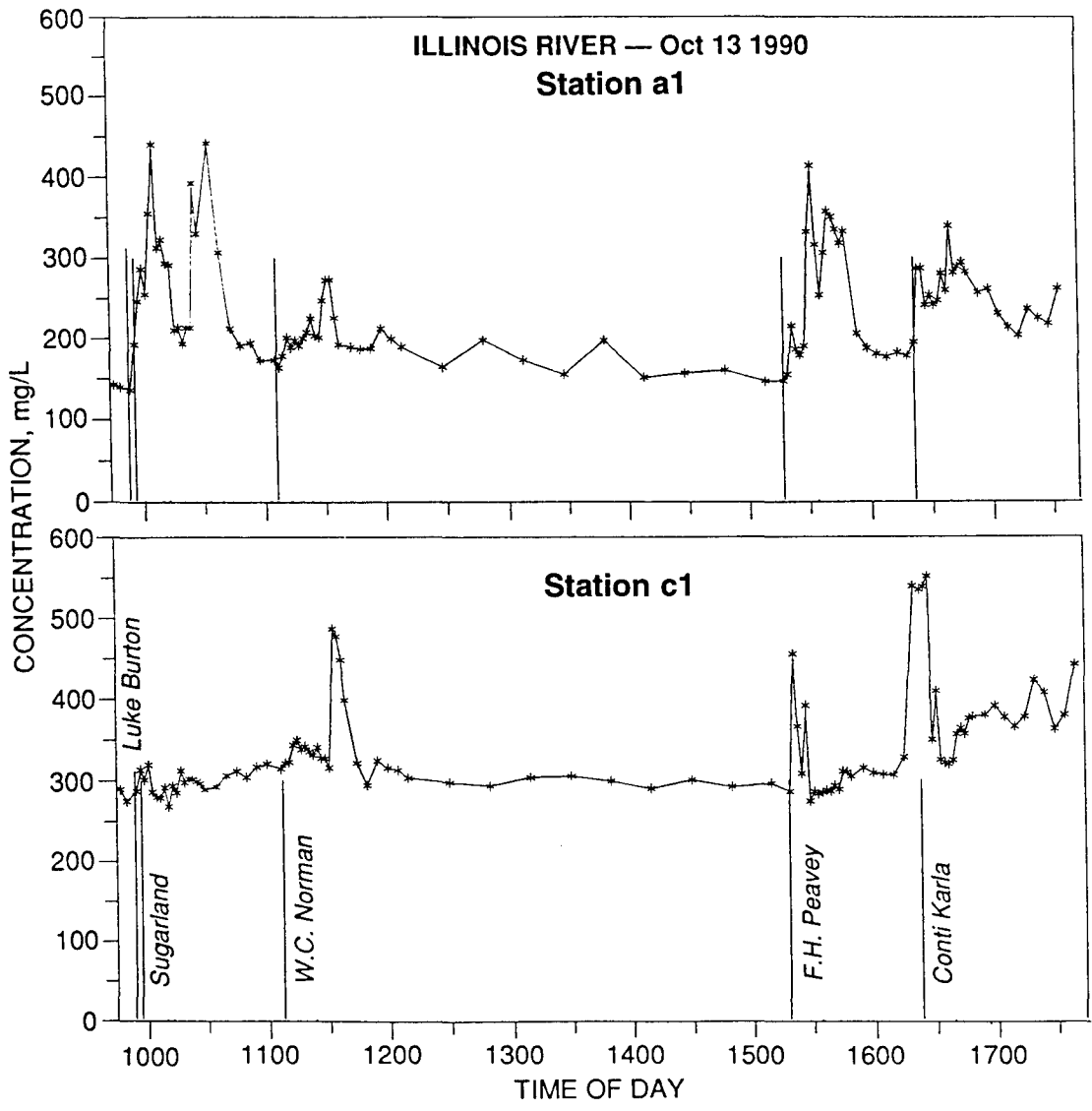


Figure 61. Sediment concentration variations for a typical day, Kampsville, RM 35.3, Illinois River

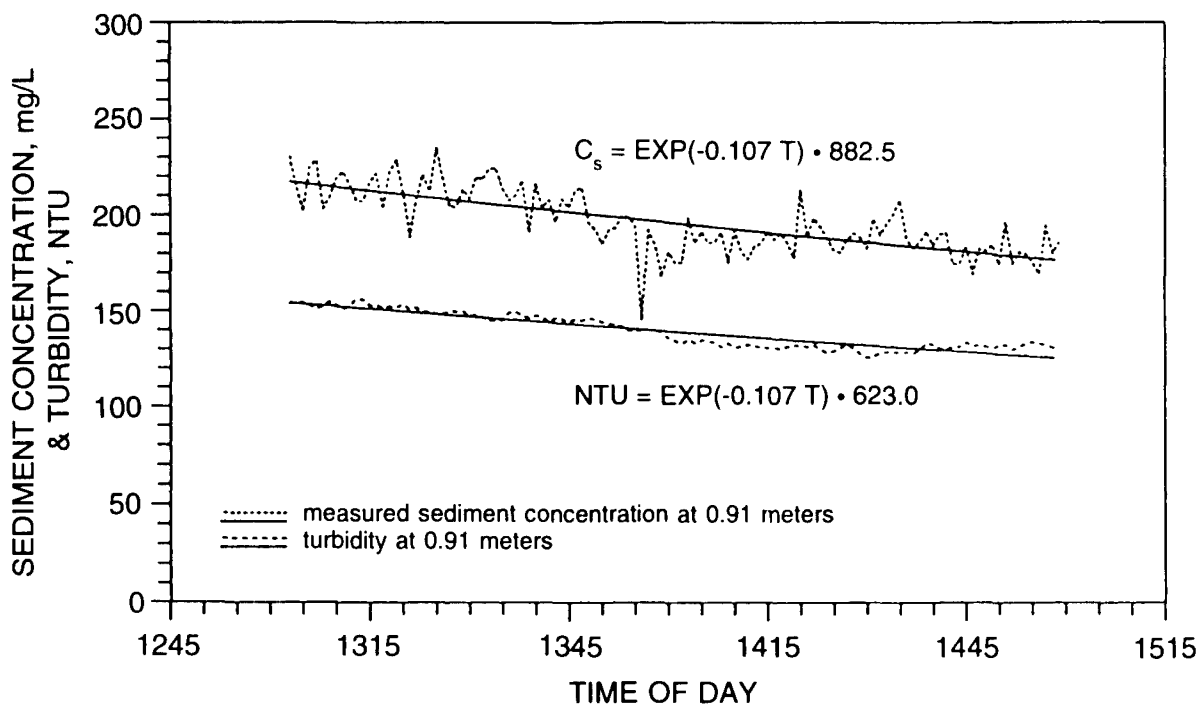


Figure 62. Suspended sediment concentrations and turbidity values versus time, McEver's Island, RM 50.1, Illinois River

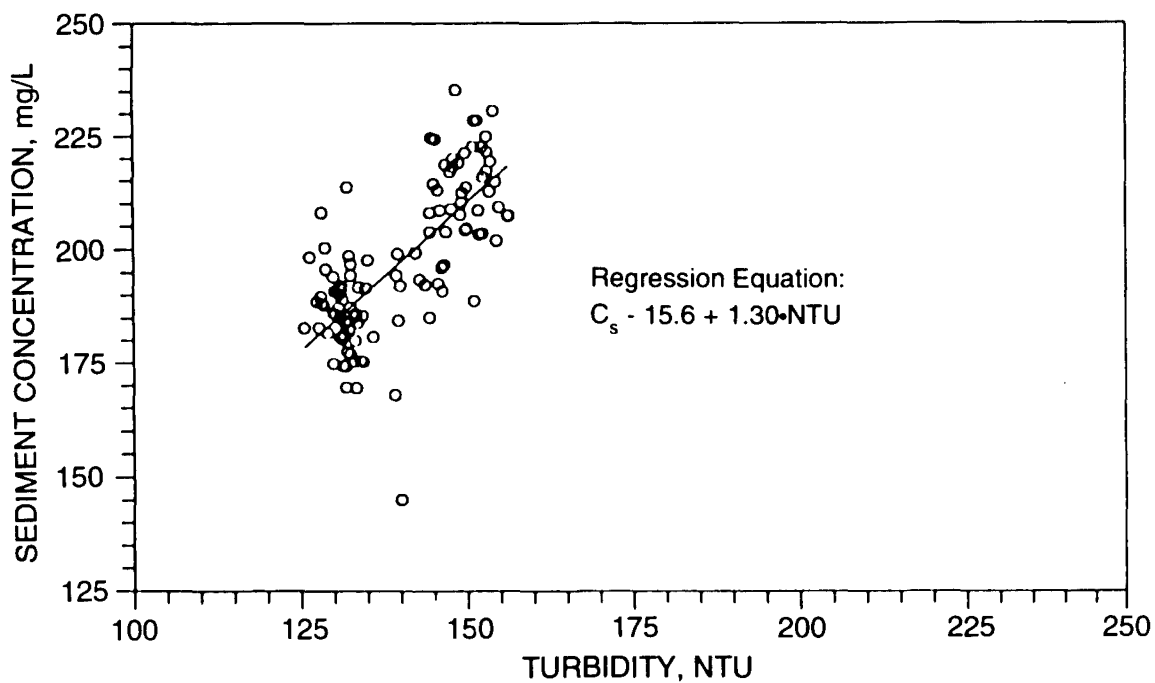


Figure 63. Scatter plot of suspended sediment concentration versus turbidity values, McEver's Island, RM 50.1, Illinois River

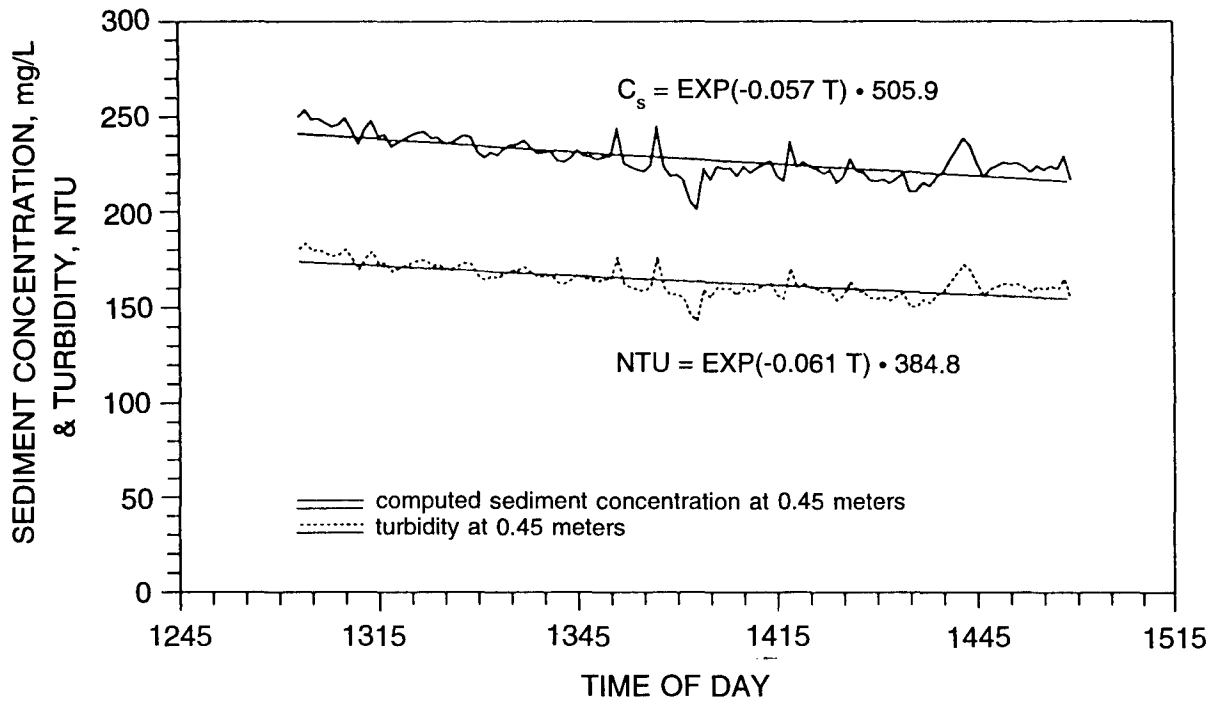


Figure 64. Measured turbidity values and computed suspended sediment concentrations versus time, McEver's Island, RM 50.1, Illinois River

Hochstein and Adams (1989)

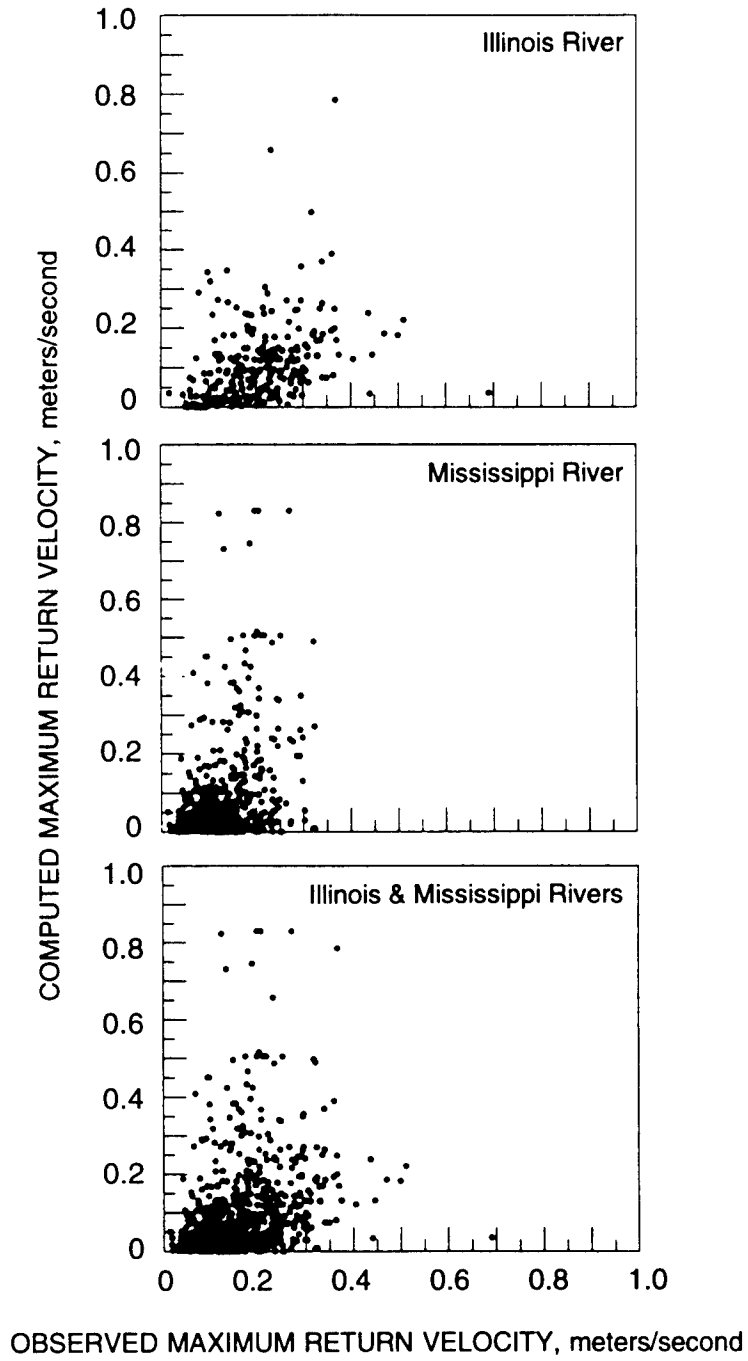


Figure 65. Comparison of computed and measured $U_{r(max)}$ using the method by Hochstein and Adams (1989)

Maynard and Siemsen (1991)

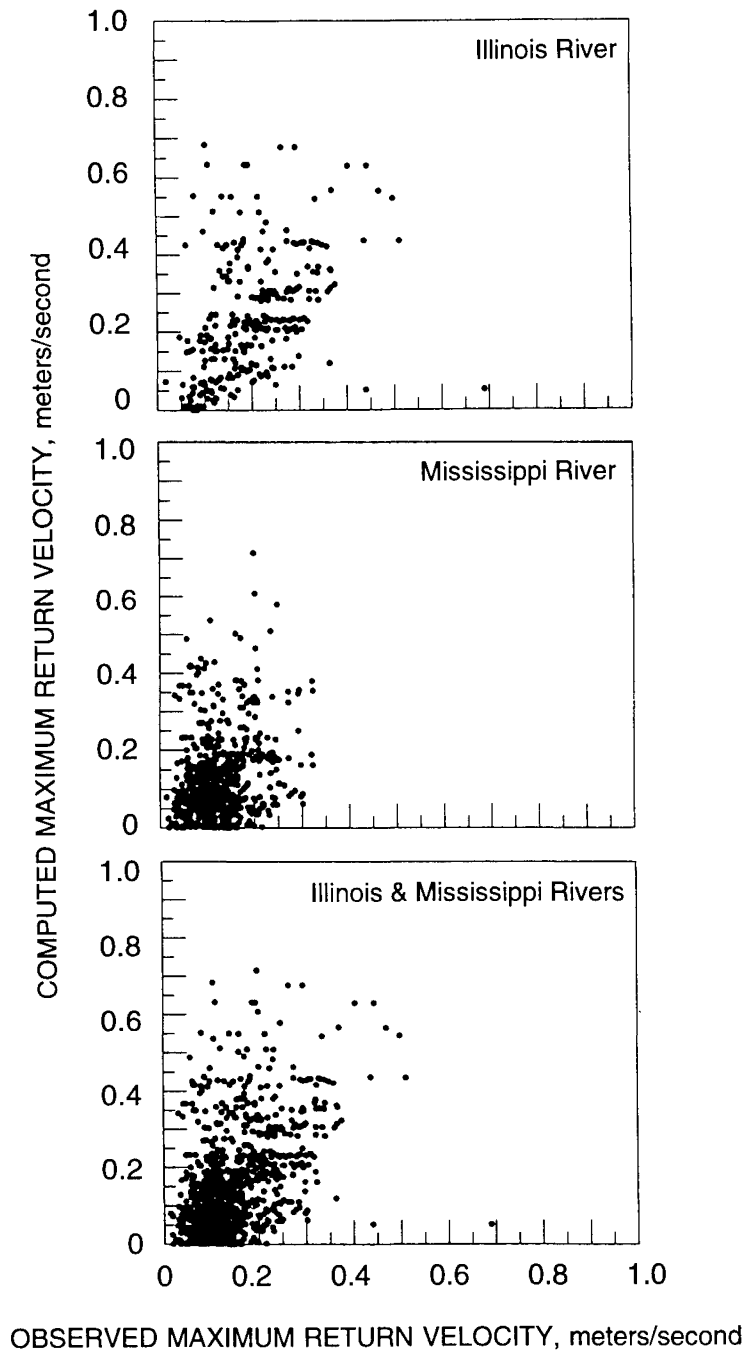


Figure 66. Comparison of computed and measured $U_{r(max)}$ using the method by Maynard and Siemsen (1991)

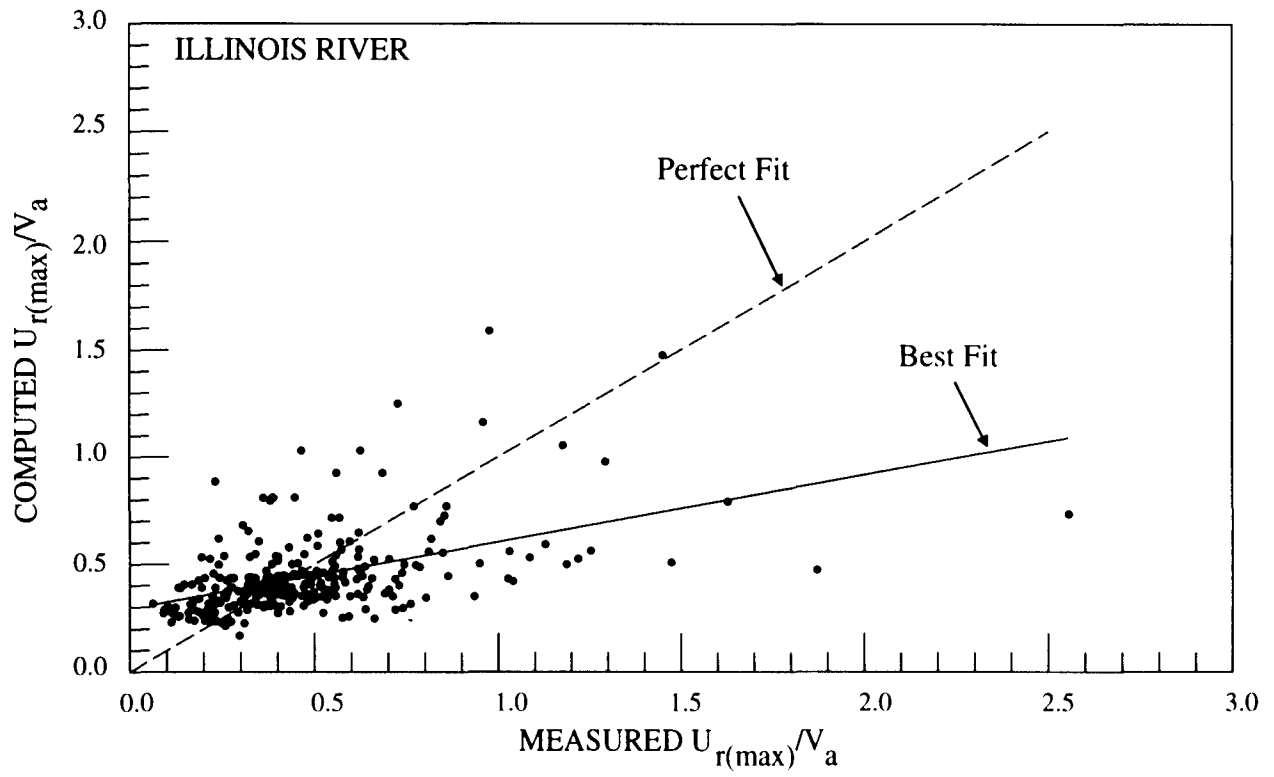


Figure 67. Comparison of computed and measured $U_{r(max)}/V_a$, Illinois River

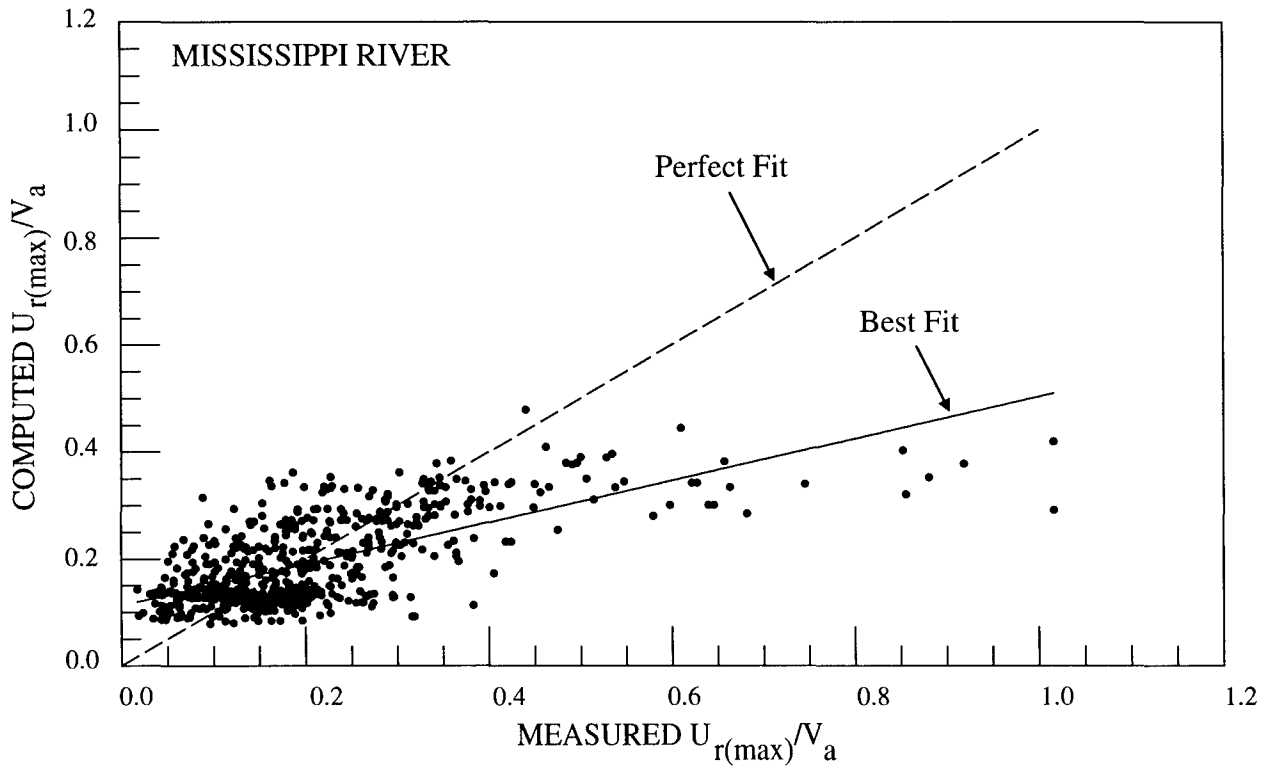


Figure 68. Comparison of computed and measured $U_{r(max)}/V_a$, Mississippi River

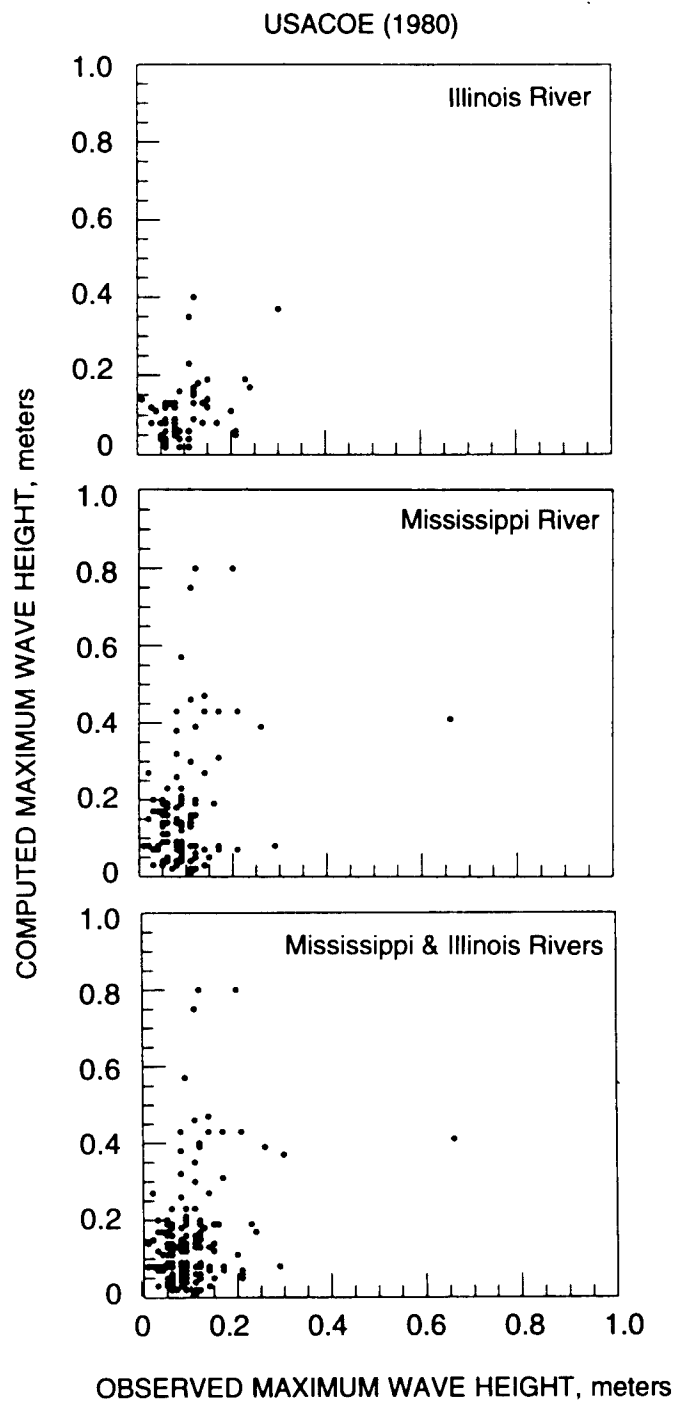


Figure 69. Comparison of computed and measured $H_{w(max)}$ using the method by USACOE (1980)

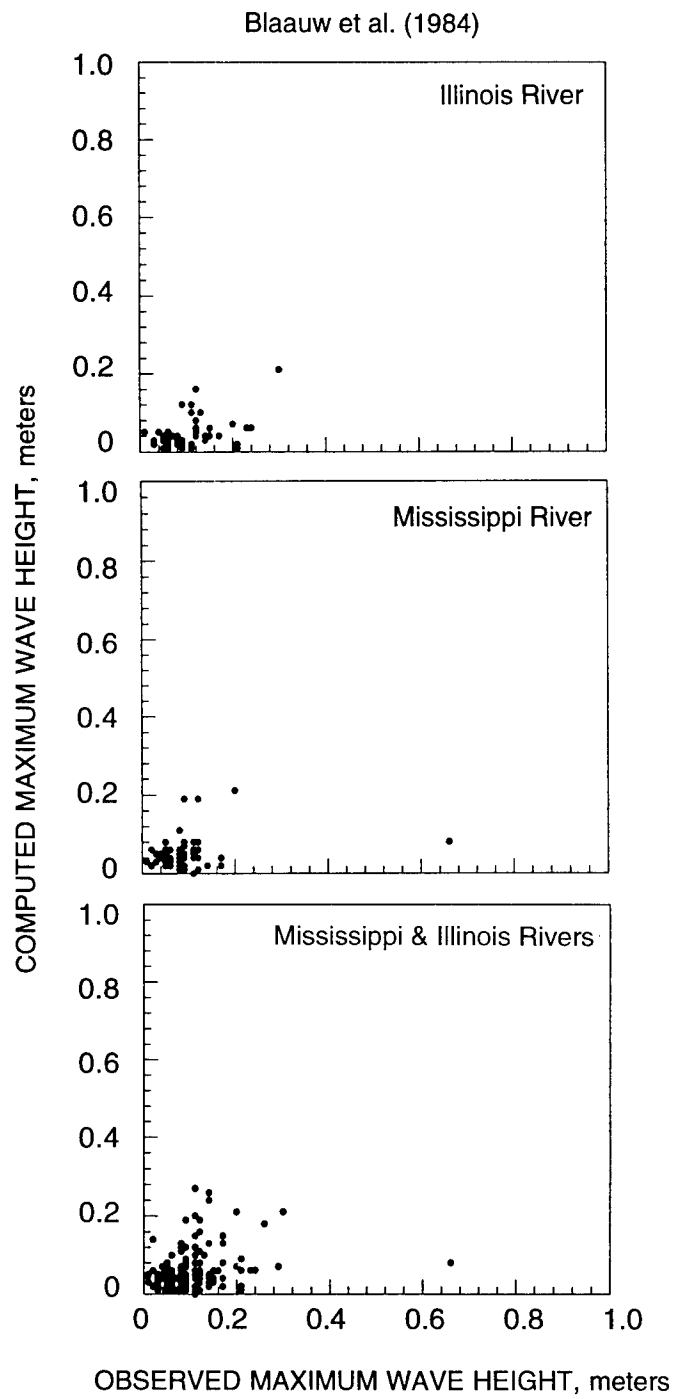


Figure 70. Comparison of computed and measured $H_{w(max)}$ using the method by Blaauw et al. (1984)

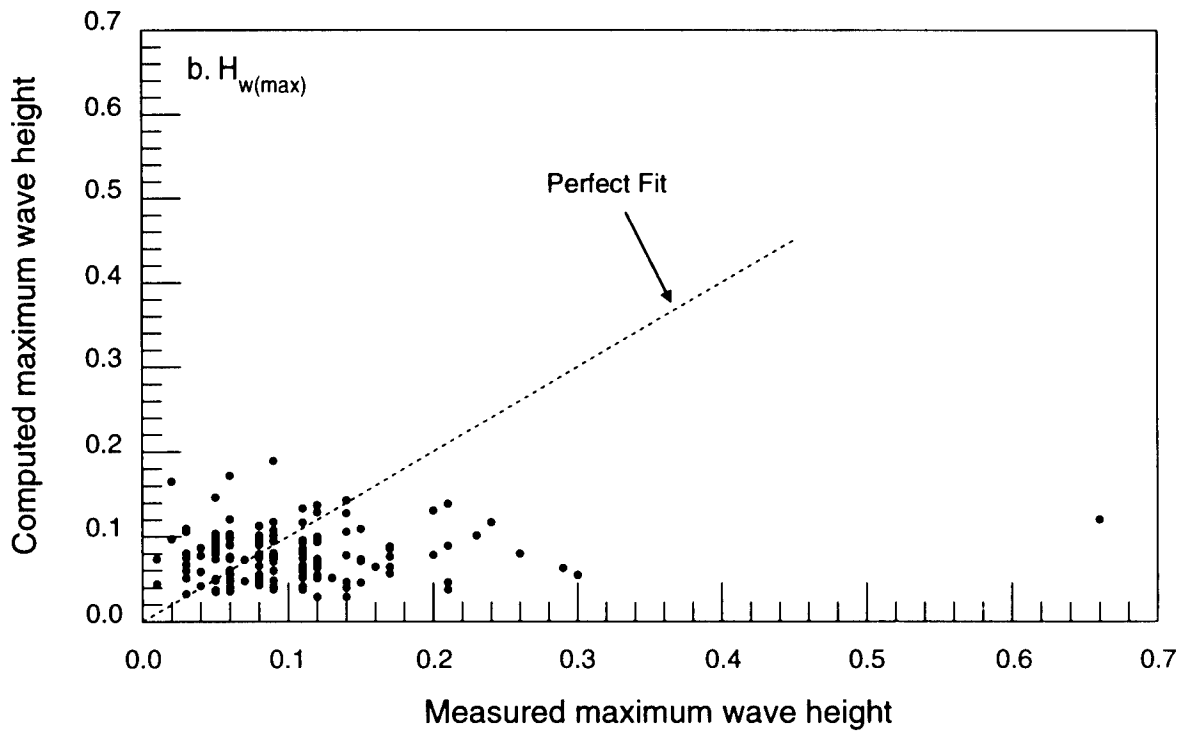
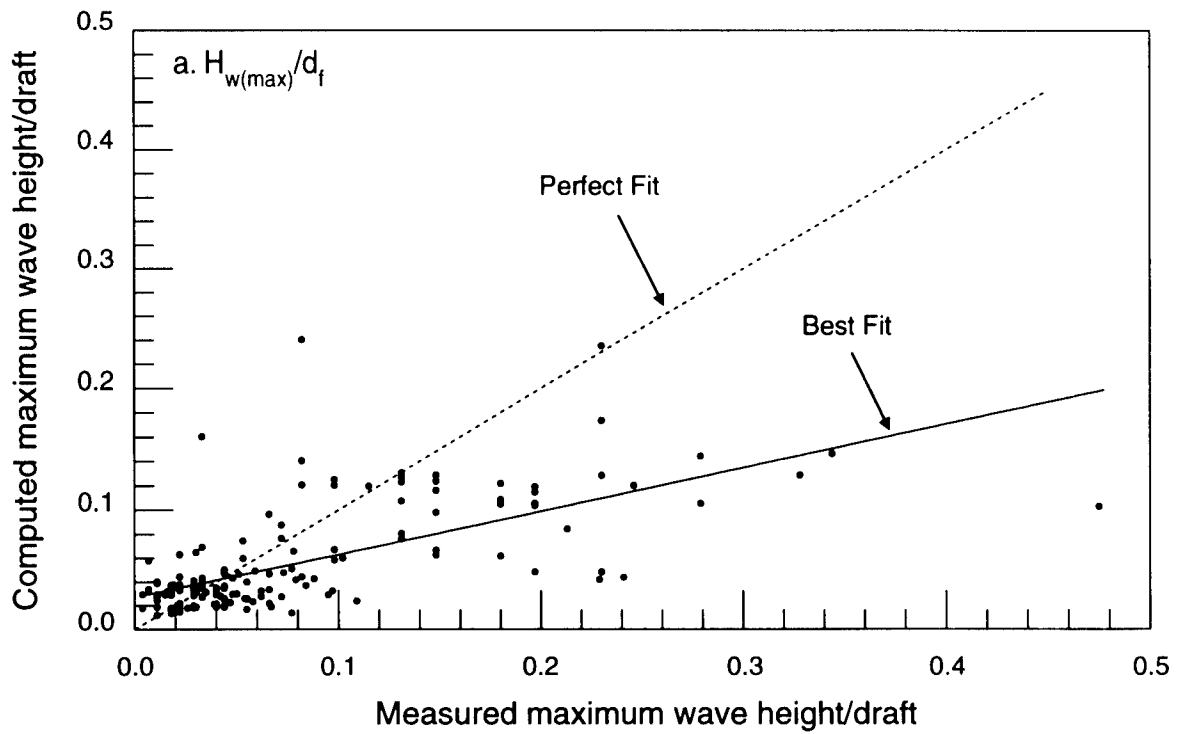


Figure 71. Comparison of (a) computed and measured $H_{w(max)}/d_f$, and (b) computed and measured $H_{w(max)}$, for the UMRS

Hochstein (1967)

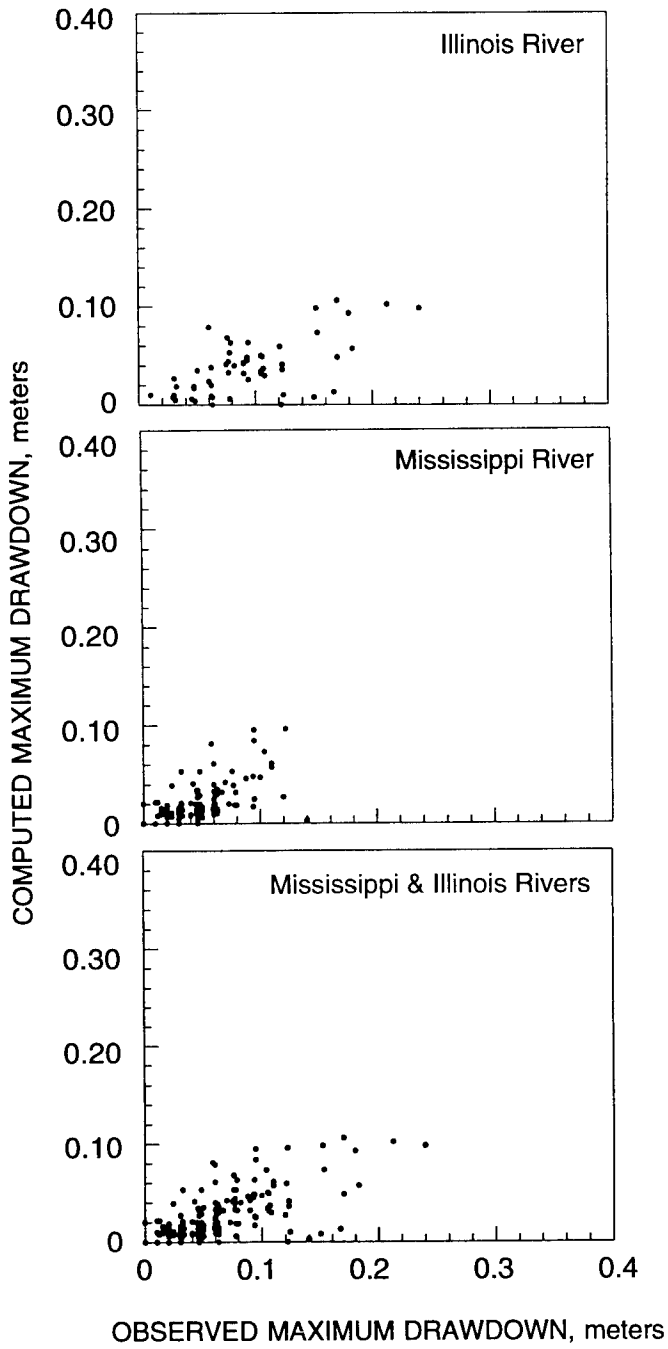


Figure 72. Comparison of computed and measured $H_{d(max)}$ using the method by Hochstein (1967)

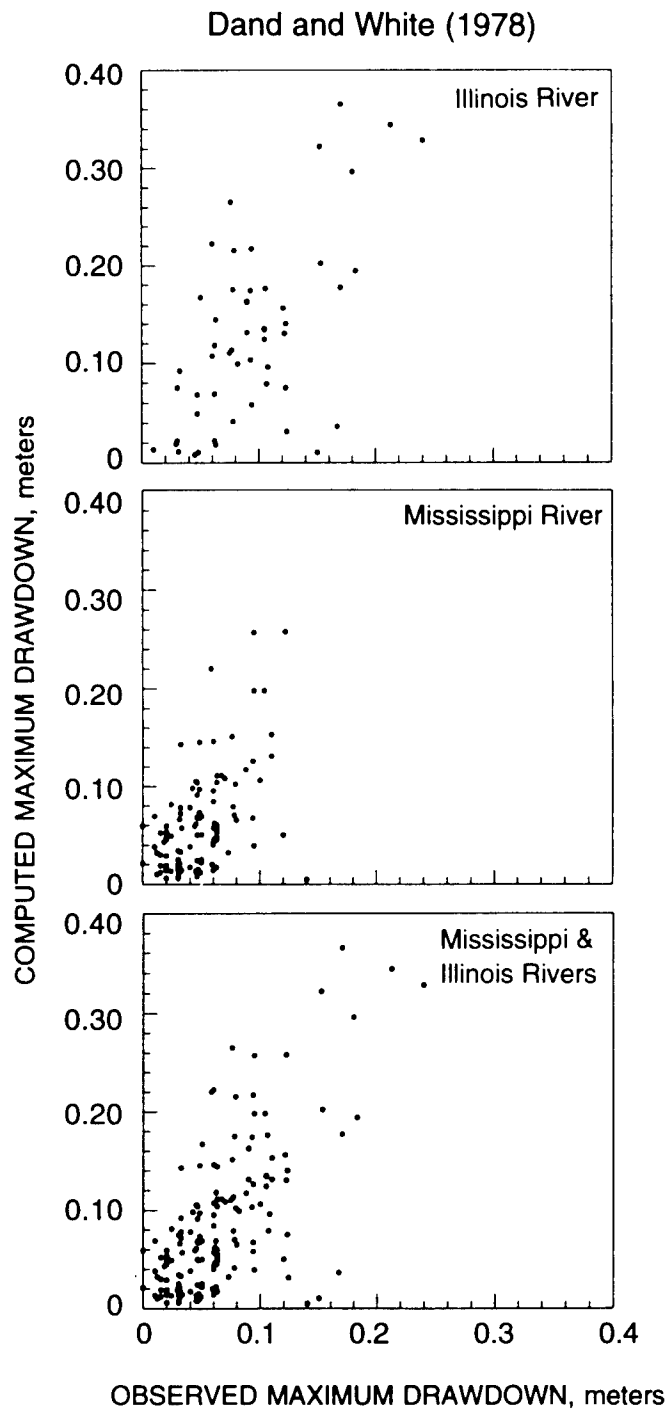


Figure 73. Comparison of computed and measured $H_{d(max)}$ using the method by Dand and White (1978)

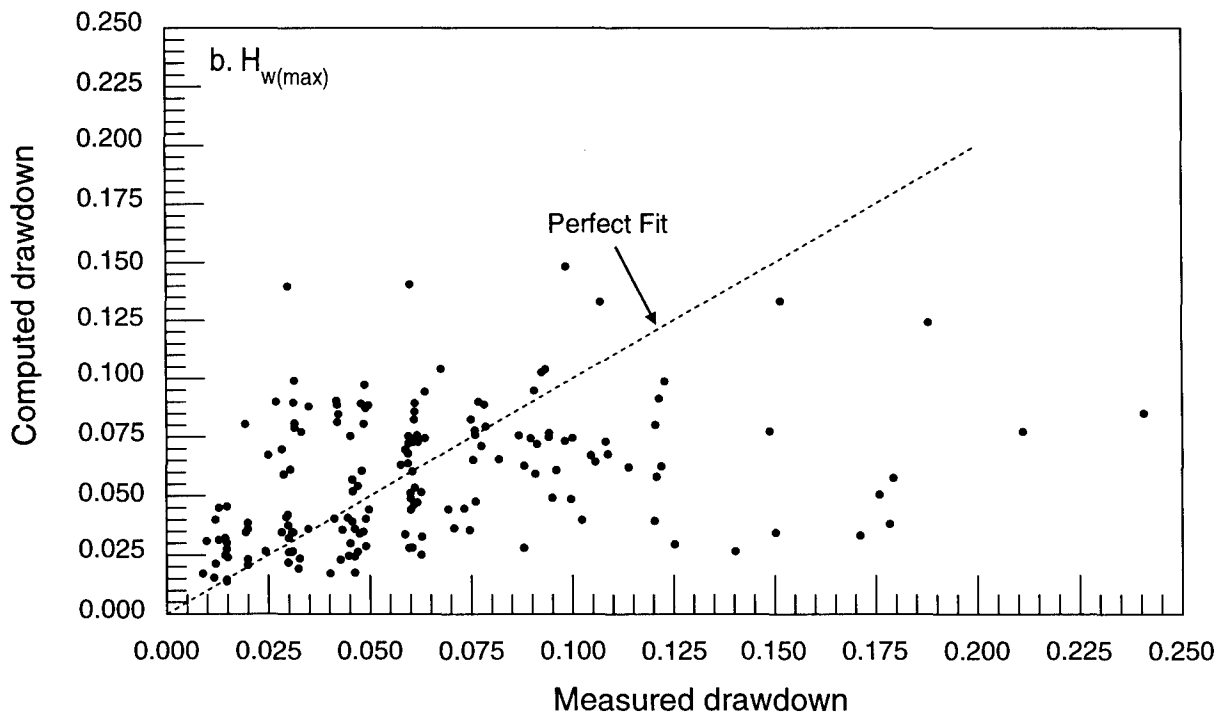
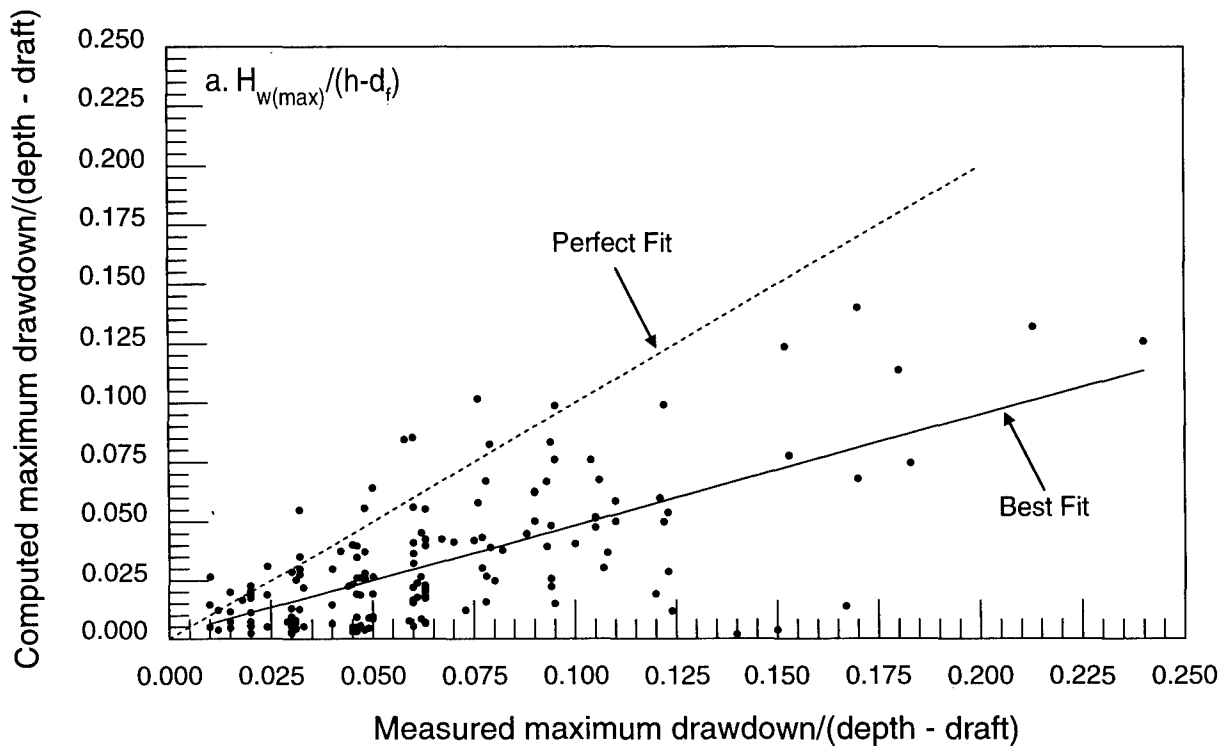


Figure 74. Comparison of (a) computed and measured $H_{d(max)}/(h-d_f)$, and (b) computed and measured $H_{d(max)}$, for the UMRS

TABLES

Table 1. Barge-Tow Variables and Ranges, after Adams (1991)

Variable	Symbol	Dimensions*	Typical values**	
			Minimum	Maximum
Barge or tow width	b	L	10.67	32.92
Barge or tow length	L	L	59.5	297.3
Barge or tow draft	d_f	L	0.61	2.74
Bow rake angle	β	°	30	90
Surface roughness	k	L	0.00005	0.0003
Towboat horsepower	HP	LF/T	600	8,000
Barge-tow speed	V_b	L/T	0	8
Propeller jet speed	V_o	L/T	0	15
Propeller flow rate	Q_j	L^3/T	0	80
Number of propellers	N_p		1	3
Open or ducted propellers	Kort		no	yes
Propeller diameter	D_p	L	1.25	3.05
Propeller rotation rate	n	1/T	0	4
Distance to a point	y	L	0	1,000
Angle to channel	α	°	0	+/-90

Notes:

*L = length, T = time, F = force.

**Standard international units (meters, joules, meters per second, cubic meters per second, and seconds).

Table 2. Target Physical Variables, after Adams (1991)

Variable	Symbol	Dimensions*	Typical values**	
			Minimum	Maximum
Velocity	V	L/T	0	10
Turbulence intensity	v^2/V^2		0	1.0
Wave height	H_w	L	0.01	5
Wave length	λ	L	1	100
Wave period	T	T	0.3	10
Wave speed	c	L/T	1.5	10
Drawdown	H_d	L	0	0.5
Sediment concentration	C_s	M/L ³	0	500
Duration of effect	t	T	0	5,000

Notes:

*L = length, T = time, M = mass

**Standard international units (meters, joules, meters per second, cubic meters per second, seconds, and milligrams per liter).

Table 3. Environmental Variables Related to Physical Effects of Commercial Navigation, after Adams (1991)

Variable	Symbol	Dimensions*	Typical values**	
			Minimum	Maximum
Average channel depth	h	L	0	30
Channel top width	W_T	L	300	2000
Channel area	A_c	L ²	1000	50,000
Energy slope	S	L/L	0	0.001
Velocity	V	L/T	0	10
Discharge	Q	L ³ /T	0	30,000
Radius of curvature	R	L	500	infinity
Particle size	d	L	0.000002	0.01
Bed form size	B_d	L	0.01	5
Wind speed	V_w	L/T	0	30
Wind wave height	H	L	0.01	2
Water temperature	T_o		-4	30

Notes:

*L = length, and T = time.

**Standard international units (meters, joules, meters per second, cubic meters per second, and seconds).

Table 4. Basic Variables and Dimensions, after Adams (1991)

<i>Variable</i>	<i>Symbol</i>	<i>Dimensions*</i>
Channel area	A_c	L^2
Submerged tow area	A_b	L^2
Maximum tow draft	D	L
Maximum channel depth	z	L
Channel top width	W_T	L
Acceleration of gravity	g	L/T^2
Barge-tow length	L	L
Towboat horsepower	HP	LF/T
Average river flow velocity	V_a	L/T
Tow or vessel speed	V_b	L/T
Energy slope	S	L/L
Unit weight	γ	F/L^3
Discharge	Q	L^3/T
Barge-tow width	b	L
Distance to vessel	y	L
Drawdown	H_d	L
Wave height	H_w	L
Kinematic viscosity	ν	L^2/T
Surface roughness	k	L
Time	t	T

Notes:

*L = length, T = time, and F = force.

Table 5. Vessel Passage Parameters, after Adams (1991)

<i>Parameter</i>	<i>Symbol</i>	<i>Definition</i>
Draft/depth ratio	DR	D/z
Blocking factor	BF	A_b/A_c
Channel Froude number	F	$V_a/[g(A_c/W_T)]^{0.5}$
Vessel draft Froude number	F_d	$V_b/(gD)^{0.5}$
Vessel length Froude number	F_l	$V_b/(gl)^{0.5}$
Vessel depth Froude number	F_z	$V_b(gz)^{0.5}$
Power ratio	P_r	$(HP/(V_b + V_a))/(wQS/V_a)$
Time ratio	t_r	tV/l
Relative distance	y/W_T	y/W_T
Relative wave height	H_w/z	H_w/z
Length Reynolds number	Re_l	$V_b l/\nu$
Relative roughness	k/L	k/l
Tow aspect ratio	L/b	l/b
Channel shape factor	W_T/z	W_T/z
Relative drawdown	H_d/z	H_d/z
Channel Reynolds number	Re_c	$V_a(A_c/W_T)/\nu$
Velocity ratio	V_b/V_a	V_b/V_a
Slope factor	$Sg/(yV_a)$	$Sg/(yV_a)$

Table 6. River Conditions Used To Generate Power Ratios, after Adams (1991)

<i>Discharge, cms</i>	<i>Slope</i>	<i>Velocity, m/s</i>	<i>Energy, J/m</i>
150	0.00002	0.15	20
300	0.00002	0.15	40
750	0.00004	0.30	100
1500	0.00008	0.60	200
3000	0.00016	0.90	533
7500	0.00020	1.20	1250

Table 7. Unit Towboat Power, after Adams (1991)

<i>Horsepower</i>	<i>kw</i>	<i>Absolute tow speed, m/s</i>					
		<i>0.3</i>	<i>0.6</i>	<i>1.0</i>	<i>2.0</i>	<i>4.0</i>	<i>8.0</i>
		<i>Unit towboat power, kJ/m</i>					
500	373	1243	622	373	187	93	47
1000	746	2487	1243	746	373	187	93
2000	1492	4973	2487	1492	746	373	187
3000	2238	7460	3730	2238	1419	560	280
4000	2984	9945	4973	2984	1492	746	373
5000	3730	12433	6217	3730	1865	933	466
6000	4476	14920	7460	4476	2238	1119	560
7000	5222	17407	8703	5222	2611	1306	653

Table 8. Barge Characteristics (USACOE, 1989)

<i>Type</i>	<i>Length, m</i>	<i>Breadth, m</i>	<i>Draft, m</i>	<i>Capacity, tons</i>
Open Hopper Barge				
Standard	53.4	7.9	0.6 - 2.7	1000
Jumbo	59.5	10.7	0.6 - 2.7	1500
Super Jumbo	76.2	12.2	0.6 - 2.7	2500
Covered Hopper Barge				
Standard	53.4	7.9	0.6 - 2.7	1000
Jumbo	59.5	10.7	0.6 - 2.7	1500
Chemical/Petroleum Barge	45.7 - 91.5	15.2 - 16.5	0.6 - 2.7	1900 - 3000
Towboats	19.8 - 48.8	7.3 - 15.2	1.5 - 2.7	300 - 7000*

Notes: *For towboats, capacity is expressed in horsepower.

**Table 9. Number of Sites Necessary
To Depict Physical Impacts of Navigation on the Upper Mississippi River System**

<i>River reach</i>	<i>Planform characteristics</i>			<i>Morphologic characteristics</i>		
	<i>S</i>	<i>GB</i>	<i>SB</i>	<i>SH</i>	<i>MD</i>	<i>DW</i>
Illinois River UMR above L&D 26	3	3	3	3	3	3
Open river	4	4	4	4	4	4
	2	2	2	2	2	2

Notes: S = straight
GB = gentle bend
SB = sharp bend
SH = shallow water
MD = medium depth
DW = deep water

**Table 10. Number of Trips Necessary
To Depict Physical Impacts of Navigation on the Upper Mississippi River System**

<i>River</i>	<i>Planform characteristics</i>			<i>Morphometry</i>			<i>Flow</i>		
	<i>S</i>	<i>GB</i>	<i>SB</i>	<i>SH</i>	<i>MD</i>	<i>DW</i>	<i>LF</i>	<i>MF</i>	<i>HF</i>
Illinois River UMR	3	3	3	3	3	3	3	3	3
	3	3	3	3	3	3	3	3	3

Notes: S = straight
GB = gentle bend
SB = sharp bend
SH = shallow water
MD = medium depth
DW = deep water
LF = low flow
MF = medium flow
HF = high flow

Table 11. Specifications of Instruments Used in the Field

<i>Instrument</i>	<i>Manufacturer</i>	<i>Data collected</i>	<i>Range</i>	<i>Accuracy</i>
S4	InterOcean	{ Vx, Vy direction depth temperature conductivity	0-350 cm/sec 0°-360° 0-70 m (-5)°-45°C 1-70 mS/cm	0.2 cm/sec 0.5° 4 mm 0.05°C 0.1mS/cm
MMB527	Marsh McBirney	{ Vx, Vy direction	±300 cm/sec 0-360°	±2% of reading 10°
MMB511	Marsh McBirney	Vx, Vy	±300 cm/sec	±2% of reading
MMB201	Marsh McBirney	V (resultant)	(-0.5)-20 ft/sec	±2% of reading
Wave gages	Illinois State Water Survey	water surface elevation	3 ft & 5 ft	0.05 ft
Turbidimeter	Orbeco-Hellige model 965	turbidity	0-1,000 NTU	0.01 NTU
ISCO pump 1680	Instrument Specialty Co.			
Wind monitor	R.M. Young	{ wind speed wind direction	0-60 m/sec 360°	1.0 m/sec 10°
Micro-Fix	Racal Survey	positioning	80 km	1 m
CR10/ SM716	Campbell Scien.	data logging		
Supersport 286 model 20	Zenith	{ program sensors, retrieve and transfer data		

Table 12. Sampling Rates Used in the Field

<i>Parameter</i>	<i>Sampling rate</i>
Velocity	1 per second
Waves	10 per second
Wind	1 per minute
Turbidity	1 per minute
Temperature	15 per hour
Suspended sediment	*

Notes: *For ambient monitoring, 3 suspended sediment samples were taken per hour. For event monitoring (during and after tow passage), suspended sediment samples were taken over a two-hour period: 20 samples the first hour, 6 samples the next half hour, and 3 samples the final half hour. Thereafter, 3 samples were taken per hour.

Table 13. Data Collection Dates and Locations

<i>Site</i>	<i>Date</i>	<i>Location</i>	<i>Station</i>
McEver's Island	5/15/89-5/19/89	RM 50.1	LHS
Apple River Island	5/14/95-5/25/95	RM 546.4	LHS
Goose Island (Trip 1)	8/20/90-8/29/90	RM 319.3	LHS
Kampsville (Trip 1)	10/9/90-10/18/90	RM 35.2	RHS
Clarks Ferry (Trip 1)	5/13/90-5/23/90	RM 468.2	RHS
Goose Island (Trip 2)	7/15/91-7/25/91	RM 319.5	LHS
Kampsville (Trip 2)	8/12/91-8/16/91	RM 35.2	RHS
Clarks Ferry (Trip 2)	10/15/91-10/20/91	RM 468.2	RHS

Notes: LHS = left-hand side and RHS = right-hand side

Table 14. Geomorphologic Characteristics of Data Collection Sites

<i>Site</i>	<i>River mile</i>	<i>Pool</i>	<i>Location</i>	<i>Deflection angle</i>	<i>Radius feet</i>	<i>Upstream point</i>	<i>Downstream point</i>
McEver's Island	50.1	Alton	upper middle river	53.2	11,300	RM 50.5	RM 49.5
Apple River Island	546.4	13	upper river	48.7	12,800	RM 546.5	RM 546.3
Goose Island (Trip 2)	319.3	22	upper river	66.7	8,200	RM 319.8	RM 319.3
Kampsville (Trip 2)	35.2	Alton	lower middle river	28	26,400	RM 35.4	RM 35.1
Clarks Ferry (Trip 2)	468.2	16	upper middle river	31	28,300	RM 468.3	RM 468.1

Table 15. Configuration of River Cross Section, Discharge, and Slope at Data Collection Sites

<i>Site</i>	<i>Top width, m</i>	<i>Avg. depth, m</i>	<i>Discharge, cms</i>	<i>Slope, m/km</i>
McEver's Island	230	3.37	212	0.006
Apple River Island	400	5.16	1,537	0.037
Goose Island (Trip 1)	418	6.04	2,856	0.069
Kampsville (Trip 1)	330	3.64	667	0.018
Clarks Ferry (Trip 1)	624	4.18	2,284	0.063
Goose Island (Trip 2)	403	5.49	1,844	0.054
Kampsville (Trip 2)	327	3.51	329	0.005
Clarks Ferry (Trip 2)	622	3.4	673	0.011

Table 16. Number of Current Meters, Suspended Sediment Sampling Intake Stations, and Wave Gages Used during Field Trips

<i>Site</i>	<i>Equipment</i>				
	<i>MMB511</i>	<i>MMB527</i>	<i>S4</i>	<i>Sediment intake stations</i>	<i>Wave gages</i>
McEver's Island	4	1	1	8	N/A
Apple River Island	4	2	2	6	1
Goose Island (Trip 1)	4	2	2	5	1
Kampsville (Trip 1)	4	2	2	9	1
Clarks Ferry (Trip 1)	6	2	5	8	1
Goose Island (Trip 2)	6	2	5	7	1
Kampsville (Trip 2)	4	2	-	N/A	1
Clarks Ferry (Trip 2)	6	2	4	N/A	1

Notes: N/A indicates data not available.

Table 17. Lateral Location of Velocity Meters at Field Sites

Lateral distance of each meter from left- or right-hand side (in meters)

<i>Site</i>	<i>MMB511/ 1001</i>	<i>MMB511/ 998</i>	<i>MMB511/ 999</i>	<i>MMB511/ 1000</i>	<i>MMB511/ 1130</i>	<i>MMB511/ 1131</i>	<i>MMB527/ 642</i>	<i>MMB527/ 332</i>	<i>S4/040</i>	<i>S4/071</i>	<i>S4/151</i>	<i>S4/832</i>	<i>S4/834</i>
McEver's Island	36.6 (L)	10.7 (L)	36.6 (L)	36.6 (L)	N/A	N/A	15.2 (L)	N/A	N/A	45.7 (L)	N/A	N/A	N/A
Apple River	4.6 (L)	32.0 (L)	32.0 (L)	9.1 (L)	N/A	N/A	61.0 (L)	97.5 (L)	149.4 (L)	112.8 (L)	N/A	N/A	N/A
Goose Island (1)	48.8 (L)	23.2 (L)	23.2 (L)	17.1 (L)	N/A	N/A	67.1 (L)	128.0 (L)	189.0 (L)	230.1 (L)	N/A	N/A	N/A
Kampsville (1)	12.9 (R)	33.5 (R)	33.5 (R)	33.5 (R)	N/A	N/A	47.2 (R)	65.5 (R)	131.4 (L)	85.7 (L)	N/A	N/A	N/A
Clarks Ferry (1)	15.2 (R)	43.0 (R)	43.0 (R)	43.0 (R)	28.0 (R)	28.0 (R)	67.1 (L)	121.9 (L)	304.8 (L)	304.8 (L)	73.5 (R)	104.0 (R)	104.0 (R)
Goose Island (2)	45.7 (L)	5.5 (L)	13.7 (L)	13.7 (L)	45.7 (L)	45.7 (L)	71.6 (L)	106.7 (L)	280.0 (L)	130.0 (L)	280.0 (L)	280.0 (L)	225.0 (L)
Kampsville (2)	12.5 (R)	22.9 (R)	22.9 (R)	22.9 (R)	N/A	N/A	53.3 (R)	76.2 (R)	N/A	N/A	N/A	N/A	N/A
Clarks Ferry (2)	25.9 (R)	41.1 (R)	41.1 (R)	41.1 (R)	68.6 (R)	68.6 (R)	67.1 (R)	70.1 (R)	89.9 (R)	N/A	304.8 (L)	259.1 (L)	104.0 (R)

Notes: Trip number is shown in parentheses following site name. N/A indicates data not available. L = left-hand side and R = right-hand side.

Table 18. Vertical Location of Velocity Meters at Field Sites

Site	<i>Distance of each meter from river bed (in meters)</i>												
	<i>MMB511/ 1001</i>	<i>MMB511/ 998</i>	<i>MMB511/ 999</i>	<i>MMB511/ 1000</i>	<i>MMB511/ 1130</i>	<i>MMB511/ 1131</i>	<i>MMB527/ 642</i>	<i>MMB527/ 332</i>	<i>S4/040</i>	<i>S4/071</i>	<i>S4/151</i>	<i>S4/832</i>	<i>S4/834</i>
McEver's Island	2.65	0.15	0.15	0.91	N/A	N/A	0.91	N/A	N/A	0.91	N/A	N/A	N/A
Apple River Island	0.2	0.15	2.74	0.22	N/A	N/A	0.46	0.91	0.91	0.91	N/A	N/A	N/A
Goose Island (1)	0.25	0.25	0.61	0.18	N/A	N/A	0.91	0.91	0.91	0.91	N/A	N/A	N/A
Kampsville (1)	0.29	0.31	1.22	2.44	N/A	N/A	0.7	0.7	0.92	0.92	N/A	N/A	N/A
Clarks Ferry (1)	0.35	0.36	1.62	2.53	0.33	1.52	0.7	0.7	1	1	1	1	1
Goose Island (2)	2.13	0.69	1.34	0.61	0.46	1.28	0.91	0.91	0.91	0.91	0.91	0.91	0.91
Kampsville (2)	0.29	0.46	1.31	2.13	N/A	N/A	0.7	0.7	N/A	N/A	N/A	N/A	N/A
Clarks Ferry (2)	0.46	0.51	1.24	2.16	0.5	1.21	0.94	0.94	1	N/A	1	1	1

Notes: N/A indicates data not available. Trip number is shown in parentheses.

Table 19. Lateral Location of Suspended Sediment Sampling Intake Nozzles at Field Sites

Site	<i>Lateral distance of each station from left- or right-hand side (in meters)</i>										
	<i>a1</i>	<i>a2</i>	<i>b1</i>	<i>b2</i>	<i>b3</i>	<i>c1</i>	<i>c2</i>	<i>c3</i>	<i>d1</i>	<i>d2</i>	<i>d3</i>
McEver's Island	13.7 (L)	13.7 (L)	18.3 (L)	18.3 (L)	18.3 (L)	24.4 (L)	24.4 (L)	24.4 (L)	N/A	N/A	N/A
Apple River Island	3.7 (L)	N/A	9.1 (L)	N/A	N/A	15.0 (L)	15.0 (L)	N/A	27.4 (L)	27.4 (L)	N/A
Goose Island (1)	8.2 (L)	N/A	16.5 (L)	16.5 (L)	N/A	25.9 (L)	25.9 (L)	N/A	N/A	N/A	N/A
Kampsville (1)	7.6 (R)	7.6 (R)	15.2 (R)	15.2 (R)	N/A	22.9 (R)	22.9 (R)	N/A	68.6 (L)	68.6 (L)	68.6 (L)
Clarks Ferry (1)	9.9 (R)	9.9 (R)	16.3 (R)	16.3 (R)	16.3 (R)	25.5 (R)	25.5 (R)	25.5 (R)	N/A	N/A	N/A
Goose Island (2)	7.6 (L)	N/A	12.2 (L)	12.2 (L)	N/A	25.9 (L)	25.9 (L)	N/A	64.0 (L)	N/A	N/A
Kampsville (2)	N/A	N/A	N/A	N/A	N/A	N/A	N/A	N/A	N/A	N/A	N/A
Clarks Ferry (2)	N/A	N/A	N/A	N/A	N/A	N/A	N/A	N/A	N/A	N/A	N/A

Notes: L = left-hand side, R = right-hand side. Trip number is shown in parentheses following site name. N/A indicates data not available.

Table 20. Vertical Location of Suspended Sediment Sampling Intake Nozzles at Field Sites

Site	<i>Distance of each station from river bed (in meters)</i>										
	<i>a1</i>	<i>a2</i>	<i>b1</i>	<i>b2</i>	<i>b3</i>	<i>c1</i>	<i>c2</i>	<i>c3</i>	<i>d1</i>	<i>d2</i>	<i>d3</i>
McEver's Island	0.15	0.61	0.15	0.61	1.22	0.15	0.61	1.85	N/A	N/A	N/A
Apple River Island	0.15	N/A	0.15	N/A	N/A	0.15	0.91	N/A	0.19	1.37	N/A
Goose Island (1)	0.23	N/A	0.23	0.61	N/A	0.23	1.52	N/A	N/A	N/A	N/A
Kampsville (1)	0.15	0.46	0.15	0.76	N/A	0.15	1.37	N/A	0.15	0.91	1.83
Clarks Ferry (1)	0.3	0.76	0.3	0.61	1.22	0.3	0.91	1.22	N/A	N/A	N/A
Goose Island (2)	0.61	N/A	0.46	0.91	N/A	0.3	1.22	N/A	0.66	N/A	N/A
Kampsville (2)	N/A	N/A	N/A	N/A	N/A	N/A	N/A	N/A	N/A	N/A	N/A
Clarks Ferry (2)	N/A	N/A	N/A	N/A	N/A	N/A	N/A	N/A	N/A	N/A	N/A

Notes: N/A indicates data not available. Trip number is shown in parentheses.

Table 21. Bed Material Size (d_{50}) at Field Sites

<i>Site</i>	<i>Main channel</i>	<i>Channel border</i>
McEver's Island	0.39 - 0.56	0.25 - 0.74
Apple River Island	0.44 - 0.59	0.34 - 0.38
Goose Island (Trip 1)	0.27 - 0.59	0.51 - 0.69
Kampsville (Trip 1)	0.26 - 0.35	0.27 - 0.34
Clarks Ferry (Trip 1)	0.32 - 0.45	0.28 - 0.46
Goose Island (Trip 2)	0.25 - 0.54	0.37 - 0.66

Notes: Bed material in mm.

Table 22. Blocking Factors at Field Sites

<i>Site</i>	<i>Barge direction</i>		
	<i>Upbound</i>	<i>Downbound</i>	<i>Both directions</i>
McEver's Island			
Max.	0.113	0.125	0.125
Mean	0.085	0.115	0.100
Min.	0.035	0.106	0.035
Apple River Island			
Max.	0.048	0.048	0.048
Mean	0.022	0.045	0.045
Min.	0.007	0.031	0.030
Goose Island (Trip 1)			
Max.	0.037	0.040	0.04
Mean	0.020	0.0369	0.03
Min.	0.009	0.010	0.01
Kampsville (Trip 1)			
Max.	0.068	0.071	0.071
Mean	0.041	0.048	0.044
Min.	0.015	0.006	0.006
Clarks Ferry (Trip 1)			
Max.	0.031	0.033	0.033
Mean	0.013	0.023	0.018
Min.	0.007	0.002	0.002
Goose Island (Trip 2)			
Max.	0.040	0.039	0.040
Mean	0.014	0.035	0.026
Min.	0.005	0.013	0.005
Kampsville (Trip 2)			
Max.	0.077	0.076	0.077
Mean	0.043	0.032	0.038
Min.	0.006	0.006	0.006
Clarks Ferry (Trip 2)			
Max.	0.042	0.042	0.042
Mean	0.014	0.024	0.021
Min.	0.008	0.003	0.003

Table 23. Draft to Depth Ratios at Field Sites

<i>Site</i>	<i>Barge direction</i>		
	<i>Upbound</i>	<i>Downbound</i>	<i>Both directions</i>
McEver's Island			
Max.	0.893	0.893	0.893
Mean	0.704	0.823	0.763
Min.	0.248	0.762	0.248
Apple River Island			
Max.	0.546	0.546	0.546
Mean	0.276	0.549	0.371
Min.	0.117	0.531	0.117
Goose Island (Trip 1)			
Max.	0.502	0.502	0.502
Mean	0.298	0.496	0.397
Min.	0.111	0.460	0.111
Kampsville (Trip 1)			
Max.	0.70	0.729	0.729
Mean	0.52	0.557	0.534
Min.	0.15	0.172	0.153
Clarks Ferry (Trip 1)			
Max.	0.663	0.663	0.663
Mean	0.321	0.543	0.440
Min.	0.138	0.140	0.138
Goose Island (Trip 2)			
Max.	0.501	0.505	0.505
Mean	0.206	0.482	0.360
Min.	0.103	0.393	0.103
Kampsville (Trip 2)			
Max.	0.780	0.780	0.780
Mean	0.546	0.524	0.546
Min.	0.171	0.171	0.171
Clarks Ferry (Trip 2)			
Max.	0.806	0.807	0.807
Mean	0.447	0.606	0.593
Min.	0.179	0.179	0.179

Table 24. Mean Values of River and Traffic Characteristics at Field Sites

<i>Site</i>	<i>V, m/s</i>	<i>Q, cms</i>	<i>BF</i>	<i>DR</i>	<i>F_i</i>	<i>F</i>
McEver's Island	0.27	212	0.09	0.7	0.046	0.406
Kampsville (1)	0.52	667	0.04	0.52	0.057	0.417
Kampsville (2)	0.29	329	0.04	0.57	0.066	0.418
Apple River Island	0.81	1537	0.02	0.28	0.068	0.431
Goose Island (1)	1.13	2856	0.02	0.3	0.051	0.301
Goose Island (2)	0.83	1844	0.01	0.21	0.062	0.407
Clarks Ferry (1)	0.82	2284	0.01	0.32	0.087	0.509
Clarks Ferry (2)	0.32	673	0.01	0.45	0.093	0.301

Notes: Trip number is shown in parentheses.

**Table 25. Mean Maximum Return Velocity
within Different Zones from Barge at Field Sites**

Site	Velocity, in m/s, by zone (distance, y/WT)					
	0.0-0.15	0.15-0.30	0.30-0.45	0.45-0.60	0.60-0.75	>0.75
Upbound Barges						
McEver's Island	N/A	N/A	0.12	0.33	0.44*	N/A
Kampsville (1)	0.25	0.22	0.21	0.2	N/A	N/A
Kampsville (2)	N/A	0.22	0.22	0.16	N/A	N/A
Apple River Island	N/A	0.14	0.11	0.09	0.20**	N/A
Goose Island (1)	N/A	0.25	0.17	0.1	0.09	N/A
Goose Island (2)	0.21	0.16	0.16	0.16	0.16	0.13
Clarks Ferry (1)	0.13	0.13	0.16	0.14**	N/A	N/A
Clarks Ferry (2)	0.12	0.11	0.09	N/A	N/A	N/A
Downbound Barges						
McEver's Island	N/A	N/A	N/A	0.15	0.35	N/A
Kampsville (1)	0.23**	0.25	0.17	N/A	N/A	N/A
Kampsville (2)	N/A	0.17	0.13	0.09	N/A	N/A
Apple River Island	N/A	0.15	0.11	0.07	N/A	N/A
Goose Island (1)	N/A	0.21	0.06	0.11	0.07	N/A
Goose Island (2)	0.16	0.16	0.14	0.13	0.11	0.16
Clarks Ferry (1)	0.17	0.16	0.15	0.17	N/A	N/A
Clarks Ferry (2)	0.13	0.09	0.1	N/A	N/A	N/A
All Barges						
McEver's Island	N/A	N/A	0.12	0.25	0.37	N/A
Kampsville (1)	0.24	0.23	0.2	0.19	N/A	N/A
Kampsville (2)	N/A	0.2	0.17	0.13	N/A	N/A
Apple River Island	N/A	0.15	0.11	0.08	0.17	N/A
Goose Island (1)	N/A	0.23	0.13	0.11	0.08	N/A
Goose Island (2)	0.18	0.16	0.15	0.14	0.13	0.14
Clarks Ferry (1)	0.15	0.15	0.15	0.16	N/A	N/A
Clarks Ferry (2)	0.13	0.1	0.1	N/A	N/A	N/A

Notes: Trip number is shown in parentheses.

*Only one data point available.

** Only two data points available.

**Table 26. Minimum and Maximum Return Velocity
within Different Zones from Barge at Field Sites**

Site	Velocity, in m/s, by zone (distance, y/WT)					
	0.0-0.15	0.15-0.30	0.30-0.45	0.45-0.60	0.60-0.75	>0.75
Upbound Barges						
McEver's Island	N/A	N/A	0.05-0.20	0.15-0.69	0.44*	N/A
Kampsville (1)	0.11-0.37	0.05-0.36	0.05-0.38	0.14-0.27	N/A	N/A
Kampsville (2)	N/A	0.09-0.36	0.06-0.35	0.11-0.24	N/A	N/A
Apple River Island	N/A	0.05-0.29	0.04-0.24	0.04-0.18	0.16-0.24**	N/A
Goose Island (1)	N/A	0.20-0.30	0.09-0.30	0.05-0.19	0.02-0.26	N/A
Goose Island (2)	0.12-0.29	0.06-0.24	0.11-0.21	0.10-0.21	0.09-0.30	0.06-0.21
Clarks Ferry (1)	0.09-0.18	0.09-0.25	0.09-0.23	0.13-0.14**	N/A	N/A
Clarks Ferry (2)	0.05-0.32	0.03-0.29	0.02-0.18	N/A	N/A	N/A
Downbound Barges						
McEver's Island	N/A	N/A	N/A	0.10-0.22	0.25-0.50	N/A
Kampsville (1)	0.14-0.32**	0.010-0.51	0.06-0.31	N/A	N/A	N/A
Kampsville (2)	N/A	0.09-0.30	0.02-0.27	0.09-0.11	N/A	N/A
Apple River Island	N/A	0.09-0.32	0.04-0.20	0.01-0.12	N/A	N/A
Goose Island (1)	N/A	0.16-0.28	0.05-0.07	0.09-0.16	0.02-0.13	N/A
Goose Island (2)	0.09-0.25	0.10-0.23	0.10-0.25	0.05-0.20	0.03-0.22	0.10-0.30
Clarks Ferry (1)	0.12-0.24	0.10-0.32	0.10-0.24	0.14-0.21	N/A	N/A
Clarks Ferry (2)	0.010-0.28	0.02-0.21	0.03-0.17	N/A	N/A	N/A
All Barges						
McEver's Island	N/A	N/A	0.05-0.20	0.10-0.69	0.25-0.50	N/A
Kampsville (1)	0.11-0.37	0.05-0.51	0.05-0.38	0.14-0.27	N/A	N/A
Kampsville (2)	N/A	0.09-0.36	0.02-0.35	0.09-0.24	N/A	N/A
Apple River Island	N/A	0.05-0.32	0.04-0.24	0.01-0.18	0.10-0.24	N/A
Goose Island (1)	N/A	0.16-0.30	0.05-0.30	0.05-0.19	0.02-0.26	N/A
Goose Island (2)	0.09-0.29	0.06-0.24	0.10-0.25	0.05-0.21	0.03-0.30	0.06-0.30
Clarks Ferry (1)	0.09-0.24	0.09-0.32	0.09-0.24	0.13-0.21	N/A	N/A
Clarks Ferry (2)	0.05-0.32	0.02-0.29	0.02-0.18	N/A	N/A	N/A

Notes: Trip number is shown in parentheses

*Only one data point available.

* Only two data point available.

Table 27. Most Frequently Occurring Intervals of Maximum Return Velocity within Different Zones from Barge at Field Sites

Site	<i>Velocity, in m/s, by zone (distance, y/WT)</i>					
	0.0-0.15	0.15-0.30	0.30-0.45	0.45-0.60	0.60-0.75	>0.75
Upbound Barges						
McEver's Island	N/A	N/A	0.1-0.15	0.25-0.3	N/A	N/A
Kampsville (1)	0.2-0.25	0.25-0.3	0.2-0.25	~ 0.2	N/A	N/A
Kampsville (2)	N/A	0.2-0.25	0.15-0.2	0.15-0.2	N/A	N/A
Apple River Island	N/A	0.15-0.2	0.1-0.15	0.05-0.1	**	N/A
Goose Island (1)	N/A	0.2-0.25	0.15-0.2	0.05-0.1	0.05-0.1	N/A
Goose Island (2)	0.2-0.25	0.1-0.15	0.15-0.2	0.15-0.2	0.1-0.15	0.1-0.15
Clarks Ferry (1)	0.1-0.15	0.1-0.15	0.1-0.15	*	N/A	N/A
Clarks Ferry (2)	0.05-0.1	0.05-0.1	0.1-0.15	N/A	N/A	N/A
Downbound Barges						
McEver's Island	N/A	N/A	N/A	0.1-0.15	0.3-0.35	N/A
Kampsville (1)	*	0.3-0.35	0.2-0.25	N/A	N/A	N/A
Kampsville (2)	N/A	0.2-0.25	0.05-0.1	0.05-0.1	N/A	N/A
Apple River Island	N/A	0.05-0.1	0.05-0.1	0.05-0.1	N/A	N/A
Goose Island (1)	N/A	0.2-0.25	0.05-0.1	0.1-0.15	0.05-0.1	N/A
Goose Island (2)	0.15-0.2	0.15-0.2	0.1-0.15	0.15-0.2	0.1-0.15	0.1-0.15
Clarks Ferry (1)	0.1-0.15	0.1-0.15	0.1-0.15	0.15-0.2	N/A	N/A
Clarks Ferry (2)	0.1-0.15	0.05-0.1	0.1-0.15	N/A	N/A	N/A
All Barges						
McEver's Island	N/A	N/A	0.1-0.15	0.15-0.2	0.3-0.35	N/A
Kampsville (1)	0.1-0.15	0.25-0.3	0.2-0.25	0.1-0.15	N/A	N/A
Kampsville (2)	N/A	0.2-0.25	0.15-0.2	0.1-0.15	N/A	N/A
Apple River Island	N/A	0.15-0.2	0.05-0.1	0.05-0.1	0.15-0.2	N/A
Goose Island (1)	N/A	0.2-0.25	0.05-0.1	0.05-0.1	0.05-0.1	N/A
Goose Island (2)	0.2-0.25	0.15-0.2	0.15-0.2	0.15-0.2	0.1-0.15	0.1-0.15
Clarks Ferry (1)	0.1-0.15	0.1-0.15	0.1-0.15	0.1-0.15	N/A	N/A
Clarks Ferry (2)	0.1-0.15	0.05-0.1	0.1-0.15	N/A	N/A	N/A

Notes: Trip number is shown in parentheses.

* Only two data points available.

Table 28. Mean Values of Maximum Return Velocity within Different Zones from Barge, Each River, All Trips

<i>Barge direction</i>	<i>Velocity, in m/s, by zone (distance, y/WT)</i>					
	<i>0.0-0.15</i>	<i>0.15-0.30</i>	<i>0.30-0.45</i>	<i>0.45-0.60</i>	<i>0.60-0.75</i>	<i>>0.75</i>
Upbound						
Ill. River	0.25	0.22	0.2	0.25	N/A	N/A
Miss. River	0.16	0.13	0.13	0.11	0.13	0.13
Downbound						
Ill. River	0.23	0.23	0.16	0.13	0.35	N/A
Miss. River	0.15	0.11	0.12	0.11	0.1	0.16
Both directions						
Ill. River	0.24	0.22	0.18	0.2	0.37	N/A
Miss. River	0.15	0.12	0.13	0.11	0.11	0.14

Table 29. Most Frequently Occurring Intervals of Maximum Return Velocity within Different Zones from Barge, Each River, All Trips

<i>Barge direction</i>	<i>Velocity, in m/s, by zone (distance, y/WT)</i>					
	<i>0.0-0.15</i>	<i>0.15-0.30</i>	<i>0.30-0.45</i>	<i>0.45-0.60</i>	<i>0.60-0.75</i>	<i>>0.75</i>
Upbound						
Ill. River	0.2-0.25	0.25-0.3	0.15-0.2	0.15-0.2	N/A	N/A
Miss. River	0.1-0.15	0.05-0.1	0.1-0.15	0.05-0.1	0.1-0.15	0.1-0.15
Downbound						
Ill. River	0.2-0.25	0.2-0.25	0.15-0.2	0.1-0.15	0.3-0.35	N/A
Miss. River	0.1-0.15	0.05-0.1	0.1-0.15	0.05-0.1	0.1-0.15	0.1-0.15
Both directions						
Ill. River	0.2-0.25	0.25-0.3	0.15-0.2	0.1-0.15	0.3-0.35	N/A
Miss. River	0.1-0.15	0.05-0.1	0.1-0.15	0.05-0.1	0.1-0.15	0.1-0.15

Table 30. Statistical Properties of Maximum Return Velocity at Field Sites and on Each River

<i>Site</i>	<i>Max.</i>	<i>Min.</i>	<i>Mean</i>	<i>Median</i>	<i>Sd. dev.</i>	<i>S. error</i>
Apple River	0.32	0.01	0.1	0.09	0.06	0.006
Clarks Ferry (1)	0.32	0.07	0.15	0.14	0.048	0.005
Clarks Ferry (2)	0.32	0.02	0.10	0.10	0.054	0.004
Goose Island (1)	0.30	0.02	0.11	0.08	0.074	0.008
Goose Island (2)	0.30	0.03	0.14	0.14	0.051	0.003
McEver's Island	0.69	0.05	0.23	0.18	0.148	0.025
Kampsville (1)	0.51	0.05	0.21	0.22	0.083	0.006
Kampsville (2)	0.36	0.02	0.17	0.17	0.079	0.010
Miss. River	0.32	0.01	0.12	0.11	0.059	0.002
Illinois River	0.69	0.02	0.21	0.20	0.094	0.006

Notes: Trip number is shown in parentheses.

Table 31. Range and Mean of Maximum Wave Height at Field Sites

	<i>Wave height, in meters</i>					
	<i>Upbound barges</i>		<i>Downbound barges</i>		<i>All barges</i>	
	<i>Range</i>	<i>Mean</i>	<i>Range</i>	<i>Mean</i>	<i>Range</i>	<i>Mean</i>
McEver's Island	0.03-0.14	0.06	0.01-0.15	0.06	0.01-0.15	0.06
Kampsville (1)	0.06-0.25	0.12	0.04-0.30	0.11	0.04-0.30	0.12
Kampsville (2)	0.03-0.21	0.09	0.01-0.20	0.1	0.01-0.22	0.1
Apple River Island	0.03-0.29	0.11	0.04-0.26	0.12	0.03-0.29	0.11
Goose Island (1)	0.09-0.17	0.12	0.11-0.66	0.25	0.09-0.66	0.16
Goose Island (2)	0.03-0.14	0.07	0.02-0.22	0.08	0.06-0.22	0.08
Clarks Ferry (1)	0.06-0.21	0.12	0.03-0.21	0.1	0.06-0.21	0.09
Clarks Ferry (2)	0.02-0.11	0.07	0.01-0.20	0.08	0.01-0.20	0.08

Notes: Trip number is shown in parentheses.

Table 32. Range and Mean of Maximum Wave Height for the Illinois and Mississippi Rivers

<i>Barge direction</i>	<i>Wave height, in meters</i>	
	<i>Mean</i>	<i>Range</i>
Illinois River		
Upbound	0.10	0.03-0.25
Downbound	0.10	0.01-0.30
Both directions	0.10	0.10-0.30
Mississippi River		
Upbound	0.09	0.02-0.29
Downbound	0.10	0.01-0.66
Both directions	0.10	0.01-0.66

Table 33. Range and Mean of Maximum Drawdown at Field Sites

<i>Site</i>	<i>Drawdown, in meters</i>						
	<i>Upbound</i>		<i>Downbound</i>		<i>All barges</i>		
	<i>Range</i>	<i>Mean</i>	<i>Range</i>	<i>Mean</i>	<i>Range</i>	<i>Mean</i>	<i>MFOI</i>
McEver's Island	0.05-0.22	0.14	0.09-0.24	0.13	0.05-0.24	0.13	0.15-0.175
Kampsville (1)	0.01-0.18	0.09	0.03-0.18	0.1	0.03-0.18	0.09	0.075-0.10
Kampsville (2)	0.01-0.09	0.06	0.01-0.17	0.08	0.01-0.17	0.08	0.075-0.10
Apple River Island	0.02-0.12	0.06	0.04-0.10	0.06	0.01-0.12	0.06	0.05-0.075
Goose Island (1)	0.02-0.09	0.05	0.03-0.09	0.06	0.01-0.09	0.06	0.025-0.075
Goose Island (2)	0.01-0.14	0.05	0.02-0.09	0.05	0.01-0.14	0.05	0.05-0.075
Clarks Ferry (1)	0.03-0.06	0.04	0.01-0.10	0.04	0.03-0.09	0.04	0.05-0.075
Clarks Ferry (2)	0.01-0.07	0.04	0.01-0.14	0.05	0.02-0.14	0.04	0.0-0.025

Notes: MFOI = most frequently occurring interval. Trip number is shown in parentheses.

Table 34. Range and Mean of Maximum Drawdown for the Illinois and Mississippi Rivers

<i>Barge direction</i>	<i>Drawdown, in meters</i>	
	<i>Mean</i>	<i>Range</i>
Illinois River		
Upbound	0.09	0.01-0.21
Downbound	0.10	0.01-0.24
Both directions	0.09	0.01-0.24
Mississippi River		
Upbound	0.05	0.01-0.14
Downbound	0.05	0.01-0.14
Both directions	0.05	0.01-0.14

Table 35. Mean Increased Suspended Sediment Concentration within Different Zones from Barge at Field Sites

Site	Concentration, in mg/L, by zone (distance, y/WT)					
	0.0-0.15	0.15-0.30	0.30-0.45	0.45-0.60	0.60-0.75	>0.75
Upbound Barges						
McEver's Island	N/A	N/A	N/A	N/A	85	143
Kampsville (1)	N/A	5	30	47	N/A	N/A
Apple River Island	N/A	N/A	N/A	19	N/A	N/A
Goose Island (1)	N/A	N/A	N/A	N/A	26	N/A
Goose Island (2)	3	4	N/A	5	55	25
Clarks Ferry (1)	N/A	N/A	8	N/A	N/A	N/A
Downbound Barges						
McEver's Island	N/A	N/A	N/A	N/A	N/A	55
Kampsville (1)	N/A	1	11	N/A	N/A	N/A
Apple River Island	N/A	N/A	N/A	10	34	N/A
Goose Island (1)	N/A	N/A	N/A	N/A	23	N/A
Goose Island (2)	6	N/A	N/A	N/A	23	27
Clarks Ferry (1)	N/A	N/A	3	7	N/A	N/A
All Barges						
McEver's Island	N/A	N/A	N/A	N/A	75	88
Kampsville (1)	N/A	3	22	47	N/A	N/A
Apple River Island	N/A	N/A	N/A	14	29	N/A
Goose Island (1)	N/A	N/A	N/A	N/A	25	N/A
Goose Island (2)	5	4	N/A	5	30	26
Clarks Ferry (1)	N/A	N/A	5	5	N/A	N/A

Notes: N/A indicates data not available. Trip number is shown in parentheses.

Table 36. Range of Increased Suspended Sediment Concentration within Different Zones from Barge at Field Sites

Site	Concentration, in mg/L, by zone (distance, y/WT)					
	0.0-0.15	0.15-0.30	0.30-0.45	0.45-0.60	0.60-0.75	>0.75
Upbound Barges						
McEver's Island	N/A	N/A	N/A	N/A	0-356	0-426
Kampsville (1)	N/A	0-72	0-181	0-146	N/A	N/A
Apple River Island	N/A	N/A	N/A	0-142	N/A	N/A
Goose Island (1)	N/A	N/A	N/A	N/A	0-130	N/A
Goose Island (2)	0-5	1-10	N/A	4-5	3-158	0-135
Clarks Ferry (1)	N/A	N/A	0-136	N/A	N/A	N/A
Downbound Barges						
McEver's Island	N/A	N/A	N/A	N/A	N/A	0-264
Kampsville (1)	N/A	1-28	0-178	N/A	N/A	N/A
Apple River Island	N/A	N/A	N/A	0-248	0-198	N/A
Goose Island (1)	N/A	N/A	N/A	N/A	0-180	N/A
Goose Island (2)	0-24	N/A	N/A	N/A	0-144	0-92
Clarks Ferry (1)	N/A	N/A	0-58	0-22	N/A	N/A
All Barges						
McEver's Island	N/A	N/A	N/A	N/A	0-356	0-426
Kampsville (1)	N/A	0-72	0-181	0-146	N/A	N/A
Apple River Island	N/A	N/A	N/A	0-248	0-198	N/A
Goose Island (1)	N/A	N/A	N/A	N/A	0-180	N/A
Goose Island (2)	0-24	1-10	N/A	4-5	0-158	0-135
Clarks Ferry (1)	N/A	N/A	0-136	0-22	N/A	N/A

Notes: N/A indicates data not available. Trip number is shown in parentheses.

Table 37. Mean Increased Suspended Sediment Concentration within Different Zones from Barge for the Illinois and Mississippi Rivers

<i>Barge direction</i>	<i>Concentration, in mg/L, by zone (distance, y/WT)</i>					
	<i>0.0-0.15</i>	<i>0.15-0.30</i>	<i>0.30-0.45</i>	<i>0.45-0.60</i>	<i>0.60-0.75</i>	<i>>0.75</i>
Upbound						
Illinois River	N/A	5	30	47	85	143
Mississippi River	3	4	8	15	30	25
Downbound						
Illinois River	N/A	1	11	N/A	N/A	54
Mississippi River	6	N/A	3	25	25	27
Both Directions						
Illinois River	N/A	3	22	25	85	88
Mississippi River	5	4	5	27	88	26

Table 38. Ranges of Increased Suspended Sediment Concentration within Different Zones from Barge for the Illinois and Mississippi Rivers

<i>Barge direction</i>	<i>Concentration, in mg/L, by zone (distance, y/WT)</i>					
	<i>0.0-0.15</i>	<i>0.15-0.30</i>	<i>0.30-0.45</i>	<i>0.45-0.60</i>	<i>0.60-0.75</i>	<i>>0.75</i>
Upbound						
Illinois River	N/A	0-72	0-181	0-147	0-356	0-426
Mississippi River	0-5	1-11	0-136	0-131	0-200	0-135
Downbound						
Illinois River	N/A	0-28	0-175	N/A	N/A	0-264
Mississippi River	0-24	N/A	0-58	0-248	0-198	0-92
Both Directions						
Illinois River	N/A	0-72	0-181	0-147	0-356	0-426
Mississippi River	0-24	1-11	0-136	0-248	0-200	0-135

Table 39. Statistical Properties of Increased Suspended Sediment Concentration at Field Sites and on Each River

<i>Site</i>	<i>Max.</i>	<i>Min.</i>	<i>Mean</i>	<i>Median</i>	<i>Sd. dev.</i>	<i>Sd. err.</i>
Apple River	248	0	18	0	43	4
Clarks Ferry (1)	136	0	5	0	15	1
Goose Island (1)	179	0	25	10	39	4
Goose Island (2)	158	0	22	7	32	3
McEver's Island	426	0	86	36	108	14
Kampsville (1)	181	0	17	0	36	3
Mississippi River	247	0	15	2	34	2
Illinois River	426	0	34	1	68	4

Notes: N/A indicates data not available. Trip number is shown in parentheses.

**Table 40. Suspended Sediment Concentration (mg/L)
at Goose Island, RM 319.3, Mississippi River, August 1990**

<i>Intake</i>	<i>Average</i>	<i>Sd. dev.</i>	<i>Maximum</i>	<i>Minimum</i>
a1 ambient	174	17	207	157
a1 event increase	42	52	182	0
a1 event maximum	100	67	193	3
c2 ambient	165	18	211	146
c2 event increase	9	17	42	0
c2 event maximum	67	87	264	3

**Table 41. Suspended Sediment Concentration (mg/L)
at Kampsville, RM 35.2, Illinois River, October 1990**

<i>Intake</i>	<i>Average</i>	<i>Sd. dev.</i>	<i>Maximum</i>	<i>Minimum</i>
a1 ambient	196	48	274	102
a1 event increase	71	41	150	28
a1 event maximum	187	116	371	47
c3 ambient	271	39	364	230
c3 event increase	17	19	37	0
c3 event maximum	75	38	130	33

Table 42. Average, Maximum, and Minimum Suspended Sediment Concentration (SSC) at Field Sites

<i>Intake</i>	<i>Ambient SSC</i>		
	<i>Avg.</i>	<i>Max.</i>	<i>Min.</i>
McEver's Island			
a1	77	158	28
a2	66	100	29
b1	126	293	47
b2	65	103	33
b3	56	88	32
c1	64	106	34
c2	60	89	34
c3	50	78	30
Kampsville, Trip 1			
a1	206	384	99
a2	181	269	95
b1	266	341	173
b2	238	285	151
c1	327	563	206
c2	269	308	227
Apple River Island			
a1	67	96	51
b1	72	85	63
c1	79	99	62
c2	71	143	56
d1	78	97	65
d2	667	80	57
Goose Island, Trip 1			
a1	181	270	152
b1	179	222	149
b2	169	203	138
c1	205	464	160
c2	162	181	147

Table 42. Concluded

<i>Intake</i>	<i>Ambient SSC</i>		
	<i>Avg.</i>	<i>Max.</i>	<i>Min.</i>
Goose Island, Trip 2			
a1	98	128	72
b1	113	159	73
b2	112	156	74
c1	95	122	71
c2	92	143	58
d1	64	68	62
e1	76	132	58
e2	81	129	68
Clarks Ferry, Trip 1			
a1	154	167	145
a2	149	160	142
b1	155	183	124
b2	157	167	145
b3	160	166	154
c1	167	213	127
c2	189	207	164
c3	190	223	159

Notes: Values in mg/L.

Table 43. Ratio of Event-Based Suspended Sediment Concentrations to Ambient Suspended Sediment Concentrations at Field Sites

<i>Intake</i>	<i>Event/ambient SSC</i>		
	<i>Avg.</i>	<i>Max.</i>	<i>Min.</i>
McEver's Island			
a1	5.74	13.08	1.17
a2	3.24	8.45	1.00
b1	2.67	6.55	1.00
b2	1.84	4.29	1.00
b3	1.85	4.10	1.00
c1	3.44	10.11	1.00
c2	1.89	4.12	1.00
c3	1.47	3.15	1.03
Kampsville, Trip 1			
a1	1.25	2.05	1.00
a2	1.22	2.01	1.00
b1	1.18	2.03	1.00
b2	1.08	1.38	1.00
c1	1.15	1.55	1.00
c2	1.05	1.21	1.00
Apple River Island			
a1	2.38	4.35	1.03
b1	1.63	2.97	1.02
c1	1.34	2.42	1.00
c2	1.21	2.21	1.00
d1	1.61	4.07	1.00
d2	1.04	1.11	1.00
Goose Island, Trip 1			
a1	1.28	2.00	1.00
b1	1.08	1.25	1.00
b2	1.09	1.22	1.02
c1	1.11	1.38	1.00
c2	1.20	1.88	1.01

Table 43. Concluded

<i>Intake</i>	<i>Event/ambient SSC</i>		
	<i>Avg.</i>	<i>Max.</i>	<i>Min.</i>
Goose Island, Trip 2			
a1	1.18	1.38	1.02
b1	1.34	2.30	1.00
b2	1.24	2.20	1.00
c1	1.18	1.45	1.00
c2	1.06	1.16	1.00
d1	1.05	1.09	1.00
e1	1.05	1.12	1.00
e2	1.05	1.23	1.01
Clarks Ferry, Trip 1			
a1	1.12	1.2	1.07
a2	1.09	1.13	1.03
b1	1.17	1.70	1.00
b2	1.12	1.20	1.08
b3	1.09	1.13	1.05
c1	1.05	1.14	1.00
c2	1.09	1.19	1.03
c3	1.23	1.86	1.01

**Table 44. Distribution of Suspended Sediment Particles,
Kampsville, Trip 1**

<i>Date</i>	<i>Time</i>	<i>Intake station</i>	<i>Dry weight, g</i>	<i>Percentage</i>		
				<i>Fine sand</i>	<i>Silt</i>	<i>Clay</i>
10/12/90	10:45 - 10:53	a1	1.1636	0.8	19.6	79.6
	10:40 - 10:53	a2	0.6856	0.8	26.7	72.5
	10:45 - 10:54	b1	1.2947	0.6	23.7	75.7
	10:45 - 10:53	b2	1.2115	0.2	25.4	74.4
	10:45 - 10:54	c1	1.1397	0.4	32.5	67.1
	10:45 - 10:54	c3	1.1964	0.4	27.9	71.7
10/13/90	13:12 - 13:17	a1	1.1918	0.9	35.7	63.4
	13:12 - 13:19	a2	1.3155	0.4	27.4	72.2
	13:12 - 13:18	b1	1.6101	0.3	37.7	62.0
	13:12 - 13:18	b2	1.4479	0.3	37.1	62.6
	13:12 - 13:18	c1	1.8757	0.2	45.3	54.5
	13:12 - 13:18	c3	1.6491	4.4	42.4	53.2

**Table 45. Distribution of Suspended Sediment Particles
for Specific Events, Kampsville, Trip 1**

<i>Date</i>	<i>Time</i>	<i>Barge</i>	<i>Intake station</i>	<i>Dry weight, g</i>	<i>Percentage</i>		
					<i>Fine sand</i>	<i>Silt</i>	<i>Clay</i>
10/15/90	09:48 - 09:54	<i>A. Randall</i>	a1	1.8782	0.4	35.8	63.8
	09:48 - 09:54	<i>A. Randall</i>	a2	1.8800	2.2	29.1	68.7
	09:48 - 09:54	<i>A. Randall</i>	b1	1.9839	0.2	40.4	59.4
	09:48 - 09:54	<i>A. Randall</i>	c1	2.0329	0.3	46.7	53.0
	09:48 - 09:54	<i>A. Randall</i>	c3	1.8598	0.4	46.4	53.2

**Table 46. Distribution of Suspended Sediment Particles,
Goose Island, Trip 1**

<i>Date</i>	<i>Time</i>	<i>Intake station</i>	<i>Dry weight, g</i>	<i>Percentage</i>		
				<i>Fine sand</i>	<i>Silt</i>	<i>Clay</i>
08/24/90	12:42 - 12:53	a1	1.9958	0.3	30.7	69.0
	12:42 - 12:53	b1	1.9637	1.2	27.8	71.0
	12:42 - 12:53	b2	2.0393	1.1	31.7	67.2
	12:42 - 12:53	c1	1.8865	5.0	33.8	61.2
	12:42 - 12:53	c2	2.0263	1.3	29.4	69.3
08/25/90	10:21 - 10:34	a1	2.1207	1.9	23.2	74.9
	10:21 - 10:38	b1	1.7704	2.4	29.0	68.6
	10:21 - 10:32	c1	2.1242	7.1	30.0	62.9
	15:29 - 15:43	a1	1.2947	0.6	35.0	64.4
	15:29 - 15:39	b1	1.2450	2.3	36.6	61.1
	15:29 - 15:39	c1	1.6579	8.5	31.6	57.9
08/26/90	09:48-09:58	a1	1.9601	0.8	40.3	58.9
	09:48-10:03	b1	1.3911	2.0	17.8	80.2
	09:48-10:03	c1	1.7110	11.2	38.4	50.4
08/27/90	11:56-12:05	a1	1.7031	0.6	26.2	73.2
	11:53-12:04	b1	2.5421	5.5	29.3	65.2
	11:55-12:06	c1	1.88051	15.7	28.6	55.7

**Table 47. Distribution of Suspended Sediment Particles
for Specific Events, Goose Island, Trip 1**

<i>Date</i>	<i>Time</i>	<i>Barge</i>	<i>Intake station</i>	<i>Dry weight, g</i>	<i>Percentage</i>		
					<i>Fine sand</i>	<i>Silt</i>	<i>Clay</i>
08/26/90	11:44 - 11:56	<i>K. Michael</i>	a1	1.1636	0.8	19.6	79.6
	13:26 - 13:35	<i>Sumac</i>	b1	0.6856	0.8	26.7	72.5

**Table 48. Distribution of Suspended Sediment Particles,
Goose Island, Trip 2**

<i>Date</i>	<i>Time</i>	<i>Intake station</i>	<i>Dry weight, g</i>	<i>Percentage</i>		
				<i>Fine sand</i>	<i>Silt</i>	<i>Clay</i>
07/22/91	14:38 - 14:45	d2	0.9599	2.4	48.9	48.7
	15:00 - 1509	b1	0.8878	3.8	30.3	65.9
	15:00 - 1507	b2	0.8878	1.9	40.3	57.8
	15:00 - 1509	e1	0.8180	1.0	31.7	67.3
	16:36 - 16:42	d1	0.9958	1.7	46.9	51.4
	16:37 - 16:42	d2	1.1943	3.0	43.2	53.8
	16:50 - 16:59	b1	1.1237	3.0	43.7	53.3
	16:50 - 16:57	b2	0.9955	2.3	40.5	57.2
	17:10 - *	d1	0.833	1.9	32.0	66.1
07/23/91	11:31 - 11:39	b1	0.8299	5.6	47.4	47.0
	11:45 - *	d1	0.7915	5.0	53.7	41.3
	11:45 - *	d2	0.8089	4.8	45.2	50.0
	11:45 - *	e1	0.8180	4.9	49.3	45.8

Notes: *Ending time was not recorded. In general, the filling time varied between 6 and 9 minutes at this site.

**Table 49. Distribution of Suspended Sediment Particles
for Specific Events, Goose Island, Trip 2**

<i>Date</i>	<i>Time</i>	<i>Barge</i>	<i>Intake station</i>	<i>Dry weight, g</i>	<i>Percentage</i>		
					<i>Fine sand</i>	<i>Silt</i>	<i>Clay</i>
07/23/91	16:25 - *	<i>Evey - T</i>	b1	1.1077	7.1	44.5	48.4
	16:25 - *	<i>Evey - T</i>	b2	1.2544	5.6	40.0	54.4
	16:30 - *	<i>Evey - T</i>	d1	0.7705	3.0	50.8	46.2
	16:30 - *	<i>Evey - T</i>	d2	1.0641	4.1	52.4	43.5
	16:30 - *	<i>Evey - T</i>	e1	0.6456	4.8	51.4	43.8

Notes: *Ending time was not recorded. In general, the filling time varied between 6 and 9 minutes at this site.

**Table 50. Distribution of Suspended Sediment Particles,
Clarks Ferry, Trip 1**

<i>Date</i>	<i>Time</i>	<i>Intake station</i>	<i>Dry weight, g</i>	<i>Percentage</i>		
				<i>Fine sand</i>	<i>Silt</i>	<i>Clay</i>
05/18/91	11:19 - 11:28	a1	5.6440	0.1	33.7	66.2
	11:19 - 11:28	a2	5.4896	0.1	26.6	73.3
	11:19 - 11:28	b1	5.2359	0.2	39.4	60.4
	11:19 - 11:28	b2	5.2568	0.2	38.0	61.8
	11:19 - 11:28	b3	6.0134	0.2	35.1	64.7
05/20/91	16:30 - *	b1	1.8645	1.2	40.3	58.5
	16:30 - *	c1	1.6799	1.2	43.1	55.7
05/21/91	10:10 - 10:21	b1	1.4145	0.7	39.9	59.4
	10:10 - 10:21	c1	1.5863	1.4	48.2	50.4
	17:01 - 17:14	e1	2.9209	41.4	31.1	27.5
	17:01 - 17:14	e2	7.6477	78.0	12.3	9.7

Notes: *Ending time was not recorded. In general, the filling time varied between 9 and 13 minutes at this site.

Table 51. Existing Methods for Computing Return Velocity

<i>Method</i>	<i>Authors</i>
1	Schijf and Jansen (1953)
2	Bouwmeester (1977)
3	Blaauw and van der Knaap (1983)
4	Fuehrer and Romisch (1977)
5	Hochstein and Adams (1989)
6	Hochstein and Adams (1989)
7	Simons et al. (1981)
8	Berger Associates, Ltd. (1981)
9	Maynord and Siemsen (1991)
10	Bhowmik et al. (1995a)

Table 52. Correlation Coefficient and Standard Error of Estimate for Methods of Computing Return Velocity

<i>Method</i>	<i>Apple R. Island</i>	<i>Clarks F., trip 1</i>	<i>Clarks F., trip 2</i>	<i>Goose, trip 1</i>	<i>Goose, trip 2</i>	<i>McEver's Island</i>	<i>Kampsville, trip 1</i>	<i>Kampsville, trip 2</i>
1	0.75 (0.056)	0.08 (0.04)	0.54 (0.043)	0.28 (0.041)	0.23 (0.046)	0.02 (0.116)	0.73 (0.045)	0.73 (0.057)
2	0.75 (0.058)	0.08 (0.043)	0.53 (0.049)	0.28 (0.042)	0.23 (0.047)	0.01 (0.140)	0.73 (0.047)	0.73 (0.060)
3	0.75 (0.056)	0.02 (0.047)	0.34 (0.052)	0.29 (0.043)	0.23 (0.064)	0.02 (0.141)	0.73 (0.047)	0.72 (0.060)
4	0.57 (0.127)	0.37 (0.208)	0.19 (0.317)	0.46 (0.063)	0.14 (0.224)	0.11 (0.231)	0.48 (0.127)	0.38 (0.038)
5	0.76 (0.047)	0.14 (0.038)	0.74 (0.026)	0.33 (0.036)	0.26 (0.040)	0.02 (0.120)	0.77 (0.037)	0.76 (0.048)
Best fit	Method 5	Method 4	Method 5	Method 4	Method 5	Method 4	Method 5	Method 5
6	0.62 (0.087)	0.04 (0.147)	0.59 (0.045)	0.55 (0.057)	0.30 (0.149)	0.16 (0.095)	0.50 (0.093)	0.56 (0.036)
7	0.40 (0.03)	0.23 (0.039)	0.11 (0.038)	0.40 (0.021)	0.19 (0.035)	0.07 (0.031)	0.41 (0.030)	0.46 (0.027)
8	0.61 (0.032)	0.03 (0.074)	0.52 (0.015)	0.64 (0.015)	0.32 (0.077)	0.28 (0.035)	0.48 (0.037)	0.45 (0.013)
9	0.48 (0.121)	0.15 (0.138)	0.26 (0.097)	0.42 (0.042)	0.30 (0.107)	0.05 (0.211)	0.53 (0.103)	0.62 (0.100)
10	0.46 (0.055)	0.05 (0.104)	0.63 (0.029)	0.46 (0.026)	0.24 (0.142)	0.43 (0.084)	0.46 (0.089)	0.33 (0.274)
Best fit	Methods 6, 8	Method 7	Methods 10, 6	Method 8	Method 8	Method 10	Methods 9, 6	Methods 9, 6

Notes: Standard error of estimate in parentheses.

**Table 53. Correlation Coefficient and Standard Error of Estimate
for Computed and Measured Return Velocity for Both Rivers
and for Directional Movement of the Barges**

<i>Method</i>	<i>Miss. R. (down)</i>	<i>Miss. R. (up)</i>	<i>Miss. R. (both)</i>	<i>Il. R. (down)</i>	<i>Il. R. (up)</i>	<i>Il. R. (both)</i>
1	0.29 (0.050)	0.42 (0.054)	0.32 (0.054)	0.44 (0.101)	0.61 (0.082)	0.53 (0.090)
2	0.29 (0.051)	0.44 (0.055)	0.33 (0.055)	0.44 (0.112)	0.58 (0.096)	0.51 (0.102)
3	0.27 (0.057)	0.48 (0.060)	0.35 (0.061)	0.43 (0.112)	0.57 (0.099)	0.50 (0.104)
4	0.07 (0.181)	0.09 (0.147)	0.09 (0.163)	0.28 (0.144)	0.33 (0.165)	0.32 (0.157)
5	0.32 (0.045)	0.46 (0.047)	0.37 (0.047)	0.40 (0.099)	0.65 (0.069)	0.52 (0.083)
Best fit	Method 5	Method 3	Method 5	Methods 1, 2	Method 5	Methods 1, 5
6	0.37 (0.118)	0.44 (0.101)	0.36 (0.114)	0.38 (0.087)	0.40 (0.0099)	0.38 (0.094)
7	0.16 (0.025)	0.24 (0.044)	0.18 (0.036)	0.37 (0.023)	0.36 (0.035)	0.34 (0.031)
8	0.32 (0.045)	0.31 (0.065)	0.32 (0.055)	0.44 (0.028)	0.30 (0.043)	0.34 (0.038)
9	0.21 (0.091)	0.28 (0.133)	0.25 (0.113)	0.43 (0.133)	0.43 (0.144)	0.43 (0.140)
10	0.27 (0.047)	0.25 (0.129)	0.24 (0.096)	0.28 (0.150)	0.18 (0.168)	0.23 (0.160)
Best fit	Method 6	Method 6	Method 6	Method 8	Method 9	Method 9

Notes: Standard error of estimate in parentheses.

Table 54. Correlation Coefficient and Standard Error of Estimate for Computed Return Velocity by Two Methods on Both Rivers

<i>Barge direction</i>	<i>Hochstein and Adams (1989)</i>		<i>Maynard and Siemsen (1991)</i>	
	<i>IL River</i>	<i>MS River</i>	<i>IL River</i>	<i>MS River</i>
Upbound	0.40 (0.099)	0.44 (0.101)	0.43 (0.144)	0.28 (0.133)
Downbound	0.38 (0.087)	0.37 (0.118)	0.43 (0.133)	0.21 (0.091)

Notes: Standard error of estimate in parentheses.

Table 55. Existing Methods for Estimating Maximum Wave Height

<i>Method</i>	<i>Authors</i>	<i>Applications</i>
1	Balanin and Bykov (1965)	All vessels
2	USACOE (1980)	Large vessels
3	Bhowmik et al. (1981b)	Barges
4	Bhowmik et al. (1982)	Barges
5	Gates and Herbich (1977)	All vessels, deep water, unrestricted channels, near the vessel
6	Blaauw et al. (1984)	Barges; coefficients are used to separate empty and loaded barges
7	PIANC (1987)	Tugboats and motor tows
8	Sorensen and Weggel (1984)	Recreational boats
9	Bhowmik (1976)	Recreational boats
10	Bhowmik et al. (1991)	Recreational boats

Table 56. Correlation Coefficient and Standard Error of Estimate for Computed and Measured Maximum Wave Height, Illinois and Mississippi Rivers

<i>Method</i>	<i>Illinois River</i>	<i>Mississippi River</i>	<i>Both Rivers</i>
1	0.18 (0.115) - ove	0.15 (0.147) - ove	0.15 (0.137) - ove
2	0.40 (0.075) - scatter	0.29 (0.149) - ove	0.29 (0.132) - ove
3	0.37 (0.209) - ove	0.23 (0.348) - ove	0.24 (0.318) - ove
4	0.13 (0.052) - scatter	0.08 (0.069) - scatter	0.09 (0.064) - scatter
5	0.013 (0.066) - scatter	0.03 (0.278) - scatter	0.03 (0.233) - scatter
6	0.44 (0.035) - ude	0.26 (0.052) - scatter	0.28 (0.048) - scatter
7	0.46 (0.067) - ude	0.22 (0.112) - scatter	0.26 (0.101) - scatter
8	0.12 (0.032) - ude	0.20 (0.044) - ude	0.17 (0.040) - ude
9	0.07 (0.726) - ove	0.11 (0.694) - ove	0.08 (0.717) - ove
10	0.31 (0.600) - ove	0.30 (0.447) - ove	0.24 (0.561) - ove
Best fit	Methods 7, 6	Methods 10, 2	Methods 2, 6

Notes: Standard error of estimate in parentheses. ove = overestimation, ude = underestimation, scatter = no clear trend.

Table 57. Existing Methods for Computing Maximum Drawdown

<i>Method</i>	<i>Authors</i>
1	Schijf and Jansen (1953)
2	Galencser (1977)
3	Gates and Herbich (1977)
4	Dand and White (1978)
5	Bhowmik et al. (1981b)
6	Balanin and Bykov (1965)
7	Hochstein (1967)
8	Bouwmeester (1977)
9	Blaauw and van der Knapp (1983)
10	Bhowmik et al. (1982)

Table 58. Correlation Coefficient and Standard Error of Estimate for Computed and Measured Maximum Drawdown, Illinois and Mississippi Rivers

<i>Method</i>	<i>Illinois River</i>	<i>Mississippi River</i>	<i>Both Rivers</i>
1	0.57 (0.005) - ude	0.53 (0.005) - ude	0.53 (0.005) - ude
2	0.34 (0.002) - ude	0.30 (0.001) - ude	0.45 (0.001) - ude
3	0.58 (0.057) - scatter	0.37 (0.057) - ove	0.48 (0.057) - ove
4	0.63 (0.072) - ove	0.54 (0.044) - ove	0.68 (0.055) - ove
5	0.55 (0.017) - ude	0.38 (0.017) - scatter	0.49 (0.017) - ude
6	0.58 (0.010) - ude	0.36 (0.010) - ude	0.48 (0.010) - ude
7	0.63 (0.022) - ude	0.57 (0.016) - scatter	0.65 (0.018) - ude
8	0.55 (0.041) - scatter	0.43 (0.030) - scatter	0.57 (0.034) - scatter
9	0.50 (0.047) - scatter	0.025 (0.233) - ove	0.01 (0.195) - scatter
10	0.51 (0.014) - ude	0.30 (0.005) - ude	0.58 (0.01) - ude
Best fit	Methods 4, 7; 3, 6	Methods 7, 4	Methods 4, 7

Notes: ove = overestimation, ude = underestimation, scatter = no clear trend. Standard error of estimate in parentheses.

Table 59. Ambient Sediment Load Computations

Site	Date	River mile	Q, cms	D, m	U, m/s	S	W, m	T, C	d50, mm	Cm, mg/L	Qsm, mt/d	Computed Qs, mt/d		
												Akers-White	Colby	Toffaleti
Mississippi River														
Apple River Island	5/22/90	546.4	1537	5.16	0.81	0.000037	367	10	0.48	80	10636	10275	3085	1175
Clarks Ferry	5/22/91	468.2	2072	4.18	0.78	0.000063	634	4	0.38	125	22404	18681	12539	2968
Goose Island (1)	8/29/90	319.3	2856	6.04	1.13	0.000069	419	21	0.46	150	37057	48071	26492	3616
Goose Island (2)	7/24/91	319.5	1880	5.56	0.84	0.000054	404	21	0.42	125	20328	107423	8461	1329
Illinois River														
McEver's Island	5/17/89	50.1	212	3.37	0.27	0.0000064	233	16	0.44	50	917	0	2	76
Kampsville (1)	10/15/90	35.2	772	3.64	0.58	0.000018	335	18	0.31	317	21169	1523	1006	378
Kampsville (2)	8/8/91	35.2	329	3.51	0.29	0.0000047	323	27	0.31	115	3272	3	27	365

Notes: Trip number is shown in parentheses.

**Table 60. Event Peak Suspended Sediment Concentration at Apple River Island,
Measured and Computed (Akers-White Method)**

<i>Tow</i>	<i>Suspended sediment concentration at each station, mg/L</i>									
	<i>a1</i> <i>Meas.</i>	<i>a</i> <i>Computed</i>	<i>b1</i> <i>Meas.</i>	<i>b</i> <i>Computed</i>	<i>c1</i> <i>Meas.</i>	<i>c2</i> <i>Meas.</i>	<i>c</i> <i>Computed</i>	<i>d1</i> <i>Meas.</i>	<i>d2</i> <i>Meas.</i>	<i>d</i> <i>Computed</i>
<i>Merlin Banta</i>	59	0	67	0	78	61	1	85	61	2
<i>Rusty Flowers</i>	108	0	78	5	81	62	6	193	62	7
<i>Tom Talbert</i>	265	1	178	0	91	65	0	76	66	1
<i>Herman Pott</i>	208	20	131	12	185	97	13	78	64	13
<i>Walter Brunson</i>	91	0	74	ND	80	212	ND	92	71	ND
<i>Dell Butcher</i>	99	0	118	0	83	68	0	75	67	0
<i>Mary Gail</i>	226	0	214	2	169	129	3	82	72	4
<i>T.S. Kunsman</i>	256	0	98	0	82	67	0	328	73	0
<i>D.R. Miller</i>	162	9	124	7	115	72	8	95	72	9
<i>Mary Gail</i>	252	0	174	0	99	78	0	95	80	1
<i>J.D. Wofford</i>	73	1	77	1	99	68	2	153	70	2
<i>Trojan</i>	90	0	88	0	99	69	1	161	71	1

Notes: ND = not detectable. Data from the period May 18-23, 1990.

**Table 61. Event Peak Suspended Sediment Concentration at Clarks Ferry (Trip 1),
Measured and Computed (Akers-White Method)**

<i>Tow</i>	<i>Suspended sediment concentration at each station, mg/L</i>										
	<i>a1</i> <i>Meas.</i>	<i>a2</i> <i>Meas.</i>	<i>a</i> <i>Computed</i>	<i>b1</i> <i>Meas.</i>	<i>b2</i> <i>Meas.</i>	<i>b3</i> <i>Meas.</i>	<i>b</i> <i>Computed</i>	<i>c1</i> <i>Meas.</i>	<i>c2</i> <i>Meas.</i>	<i>c3</i> <i>Meas.</i>	<i>c</i> <i>Computed</i>
<i>Jemco Towing</i>	179	163	14	188	174	ND	14	194	196	295	64
<i>Pearl B.</i>	ND	152	1	174	171	169	1	199	198	190	1
<i>Conti-Afton</i>	156	161	0	176	171	166	0	210	202	200	1
<i>Sunflower-1</i>	ND	ND	1	193	ND	ND	1	190	ND	ND	35
<i>Am. Beauty-1</i>	ND	ND	1	211	ND	ND	2	186	ND	ND	38
<i>Dell Butcher-2</i>	ND	ND	4	173	ND	ND	5	145	ND	ND	35
<i>Hornet</i>	ND	ND	4	139	ND	ND	4	138	ND	ND	38
<i>Volunteer State</i>	ND	ND	4	210	ND	ND	4	144	ND	ND	34

Notes: ND = not detectable. Data from the period May 16-22, 1990.

Table 62. Event Peak Suspended Sediment Concentration at Goose Island (Trip 1), Measured and Computed (Akers-White Method)

<i>Tow</i>	<i>Suspended sediment concentration at each station, mg/L</i>							
	<i>a1</i> <i>Meas.</i>	<i>a</i> <i>Computed</i>	<i>b1</i> <i>Meas.</i>	<i>b2</i> <i>Meas.</i>	<i>b</i> <i>Computed</i>	<i>c1</i> <i>Meas.</i>	<i>c2</i> <i>Meas.</i>	<i>c</i> <i>Computed</i>
<i>Dell Butcher</i>	332	0	252	242	1	253	190	7
<i>W.C. Norman</i>	258	0	217	212	1	203	236	5
<i>Normania</i>	268	2	216	210	3	192	277	14
<i>Dave Carlton</i>	199	2	192	191	3	193	178	13
<i>H.C. Blaske</i>	155	0	153	160	0	193	155	5
<i>Teresa Renee</i>	164	5	163	144	6	167	155	25
<i>Trojan Warrior</i>	193	0	169	144	0	186	277	4
<i>Hoosier State</i>	160	5	167	154	6	179	194	24
<i>Kevin Michael</i>	159	2	161	154	3	180	147	13
<i>Sumac</i>	195	1	176	181	2	197	155	8
<i>Twin Cities</i>	297	0	183	173	0	195	160	6
<i>Coop. Vanguard</i>	187	3	179	164	4	191	155	19
<i>H.M. Clements</i>	360	3	226	216	3	252	265	17

Notes: Data from the period August 24-27, 1990.

Table 63. Event Peak Suspended Sediment Concentration at Goose Island (Trip 2),
Measured and Computed (Akers-White Method)

Tow	Suspended sediment concentration at each station, mg/L												
	<i>a1</i>	<i>a</i>	<i>b1</i>	<i>b2</i>	<i>b</i>	<i>c1</i>	<i>c2</i>	<i>c</i>	<i>d1</i>	<i>d</i>	<i>e1</i>	<i>e2</i>	<i>e</i>
	Meas.	Computed	Meas.	Meas.	Computed	Meas.	Meas.	Computed	Meas.	Computed	Meas.	Meas.	Computed
<i>James F. Neal</i>	148	0	133	113	0	132	154	0	ND	13	ND	ND	25
<i>H.M. Clements</i>	120	0	118	110	0	123	137	0	ND	95	ND	ND	76
<i>F.T. Heffelfinger</i>	104	0	110	110	0	125	97	0	ND	10	ND	ND	ND
<i>Queen City</i>	93	0	92	88	0	93	62	ND	ND	10	ND	ND	ND
<i>H.M. Clements</i>	99	ND	99	129	0	77	74	0	ND	5	ND	ND	ND
<i>F.T. Heffelfinger</i>	111	ND	105	136	6	103	80	0	ND	64	ND	ND	ND
<i>Lil Charley</i>	ND	ND	131	151	ND	ND	ND	ND	ND	26	ND	ND	ND
<i>C.W. Rushing</i>	ND	ND	150	162	0	ND	ND	0	ND	10	ND	ND	ND
<i>Conti-Nan</i>	ND	ND	132	128	0	ND	ND	ND	ND	73	136	139	ND
<i>Conti-Karla</i>	ND	ND	163	184	ND	ND	ND	0	ND	4	92	129	20
<i>Hornet</i>	ND	0	125	103	0	ND	ND	0	ND	12	ND	ND	26
<i>Coop. Ambassador</i>	ND	1	145	107	14	ND	ND	12	68	19	70	71	107
<i>Eastern</i>	ND	0	254	184	0	ND	ND	1	70	51	74	71	48
<i>S.M. Fleming</i>	ND	2	280	231	28	ND	ND	27	72	76	74	70	107
<i>Kevin Michael</i>	ND	ND	142	151	ND	ND	ND	ND	69	10	77	74	51
<i>A.M. Thompson</i>	ND	ND	165	126	0	ND	ND	1	67	10	67	75	67
<i>Lil Charley</i>	ND	ND	165	110	27	ND	ND	30	70	66	70	73	53
<i>Badger</i>	ND	ND	165	151	0	ND	ND	0	62	17	65	69	30
<i>Kay D</i>	ND	ND	181	174	0	ND	ND	1	63	36	65	70	41
<i>Evey-T</i>	ND	ND	158	96	ND	ND	ND	ND	66	67	67	78	134

Notes: ND = not detectable. Data from the period July 18-23, 1991.

**Table 64. Event Peak Suspended Sediment Concentration at McEver's Island,
Measured and Computed (Akers-White Method)**

<i>Tow</i>	<i>Suspended sediment concentration at each station, mg/L</i>										
	<i>a1</i> <i>Meas.</i>	<i>a2</i> <i>Meas.</i>	<i>a</i> <i>Computed</i>	<i>b1</i> <i>Meas.</i>	<i>b2</i> <i>Meas.</i>	<i>b3</i> <i>Meas.</i>	<i>b</i> <i>Computed</i>	<i>c1</i> <i>Meas.</i>	<i>c2</i> <i>Meas.</i>	<i>c3</i> <i>Meas.</i>	<i>c</i> <i>Computed</i>
<i>Mary Ellen</i>	292	58	5	145	35	34	47	149	377	33	ND
<i>Elaine Jones</i>	385	245	5	352	146	134	47	377	140	97	ND
<i>Nicholas Duncan</i>	70	87	8	68	57	59	0	54	53	53	ND
<i>Mobil Leader</i>	469	244	ND	310	105	115	ND	230	152	89	0
<i>Reliance</i>	431	143	1	304	177	101	9	187	119	52	0
<i>Coop. Vanguard</i>	389	243	1	322	125	85	3	199	126	84	0
<i>M. E. Norman</i>	298	140	0	293	88	88	0	99	89	72	0
<i>Illini</i>	78	155	0	168	108	ND	0	82	72	64	0

Notes: ND = not detectable. Data from the period May 17-18, 1989.

**Table 65. Event Peak Suspended Sediment Concentration at Kampsville (Trip 1),
Measured and Computed (Akers-White Method)**

<i>Tow</i>	<i>Suspended sediment concentration at each station, mg/L</i>											
	<i>a1</i>	<i>a</i>	<i>b1</i>	<i>b2</i>	<i>b</i>	<i>c1</i>	<i>c2</i>	<i>c</i>	<i>d1</i>	<i>d2</i>	<i>d3</i>	<i>d</i>
	<i>Meas.</i>	<i>Computed</i>	<i>Meas.</i>	<i>Meas.</i>	<i>Computed</i>	<i>Meas.</i>	<i>Meas.</i>	<i>Computed</i>	<i>Meas.</i>	<i>Meas.</i>	<i>Meas.</i>	<i>Computed</i>
<i>Mr. Aldo</i>	106	0	350	162	0	230	ND	0	ND	ND	ND	0
<i>Floyd Blaske</i>	157	0	248	187	0	253	ND	24	ND	ND	ND	53
<i>Luke Barton</i>	246	0	257	210	0	313	243	22	ND	ND	ND	61
<i>Sugarland</i>	286	0	288	229	0	320	251	21	ND	ND	ND	68
<i>W.C. Norman</i>	189	0	276	242	0	333	264	0	ND	ND	ND	3
<i>F.H. Peavey</i>	214	0	ND	ND	0	455	246	21	ND	ND	ND	57
<i>Conti-Karla</i>	267	0	ND	ND	0	551	279	30	ND	ND	ND	63
<i>Mr. Paul</i>	201	0	306	274	0	ND	ND	1	ND	ND	ND	3
<i>Rambler</i>	278	0	341	375	0	ND	ND	0	ND	ND	ND	22
<i>Mr. Lawrence</i>	357	0	348	363	0	ND	ND	39	ND	ND	ND	82
<i>Mallard</i>	277	0	320	275	0	ND	ND	23	ND	ND	ND	43
<i>Charles Lehman</i>	379	0	444	305	0	ND	ND	43	ND	ND	ND	75
<i>Nicholas Duncan</i>	ND	0	ND	ND	0	ND	ND	22	ND	ND	ND	66
<i>Ardyce Randall</i>	209	0	329	270	0	349	295	ND	ND	ND	ND	7
<i>Mr. Paul</i>	209	0	281	249	0	336	280	35	ND	ND	ND	70
<i>Exxon St. Louis</i>	379	0	316	285	0	448	305	38	ND	ND	ND	88
<i>Margaret O.</i>	311	0	317	286	0	373	319	0	ND	ND	ND	0
<i>A.L. Smith</i>	175	0	232	211	0	563	333	3	ND	ND	ND	12
<i>Ste. Genevieve</i>	261	0	ND	ND	0	328	287	24	478	346	529	39
<i>Nicole Brent</i>	223	0	252	208	0	ND	ND	13	ND	ND	ND	39
<i>F.H. Peavey</i>	230	0	252	215	0	ND	ND	1	ND	ND	ND	1

Notes: ND = not detectable. Data from the period October 12-17, 1990.

**Table 66. Event Peak Suspended Sediment Concentration at Apple River Island,
Measured and Computed (Toffaletti Method)**

<i>Tow</i>	<i>Suspended sediment concentration at each station, mg/L</i>									
	<i>a1</i>	<i>a</i>	<i>b1</i>	<i>b</i>	<i>c1</i>	<i>c2</i>	<i>c</i>	<i>d1</i>	<i>d2</i>	<i>d</i>
	<i>Meas.</i>	<i>Computed</i>	<i>Meas.</i>	<i>Computed</i>	<i>Meas.</i>	<i>Meas.</i>	<i>Computed</i>	<i>Meas.</i>	<i>Meas.</i>	<i>Computed</i>
<i>Merlin Banta</i>	59	0	67	1	78	61	0	85	61	0
<i>Rusty Flowers</i>	108	2	78	1	81	62	1	193	62	1
<i>Tom Talbert</i>	265	2	178	0	91	65	0	76	66	0
<i>Herman Pott</i>	208	8	131	2	185	97	1	78	64	1
<i>Walter Brunson</i>	91	2	74	ND	80	212	ND	92	71	ND
<i>Dell Butcher</i>	99	0	118	0	83	68	0	75	67	0
<i>Mary Gail</i>	226	2	214	1	169	129	1	82	72	1
<i>T.S. Kunsman</i>	256	0	98	0	82	67	0	328	73	0
<i>D.R. Miller</i>	162	5	124	2	115	72	1	95	72	1
<i>Mary Gail</i>	252	0	174	0	99	78	0	95	80	0
<i>J.D. Wofford</i>	73	2	77	1	99	68	0	153	70	0
<i>Trojan</i>	90	2	88	0	99	69	0	161	71	0

Notes: ND = not detectable. Data from the period May 18-23, 1990.

**Table 67. Event Peak Suspended Sediment Concentration at Clarks Ferry (Trip 1),
Measured and Computed (Toffaletti Method)**

	<i>Suspended sediment concentration at each station, mg/L</i>										
	<i>a1</i>	<i>a2</i>	<i>a</i>	<i>b1</i>	<i>b2</i>	<i>b3</i>	<i>b</i>	<i>c1</i>	<i>c2</i>	<i>c3</i>	<i>c</i>
<i>Tow</i>	<i>Meas.</i>	<i>Meas.</i>	<i>Computed</i>	<i>Meas.</i>	<i>Meas.</i>	<i>Meas.</i>	<i>Computed</i>	<i>Meas.</i>	<i>Meas.</i>	<i>Meas.</i>	<i>Computed</i>
<i>Jemco Towing</i>	179	163	2	188	174	ND	2	194	196	295	2
<i>Pearl B.</i>	ND	152	1	174	171	169	1	199	198	190	1
<i>Conti-Afton</i>	156	161	0	176	171	166	0	210	202	200	1
<i>Sunflower-1</i>	ND	ND	1	193	ND	ND	1	190	ND	ND	1
<i>American Beauty-1</i>	ND	ND	1	211	ND	ND	1	186	ND	ND	1
<i>Dell Butcher-2</i>	ND	ND	1	173	ND	ND	1	145	ND	ND	1
<i>Hornet</i>	ND	ND	1	139	ND	ND	1	138	ND	ND	1
<i>Volunteer State</i>	ND	ND	1	210	ND	ND	1	144	ND	ND	1

Notes: ND = not detectable. Data from the period May 16-22, 1990.

**Table 68. Event Peak Suspended Sediment Concentration at Goose Island (Trip 1),
Measured and Computed (Toffaletti Method)**

<i>Tow</i>	<i>Suspended sediment concentration at each station, mg/L</i>							
	<i>a1</i>	<i>a</i>	<i>b1</i>	<i>b2</i>	<i>b</i>	<i>c1</i>	<i>c2</i>	<i>c</i>
	<i>Meas.</i>	<i>Computed</i>	<i>Meas.</i>	<i>Meas.</i>	<i>Computed</i>	<i>Meas.</i>	<i>Meas.</i>	<i>Computed</i>
<i>Dell Butcher</i>	332	1	252	242	1	253	190	2
<i>W.C. Norman</i>	258	1	217	212	2	203	236	3
<i>Normania</i>	268	1	216	210	2	192	277	3
<i>Dave Carlton</i>	199	1	192	191	1	193	178	2
<i>H.C. Blaske</i>	155	1	153	160	2	193	155	4
<i>Teresa Renee</i>	164	1	163	144	1	167	155	2
<i>Trojan Warrior</i>	193	1	169	144	2	186	277	4
<i>Hoosier State</i>	160	1	167	154	2	179	194	3
<i>Kevin Michael</i>	159	1	161	154	1	180	147	2
<i>Sumac</i>	195	1	176	181	1	197	155	2
<i>Twin Cities</i>	297	1	183	173	2	195	160	3
<i>Coop. Vanguard</i>	187	1	179	164	1	191	155	3
<i>H.M. Clements</i>	360	1	226	216	2	252	265	3

Notes: Data from the period August 24-27, 1990.

Table 69. Event Peak Suspended Sediment Concentration at Goose Island (Trip 2),
Measured and Computed (Toffaletti Method)

Tow	Suspended sediment concentration at each station, mg/L												
	<i>a1</i>	<i>a</i>	<i>b1</i>	<i>b2</i>	<i>b</i>	<i>c1</i>	<i>c2</i>	<i>c</i>	<i>d1</i>	<i>d</i>	<i>e1</i>	<i>e2</i>	<i>e</i>
	Meas.	Computed	Meas.	Meas.	Computed	Meas.	Meas.	Computed	Meas.	Computed	Meas.	Meas.	Computed
<i>James F. Neal</i>	148	0	133	113	0	132	154	0	ND	1	ND	ND	2
<i>H.M. Clements</i>	120	0	118	110	0	123	137	0	ND	4	ND	ND	4
<i>F.T. Heffelfinger</i>	104	0	110	110	0	125	97	0	ND	1	ND	ND	ND
<i>Queen City</i>	93	0	92	88	0	93	62	ND	ND	1	ND	ND	ND
<i>H.M. Clements</i>	99	ND	99	129	0	77	74	0	ND	0	ND	ND	ND
<i>F.T. Heffelfinger</i>	111	ND	105	136	0	103	80	0	ND	2	ND	ND	ND
<i>Lil Charley</i>	ND	ND	131	151	ND	ND	ND	ND	ND	1	ND	ND	ND
<i>C.W. Rushing</i>	ND	ND	150	162	0	ND	ND	0	ND	1	ND	ND	ND
<i>Conti-Nan</i>	ND	ND	132	128	0	ND	ND	ND	ND	3	136	139	ND
<i>Conti-Karla</i>	ND	ND	163	184	ND	ND	ND	0	ND	0	92	129	2
<i>Hornet</i>	ND	0	125	103	0	ND	ND	0	ND	1	ND	ND	2
<i>Coop. Ambassador</i>	ND	0	145	107	1	ND	ND	1	68	1	70	71	5
<i>Eastern</i>	ND	0	254	184	1	ND	ND	0	70	2	74	71	3
<i>S.M. Fleming</i>	ND	0	280	231	1	ND	ND	1	72	3	74	70	5
<i>Kevin Michael</i>	ND	ND	142	151	ND	ND	ND	ND	69	1	77	74	3
<i>A.M. Thompson</i>	ND	ND	165	126	0	ND	ND	0	67	1	67	75	3
<i>Lil Charley</i>	ND	ND	165	110	1	ND	ND	1	70	2	70	73	3
<i>Badger</i>	ND	ND	165	151	0	ND	ND	0	62	1	65	69	2
<i>Kay D</i>	ND	ND	181	174	0	ND	ND	0	63	1	65	70	2
<i>Evey-T</i>	ND	ND	158	96	ND	ND	ND	ND	66	2	67	78	5

Notes: ND = not detectable. Data from the period July 18-23, 1991.

**Table 70. Event Peak Suspended Sediment Concentration at McEver's Island,
Measured and Computed (Toffaletti Method)**

<i>Tow</i>	<i>Suspended sediment concentration at each station, mg/L</i>										
	<i>a1</i> <i>Meas.</i>	<i>a2</i> <i>Meas.</i>	<i>a</i> <i>Computed</i>	<i>b1</i> <i>Meas.</i>	<i>b2</i> <i>Meas.</i>	<i>b3</i> <i>Meas.</i>	<i>b</i> <i>Computed</i>	<i>c1</i> <i>Meas.</i>	<i>c2</i> <i>Meas.</i>	<i>c3</i> <i>Meas.</i>	<i>c</i> <i>Computed</i>
<i>Mary Ellen</i>	292	58	8	145	35	34	27	149	377	33	ND
<i>Elaine Jones</i>	385	245	8	352	146	134	27	377	140	97	ND
<i>Nicholas Duncan</i>	70	87	11	68	57	59	0	54	53	53	ND
<i>Mobil Leader</i>	469	244	ND	310	105	115	ND	230	152	89	2
<i>Reliance</i>	431	143	4	304	177	101	12	187	119	52	1
<i>Coop. Vanguard</i>	389	243	3	322	125	85	6	199	126	84	0
<i>M. E. Norman</i>	298	140	0	293	88	88	1	99	89	72	0
<i>Illini</i>	78	155	1	168	108	ND	1	82	72	64	0

Notes: ND = not detectable. Data from the period May 17-18, 1989.

Table 71. Event Peak Suspended Sediment Concentration at Kampsville (Trip 1),
Measured and Computed (Toffaletti Method)

Tow	Suspended sediment concentration at each station, mg/L											
	a1 Meas.	a Computed	b1 Meas.	b2 Meas.	b Computed	c1 Meas.	c2 Meas.	c Computed	d1 Meas.	d2 Meas.	d3 Meas.	d Computed
Mr. Aldo	106	0	350	162	0	230	ND	0	ND	ND	ND	0
Floyd Blaske	157	0	248	187	0	253	ND	13	ND	ND	ND	21
Luke Barton	246	0	257	210	0	313	243	12	ND	ND	ND	24
Sugarland	286	0	288	229	0	320	251	11	ND	ND	ND	24
W.C. Norman	189	0	276	242	0	333	264	0	ND	ND	ND	1
F.H. Peavey	214	0	ND	ND	0	455	246	11	ND	ND	ND	22
Conti-Karla	267	0	ND	ND	0	551	279	16	ND	ND	ND	24
Mr. Paul	201	0	306	274	0	ND	ND	1	ND	ND	ND	1
Rambler	278	0	341	375	0	ND	ND	1	ND	ND	ND	3
Mr. Lawrence	357	1	348	363	0	ND	ND	20	ND	ND	ND	16
Mallard	277	0	320	275	0	ND	ND	12	ND	ND	ND	7
Charles Lehman	379	0	444	305	0	ND	ND	21	ND	ND	ND	14
Nicholas Duncan	ND	0	ND	ND	0	ND	ND	12	ND	ND	ND	12
Ardyce Randall	209	0	329	270	0	349	295	ND	ND	ND	ND	1
Mr. Paul	209	0	281	249	0	336	280	18	ND	ND	ND	13
Exxon St. Louis	379	0	316	285	0	448	305	19	ND	ND	ND	17
Margaret O.	311	0	317	286	0	373	319	0	ND	ND	ND	0
A.L. Smith	175	0	232	211	0	563	333	3	ND	ND	ND	2
Ste. Genevieve	261	0	ND	ND	0	328	287	13	478	346	529	6
Nicole Brent	223	0	252	208	0	ND	ND	8	ND	ND	ND	6
F.H. Peavey	230	0	252	215	0	ND	ND	1	ND	ND	ND	0

Notes: ND = not detectable. Data from the period October 12-17, 1990.

REFERENCES

REFERENCES

- Adams, J.R. 1991. *Identification of Study Approaches To Determine Physical Impacts of Commercial Navigation on the Upper Mississippi River*. Illinois State Water Survey Contract Report 531, and Long-Term Resources Monitoring Program Special Report 92-S005, 53 p.
- Adams, J.R. 1992. *Sediment Concentration Changes Caused by Barge Tows*. Proceedings of Water Forum '92, Hydraulics Division, ASCE, Baltimore, MD, August 2-5:677-682.
- Adams, J.R., N.G. Bhowmik, and E. Delisio. 1989. *Measuring Resuspension of Sediment by Barge Tows*. Proceedings of the International Symposium on Sediment Transport, New Orleans, LA, August 14-18: 765-770.
- Adams, J.R., and E. Delisio. 1991. *Ambient Suspended Sediment Concentration and Turbidity Levels*. Proceedings of the 1991 ASCE National Conference on Hydraulic Engineering. Nashville, TN, July 29-August 2:865-869.
- Akers, P., and W.R. White. 1973. Sediment transport: new approach and analysis. *Journal of the Hydraulic Division*, ASCE, no. 99, HY11:2041-2060.
- American Society of Civil Engineers. 1990. *Sediment and Aquatic Habitat Associations in River Systems*. ASCE Task Committee on Sediment Transport and Aquatic Habitats: Milhous, R.T., MacArthur R.C., Shields, F.D., and J.R. Adams. Proceedings of the National Conference on Hydraulic Engineering, ASCE, San Diego, July 30-August 3.
- Bagnold, R.A. 1966. *An Approach to the Sediment Transport Problem from General Physics*. U.S. Geological Survey Professional Paper 422-I, 37p.
- Balanin, V.V., and L.S. Bykov. 1965. *Selection of Leading Dimensions of Navigation Canal Sections and Modern Methods of Bank Erosion*. S.1-4. Proceedings of the 21st International Navigation Congress, PIANC. Stockholm:151-170.
- Berger Associates, Ltd. 1981. *Analysis of Impact of Navigation on the Tennessee-Tombigbee Waterway*. Berger Associates, Ltd., Louis Berger and Associates, Inc.
- Bhowmik, N.G. 1976. *Development of Criteria for Shore Protection against Wind-Generated Waves for Lakes and Ponds in Illinois*. University of Illinois Water Resources Center Research Report 107 and Illinois State Water Survey Contract Report 170.
- Bhowmik, N.G., J.R. Adams, A.P. Bonini, C.Y. Guo, D.J. Kisser, and M.A. Sexton. 1981a. *Resuspension and Lateral Movement of Sediment by Tow Traffic on the Upper Mississippi and Illinois Rivers*. Illinois State Water Survey Contract Report 269.
- Bhowmik, N.G., M. Demissie, and C.-Y. Guo. 1982. *Waves and Drawdown Generated by River Traffic on the Illinois and Mississippi Rivers*. Illinois State Water Survey Contract Report 293 and University of Illinois Water Resources Center Research Report 167.
- Bhowmik, N.G., M. Demissie, and S. Osakada. 1981b. *Waves and Drawdown Generated by River Traffic on the Illinois and Mississippi Rivers*. Illinois State Water Survey Contract Report 271, submitted to the Environmental Work Team, Upper Mississippi River Basin Commission, September 1.
- Bhowmik, N.G., M.T. Lee, W.C. Bogner, and W.P. Fitzpatrick. 1981c. *The Effects of Illinois River Traffic on Water and Sediment Input to a Side Channel*. Illinois State Water Survey Contract Report 270, submitted to the Environmental Work Team, Upper Mississippi River Basin Commission, September 1.
- Bhowmik, N.G., T.W. Soong, W.F. Reichelt, and N. Seddik. 1991. *Waves Generated by Recreational Traffic on the Upper Mississippi River System*. Illinois State Water Survey Research Report 117. Prepared for the U.S. Fish and Wildlife Service, Environmental Management Technical Center, Onalaska, WI.

- Bhowmik, N.G., T.W. Soong, and R.J. Xia. 1993a. *Physical Effects of Barge-Tows on the Upper Mississippi River System: Analyses of Existing Data Collected by the Illinois State Water Survey from the Clarks Ferry Site on the Mississippi River*. Progress Report 1. Illinois State Water Survey, Champaign, IL.
- Bhowmik, N.G., T.W. Soong, and R.J. Xia. 1993b. *Physical Effects of Barge-Tows on the Upper Mississippi River System: Analyses of Existing Data Collected by the Illinois State Water Survey from the Kampsville Site on the Illinois River*. Progress Report 2. Illinois State Water Survey, Champaign, IL.
- Bhowmik, N.G., T.W. Soong, R.J. Xia, and M. Bera. 1994a. *Physical Effects of Barge-Tows on the Upper Mississippi River System: Analyses of Existing Data Collected by the Illinois State Water Survey from the McEver's Island Site on the Illinois River*. Progress Report 3A. Illinois State Water Survey, Champaign, IL.
- Bhowmik, N.G., T.W. Soong, R.J. Xia, and M. Bera. 1994b. *Physical Effects of Barge-Tows on the Upper Mississippi River System: Analyses of Existing Data Collected by the Illinois State Water Survey from the Apple River Island Site on the Mississippi River*. Progress Report 3B. Illinois State Water Survey, Champaign, IL.
- Bhowmik, N.G., T.W. Soong, R.J. Xia, and M. Bera. 1994c. *Physical Effects of Barge-Tows on the Upper Mississippi River System: Analyses of Existing Data Collected by the Illinois State Water Survey from the Goose Island Site on the Mississippi River*. Progress Report 3C. Illinois State Water Survey, Champaign, IL.
- Bhowmik, N.G., and R.J. Xia. 1992. *Hydraulic and Geomorphic Classification of the Upper Mississippi River System: Pilot Study of Three Pools*. ASCE Proceedings, 1992 National Conference on Hydraulic Engineering, Baltimore, MD, August 2-6:666-671.
- Bhowmik, N.G., and R.J. Xia. 1993. *Turbulent velocity fluctuations in natural rivers*. Proceedings of Hydraulic Division, ASCE, V2:1677-1682.
- Bhowmik, N.G., R.J. Xia, B.S. Mazumder, and T.W. Soong. 1995a. Return flow in rivers due to navigation traffic. *Journal of Hydraulic Engineering*, ASCE, Vol. 121, No. 12, Dec. 1993:914-918.
- Bhowmik, N.G., R.J. Xia, B.S. Mazumder, and T.W. Soong. 1995b. Distribution of turbulent velocity fluctuations in a natural channel. *Journal of Hydraulic Research*. Vol. 33, No.5:649-661.
- Bhowmik, N.G., and R.J. Xia. 1996. *Hydraulic and Geomorphic Classification of the Upper Mississippi River System: Pilot Study of Three Pools*. Illinois State Water Survey Contract Report (In Press).
- Blaauw, H. G., and F.M.C. van der Knaap. 1983. *Prediction of Squat of Ships Sailing in Restricted Water*. Publication No. 302 8th International Harbor Congress, Delft Hydraulic Laboratory, Delft, The Netherlands.
- Blaauw, H. G., F.M.C. van der Knaap, D.T. de Groot, and K.W. Pilarczyk. 1984. *Design of Bank Protection of Inland Navigation Fairways*. Publication No. 320. Presented at the International Conference on Flexible Armoured Revetments Incorporating Geotextiles, London, England. March 29-30, 1984.
- Bouwmeester, J. 1977. *Calculation of Return Flow and Water Level Depression; New Method*. 24th International Navigation Congress, SI-3, PIANC, Brussels, Belgium. 148-151.
- Bridgeman, P.W. 1931. *Dimensional Analysis*. Yale University Press, New Haven, CT.
- Buchanan, T.J., and W.P. Somers. 1969. *Stage Measurement at Gaging Stations*. Techniques of Water Resources Investigations of the U.S. Geological Survey, Book 3, Chapter C7, 28p.
- Carter, R.W., and J. Davidian. 1968. *General Procedure for Gaging Streams*. Techniques of Water Resources Investigations of the U.S. Geological Survey, Book 3, Chapter A6, 12p.

- Colby, B.R. 1964a. *Practical Computation of Bed-Material Discharge*. Journal of the Hydraulics Division, ASCE, Vol. 90, No. HY2, Proceeding Paper 3843, March.
- Colby, B.R. 1964b. *Discharge of Sands and Mean Velocity Relationships in Sand-Bed Streams*. Professional Paper 462-A, U.S. Geological Survey, Washington, D.C.
- Daily, J.W., and D.R.F. Harleman. 1973. *Fluid Dynamics*. Addison-Wesley Publishing Company, Inc. Reading, Massachusetts, USA, 454p.
- Dand, I.W., and W.R. White. 1978. *Design of Navigation Canals*. Proceedings, Symposium on Aspects of Navigability of Constraint Waterways, Including Harbor Entrances, Vol. 2, Paper 3, Delft, The Netherlands.
- Demissie, M., L. Keefer, and R.J. Xia. 1992. *Erosion and Sedimentation in the Illinois River*. Illinois State Water Survey Contract Report 519. 123p.
- Einstein, H.A. 1950. *The Bed Load Function for Sediment Transport in Open Channels*. Technical Bulletin 1026, U.S. Department of Agriculture, Soil Conservation Service, Washington, D.C.
- Fuehrer, M., and R. Romisch. 1977. *Effects of Modern Ship Traffic on Inland and Ocean Waterways and Their Structures*. 24th International Navigation Congress, SI-3, PIANC, Brussels, Belgium, pp. 79-93.
- Galencser, G.J. 1977. *Drawdown Surge and Slope Protection, Experimental Results*. Proceedings of the 24th International Congress, Leningrad.
- Garthune, R.S., B. Rosenberg, D. Cafiero, and C.R. Olson. 1948. *The Performance of Model Ships in Relation to the Design of the Ship Canal*. Report no. 601, David Taylor Model Basin.
- Gates, E.D., and J.B. Herbich. 1977. *Mathematical Model To Predict Behavior of Deep-Draft Vessels in Restricted Waterways*. Corps of Engineers Report No. 200, Texas A & M University, College Station, TX.
- Guy, H.P. 1969. *Laboratory Theory and Methods for Sediment Analysis*. Techniques of Water Resources Investigations of the U.S. Geological Survey, Book 5, Chapter C1, 58p.
- Guy, H.P. 1970. *Fluvial Sediment Concept*. Techniques of Water Resources Investigations of the U.S. Geological Survey, Book 3, Chapter C1, 55p.
- Guy, H.P., and V.W. Norman. 1982. *Field Methods for Measurement of Fluvial Sediment*. Techniques of Water Resources Investigations of the U.S. Geological Survey, Book 3, Chapter C2, 59p.
- Henderson, F.M. 1966. *Open Channel Flow*. The Macmillan Company, New York.
- Hochstein, A.B. 1967. *Navigation Use of Industrial Canals*. Water Transportation, Moscow Publishing House, U.S.S.R.
- Hochstein, A.B., and C.E. Adams. 1989. Influence of vessel movements on stability of restricted channels. *Journal of Waterway, Port, Coastal, and Ocean Engineering*, ASCE, 115(5):444-465.
- Illinois State Water Survey. 1989. Progress Report for SCFW 14-16-003-88973. Illinois State Water Survey, Champaign, IL., 26p.
- InterOcean Systems, Inc. 1990. *S4 Users Manual*. Third edition. InterOcean Systems, Inc. 3540 Aero Court, San Diego, CA 92123, 90p.
- Kuo, C.Y., D.M. Jordan, K.J. Ying, and G.V. Loganathan. 1988. *Vessel Induced Physical Effects Related to Navigation Changes on the Kanawha River, West Virginia*. Prepared for U.S. Army Corps of Engineers, Huntington District, Huntington, WV.
- Latorre, R. 1985. Shallow river pushboat preliminary design. *Journal of Waterway, Port, Coastal, and Ocean Engineering*, ASCE, Vol. 111, No. 4, July:678-692.
- Laursen, E.M. 1958. The total sediment load of streams. *Journal of the Hydraulics Division*, ASCE, Vol. 84(1):1530 1-36.

- Maynard, S.T. 1988. *Investigation of Velocities Induced by Commercial Navigation*. Summary Report. Department of the Army, Waterways Experiment Station, U.S. Army Corps of Engineers, Vicksburg, MS.
- Maynard, S.T., and T. Siemsen. 1991. *Return Velocities Induced by Shallow-draft Navigation*. Proceedings of Hydraulic Division, ASCE Conference, ASCE, 1:894-899.
- Mazumder, B.S., N.G. Bhowmik, and T.W. Soong. 1991. *Turbulence and Reynolds Stress Distribution in a Natural River*. Proceedings of Hydraulic Division, ASCE Conference, ASCE, 1:906-911.
- Mazumder, B.S., N.G. Bhowmik, and T.W. Soong. 1993. Turbulence in rivers due to navigation traffic. *Journal of Hydraulic Engineering*, ASCE, Vol. 119, No. 5:581-597.
- McNown, J.S. 1976. Sinkage and resistance for ships in channels. *Journal of Waterways, Harbors, and Coastal Engineering*, ASCE, Vol. 102, No. WW1:287-300.
- Ofuya, A.O. 1970. *Shore Erosion — Ship and Wind Waves, St. Clair, Detroit and St. Lawrence Rivers*. Department of Public Works of Canada, Design Branch. Report No.21.
- Owen, D., editor. 1988. *Inland River Record 1988-1989*. The Waterway Journal, St. Louis, MO.
- PIANC. 1987. *Guidelines for the Design and Construction of Flexible Revetment Incorporating Geotextiles for Inland Waterways*. Report, Working Group 4, Permanent Technical Committee I (Supplement to Bulletin No. 57). Brussels, Belgium.
- Rasmussen, J.L., and J.H. Wlosinski. 1988. *Operating Plan of the Long-Term Resource Monitoring Program for the Upper Mississippi River System*. U.S. Fish and Wildlife Service, Environmental Management Technical Center, LaCrosse, WI.
- Rouse, H., editor. 1959. *Advanced Mechanics of Fluids*. John Wiley & Sons, New York.
- Schijf, J.B., and P.P. Jansen. 1953. *Section I*. 18th International Navigation Congress, Rome, Italy:175-197.
- Sharp, B.B., and J.D. Fenton. 1968. *A model investigation of squat*. Dock Harbor Authority, 48(S77), November 1968:242-244.
- Simons, D.B., R.M. Li, Y.H. Chen, S.S. Ellis, and T.P. Chang. 1981. *Investigation of Effects of Navigation Traffic Activities on Hydrologic, Hydraulic, and Geomorphic Characteristics*. Report for the Environmental Work Team, Upper Mississippi River Commission Master Plan, Minneapolis, MN.
- Soong, T.-W., W.C. Bogner, and W.F. Reichelt. 1990. *Field Data Acquisition for Determining the Physical Impacts of Navigation*. Proceedings of the National Conference on Hydraulic Engineering, San Diego, CA, July 30-August 3, 1990:616-621.
- Sorensen, R.M., and J.R. Weggel. 1984. *Development of Ship Wave Design Information*. Proceedings, 19th International Conference on Coastal Engineering, ASCE, Houston, TX. ASCE:3227-3243.
- Stefan, H.G., and M.J. Riley. 1985. Mixing of a stratified river by barge tows. *Water Resources Research*, Vol. 21, No. 8:1085-1094.
- Toffaletti, F.B. 1969. *Definitive computations of sand discharge in Rivers*. Journal of the Hydraulics Division, ASCE, Vol. 95, No. HY1, Proceeding Paper 6350.
- Tothill, J.T. 1966. *Ships in Restricted Channels — a Correlation of Model Tests, Field Measurements and Theory*. Society of Naval Architecture and Marine Engineering, February:111-128.
- Upper Mississippi River Basin Commission. 1982. *Comprehensive Master Plan for the Management of the Upper Mississippi River System*. Environmental Report. Prepared by the Environmental Work Team for the Upper Mississippi River Basin Commission.

- U.S. Army Corps of Engineers. 1980. *Gallipolis Lock and Dam Replacement, Ohio River, Phase I Advanced Engineering and Design Study*. General Design Memorandum, Appendix J, Volume 1, Environmental and Social Impact Analysis. U.S. Army Corps of Engineers, Huntington District.
- U.S. Army Corps of Engineers. 1982. *Upper Mississippi Navigation Charts*. U.S. Army Corps of Engineers, North Central Division.
- U.S. Army Corps of Engineers. 1988. *Final Environmental Impact Statement: Second Lock at Locks and Dam No. 26 (Replacement) Mississippi River, Alton, Illinois, and Missouri*. U.S. Army Corps of Engineers, St. Louis District.
- U.S. Army Corps of Engineers. 1989. *Report on the Upper Mississippi River and Illinois Waterway Navigation Systems*. U.S. Army Corps of Engineers, Rock Island District, 35p.
- U.S. Army Corps of Engineers. 1991. *Plan of Study for Navigation Effects of the Second Lock, Melvin Price Lock and Dam, Mississippi River, Alton, Illinois, and Missouri*. Army Corps of Engineers, St. Louis District.
- U.S. Fish and Wildlife Service. 1992. *Operating Plan for the Upper Mississippi River System, Long-Term Resources Monitoring Program*. EMTC-91-P002, Environmental Management Technical Center, Onalaska, WI., 183 p.
- Vanoni, V.A., editor. 1975. *Sedimentation Engineering*. ASCE Manuals and Reports on Engineering Practice, No. 54, New York.
- Weggel, J.R., and R.M. Sorensen. 1986. *Ship Wave Prediction for Port and Channel Design*. Proceedings of a Specialty Conference on Innovation in Port Engineering and Development in the 1990s. Oakland, CA, May 19-21, 1986. Paul H. Sorensen (ed.), ASCE:791-814.

REPORT DOCUMENTATION PAGE			Form Approved OMB No. 0704-0188
Public reporting burden for this collection of information is estimated to average 1 hour per response, including the time for reviewing instructions, searching existing data sources, gathering and maintaining the data needed, and completing and reviewing the collection of information. Send comments regarding this burden estimate or any other aspect of this collection of information, including suggestions for reducing this burden, to Washington Headquarters Services, Directorate for Information Operations and Reports, 1215 Jefferson Davis Highway, Suite 1204, Arlington, VA 22202-4302, and to the Office of Management and Budget, Paperwork Reduction Project (0704-0188), Washington, D.C. 20503			
1. AGENCY USE ONLY (Leave blank)	2. REPORT DATE July 1998	3. REPORT TYPE AND DATES COVERED	
4. TITLE AND SUBTITLE Physical changes associated with navigation traffic on the Illinois and Upper Mississippi Rivers		5. FUNDING NUMBERS	
6. AUTHOR(S) Nani G. Bhowmik, David Soong, J. Rodger Adams, Renjie Xia, and Bijoy S. Mazumder			
7. PERFORMING ORGANIZATION NAME AND ADDRESS Illinois State Water Survey Hydrology Division 2204 Griffith Drive Champaign, Illinois 61820		8. PERFORMING ORGANIZATION REPORT NUMBER	
9. SPONSORING/MONITORING AGENCY NAME(S) AND ADDRESS(ES) U.S. Geological Survey Environmental Management Technical Center 575 Lester Avenue Onalaska, Wisconsin 54650		10. SPONSORING/MONITORING AGENCY REPORT NUMBER 98-S001	
11. SUPPLEMENTARY NOTES			
12a. DISTRIBUTION/AVAILABILITY STATEMENT Release unlimited. Available from National Technical Information Service, 5285 Port Royal Road, Springfield, VA 22161 (1-800-553-6847 or 703-487-4650. Available to registered users from the Defense Technical Information Center, Attn: Help Desk, 8725 Kingman Road, Suite 0944, Fort Belvoir, VA 22060-6218 (1-800-225-3842 or 703-767-9050).		12b. DISTRIBUTION CODE	
13. ABSTRACT (Maximum 200 words) This report summarizes the investigation conducted by the Illinois State Water Survey on the physical changes associated with the movement of navigation traffic on the Illinois and Upper Mississippi Rivers. This research project was partially funded by the Environmental Management Technical Center of the U.S. Geological Survey and the U.S. Army Corps of Engineers. Project activities were conducted through the Illinois Department of Natural Resources. Research results have also been presented at technical society meetings and published in a number of journals.			
14. SUBJECT TERMS Barge traffic, current, draw down, Illinois River, Mississippi River, navigation traffic, return velocity, sediment resuspension, suspended sediment, turbidity, water quality		15. NUMBER OF PAGES 205 pp.	16. PRICE CODE
17. SECURITY CLASSIFICATION OF REPORT Unclassified	18. SECURITY CLASSIFICATION OF THIS PAGE Unclassified	19. SECURITY CLASSIFICATION OF ABSTRACT Unclassified	20. LIMITATION OF ABSTRACT